P-282

IN-26895

DOE/NASA/0290-02
NASA CR-175047
WAESD-TR-85-0030

GAS COOLED FUEL CELL SYSTEMS TECHNOLOGY DEVELOPMENT

FINAL REPORT FOR THE SECOND LOGICAL UNIT OF WORK
CONTRACT PERIOD: MAY 1983 – MAY 1984

J. M. Feret
Westinghouse Electric Corporation
Advanced Energy Systems Division
Pittsburgh, PA 15236-0864

AUGUST 1986

Prepared for
NATIONAL AERONAUTICS AND SPACE ADMINISTRATION
Lewis Research Center
Under Contract DEN 3-290

For
U.S. DEPARTMENT OF ENERGY
Morgantown Energy Technology Center

(NASA-CR-175047) GAS COOLED FUEL CELL N86-31984
SYSTEMS TECHNOLOGY DEVELOPMENT Final
Report, May 1983 - May 1984 (Westinghouse
Electric Corp.) 282 p CSCL 10A Unclas
G3/44 43679

DISCLAIMER

Printed in the United States of America

Available from

National Technical Information Service
U.S. Department of Commerce
5285 Port Royal Road
Springfield, VA 22161

NTIS price codes[1]

Printed copy: A04
Microfiche copy: A01

---

[1] Codes are used for pricing all publications. The code is determined by the number of pages in the publication. Information pertaining to the pricing codes can be found in the current issues of the following publications, which are generally available in most libraries: Energy Research Abstracts (ERA); Government Reports Announcements and Index (GRA and I); Scientific and Technical Abstract Reports (STAR); and publication, NTIS-PR-360 available from NTIS at the above address.

WAESD-TR-85-0030
DOE/NASA/0290-02
NASA CR-175047

GAS COOLED FUEL CELL SYSTEMS TECHNOLOGY DEVELOPMENT

Final Report for the Second Logical Unit of Work
Contract Period: May 1983 - May 1984

J. M. Feret
Westinghouse Electric Corporation
Advanced Energy Systems Division
Pittsburgh, PA 15236-0864

August 1986

Prepared for
NATIONAL AERONAUTICS AND SPACE ADMINISTRATION
Lewis Research Center
Under Contract DEN 3-290

for
U. S. DEPARTMENT OF ENERGY
Morgantown Energy Technology Center
Morgantown, West Virginia 26505

Under Interagency Agreement DE-AI21-80ET17088

ACKNOWLEDGEMENTS

The following personnel contributed to this Final Report

M. S. Barrett
D. E. Dickey
G. G. Elia
J. M. Feret
L. L. France
N. Haines
R. R. Holman
T. K. Houghtaling
J. L. Kelly
H. D. Kulikowski
A. K. Kush
R. F. Lampe
J. R. Lance
M. T. Le
B. L. Pierce
J. F. Pierre
R. Rosey
E. F. Saladna
F. R. Spurrier
S. Venkatesh
D. A. Wiseman
B. M. Woodle
M. K. Wright
J. F. Zippay

TABLE OF CONTENTS

TABLE OF CONTENTS (CONTINUED)

LIST OF FIGURES

LIST OF FIGURES (CONT'D)

LIST OF FIGURES (CONT'D)

LIST OF FIGURES (CONT'D)

LIST OF TABLES

LIST OF TABLES (CONT'D)

LIST OF TABLES (CONT'D)

LIST OF TABLES (CONT'D)

LIST OF ACRONYMS

AICM	Acid Inventory Control Member
BOU	Beginning of Use
COE	Cost of Electricity
CT	Combustion Turbine
DHE	Dynamic Hydrogen Electrode
DSC	Differential Scanning Calorimetry
EOU	End of Use
EPRI	Electric Power Research Institute
ERC	Energy Research Corporation
ETU	Electrolyte Take-Up
FCS	Fuel Cell System
FEP	Fluorinated Ethylene-Propylene
FHS	Fuel Handling System
FMEA	Failure Mode Control System
FPS	Fuel Processing System
ICD	Interface Control Drawing
ICS	Instrumentation and Control System
LVDT	Linear Variable Displacement Transducer
O&M	Operating and Maintenance
OCV	Open Circuit Voltage
PAFC	Phosphoric Acid Fuel Cell
PCS	Power Conditioning System
PDS	Purchasing Department Specifications
PES	Polyethersulfone
PFA	Perfluoroalkoxyethylene
RES	Rotating Equipment System
RHE	Reversible Hydrogen Electrode
SGS	Steam Generation System
SRG	Simulated Reformer Gas
TAG	Technical Assessment Guide
TBD	To Be Determined
TGA	Thermogravimetric Analysis
UES	Utility Equipment System
UPP	Utility Power Plant
W	Westinghouse
WBS	Work Breakdown Structure
WDPF	Westinghouse Distributed Process Family

1.0 SUMMARY

This report addresses the work performed during the Second Logical Unit of Work of a multi-year program designed to develop a phosphoric acid fuel cell (PAFC) for electric utility power plant application. The Second Logical Unit of Work, which covers the period May 14, 1983 through May 13, 1984, was funded by the U.S. Department of Energy, Office of Fossil Energy, Morgantown Energy Technology Center, and managed by the NASA Lewis Research Center. The PAFC Technology Development Program efforts were performed by a team comprised primarily of personnel from the Westinghouse Advanced Energy Systems Division and the Energy Research Corporation (a division of St. Joe Minerals Corporation), in parallel and integrated with the Utility Power Plant Program which was sponsored by Westinghouse, a host utility, the Electric Power Research Institute, the Empire State Electric Energy Research Corporation, and other participating organizations.

1.1 Scope of Work

The major elements of work to be performed in the multi-year program have been integrated into a Work Breakdown Structure (WBS) as shown in Figure 1-1. This WBS establishes the basic framework for all contractually required effort and thereby provides a uniform structure for planning, assessing progress achieved, controlling costs, etc.

The Second Logical Unit of Work comprised twenty WBS tasks (see Table 1-1) for which specific objectives, schedular and cost plans, and deliverables have been established.

1.2 Technical Objectives

The primary objectives established to be achieved in the Second Logical Unit of the program were:

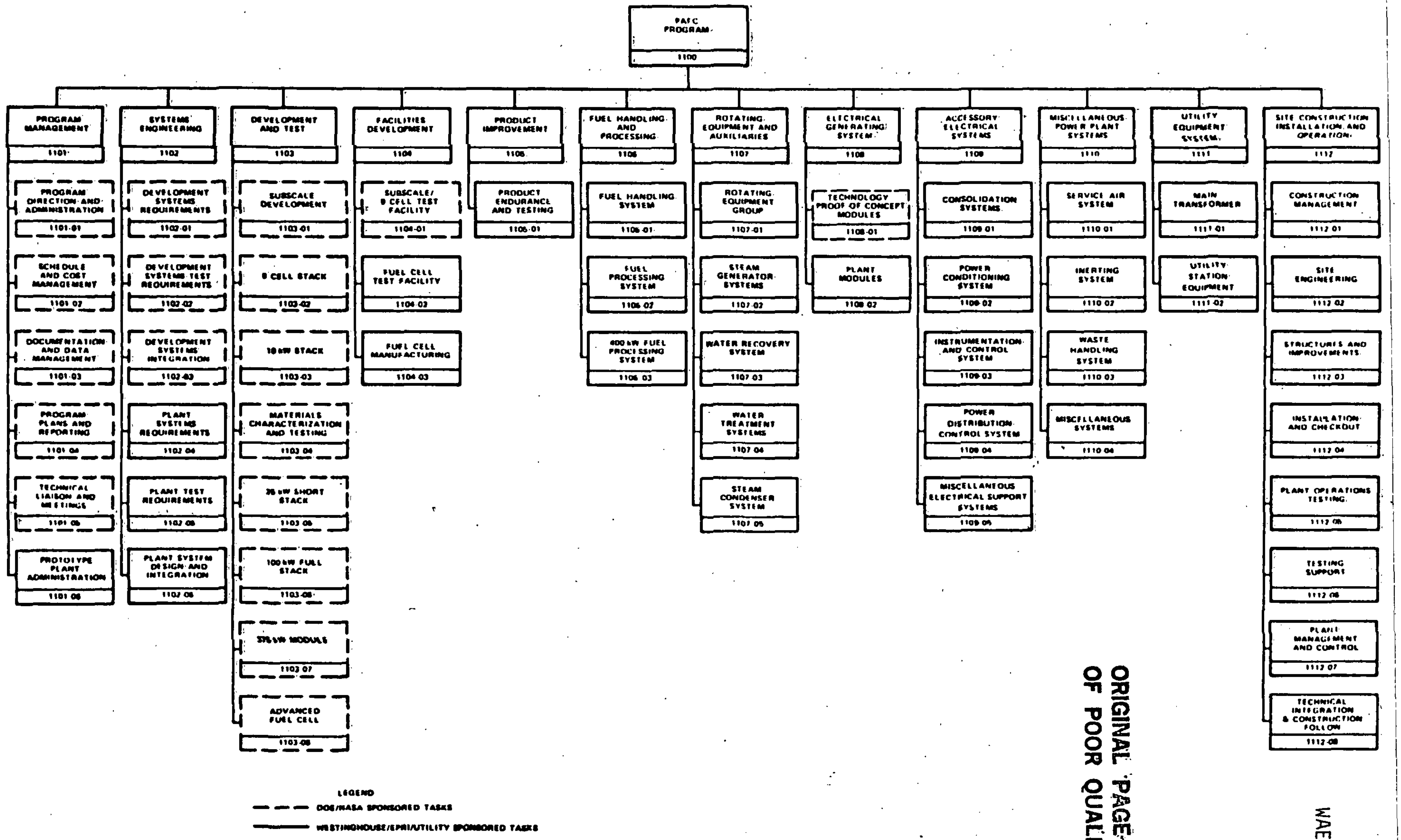

Figure 1-1. Westinghouse PAFC Program Work Breakdown Structure

TABLE 1-1

PHOSPHORIC ACID FUEL CELL TECHNOLOGY DEVELOPMENT PROGRAM SECOND LOGICAL UNIT TASKS

WBS TASK NO.	DESCRIPTION
1101	Program Management
1102-01-100	System Analyses
1102-01-200	Fuel Cell, Fuel Processing, Power Conditioning, Rotating Equipment, and Instrumentation and Control Systems Design Requirements
1102-01-300	Fuel Cell Requirements
1102-02-200	100 kW Full Stack Fuel Cell Test Specification
1102-02-300	25 kW Short Stack Fuel Cell Test Specification
1102-02-400	Fuel Cell Hardware Test Specifications
1102-02-500	Fuel Cell Manufacturing Processes Specifications
1102-03-100	Fuel Cell System Design
1102-03-300	Systems Interface Requirements and Control
1103-01	Subscale Fuel Cell Development
1103-02	9-Cell Stack Development
1103-03	10 kW Fuel Cell Stack Development
1103-04	Fuel Cell Materials Characterization and Testing
1103-05	25 kW Short Stack Development
1103-06	100 kW Full Stack Development
1103-07	375 kW Module Development
1103-08	Advanced Fuel Cell Development
1104-01	Subscale 2 x 2 Inch Cell and 9-Cell Testing Facilities Development
1108-01	Technology Proof-of-Concept Module Fuel Cell System

- Establish the final system-level requirements for the Fuel Cell, Fuel Processing, Power Conditioning, Rotating Equipment, and Instrumentation and Control Systems.

- Develop the Fuel Cell System preliminary design.

- Reduce the total fuel cell resistance to less than 0.2 mΩ.

- Increase the average cell beginning of use performance at pressure on the order of 50 mV, and improve the long term performance of the fuel cell to a 2 mV loss per 1000 hours of operation.

- Develop an optimum stack startup procedure from ambient conditions to the nominal operating conditions: 480 kPa (70 psia), 190°C (374°F), and 325 mA/cm^3 (300 A/ft^2) operating on reformate hydrogen (83 percent utilization) and air (50 percent utilization), and changes above/below these nominal conditions.

- Develop performance repeatable and cost effective manufacturing processes for the electrodes, matrices, and cooling and bipolar plates.

Considerable progress was achieved relative to each of these objectives and is summarized below:

- System level design requirements were established for the Fuel Cell, Fuel Processing, Power Conditioning, Rotating Equipment, and Instrumentation and Control Systems. This was accomplished by the performance of numerous studies and analyses which addressed the areas of system trade-offs, performance, operation, and maintenance. The specifications prepared for these systems include functional, operational, interface, and quality assurance requirements based on the selected plant design parameters: 1) 7.5 MW gross electrical output (7.2 MW net), 2) a heat rate of less than 9500 kJ/kWh

(9000 BTU/kWh), 3) full power operation with naphtha as the backup fuel, and 4) automatic control during all power operations.

A number of modifications were incorporated into the PAFC power plant design which resulted in improved performance, or a simpler configuration. These requirements, studies, and modifications are discussed in detail in Section 2.1.

- The Fuel Cell System preliminary design was fully developed. A complete design description, system maintenance requirements, and structural analysis are presented in Sections 2.2 and 2.3. The system interface requirements were identified and are documented in Section 2.3.2.

- Technology in the fuel cell development program has progressed significantly. Subscale cell testing verified stack design and manufacturing processes, as well as provided a base for stack scaling. The various test plans and results are reported in Section 3.1.

- The nine cell stack design has been further developed and refined. The primary areas of improvement were electrode edge sealing, acid transport within the cells, and manifold sealing. Additionally, new manufacturing, startup, and operating procedures resulted a substantial 48 mV increase in cell performance, while a further increase of 30 mV is projected due to thinner matrices. Complete details and testing results are given in Section 3.2.

- Based on the achievements in the nine cell stack area, the 10 kW, 25 kW, and 100 kW stacks were re-designed, incorporating a new inverted cell configuration. This configuration provides improved acid transport. The development status and design description of each of these stacks are presented in Sections 3.3 through 3.5.

- The 375 kW module design, necessary to the utility plant application, was updated to incorporate advancements achieved by the fuel cell technology program. The major changes included addition of a continuous acid supply system, addition of electric heaters to maintain higher internal temperatures, and the inverted cell stack design. A complete design description, including maintenance and replacement schedules, of the 375 kW module is given in Section 3.6.

- The characterization of various raw materials utilized in the manufacture of repeating cell components was addressed. Specifically, plate resistivity, porosimetry, and corrosion, seal materials, electrode materials, and other stack materials were evaluated. The comprehensive results of this effort are reported in Section 3.7.

- The advanced fuel cell development effort achieved considerable success by defining performance goals and identifying problem areas. A Performance Improvement Work Plan was formulated and implemented to improve cell performance and reduce variance. The areas primarily addressed were alternate catalyst evaluation and support, manufacturing, cell resistance, plate coatings and corrosion, acid management, and impurity effects. A complete summary of this effort is presented in Section 3.8.

- A new presurized test facility, SE-1, was constructed and checked out at ERC. This facility, which is capable of accommodating a full sized (12x17 in.) nine cell stack, improved upon past ERC facilities by incorporating advanced methods of measurement and control. This facility is described in Section 4.0.

The aggregate of this effort resulted in the revision of manufacturing and stack assembly procedures, stack design, and system specifications. These, along with the associated drawings, were updated and released.

2.0 SYSTEMS ENGINEERING (WBS 1102)

The objectives of this task were to develop the final system-level design requirements for the Fuel Cell, Fuel Processor, Power Conditioning, Rotating Equipment, and the Instrumentation and Control Systems (FCS, FPS, PCS, RES, and ICS, respectively). The following sections summarize the results of analyses and design studies performed.

2.1 Development System Requirements (WBS 1102-01)

This section summarizes system analysis, technology assessments, and the resulting design requirements for the FCS, FPS, PCS, RES, and ICS.

2.1.1 System Analyses (WBS 1102-01-100)

The primary objectives of the system analysis effort were to perform system trade-off studies, performance analyses, and operational studies to establish preliminary system level design requirements.

These analyses identified the functional and conceptual interface requirements in conjunction with the Task 1102-04-100 Plant Systems Analyses effort. System level trade-off studies that considered heat rate, power level, cost of electricity (COE), operating characteristics, and development risk were performed to select system level design requirements for each of these systems for a prototype power plant that produces 7.5 MW_e DC with a heat rate goal of less than 9500 kJ/kWh (9000 Btu/kWh). The effect upon plant performance and operating characteristics for startup, steady-state, shutdown, and malfunction conditions associated with these systems was determined by utilizing appropriate steady-state, transient, and controllability analysis models.

A number of design modifications were incorporated into the PAFC power plant. These modifications include:

- Provide addition of 100 cells per module.
- Incorporate the functions of the FPS turbocompressor into the RES.
- Make plant operation at a lower pressure level at part power compatible with RES recommended speed.
- Provide part of the steam required for reforming in the FPS.
- Design for full power beginning of use with naphtha fuel.

The above items resulted in improved performance or a simpler configuration.

2.1.1.1 Performance and Operational Studies

Four normal power plant operating points were established in the First Logical Unit. These are: (1) full power beginning of use (BOU), (2) full power end of use (EOU), (3) part power BOU, and (4) part power (EOU). The full power BOU point is identified as the baseline prototype power plant design. The EOU condition is defined at a cell voltage degradation of 80 mV. Though the remaining fuel cell operating parameters (temperature, pressure, current density, etc.) remain constant at BOU and EOU for full and part power modes respectively, there is a difference in the operating parameters between full and part power. The full power BOU operating conditions for the fuel cell are 190°C (374°F), 480 kPa (70 psia), and 300 mA/cm^2 (280 A/ft^2) producing a cell voltage of 0.690 V (0.610 V at EOU). The corresponding part power conditions are 190°C (374°F), 207 kPa (30 psia), and 75 mA/cm^2 (70 A/ft^2), which result in a BOU cell voltage of 0.752 V (0.672 V at EOU). The part power operating pressure represents a pressure level compatible with the RES speed. Part power operation at constant temperature maintains the pressure level of the steam generators. The performance summary for these operating points is given in Table 2-1, where the heat rates have been reduced from one to four percent below the First Logical Unit values.

TABLE 2-1
PERFORMANCE SUMMARY

	FULL POWER		PART POWER	
	BOU	EOU	BOU	EOU
Cell Voltage (mV)	690	610	752	672
Pressure, kPa (psia)	480 (70)	480 (70)	207 (30)	207 (30)
Temperature, °C (°F)	190 (374)	190 (374)	190 (374)	190 (374)
Current Density, mA/cm^2 (A/ft^2)	300 (280)	300 (280)	75 (70)	75 (70)
Gross DC, kW	7500	6625	2042	1825
Gross AC, kW	7200	6360	1878	1679
Net RES, kW	98	103	-233	-203
Parasitic Losses, kW	202	202	64	66
Net AC, kW	7096	6243	1581	1410
Thermal Input, GJ/h $(10^6$ Btu/h)	62.6 (59.39)	62.6 (59.39)	16.1 (15.23)	16.1 (15.23)
Plant Heat Rate, kJ/kWh (Btu/kWh)	8875 (8370)	10,028 (9510)	10,155 (9630)	11,388 (10,800)

2.1.2 Fuel Cell, Fuel Processing, Power Conditioning, Rotating Equipment, and Instrumentation and Control Systems Design Requirements (WBS 1102-01-200)

Updated system design requirements were prepared for the FCS, FPS, PCS, RES, and ICS. These specifications include functional, operation, interface, and quality assurance requirements.

2.1.2.1 Fuel Cell System

The primary function of the FCS is to produce DC electric power and thermal energy using air-cooled 375 kW fuel cell modules. The fuel cell modules transform the chemical energy from the fuel and oxidant reaction (hydrogen-rich feed gas supplied by the FPS and oxygen in the form of pressurized air supplied by the RES) into electrical energy.

Design requirements established for the FCS include:

- Provide a gross electrical output of 7.5 MW DC at full power operating conditions at BOU.
- Control electrical output based on current demand. The design basis (BOU full power) fuel cell module current output is 325 amps.
- Provide hydrogen utilization consistent with fuel cell performance characteristics and FPS performance requirements. The design hydrogen utilization is 83 percent.
- Equalize fuel and process air flows to the individual fuel cell modules and provide for on-line checking for cross leakage between the anode and the cathode.
- Design for stable operation at power operation conditions and for response to the transient operating conditions within the appropriate time frames.

- Maintain fuel cell module temperatures greater than 107°C (225°F) during STANDBY.

- Maintain the fuel cell temperature between 38°C (100°F) and 54°C (130°F) during shipping, handling, maintenance, installation and non-power operating conditions to prevent solidification of the installed phosphoric acid.

- Maintain the air pressure level between 205 and 480 kPa (30 - 70 psia). The system design shall include the capability to isolate any fuel cell module or modules without causing significant pressure differentials across individual cells.

- Maintain the fuel cells in a dry inert atmosphere having a dew point of -23°C (10°F) or less during shipping, handling, installation, and non-power operating conditions to limit phosphoric acid water-content.

- Design for operation on the fuel cell anode supply composition defined in Table 2-2.

- Design to allow replenishment of fuel cell phosphoric acid during operation and shutdown.

2.1.2.2 Fuel Processing System

The primary function of the FPS is to convert steam and hydrocarbon fuel (either natural gas or naphtha) to a hydrogen-rich gas for use in the fuel cells. Fuel is provided by the Fuel Handling System (FHS) as natural gas or as liquid naphtha. Fuel cell anode exhaust is used to provide thermal energy for the reforming process. Steam and feedwater are supplied by the Steam Generation System (SGS). Pressurized air for combustion is provided by the RES.

Secondary functions of the FPS are to reduce impurities (hydrogen sulfide, etc.) from the fuel stream which are detrimental to fuel cell performance, to

TABLE 2-2
FUEL CELL ANODE SUPPLY COMPOSITION REQUIREMENTS

Component	Composition (volume fraction) Design Basis	Acceptable Limit
Hydrogen	.742	> 0.50
Carbon Dioxide	.182	diluent
Carbon Monoxide	.008	< 0.01
Water	.044	< 0.06
Methane	.014	< 0.05
Nitrogen	.010	diluent

Impurities	Composition (ppm by volume)
H_2S	< 100
COS	< 100
Olefins	< 300
Higher Hydrocarbons (C_2^+)	< 1000
NH_3	< 10
Cl	< 1
Metal Ions	< 1 (by weight)
Tar/Oils	< 0.05 (by weight)
Particulates	< 0.05 (by weight)

remove water from the process gas stream, and to provide process heat for steam generation.

The FPS "top level" design requirements are summarized in Table 2-3.

2.1.2.3 Power Conditioning System

The primary functions of the PCS are to control the magnitude of the direct currents generated by the FCS, to combine these currents, and to convert them to alternating currents suitable for application to a distribution system and to an electric utility transmission network through the Utility Equipment System (UES).

Secondary functions are to control fuel cell module electrical loading, provide appropriate fault protection, harmonic reduction, power factor correction capability, and means of integrating system control and monitoring into the overall power plant.

The PCS design will be designed to meet the performance and equipment requirements identified in Tables 2-4 and 2-7 based on the input and output conditions as specified in Tables 2-5 and 2-6.

2.1.2.4 Rotating Equipment System

The primary functions of the RES are to provide and circulate a supply of clean pressurized air to the FCS and to provide clean pressurized air to the FPS. The air provides a source of oxygen for both the FPS combustion and the cathode side of the fuel cells and also removes thermal energy produced by the exothermic reaction within the FCS. The RES uses steam generated in the SGS, cathode exhaust gas from the FCS and combustion exhaust gas from the FPS to develop mechanical shaft power to help drive circulating and compressing equipment, thus helping to maximize the overall power plant efficiency. Key operating statepoints are summarized in Table 2-8.

TABLE 2-3
FPS TOP LEVEL DESIGN REQUIREMENTS

PERFORMANCE	
H_2 Production Rate, normal m^3/s (SCFD)	
• Gross	1.5 (4.9×10^6)
• Net (Hydrogen Utilized)	1.3 (4.1×10^6)
Natural Gas Feedrate,* kg/s (lb/h)	0.34 (2,720)
OPERATIONAL	
Cold Start to Standby, hours	< 4
Standby to Min. Power, hours	< 1/2
Min. to Max. Power, Percent Full Power per min	7.7
Operating Range, Percent production rate	23-100
Operation	Automatic Dispatch from Standby to Full Power
Start/Stop Cycles (Over Lifetime)	
- Warm Startup/Warm Shutdown	10,000
- Cold Startup/Cold Shutdown	150
GENERAL	
Fuel Capability	Natural Gas/Naphtha
Availability, Percent	95
Design Life, Years	25
Maximum Plot Plan Area, m^2 (ft^2)	230 (2500)
Maximum Height of Equipment Above Grade, m (ft)	9.1 (30)
Noise Level (db)	55
Transportability	Common Carrier Truck (For all subsystems except reformer)

* Includes raw fuel used as reformer furnace fuel

TABLE 2-4
PCS PERFORMANCE REQUIREMENTS

Power Conversion	
Rated Full Power Input	7.5 MWDC
Rated Full Power Output	7.2 MWAC
Rated Part Power Input	1.875 MWDC
Rated Part Power Output	1.725 MWAC
Minimum Operating Input	.75 MWDC
Efficiency	
Full Power	96 percent
Part Power	92 percent
Power Factor	
Normal	Unity - Part to Full Load
Excess VARs Available	1.4 MVAR - Full Load, Rated Voltage 5.4 MVAR - Part Load, Rated Voltage +6.8 MVAR or - 3.4 MVAR - Zero Load
Fault Protection	
DC Power	Electronic circuit interruption
AC Power	Circuit breaker
Response Time	
Controlled Power Change	.5 seconds over operating range
Controlled MVAR Change	.1 seconds over operating range
Fault Clearing Trip	.05 seconds
Harmonic Distortion	Maximum total harmonic distortion of 3 percent RMS of fundamental voltage and 1 percent for any one individual component when operating into a system with 250 MVA short circuit capacity.

TABLE 2-4

PCS PERFORMANCE REQUIREMENTS (CONT'D)

Manual Control	To bring system to STANDBY condition during plant startup and for system checkout.
Automatic Control	For all normal power operation via plant computer.
Power Dispatch	In response to changes in currents from fuel cell modules.
Reactive Power Dispatch	In response to command signals from plant computer independent of real power dispatch.
Power Level Control Accuracy	± 150 kW
Electromagnetic Interference	Shall not result in misoperation of local communications equipment or any sensitive loads.
Black Start Capability	None
Low Power Bleed Loading	Provide 50 ± 2.5 ohm load for each group of 5 modules - to load modules before PCS is connected.

TABLE 2-5
PCS INPUT FROM FUEL CELL SYSTEM

Number of Fuel Cell Modules	20
Nominal Input Per Module	
	375 kW Module
Full Power - Beginning of Use	
Current, amps	325
Voltage, volts DC	1156
Power, kWDC	375
Full Power - End of Use	
Current, amps	325
Voltage, volts DC	1025
Power, kWDC	333
Part Power - Beginning of Use	
Current, amps	80
Voltage, volts DC	1260
Power, kWDC	100
Part Power - End of Use	
Current, amps	80
Voltage, volts DC	1130
Power, kWDC	90
Module Voltage Maximum Limit	1300 V (sustained more than 1 second)
Module Current Maximum Limit	450A (sustained more than 1 second)
Module Minimum Controlled Current	50A
Module Low Power Bleed Current	5 to 10A during shutdown operation
Module Ripple Current Limit	100A peak to peak, 180 or 360 Hertz
Module Effective Resistance	.95 ohm during power operation
Module Effective Capacitance	Variable with magnitude of maximum current reached during a load change 24 MFD for 100A maximum 120 MFD for 350A maximum

TABLE 2-6

PCS OUTPUT TO UTILITY EQUIPMENT SYSTEM

Output Voltage	13,800 VAC, 3 phase, 60 Hz	
System Performance Degradation Performance (Resulting from utility AC grid voltage variations)	Bus Voltage Variation	System Impact
	±5 Percent	Rated Power
	>+5 Percent to +10 Percent (continuous)	95 Percent of Rated Power
	<-5 Percent to -10 Percent (continuous)	95 Percent of Rated Power
	<-10 Percent to -20 Percent	85 Percent of Rated Power
	>+10 Percent or -20 Percent	Unpredictable
Utility System Unbalance	Rated Power Output with up to 3 Percent unbalance and 2 Percent negative sequence voltage	
Frequency	Rated Power Output - 57 - 61 Hertz (Trips off line outside this range due to transformer core limitations)	

TABLE 2-7
PCS EQUIPMENT DESIGN REQUIREMENTS

Design Life	25 years 10000 Operations (mechanical)	
Availability	99 Percent	
Reliability	99.5 Percent	
Structural Welding	AWS D1.1	
Structural Design	ANSI A58.1 (Seismic Zone 4)	
Footprint	43.5 m^2 (1500 ft^2) maximum	
Environment	Temperature	-29°C to 49°C (-20°F to 120°F)
	Humidity	100 percent
	Pressure	85-110 kPa (12.5-16 Psia)
	Altitude	1525 m (5000 ft)
Governing Electrical Code	National Electrical Code (NFPA No. 70 - Latest Revision)	
Shipment	Truck Transportable (maximum size modules 3.5 m (11'-6") high x 2.25 m (7'-6") wide x 9.5 m (31'-6") long, 18600 kg (41,000 lbs) - shock loads of up to 3 g during shipment)	

TABLE 2-7

PCS EQUIPMENT DESIGN REQUIREMENTS (CONT'D)

Maintenance Requirements	Clearance for removal of major component and assemblies Replaceable air filters Self checking diagnostic circuits Conservative thermal margins 24 hours/year scheduled maintenance downtime
Controlled Mechanical Interfaces	Equipment foundations Equipment fencing Fire protection alarms
Controlled Electrical Interfaces	(+) or (-) connection to each FCS module 13.8 KVAC output connections to a Utility Equipment System 480 VAC power feeder from Power Distribution System Ground connections from Power Distribution System Control interface with Westinghouse WDPF Data Highway

TABLE 2-8
RES OPERATING STATEPOINTS

	Full Power EOU	Part Power BOU
● Air Circulator		
Flow, kg/h (lb/h)	642, 200 (1,416,000)	102,490 (225,950)
Inlet Pressure, kPa (psia)	482 (70)	207 (30)
Inlet Temperature, °C (°F)	146 (294)	117 (243)
Outlet Pressure, kPa (psia)	489 (71)	207 (30)
Outlet Temperature, °C (°F)	147 (297)	141 (286)
Fluid	Air	Air
● Centrifugal Compressor (Two Stages)		
Flow, kg/h (lb/h)	33,790 (74,490)	17,919 (39,480)
Inlet Pressure, kPa (psia)	101.3 (14.7)	101.3 (14.7)
Inlet Temperature, °C (°F)	27 (80)	27 (80)
Outlet Pressure, kPa (psia)	482 (70)	207 (30)
Outlet Temperature, °C (°F)	146 (294)	117 (243)
Fluid	Air	Air
● Steam Turbine		
Flow, kg/h (lb/h)	8,193 (18,060)	1,126 (2,476)
Inlet Pressure, kPa (psia)	365 (53)	365 (53)
Inlet Temperature, °C (°F)	140 (284)	140 (284)
Outlet Pressure, kPa (psia)	21 (3)	21 (3)
Outlet Temperature, °C (°F)	61 (141)	61 (141)
Fluid	Steam	Steam
● Cathode Gas Expander		
Flow, kg/h (lb/h)	28,230 (62,230)	11,730 (25,860)
Inlet Pressure, kPa (psia)	475 (69)	200 (29)
Inlet Temperature, °C (°F)	193 (379)	172 (341)

TABLE 2-8
RES OPERATING STATEPOINTS (CONT'D)

	Full Power EOU	Part Power BOU
Outlet Pressure, kPa (psia)	110 (16)	110 (16)
Outlet Temperature, °C (°F)	27 (146)	114 (238)
Fluid	Air (O_2 depleted)	Air (O_2 depleted)
● Combustion Gas Expander		
Flow, kg/h (lb/h)	9,288 (20,480)	2,457 (5,416)
Inlet Pressure, kPa (psia)	352 (51)	138 (20)
Inlet Temperature, °C (°F)	440 (824)	434 (813)
Outlet Pressure, kPa (psia)	110 (16)	110 (16)
Outlet Temperature, °C (°F)	295 (563)	408 (767)
Fluid	Combustion Products	

Table 2-9 gives the power summary for the RES design for full and part power at BOU and EOU conditions. The BOU part power case requires the most power from the electric motor, 231 kW (310 HP). Table 2-10 lists the RES design requirements. A compact arrangement of the RES is illustrated in Figure 2-1.

2.1.2.5 Instrumentation and Control System

The primary functions of the ICS are to provide real time monitoring of all plant parameters and provide warnings of deviations from normal operating conditions or plant configuration, to control all startup, power and shutdown operations of plant systems, and to implement automatic corrective action in the event of faulted or emergency conditions. Secondary functions are to provide data recordings of plant parameters, plant configuration status, and alarm event sequences for overall plant performance evaluation use and event documentation.

The ICS will be designed to meet the performance requirements identified in Table 2-11, based on the numbers of inputs and outputs specified in Table 2-12.

Table 2-13 lists equipment design requirements that will be met, and Figure 2-2 shows the basic system configuration in block diagram form.

2.1.3 Fuel Cell Requirements (WBS 1102-01-300)

The fuel cell baseline technology requirements development effort needed to meet the PAFC system design and operation goals imposed by FCS performance requirements is discussed in this section. Current fuel cell technology and the anticipated improvements resulting from the development effort are identified and compared to the prototype plant requirements and goals.

2.1.3.1 Approach and Assumptions

The overall objectives of the fuel cell requirements effort were to establish the baseline fuel cell technology requirements, define goals for design and

TABLE 2-9
RES POWER SUMMARY

	Full Power		Part Power	
	BOU	EOU	BOU	EOU
Steam Turbine (kW)	561	672	46	77
Combustion Gas Expander (kW)	458	458	22	22
Cathode Gas Expander (kW)	1175	1175	207	207
Air Compressor (kW) (Two Stages)	-1842	-1842	-492	-492
Air Circulator (kW)	-255	-360	-14	-16
Motor Power Required (kW)	97	103	-231	-202

TABLE 2-10
RES DESIGN REQUIREMENTS

Performance	
See Operating Statepoints	(Table 2-8)
Operational	
Warm Startup/Warm Shutdown Cycles	10,000
Cold Startup/Cold Shutdown Cycles	150
Operating Range, Percent of Rated Speed	70 - 100
Operation	Automatic Dispatch from Standby to Full Power
General	
Availability Percent	94
Design Life, years	25
Maximum Plot Plan Area, m^2 (ft^2)	50 (525)
Maximum Height of Equipment Above Grade, m (ft)	9.1 (30)
Noise Level (db) at plant parameter	55
Transportability	Common Carrier Truck

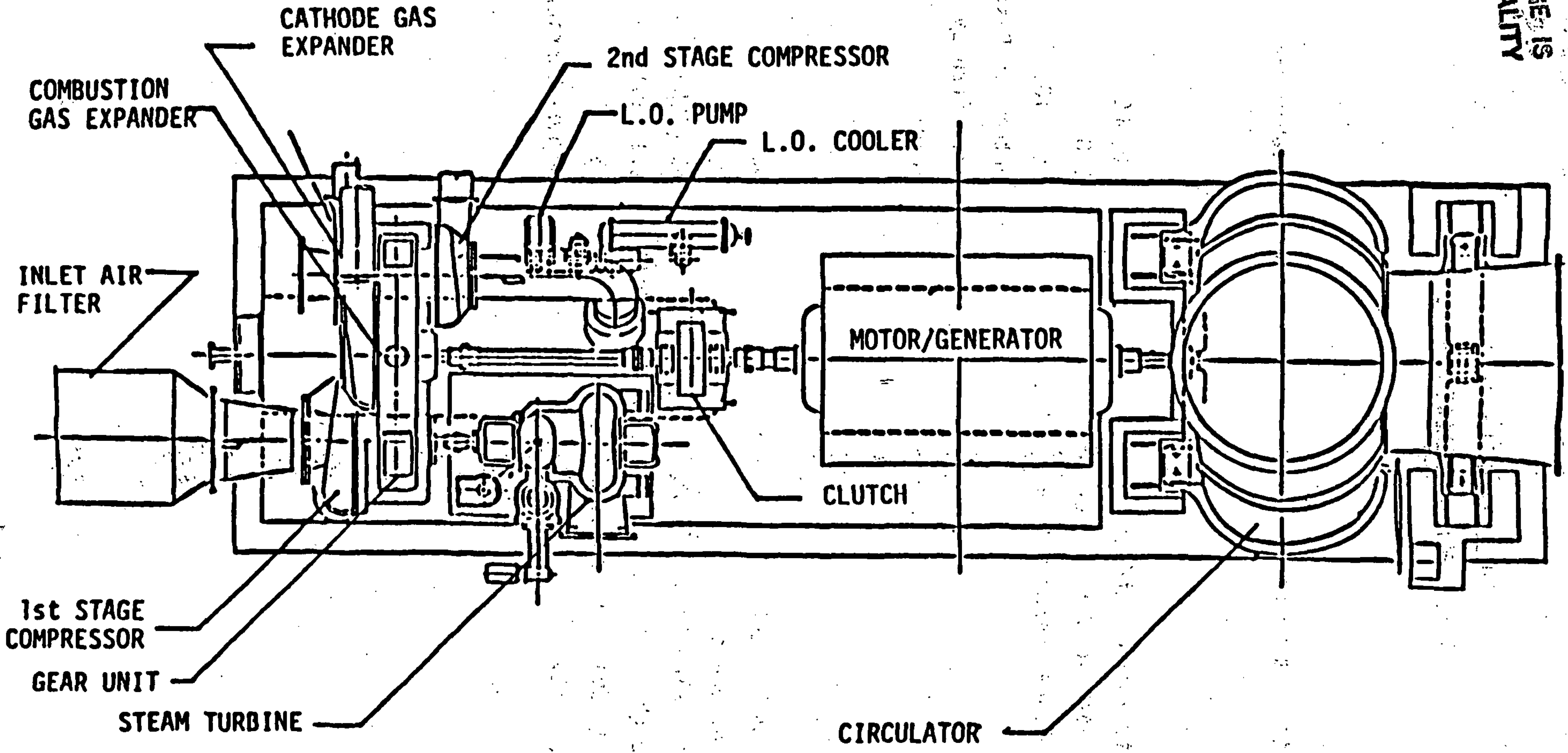

Figure 2-1. Rotating Equipment System Arrangement

TABLE 2-11
ICS TOP LEVEL DESIGN REQUIREMENTS

System Type	Westinghouse WDPF distributed control system using local programmable controllers, data highway, and central control room.
Manual Control	Between COLD STOP and STANDBY from local control stations of individual systems or central control room.
Automatic Control	During POWER operations from local control stations of individual systems or central control room or remote utility dispatch room.
Alarms	Lock-in type warnings of deviations from normal operating condition or plant configuration and identification of fault and emergency conditions and sequence of occurence.
Monitoring	Real time indications of plant alignment and operating parameters.
Redundancy	As required to achieve desired reliability and accomplish safe shutdown.
Uninterruptible Power Supply	As required to monitor plant status after loss of plant power.
Software	User friendly - no previous computer programming experience required.
Diagnostics	Self checking and failure diagnostic programming built in.

TABLE 2-12
ICS INPUT/OUTPUT REQUIREMENTS

Type of I/O	No. Required*	Electrical Characteristic	Function
Digital Input	768	384-TTL, 192-25VDC, 192-115VAC	Level, temp., and pressure switches, limit switches, events, handshakes, binary data
Digital Output	768	384-TTL, 192-115VAC, 192-Relay	Digital controls, contactors, inhibits, enables, handshakes, binary data
Analog Input			
• Thermocouple	288	Type K	Temperature sensors
• High level	288	0-5 VDC	from level, pressure, flow, voltage and current sensors and strain gauges
Analog Output			
• High level	72	0-5 VDC	To meters, trend recorders, analog devices
• PID Controller	72	4-20 ma	Closed loop controllers
TOTAL	2,256	(720 Analog, 1536 Digital)	

*Current estimate

TABLE 2-13
ICS EQUIPMENT DESIGN REQUIREMENTS

Response Times	
Controller computational frequency	TBD
Operator display update	TBD
Multiplexer scan rate	TBD
Time to change display format	TBD
Alarm scan rate	TBD
Alarm timing resolution	TBD
Accuracy	
Type of Measurement	Error
TBD	TBD (percent of full scale)
Control Accuracy	± 2 percent Power
Design Life	25 years 10,000 operations (mechanical)
Availability	99 percent
Reliability	99.8 percent
Structural Welding	AWS D1.1
Structural Design	ANSI A58.1 (Seismic Zone 4)
Configuration	93 m^2 (1000 ft^2) maximum footprint. Skid mounted, prewired assemblies with weather/explosion proof enclosures as required. See Figures 2-8 and 2-9.

TABLE 2-13
ICS EQUIPMENT DESIGN REQUIREMENTS (CONT'D)

Environment	Temperature -29°C to 49°C (-20°F to 120°F) 15°C to 32°C ((60°F to 90°F) inside enclosure) Humidity 100 percent Pressure 85-110 kPa (12.5-16 psia)
Governing Electrical Code	National Electrical Code (NFPA No. 70, latest revision)
Shipment	Truck transportable (maximum size modules 3.5 m (11'-6") high x 2.25 m (7'-6") wide x 9.5 m (31'-6") long, 18600 kg (41,000 lbs) - shock loads of up to 3 g during shipment)
Maintenance Requirements	Clearance for removal of major components and assemblies Conservative thermal design margins On-line diagnostic and verification capability and software
Controlled Mechanical Interfaces	Equipment foundations Fire protection alarms
Controlled Electrical Interfaces	All wiring to other plant systems

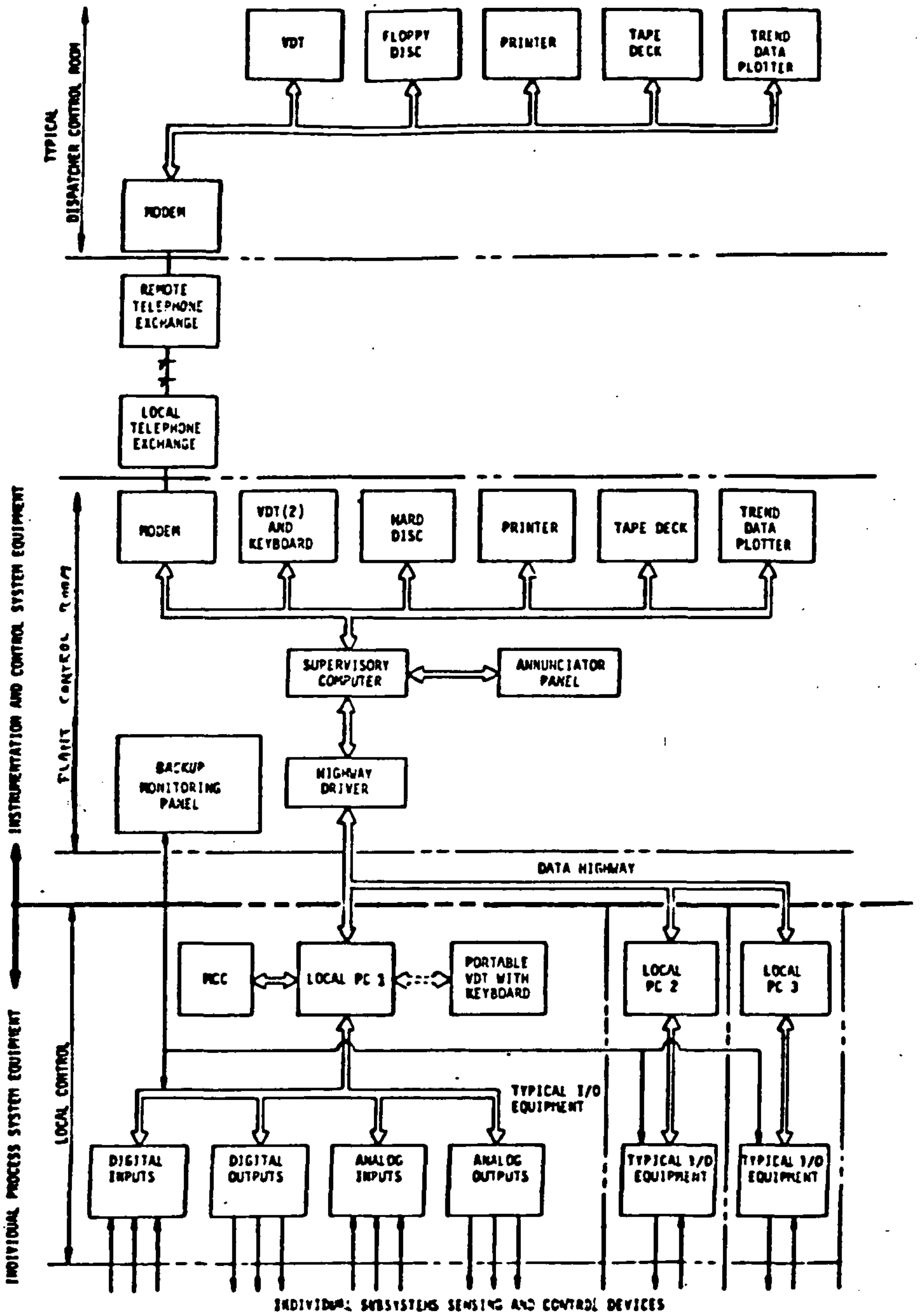

Figure 2-2. Instrumentation and Control System Functional Block Diagram

development of the fuel cells, and determine further development effort required. Specific efforts during this reporting period were to:

- determine fuel cell testing performance and technology baseline requirements to meet system development goals.
- establish and update the PAFC technology database needed for system development requirements assessments.
- define the fuel cell design and operating requirements for the continuing development testing to ensure meeting system requirements.
- provide projected fuel cell requirements for the PAFC module design specification and update as required.

The key baseline fuel cell technology existing at the beginning of this reporting period and from which the fuel cell development requirements effort progressed included design and fabricating processes for:

- nominal 30.5 cm x 43 cm (12 in. x 17 in.) "Z" channel process gas routing bipolar plates and double branched (tree) cooling plates.
- rolled electrode catalyst layers dry bonded to Teflon wet-proofed Stackpole backing paper.
- five cells between cooler plates
- a matrix utilizing .25 mm (10 mil) thickness MAT-1 and nominal .20 mm (8 mil) thickness SiC layer.
- performance development testing to be conducted with simulated reformer gas (SRG) fuel and oxidized with air.

- Viton seals selected as the first baseline (more detail is presented in Section 3.2.1.1 Stack Elastomer Edge Seal Development).
- nominal 48 cm^3 (12.7×10^{-3} gal) of phosphoric acid applied at 97 percent concentration for each cell.

During this development period variations in fuel cell assemblies of alternate electrodes, processes, seal materials, seal configuration and acid loadings were investigated. However, the above baseline configuration was the basis for comparison of the technology development.

2.1.3.2 Technology Assessment Updates

During the First Logical Unit, the reference PAFC design technology baseline was not fully established for assessing development efforts for meeting prototype power plant applications. Effort was directed during this earlier period toward upgrading technology to improve performance. This is noted in Table 2-14, where the parameters developed in the First Logical Unit effort were updated to concur with the fuel cell prototype performance goals determined during this reporting period. A review of the prototype goals resulted in the definition of potentially more compatible fuel cell and plant (systems) operating conditions for the specified plant requirements (Refer to Section 2.1.2). PAFC development goals and test performance experienced during this reporting period are presented in Table 2-15.

Although most of the fuel cell operating parameters that were needed for design and concept assessments had some level of definition, the impacts of the selected operating conditions on cell life, overall stack performance, economics, and risk were not definable since corresponding test data were not available. Work continues to identify the parameter trade-offs and sensitivity of the fuel cell to its operating requirements in plant system conditions.

TABLE 2-14

KEY PAFC DESIGN PARAMETERS, VALUES, AND CONSTRAINTS[1]

Parameter Identity	Time	Level	Origin/Comments
Maximum Voltage (Cell)	Continuous	<800 mV	Corrosion Constraint to < 800 mV from life performance
Minimum Voltage (Cell)		None	Functional Constraint - minimum design voltage required
Current Density (Min)	(TBD) h	0-75 mA/cm^2 (0-70 A/ft^2)	Corrosion Constraint - Voltage dependent - requires further development data to set time limit at temperature
Current Density (Min)	Continuous	> 75-100[2] mA/cm^2 (70-93 A/ft^2)	Corrosion Constraint[2] - function of temperature and pressure and not yet characterized
Current Density (Max)	Continuous	<400 mA/cm^2 (370 A/ft^2)	Performance Constraint - low efficiency and cell performance (requires trade-offs - efficiency versus cost)
Temperature (Nom Max)	(TBD) h	220°C (426°F)	Performance Constraint - electrode life requirements from impact of electrolyte loss
Temperature (Max)	Continuous	190-200°C (375-398°F)	Performance Constraint - temperature control requires ΔT variance and maximum local temperature in cell is constraint
Temperature (Min)	Continuous	(TBD)	Performance Constraint - temperature control for acid conc., performance variance & CO poisoning
Pressure (Max)	Continuous	690 kPa (100 psia)	Performance Constraint - trade-off studies of system operating cost versus pressure level needed
Pressure Difference Process Gases (Max)	Instantaneous	34.5 kPa (5 psia)	Functional Constraint - design condition imposed on gas separation, cell assembly and sealing
Coolant Temperature (Min)	Continuous	110-150°C (230-302°F)	Performance Constraint - temperature control of cell acid concentration and performance (characterization TBD)
Coolant Temperature (Max)	(TBD) h	200°C (398°F)	Performance Constraint - life requirement impact from excessive cell temperature conditions

TABLE 2-14

KEY PAFC DESIGN PARAMETERS, VALUES AND CONSTRAINTS[1] (CONT'D)

Parameter Identity	Time	Level	Origin/Comments
Cell Coolant Diff. Pressure (Max)	Instantaneous	(TBD)	Functional Constraint - design limit for separation requirement and cell assembly and sealing
Reactant Diff. Pressure (Max)	Continuous	(TBD)	Functional Constraint - design limit for separation requirement and cell assembly and sealing
Cell Stack Temp Diff. (Max to Min)	(TBD) h	20-50°C (36-90°F)	Performance Constraint - life requirement impact
Cell Stack Temp Diff. (Max to Min)	Continuous	∼ 20°C (36°F)	Performance Constraint - life requirement impact
Transient Rates - Power	Startup Shutdown	(TBD) (TBD)	Performance Constraint - life requirement impact
Stack Mechanics:			
- Contact Resistances	Continuous	<20mΩ-cm^2 (8mΩ-in^2)	Performance Constraint for practical losses (<2 percent output)
- Clamping Load (Initial)	Continuous	70-210 kPa (20-60 psi)	
- Clamping Load (Min)	Continuous	(TBD)∼6.9 kPa (1 psi)	Performance Constraint - leakage and electrical losses - high contact resistance
- Creep Rates/ Strengths	--	(TBD)	Performance Constraint - life requirements impacts
- Maximum Stack Height (Module Unit)	--	3.3 m (10 ft)	Imposed Constraint - truckability
- Maximum Width (Module Unit)	--		Imposed Constraint - truckability

TABLE 2-14

KEY PAFC DESIGN PARAMETERS, VALUES AND CONSTRAINTS[1] (CONT'D)

Parameter Identity	Time	Level	Origin/Comments
- Maximum Weight (Module Unit)	--		Imposed Constraint - truckability
- Maximum Output Voltage (Stack)	Instantaneous	< 400V DC	Functional Constraint - design limit is fixed as function of number cells in stack at O.C. voltage
- Maximum Output Voltage (Stack)	Continuous	< 300V DC	Nominal design condition
- Minimum Output Voltage (Unit)	Continuous	> 2000V DC	Functional Constraint - nominal design condition Performance Constraint - conversion efficiency

---

(1) Condensed list of key constraints remaining after having assumed fixed process controls and fixed performance parameters for baselined reference design. These parameters are needed for further design and operating requirements definition.

(2) Corrosion impact - not yet determined.

(3) Amount of H_3PO_4 vaporized; currently perceived upper limit.

TABLE 2-15

PAFC DEVELOPMENT GOALS

Cell Performance:(1)

Primary	Goal	Prototype Demonstration
• Voltage:		
Cell Potential - avg. mV/cell		
2 x 2 @ Design(2)	705	678 ± 12
12 x 17 @ Design(2)	680	645 ± 12
• Endurance		
Voltage Loss - mV/1000 h	2	10-15
Corrosion Loss - cm/yr (mil/yr)	2 (2.54×10^{-3})	NA
Secondary		
• Catalyst		
Anode Loading - mg/cm^2 (lb/ft^2)	0.25 ($.5 \times 10^{-3}$)	0.30 ($.5 \times 10^{-3}$)
Cathode Loading - mg/cm^2 (lb/ft^2)	0.50 (1.0×10^{-3})	0.50 (1.0×10^{-3})
• Oxidant Utilization with Air:		
Oxygen(3) - percent	50	50
• Fuel Utilization with SRG:		
Hydrogen(3) - percent	83	83
• Operating Temp. of Cell:		
Cell Avg. Temp. - °C (°F)	190 (374)	190 (374)

---

(1) Fixed Parameters:
Natural gas feedstock
ERC-Westinghouse Air Cooled System Configuration
Mark II "zee"-"tree" Plates
MAT-1 matrix
1982 Process Specs/Fab Controls

(2) Design Conditions (Beginning of Use):
480 kPa (70 psia) Pressure Level
190°C (374°F) Average Cell Temperature
325 mA/cm^2 (300 A/ft^2) Average Cell Current Density Loading
Acid Control Equilibrium
80 percent H_2 Utilization (SRG)
50 percent Air utilization

(3) At 485 kPa (4.8 Atm)

2.1.3.3 PAFC Module and 100 kW Stack Fuel Cell Requirements

The performance and design requirements for the 100 kW stack and module design defined in the First Logical Unit report were assessed and updated during this reporting period. Revised requirements are presented in Table 2-16 for the key PAFC operating parameters.

2.2 Fuel Cell System Requirements (WBS 1102-02)

The primary objective of this task is to develop test specifications in accordance with the FCS requirements discussed in the previous section for subscale (2x2 in.) fuel cells, nine and ten cell stacks, 10 kW stack and the 25 kW stacks. The test specifications include requirements for steady state and transient performance, endurance, key statepoint data, gas analyses and chemistry, and structural considerations. The following sections summarize the results of these efforts.

2.2.1 25 kW Stack Fuel Cell Test Specification (WBS 1102-02-300)

Although a preliminary 25 kW stack specification has not been issued, system performance requirements and design requirements were identified and documented during the First Logical Unit of Work. Updated 25 kW stack performance requirements are given in Table 2-17.

2.2.2 Fuel Cell Hardware Test Specifications (WBS 1102-02-400)

A number of subscale cell and nine cell stack test specifications were issued to perform tests to obtain the technology characterization for fuel cell and stack design and performance prediction. The 10 kW stack test and measurement requirements and testing conditions were defined and the test specification initiated.

Subscale cell test specifications were issued for a group of technology characterization tests and quality verification tests. A summary of the

TABLE 2-16

100 kW STACK PERFORMANCE AND DESIGN REQUIREMENTS

PARAMETER	UNITS	NOMINAL	DESIGN RANGE
POWER	kW_{dc}	94	0 < 120
TEMPERATURE	°C(°F)		
Oxidant Inlet*		182 (360)	Amb. to 204 (400)
Coolant Inlet		143 (290)	Amb. to 160 (320)
Fuel Inlet		190 (374)	Amb. to 204 (400)
Plate Avg.		190 (374)	Amb. to 204 (400)
*Same as coolant outlet.			
PRESSURE	kPa (psia)	485 (70)	101-107 (15-85)
FLOW	g/s (lb/hr)		
Fuel 83% H_2 util.		12.6 (100)	15 (< 120)
Oxidant (air) 50% O_2 Util.		97.6 (775)	113 (< 900)
Coolant (air)		1934 (15,350)	2268 (< 18,000)
CELL VOLTAGE	mV		
Open Circuit		920	0 - 1000
Operating Limit		800	
Operating Design Point		680	600 - 690
CELL CURRENT DENSITY	mA/cm^2 (A/ft^2)		
Minimum Operating		50 (47)	0 < 400 (372)
Design Point		325 (300)	250-400 (235-372)
FUEL STACK VOLTAGE	Volts		
Open Circuit		360	< 385
Operating Limit		315	< 335
Operating Point		270	210-335
FULL STACK CURRENT	Amps	350	0 < 430

TABLE 2-17
25 kW STACK PERFORMANCE REQUIREMENTS

The performance requirements for the 25 kW stack design are listed below:

PARAMETERS	UNITS	NOMINAL	DESIGN RANGE
POWER	KW_{dc}	25	< 30
TEMPERATURE	°C (°F)		
Oxidant Inlet		(184) 363	(149-204) 300-400
Coolant Inlet		(136) 277	(110-160) 230-320
Fuel Inlet		(190) 375	(149-204) 300-400
Plate Avg.		(190) 375	(149-204) 300-400
PRESSURE	kPa (Atm)	485 (4.8)	101-606 (1 - 6)
FLOW	g/s (lb/hr)		
Fuel		1.1 (8.75)	1.1 (8.75)
Oxidant (air)		26.3 (209)	<52.7 (< 418)
Coolant (air)		419 (3325)	365-548 (2900-4350)
CELL VOLTAGE	mV		
Open Circuit		920	< 1100
Operating Limit		800	
Operating Point		680	500-800
CELL CURRENT DENSITY	mA/cm^2 (A/ft^2)	325 (300)	< 400 (372)

subscale test specifications issued is given in Table 2-18. The purpose of the first group of tests was to: (1) verify process and fabrication reproducibility and the process control requirements, (2) establish comparative capabilities of electrodes with other vendor catalysts, (3) to determine the impact of some process variables and material sources, and (4) to meet the requirements stipulated in the technology development program.

Test specifications were defined and issued for nine cell stacks W009-08, -09, -10 and -11. Test article data and the test operations are listed in Tables 2-19 and 2-20. Revisions were issued for stacks W009-08, -09 and -11 to accommodate changes in the test plan. Test results and conclusions derived from these test plans from the experiments that had been conducted are presented in Section 3.0.

2.2.3 Fuel Cell Manufacturing Process Specifications

The Nine Cell Stack Subassembly Procedure (PAFC-006) and Final Assembly Procedure (PAFC-007) were modified for each stack fabricated during the report period. The modifications to the procedures were made to accommodate the design changes peculiar to each stack.

Disassembly procedures were prepared and utilized for stacks W-009-04 and W-009-10.

2.3 Systems Integration (WBS 1102-03)

2.3.1 Fuel Cell System Design (WBS 1102-03-100)

FUEL CELL SYSTEM PRELIMINARY DESIGN DESCRIPTION

The FCS (Figure 2-3) consists of groups of ten fuel cell modules supported in two rows of five together with their piping on an elevated platform. Two such ten-module groups are employed in a 7.5 MW plant. The fuel cell module design is described in Section 3.6. Each module has an overall height of approximately 3.5 m (11 ft 6 in.) and diameters of 1.4 m (4 ft 6 in.) over the

TABLE 2-18
SUBSCALE TEST SPECIFICATIONS ISSUED

Test Specification	Test Objective
TS 2 X 2-001	- Reproducibility (Fab, Ass'y & Test)
TS 2 X 2-002	- Five Manufacturing Variable Effects
TS 2 X 2-004	- Initial Baseline Electrode Characterization at Pressure
TS 2 X 2-005	- Initial Baseline Electrode Characterization
TS 2 X 2-006	- Screening of Alternate Vendor Catalyst
TS 2 X 2-007	- Alternate Backing Paper/Process Evaluation
TS 2 X 2-008	- Electrode Bonding and Sintering Assessment
TS 2 X 2-010	- 10 kW Stack Electrode Performance
TS 2 X 2-011	- Alternate Acid Transport Evaluation
TS 2 X 2-012	- Manufacturing Variables Evaluation, Catalyst and Backing Paper Wet Proofing
TS 2 X 2-013	- 10 kW Stack Electrode Quality Verification
TS 2 X 2-014	- Pressurized Endurance Demonstration
TS 2 X 2-015	- Screening of Manufacturing Variables
TS 2 X 2-016	- Non-Electrode Catalyst Poison/Contamination Assessment

TABLE 2-19
NINE CELL STACK TEST ARTICLE DATA

STACK ID W009	-06	-07	-08	-09	-10	-11
Cells 1 & 2	Baseline	Dry Laminated (900° HT Catalyst)	Baseline	------- Dry Laminated ---------- (900° HT Catalyst)		
Cells 3-7	Baseline	Baseline	Baseline	------- Dry Laminated ---------- (900° HT Catalyst)		
Cells 8 & 9	Baseline	Dry Laminated (900° HT Catalyst)	Baseline	------- Dry Laminated ---------- (900° HT Catalyst)		
MAT-1 Matrix	Yes	Yes	Yes	No	Yes	Yes
Bipolar Plates	Machined, 900° HT---------		Molded	A99 Regrind	Molded -------------	
Seals	Teflon ------------------		Viton	Viton	Viton	Viton
Acid	97% 50 ml	93% 46.5 ml	93% 42 ml*	98% 27 ml*	98% 45 ml*	98% 45 ml%
Load Instrument	No	Yes	No	No	No	Yes
Additional Tests	Start/Stop	Load Var.	Start/Stop	Start/Stop	Start/Stop	Load Var.

---

*Stack to be acid wicked at 130°F, dry room conditions for 3 to 7 days prior to testing.

TABLE 2-20
NINE CELL STACK TEST PLAN SEQUENCE(1)

PHASE I				PHASE II
STEP 1 ATMOSPHERIC TESTS	STEP 2 PRESSURIZE	STEP 3 STEADY STATE PRESSURIZED	STEP 4 MAPPING PRESSURIZED	ADDITIONAL OPTIONAL TEST(4)
< 50 Hrs	4 Hrs	500 Hrs	< 100 Hrs	500 Hrs
● Repeatability(2) ● Open Circuit Voltage ● Conditioning	● Startup to part power ● Up to full rated power condition ● Initiate SRG	● Polarization(3) ● Conditions 375°F 70 psia 40% air, 83% H_2 325 mA/cm^2	● 16 points ● Polarization @ end of mapping	● Shutdown ● Polarization ● Open Circuit Voltage ● Operational Transients - Endurance - Additional Mapping - Start/Stop Sequence Cycling - Other Development Options

Noted: (1) All full pressurized tests run with SRG except H_2 gain

(2) Verify measurements with stack installed and stack control repeatability within uncertainty required.

(3) Minimum of four points - H_2 utilization constant, oxidant flow rate held at four utilization levels each point from 25% to 60%.

(4) Continued operation for up to 500 hours on SRG and TBD options, transients (continuing development may extend these options).

ORIGINAL PAGE IS
OF POOR QUALITY

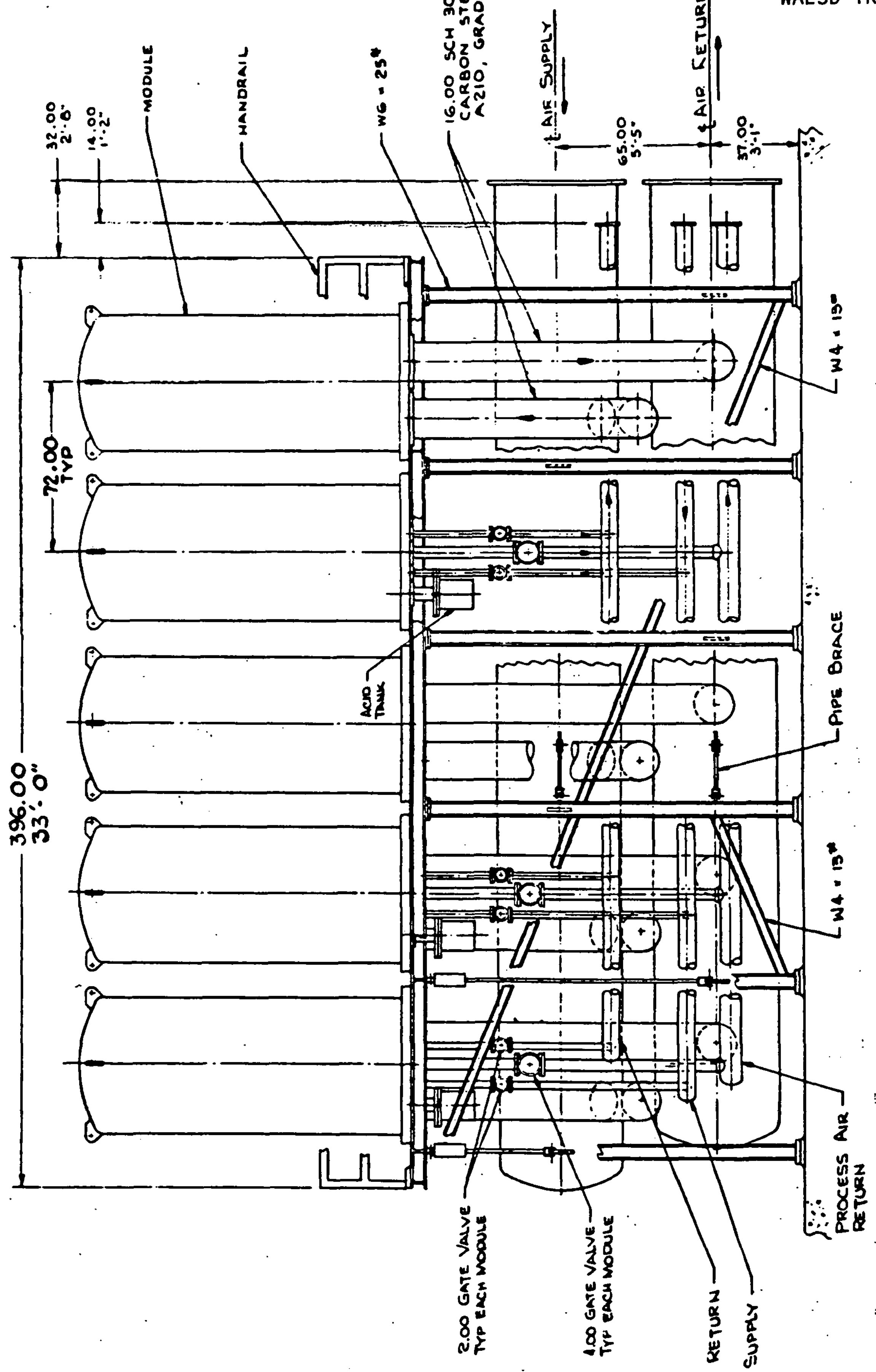

Figure 2-3. Fuel Cell System Preliminary Design

pressure vessel cylinder and 1.7 m (5 ft 6 in.) over its lower flange and support region. The weight of each module is approximately 5500 kg (6 tons).

Each of the fuel cell modules is designed to be truck transportable by common carrier. The module dimensions and weight are within the envelope permissible for truck transportation. The structural design of the modules is such that they can withstand the loads imposed by this type of transportation, as well as expected seismic loads. The module pressure vessels will be designed in accordance with Section VIII (Division 1) of the ASME Pressure Vessel Code.

Cooling and process air is supplied through a 1.2 m (4 ft) diameter pipe which traverses the length of the system immediately below the platform and midway between the two rows of modules. Air is extracted from this pipe and is supplied to each module through a short 40 cm (16 in.) diameter branch pipe. The cooling air, after traversing the module internals, is returned through another 40 cm (16 in.) line to a 1.2 m (4 ft) diameter air return line, supported immediately below the air supply line, midway between the rows of modules. A portion of the spent cooling air is extracted for use as process air internally to each module.

The 15 cm (6 in.) diameter fuel inlet and outlet lines are supported in two rows immediately below the outermost edges of the mounting platform. The fuel lines and the 20 cm (8 in.) diameter process air return lines, which are similarly supported, are connected to penetrations at the module pressure vessel lower head through lengths of small diameter piping. This piping is 5 cm (2 in.) diameter in the case of the fuel supply and return, and 10 cm (4 in.) diameter in the case of the process air return.

The symmetry of the piping arrangement provides for uniform distribution of fuel, cooling and process air between the modules comprising the FCS. The pipe sizes are selected so that the pressure drops through the fuel cell stacks dominate the flow resistances in the system, thus promoting equal flow distribution between modules as well as between the fuel cells within a module.

Shutoff valves are provided in all the fuel and process air connections to the modules to enable any of the modules to be shut down independently of the system. Valves are not provided in the 40 cm (16 in.) cooling air connecting lines to the modules so that continued operation of the fuel cell system with a module or modules shut down will therefore result in the continued circulation of cooling air through the shut down module or modules. The modules and their piping system and valves are completely encased in thermal insulation to reduce heat losses to acceptable levels.

Cable trays, located below the platform, support the electrical power leads and instrumentation lines between the modules and the PCS and ICS.

The overall height of the FCS is 8 m (25 ft). The overall length and width of the ten module assembly are approximately 10 m (33 ft) and 7 m (23 ft), respectively. The module support platform is approximately 4 m (14 ft) above foundation level. Foundation level must be located approximately 1.5 m (5 ft) below ground to provide for module handling using a permanent overhead crane and meet the 9.1 m (30 ft) height limitation of the crane.

The physical location of the FCS ten module groups in relation to the interfacing plant systems is suitably arranged so that the thermal expansion effects in the large 1.2 m (4 ft) diameter cooling air pipes can be accommodated by hinged bellows without overstressing the pipes in bending or exceeding limiting axial loads and movements at the FCS interfaces.

The smaller process gas piping is less constrained in this respect due to the substantially smaller diameters involved. However, some modification of the process gas piping geometry within the FCS is required to increase the bending flexibility of the vertical legs to accommodate thermal expansion of the horizontal piping.

2.3.1.1 Fuel Cell System Maintenance

Access is provided to the fuel cell modules from below for attention to electrical connections and acid replenishment systems. Access to the piping and shutoff valves below the ten module group is also available. Access is also provided from the sides of each ten module group and via an aisle between the two five module rows within each ten module group to facilitate removal of the pressure vessel flange bolts when fuel cell cartridges must be replaced.

Detailed maintenance requirements for all of the components of the FCS have not yet been defined. However, an initial assessment of the module maintenance requirements including acid replenishment and cartridge replacement, is included in Sections 3.6.4 and 3.6.5. As the FCS design matures and specific items of equipment are selected, such as valves, pipe hangers, instrumentation, etc., additional maintenance requirements may be identified.

2.3.1.2 Structural Analysis

A structural analysis of the entire fuel cell system piping and support structure was initiated using the finite element computer program ANSYS. Figure 2-4 illustrates a three-dimensional view of the entire FCS piping and support structure model containing over 1100 elements. The purpose of this analysis is to demonstrate that the stresses in the piping and support structure are within allowable limits or to recommend design changes to insure structural adequacy of all components. The allowable design stresses are based upon ANSI B31.1 (1980 edition) Power Piping Code and the ASME B&PV code, Section VIII (1983 edition), Division 1, Appendix G.

The finite element model includes all large and small pipes, support structure, and the module vessel baseplates. The weights of the vessels are included as mass elements acting at the center of the baseplates. The work platform and handrails were not included as structures; however, their weights were included. The bolted connection between each vessel base and the support beams was included. Specific details of this connection will be considered in the thermal stress analysis. Flexibility factors for the pipe elbows and stress intensification factors at the pipe connections are included based on the ANSI B31.1 Power Piping Code.

ORIGINAL PAGE IS
OF POOR QUALITY

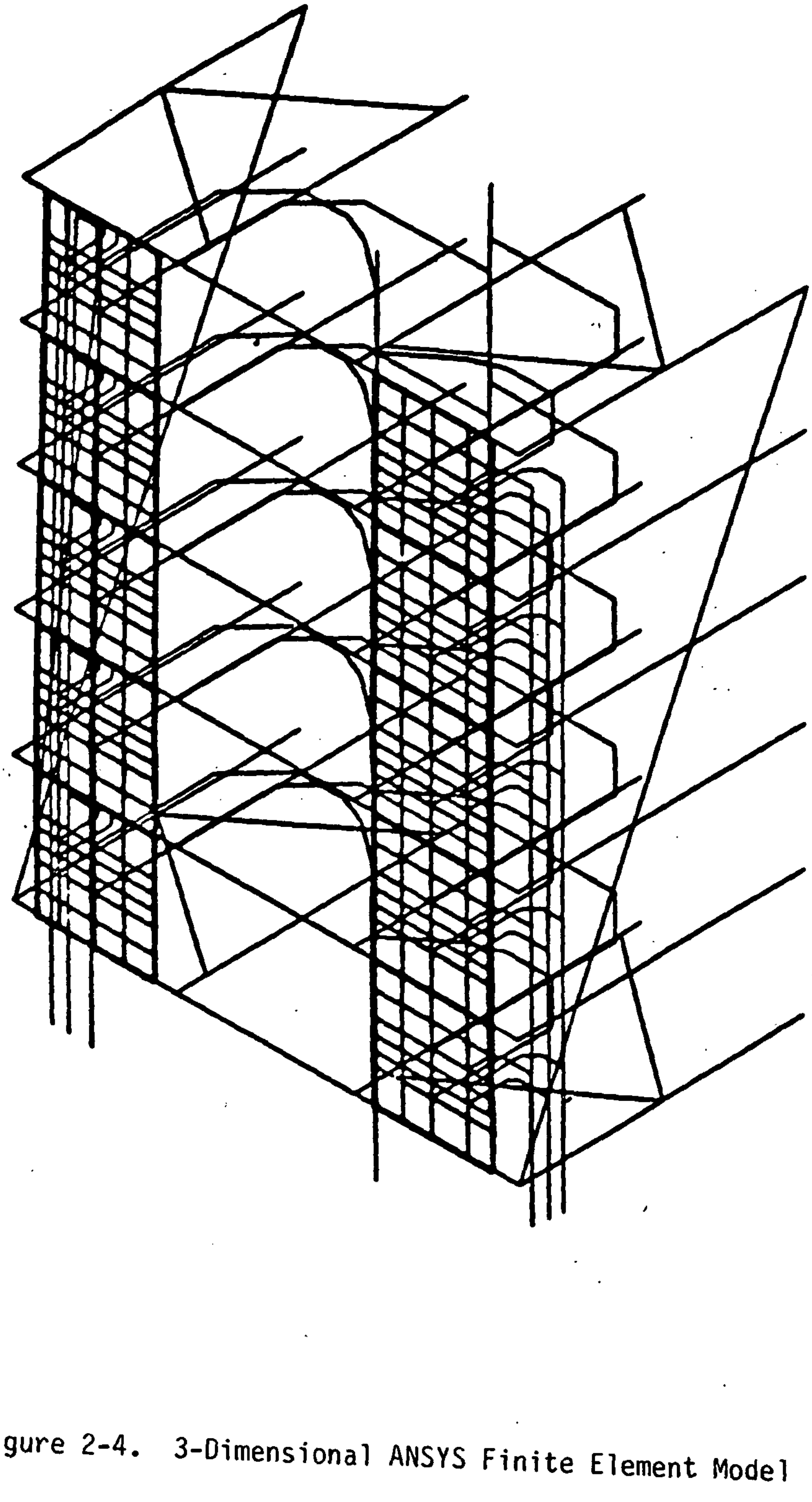

Figure 2-4. 3-Dimensional ANSYS Finite Element Model

The loading conditions considered in the analysis included dead weight, earthquake loads (1/2 g), thermal expansion (assuming a -29°C (-20°F) day based on EPRI TAG guidelines), and internal piping pressure. The frame columns are assumed to be rigidly connected to the concrete base.

This analysis effort is now in progress; however, no results or conclusions are available at this time.

2.3.2 Systems Interface Requirements and Control (WBS 1102-03-300)

This section presents the drawings which will be used to define and control the developmental systems interfaces. The Interface Control Drawings (ICDs) illustrate each system in simplified form and show the interfaces with other plant systems. These drawings were developed as part of a complete ICD package for each plant system which also contains information regarding each interface, foundations and supports requirements, electrical interface requirements, and measurements requirements. The ICD packages provide the means to identify and maintain control of all interfaces as needed throughout each system's design development. The developmental systems ICDs which are shown in Figures 2-5 through 2-9 are listed below.

System	Figure No.
FCS	2-5
FPS	2-6
RES	2-7
PCS	2-8
ICS	2-9

ORIGINAL PAGE IS
OF POOR QUALITY

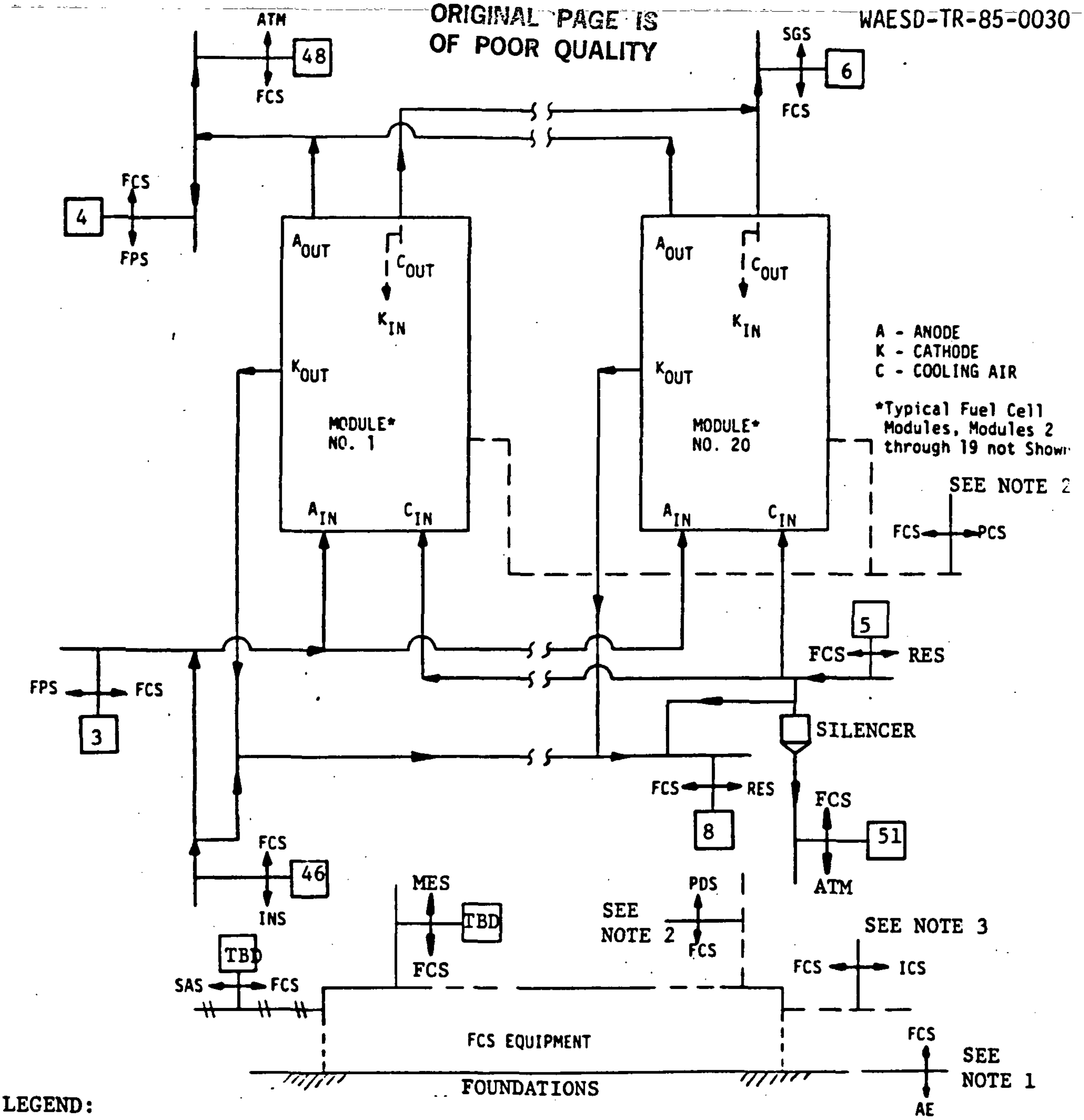

LEGEND:

xx - Plant Interface Number
FCS, PCS, etc. - System Acronyms
AE - Architect Engineer
ATM - Atmosphere

NOTES:
1. Equipment foundations and supports by AE
2. Electrical power interfaces with PDS and PCS
3. Electrical control interfaces with ICS

Figure 2-5. Fuel Cell System Interface Control Drawing

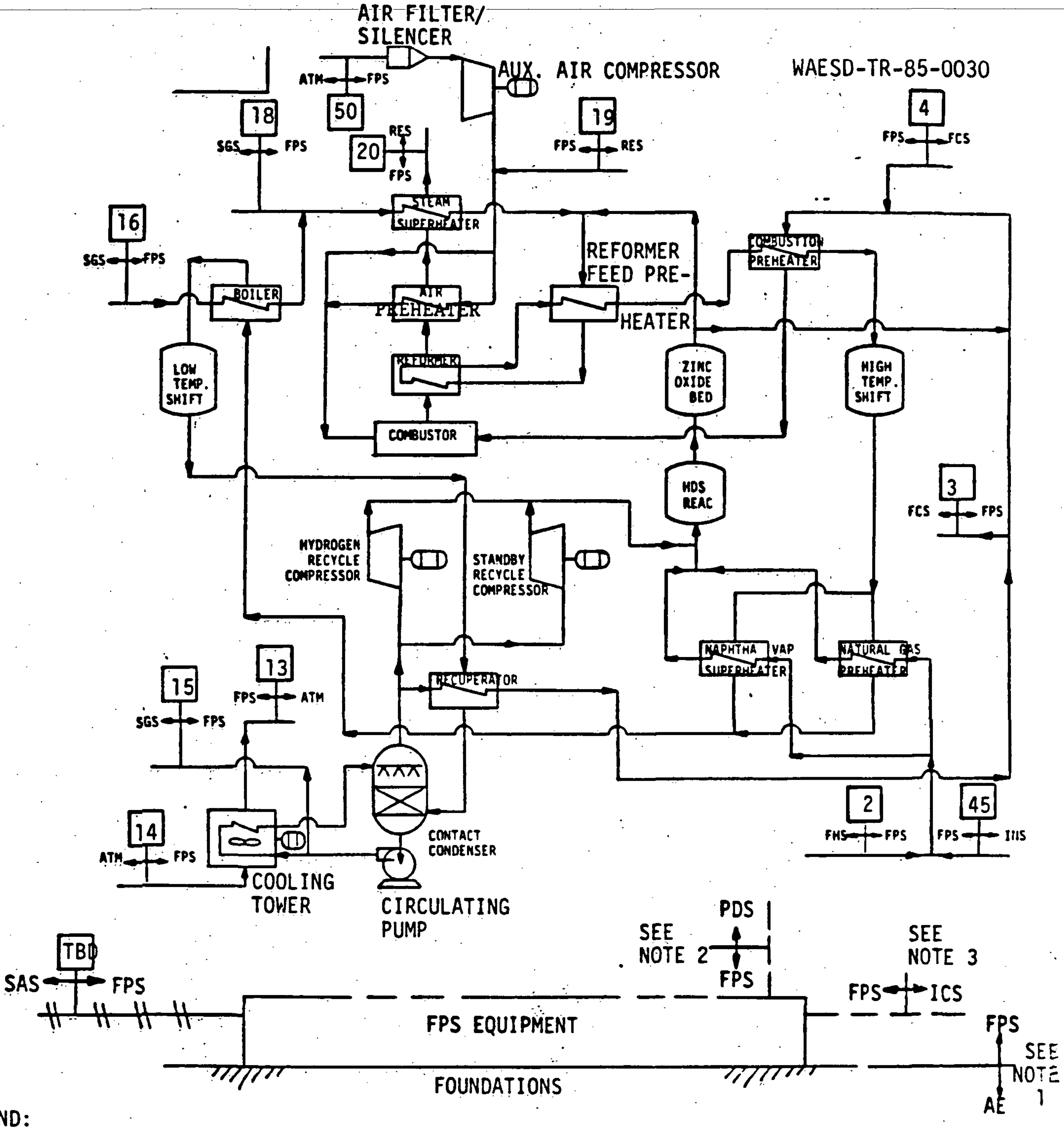

LEGEND:

xx - Plant Interface Number

FPS, RES, etc. - System Acronyms

AE - Architect Engineer

ATM - Atmosphere

NOTES:
1. Equipment foundations and supports by AE
2. Electrical power interfaces with PDS
3. Electrical control interfaces with ICS

Figure 2-6. Fuel Processing System Interface Control Drawing

ORIGINAL PAGE IS
OF POOR QUALITY

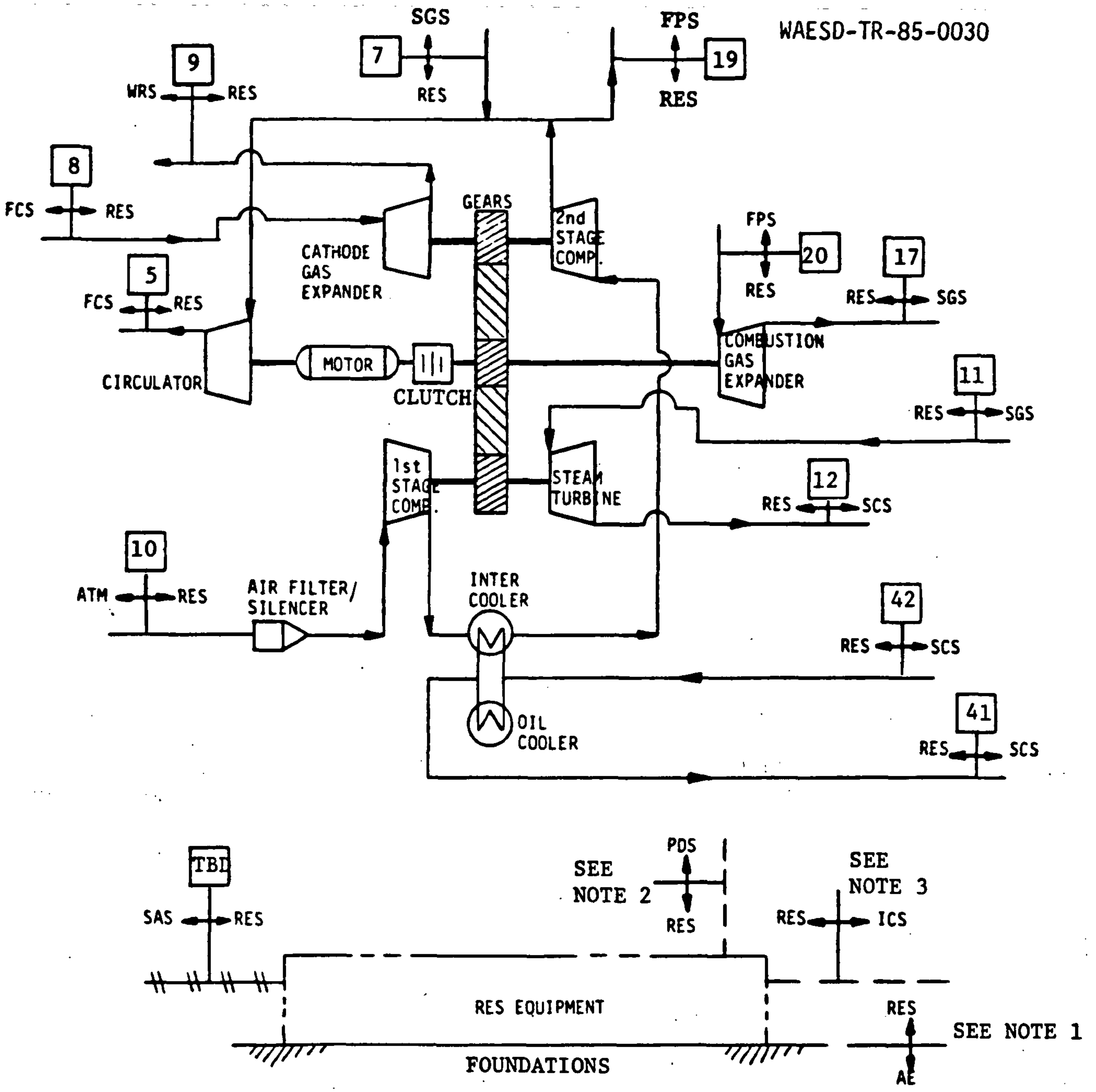

LEGEND:

xx - Plant Interface Number

RES, SGS, etc. - System Acronyms.

AE - Architect Engineer.

ATM - Atmosphere.

NOTES:
1. Equipment foundations and supports by AE
2. Electrical power interfaces with PDS
3. Electrical control interfaces with ICS

Figure 2-7. Rotating Equipment System Interface Control Drawing

LEGEND:

PCS, PDS, etc. - System Acronymns

AE - Architect Engineer

NOTES:

1. Equipment foundations and supports by AE
2. Electrical power interfaces with PDS, FCS and UES
3. Electrical control interfaces with ICS

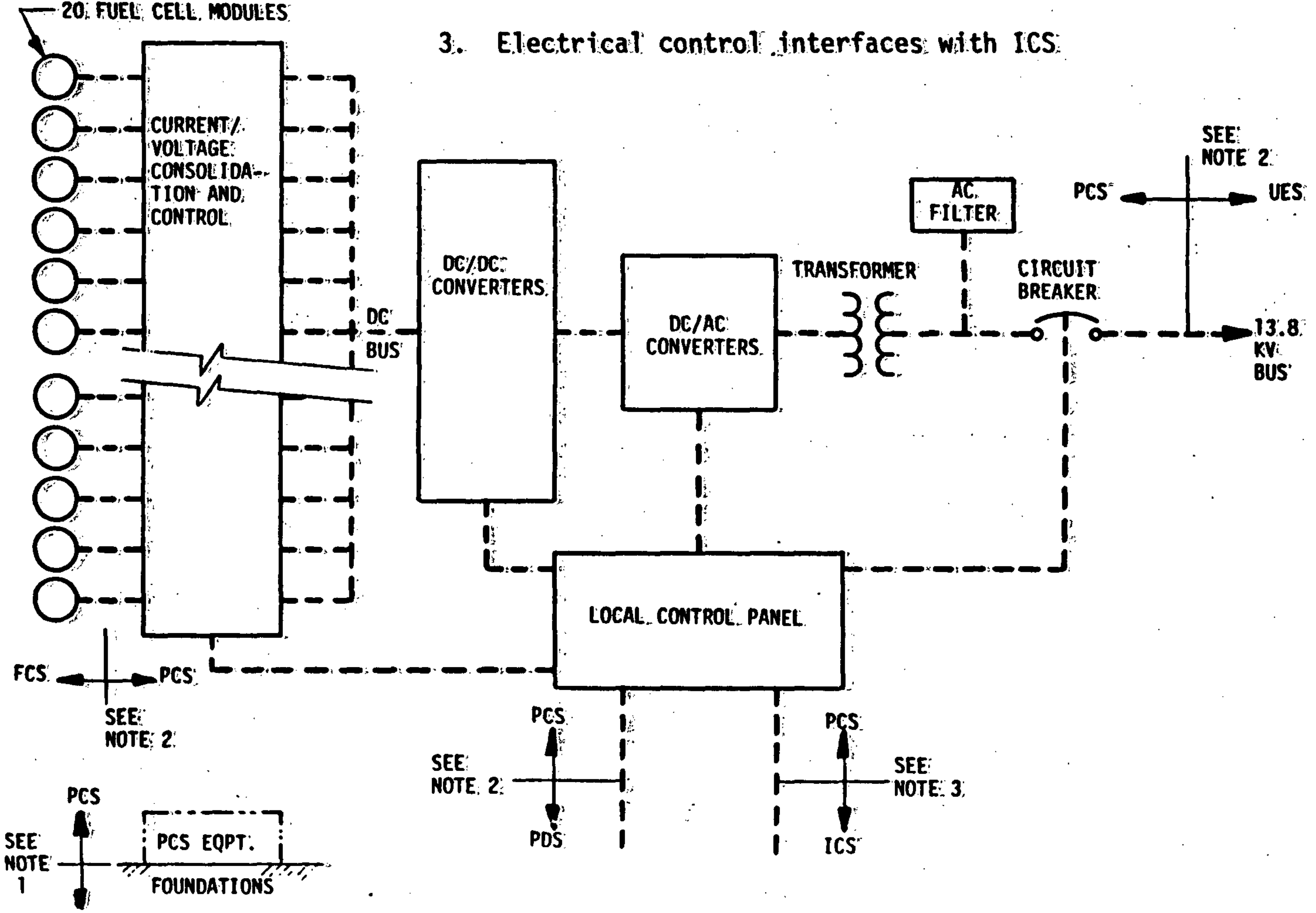

Figure 2-8. Power Conditioning System Interface Control Drawing

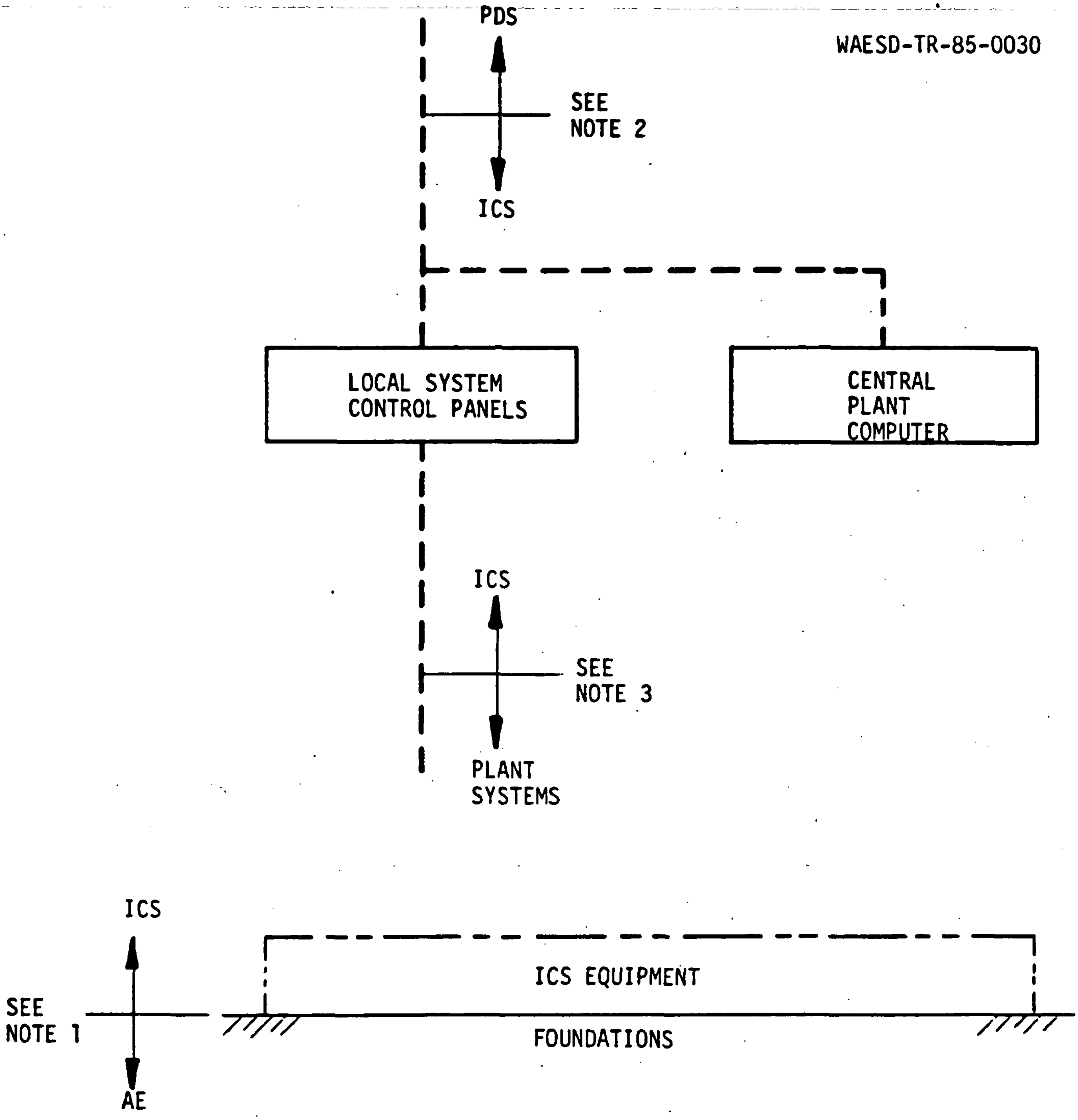

LEGEND:
ICS, PDS, etc. - System Acronyms
AE - Architect Engineer

NOTES:
1. Equipment foundations and supports by AE
2. Electrical power interfaces with PDS

3. See individual plant systems ICD's for interface requirements with ICS

Figure 2-9. Instrumentation and Control System Interface Control Drawing

3.0 FUEL CELL DEVELOPMENT AND TEST (WBS 1103)

3.1 Subscale Fuel Cell Development (WBS 1103-01)

3.1.1 Design and Assembly Status

The principal subscale design and assembly procedure utilized was that developed during the First Logical Unit of Work. Gasket requirements were revised to accommodate cells assembled without MAT-1 matrix material as well as cells with alternate matrix material.

A metal end plate design was evaluated to provide suitable end plates for pressurized endurance testing of up to 5,000 hours. Gold plating of tantalum was considered but since a reliable plating process was not readily available, it was concluded that gold plated nickel 200 would be evaluated. To select the gold plating process for the nickel 200 design, four simplified end plates with various types of gold plating were corrosion tested by immersion in 97 w/o H_3PO_4 at 190°C (374°F), 485 kPa (4.8 atms.), with no applied potential for over 100 hours. Following visual examination, three types of coating were subjected to a second pressurized, 485 kPa (4.8 atm.), corrosion test for an additional 500 hours. The gold plating selected was a combination of 5 microns (.2 mils) of gold applied by electroplating. Five cells were assembled utilizing gold plated hardware and tested, four at pressure and one unpressurized. The gold plating failed during cell operation.

Work was initiated on heat treating sections of subscale 900°C (1650°F) heat treated carbon end plates to 2700°C (4950°F). Based on the success of this work on high temperature heat treatment of carbon end plates and the relatively poor performance of cells built with gold plated nickel 200 plates, it was concluded that the effort would be concentrated on procuring 2700°C (4950°F) heat treated carbon end plates for pressurized endurance evaluation of baseline and alternate catalysts.

A design revision was completed and drawings prepared for a subscale cell using heat treated carbon end plates that can accommodate a variety of matrices. The matrix size was increased to the cathode size and is now larger than the anode, making the subscale configuration similar to the stack configuration. Anode and cathode gasket widths were modified to provide a 0.25 cm (0.10 in.) overlap between the anode gasket and the matrix or between the anode gasket and the cathode if a matrix is not used. This overlap should decrease the possibility of cell cross leakage in this area. Teflon gaskets (of different thicknesses) are included to facilitate disassembly of the cell after testing and to provide capability to adjust for variation in electrode and gasket thickness. The design provides for a nominal 12 percent electrode compression coupled with a 15 - 20 percent elastomer seal compressive strain range.

3.1.2 Subscale Testing

A total of 160 cells, unpressurized and pressurized, were assembled and tested at Westinghouse. With the exception of five cells, all the testing was based on test plans, and the status of these test plans and cells built is provided in Table 3-1.

An additional sixty-nine subscale fuel cells were assembled and tested during this period. Testing of eleven subscale cells assembled during the first logical unit of work was also conducted. These cells were tested to address various areas of work (Table 3-2) as identified in the performance improvement work plan developed by Westinghouse and ERC to achieve the power plant performance goals. Table 3-3 summarizes the test data. Specific test objectives and results for these cells are discussed under relevant subsections of Task 1103-08.

The overall objectives of the various test plans are:

- To establish the baseline technology with existing ERC/W design/processes.

TABLE 3-1

CELLS TESTED UNDER VARIOUS TEST PLANS

Test Specification	Cells Built and Tested
TS 2X2-002, Rev. 0	CAS-001 through -016, -001-S1, 005-S1
TS 2X2-002, Revs. 1 and 2	CAS-061 through -072, CAS-112 through -115
TS 2X2-004, Rev. 2 and 4	CPS-017 through -024, CPS-018-S1, -020-S1, -021-S1, -023-S1, -023-S2, CPS-045 through -047
TS 2X2-004, Rev. 3	CPS-026, CPS-028, -029, CPS-031
TS 2X2-005, Revs. 2 and 3	CAS-017, -023, -090, -091, -096 -097
TS 2X2-006, Rev. 0	CAS-026 through -039
TS 2X2-006, Rev. 1	CAS-047 through -049, CAS-051 through -060, CAS-100 through -106, CAS-108
TS 2X2-007, Revs. 0 and 1	CAS-040 through -045, CAS-073 through -076
TS 2X2-008, Rev. 0	DAS-001 through -010
TS 2X2-010, Rev. 0	QAS-001, -002, -015, -016, -019 through -024, DAS-047, -048
TS 2X2-013, Revs. 0, 1, 2, 3 and 4	QAS-006 through -009, QAS-009-S1, QAS-016 through -020, QAS-019-S1, QAS-019-S2, QAS-025 through -027, QAS-009 through -020
TS 2X2-014, Rev. 0 and 1	CPS-033 through -036
TS 2X2-016	CAS-116 through -121

TABLE 3-2

SUMMARY OF SUBSCALE CELLS TESTED

Test Purpose	Number of Cells Tested	Task 1103-08 Reference Section
Alternate Catalyst	19	1.1
Alternate Catalyst Support	7	1.2
Electrode Manufacturing	14	1.3
Cell Resistance	10	1.4
Plate Corrosion	9	1.5
Quality Control	6	1.8
Miscellaneous	15	-
Total	80	

ORIGINAL PAGE IS
OF POOR QUALITY

TABLE 3-3
SUMMARY OF SUBSCALE TEST DATA

ATMOSPHERIC TESTS

TEST CONDITIONS (UNLESS OTHERWISE NOTED)

TEMPERATURE : 190 C
PRESSURE : 1 ATM.
CURRENT DENSITY : 200 MA/CM2
FUEL : H2, 83% UTILIZATION
OXIDANT : AIR, 25% UTILIZATION

CELL NO.	INITIAL PERFORMANCE			PEAK PERFORMANCE			PRESENT PERFORMANCE			CATHODE			ANODE			CELL MATRIX	TEST SPEC	TEST OBJECTIVE	TEST TERMINATION DATE
	OCV	MV	IR	HOURS	MV	IR	HOURS	MV	IR	CATA.	BOND.	SINT.	CATA.	BOND.	SINT.				
3009	928	643	5.7	552	643	6.1	11,064	620	7.5	H.T.PT	DRY	AIR	PT	WET	AIR	MAT-1		ENDURANCE TEST OF H.T. PT CATALYST	
3020	919	628	6.3	264	655	6.0	840	647	6.0	H.T.PT	WET	AIR	PT	WET	AIR	MAT-1		ENDURANCE TEST OF H.T. PT CATALYST	05/20/83
3029	867	647	5.7	240	677	5.6	4,968	618	10.7	H.T.PT	WET	AIR	PT	WET	AIR	SIC		ENDURANCE TEST OF H.T. PT CATALYST	11/15/83
3030	931	607	8.0	144	625	7.8	2,136	613	8.8	PT	DRY	STEAM	PT	WET	AIR	SIC		EVALUATION OF SHAWINIGAN CATALYST SUPPORT	09/19/83
3031	923	574	7.7	120	629	6.8	2,112	621	7.0	PT	DRY	STEAM	PT	WET	AIR	SIC		EVALUATION OF SHAWINIGAN CATALYST SUPPORT	09/19/83
3032	831	641	7.4	96	660	7.8	1,344	646	7.8	PT/CR	WET	AIR	PT	WET	AIR	SIC		EVALUATION OF PT/CR CATALYST	08/22/83
3033	933	622	7.5	24	664	7.6	1,272	644	8.4	PT/CR	WET	AIR	PT	WET	AIR	SIC		EVALUATION OF PT/CR CATALYST	08/22/83
3034	838	596	3.7	120	672	3.8	4,896	605	6.8	H.T.PT	DRY	STEAM	PT	WET	AIR	MAT-1		EVALUATION OF THIN (3 MIL) SIC LAYER	01/10/84
3035	862	647	5.3	744	661	5.0	5,160	634	4.7	H.T.PT	DRY	STEAM	PT	WET	AIR	MAT-1		EVALUATION OF THIN (3 MIL) SIC LAYER	02/01/84
3036	889	614	5.0	648	671	4.5	1,680	666	4.0	H.T.PT	DRY	STEAM	PT	WET	AIR	MAT-1		EVALUATION OF THIN (3 MIL) SIC LAYER	09/13/83
3037	965	622	6.9	432	641	6.3	2,040	576	6.3	PT	DRY	STEAM	PT	WET	AIR	MAT-1		EVALUATION OF SHAWINIGAN CATALYST SUPPORT	10/07/83
3038	920	608	6.5	1,512	643	5.0	7,584	630	4.9	PT	DRY	STEAM	PT	WET	AIR	MAT-1		ENDURANCE TEST OF SHAWINIGAN CATALYST SUPPORT	
3039	920	614	9.0	1,464	640	8.9	1,464	640	8.9	H.T.PT	DRY	STEAM	PT	WET	AIR	SIC		EVALUATION OF WESTINGHOUSE CATHODE	11/15/83
3040	897	598	12.5	600	620	11.7	1,464	614	12.0	H.T.PT	DRY	STEAM	PT	WET	AIR	SIC		EVALUATION OF WESTINGHOUSE CATHODE	11/15/83
3041	905	630	8.1	456	654	7.7	3,288	633	8.1	H.T.PT	DRY	STEAM	PT	WET	AIR	SIC		EVALUATION OF WESTINGHOUSE CATHODE	02/05/84
3042	745	624	3.5	96	638	3.5	120	638	3.5	H.T.PT	DRY	STEAM	PT	WET	AIR	SIC		EVALUATION OF PTFE GASKETS	10/31/83
3043	840	632	4.8	120	662	3.6	120	662	3.6	H.T.PT	DRY	STEAM	PT	WET	AIR	SIC		EVALUATION OF PTFE GASKETS	11/09/83
3044	915	659	4.9	744	679	5.0	3,480	665	5.4	H.T.PT	WET	AIR	PT	WET	AIR	SIC		EVALUATION OF PTFE GASKET/WESTINGHOUSE HARDWARE	04/08/84
3045	900	602	4.7	1,656	665	4.5	2,952	626	4.5	H.T.PT	WET	AIR	PT	WET	AIR	MAT-1		EVALUATION OF PTFE GASKET/WESTINGHOUSE HARDWARE	04/04/84
3046	749	636	5.6	0	636	5.6	1,536	525	9.8	H.T.PT	WET	AIR	PT	WET	AIR	SIC			
3047	810	577	7.6	216	671	5.7	672	605	6.1	H.T.PT	WET	AIR	PT	WET	AIR	SIC		EVALUATION OF VITON GASKET/WESTINGHOUSE HARDWARE	03/20/84
3048	853	626	5.9	216	653	5.6	672	648	6.0	H.T.PT	WET	AIR	PT	WET	AIR	MAT-1		EVALUATION OF VITON GASKET/WESTINGHOUSE HARDWARE	03/20/84
3049	860	582	10.5	888	651	8.1	1,224	634	7.9	H.T.PT	DRY	AR	PT	WET	AR	MAT-1		EVALUATION OF START-UP PROCEDURE	
3050	860	626	5.9	404	665	6.1	404	665	6.1	H.T.PT	DRY	AR	PT	WET	AR	MAT-1		EVALUATION OF 2700 C HEAT-TREATED PLATES	
QC01	925	631	6.6	120	638	6.8	1,153	633	6.3	PT	WET	AIR	PT	WET	AIR	MAT-1		QUALITY CONTROL FOR STACK E-009-02	01/10/84
QC02	925	635	6.6	0	635	6.6	1,032	398	6.8	PT	WET	AIR	PT	WET	AIR	MAT-1		QUALITY CONTROL FOR STACK E-009-02	01/05/84
QC03	920	627	8.0	96	634	8.0	1,032	620	9.2	PT	WET	AIR	PT	WET	AIR	SIC		QUALITY CONTROL FOR STACK E-009-02	01/19/84
QC04	925	635	7.8	96	644	7.8	1,032	631	8.9	PT	WET	AIR	PT	WET	AIR	SIC		QUALITY CONTROL FOR STACK E-009-02	01/19/84
MF01P	875	596	6.8	312	625	7.0	1,032	599	7.7	H.T.PT	DRY	CO2	PT	WET	AIR	SIC	E-006	EVALUATION OF MANUFACTURING VARIABLES	02/01/84
MF02P	920	620	6.6	360	638	7.0	1,032	608	7.7	H.T.PT	DRY	N2	PT	WET	AIR	SIC	E-006	EVALUATION OF MANUFACTURING VARIABLES	02/01/84
MF03P	920	609	6.9	480	631	8.0	1,032	606	9.6	H.T.PT	DRY	AR	PT	WET	AIR	SIC	E-006	EVALUATION OF MANUFACTURING VARIABLES	02/01/84
MF04P	865	642	5.8	0	642	5.8	384	413	7.0	H.T.PT	DRY	STEAM	PT	WET	AIR	SIC	E-006	EVALUATION OF MANUFACTURING VARIABLES	01/05/84
MF05S	930	660	7.2	408	671	7.6	1,728	638	8.2	H.T.PT	DRY	AR	PT	WET	AIR	SIC	E-006	EVALUATION OF MANUFACTURING VARIABLES	04/05/84
MF06S	925	629	7.0	576	659	7.0	1,752	645	7.7	H.T.PT	DRY	AR	PT	WET	AIR	MAT-1	E-006	EVALUATION OF MANUFACTURING VARIABLES	04/06/84
PC01	930	668	3.6	264	676	3.7	624	670	3.8	H.T.PT	DRY	AR	PT	WET	AIR	MAT-1	E-001	EVALUATION OF PLATE CORROSION	11/07/83
PC02	940	668	4.1	240	671	4.2	600	646	4.8	H.T.PT	DRY	AR	PT	WET	AIR	MAT-1	E-001	EVALUATION OF PLATE CORROSION	11/08/83
PC03	925	654	4.7	264	660	5.0	600	650	5.1	H.T.PT	DRY	AR	PT	WET	AIR	MAT-1	E-001	EVALUATION OF PLATE CORROSION	11/14/83
PC04	905	623	4.0	432	670	4.0	600	668	4.0	H.T.PT	DRY	AR	PT	WET	AIR	MAT-1	E-001	EVALUATION OF PLATE CORROSION	11/14/83
PC05	907	628	5.1	240	650	5.3	600	614	8.0	H.T.PT	DRY	AR	PT	WET	AIR	MAT-1	E-001	EVALUATION OF PLATE CORROSION	11/15/83
PC06	915	638	4.2	312	669	4.4	336	669	4.4	H.T.PT	DRY	AR	PT	WET	AIR	MAT-1	E-001	EVALUATION OF PLATE CORROSION	11/04/83
PC07	940	643	7.2	336	659	7.5	552	651	7.7	H.T.PT	DRY	AR	PT	WET	AIR	MAT-1	E-001	EVALUATION OF PLATE CORROSION	02/22/84
PC08	920	607	9.6	0	607	9.6	576	508	10.7	H.T.PT	DRY	AR	PT	WET	AIR	MAT-1	E-001	EVALUATION OF PLATE CORROSION	04/19/84
AS02	900	634	8.4	576	654	7.0	2,088	647	7.0	H.T.PT	DRY	AR	PT	WET	AR	SIC	E-002	EVALUATION OF ALTERNATE CATALYST SUPPORTS	05/06/84
AS05	915	595	7.8	360	623	7.0	528	614	7.2	H.T.PT	DRY	AR	PT	WET	AR	SIC	E-002	EVALUATION OF ALTERNATE CATALYST SUPPORTS	02/24/84
AS06	902	622	9.0	1,200	637	8.5	2,088	634	8.7	H.T.PT	DRY	AR	PT	WET	AR	SIC	E-002	EVALUATION OF ALTERNATE CATALYST SUPPORTS	05/06/84
AS08	743	644	7.0	240	648	6.2	1,152	579	7.7	H.T.PT	DRY	AR	PT	WET	AR	SIC	E-002	EVALUATION OF ALTERNATE CATALYST SUPPORTS	03/27/84
AS09	---	---	---	---	---	---	360	280	15.5	H.T.PT	DRY	AR	PT	WET	AR	SIC	E-002	EVALUATION OF ALTERNATE CATALYST SUPPORTS	02/24/84
AS17	---	---	---	---	---	---	360	423	13.0	H.T.PT	DRY	AR	PT	WET	AR	SIC	E-002	EVALUATION OF ALTERNATE CATALYST SUPPORTS	02/24/84

ORIGINAL PAGE IS
OF POOR QUALITY

TABLE 3-3
SUMMARY OF SUBSCALE TEST DATA (CONT'D)

MF01	925	670	7.1	408	677	7.2	1,920	654	7.7	H.T.PT	DRY	CO2	PT	WET	AR	SIC	E-006	EVALUATION OF MANUFACTURING VARIABLES	
MF02	872	650	8.4	129	654	8.3	1,920	635	12.2	H.T.PT	DRY	N2	PT	WET	AR	SIC	E-006	EVALUATION OF MANUFACTURING VARIABLES	
MF03	930	657	8.8	744	662	9.4	1,920	645	10.4	H.T.PT	DRY	AR	PT	WET	AR	SIC	E-006	EVALUATION OF MANUFACTURING VARIABLES	
MF04	925	660	8.5	0	660	8.5	696	481	10.5	H.T.PT	DRY	STEAM	PT	WET	AR	SIC	E-006	EVALUATION OF MANUFACTURING VARIABLES	04/04/84
MF05	925	665	6.4	285	680	6.7	789	680	6.7	H.T.PT	DRY	AR	PT	WET	AR	SIC	E-006	EVALUATION OF MANUFACTURING VARIABLES	
MF06	915	642	7.0	408	664	7.3	576	629	7.3	H.T.PT	DRY	AR	PT	WET	AR	SIC	E-006	EVALUATION OF MANUFACTURING VARIABLES	
MF07	925	650	6.6	621	677	6.7	789	676	6.7	H.T.PT	DRY	AR	PT	WET	AR	SIC	E-006	EVALUATION OF MANUFACTURING VARIABLES	
MF08	880	666	6.5	621	681	6.5	789	679	6.6	H.T.PT	DRY	AR	PT	WET	AR	SIC	E-006	EVALUATION OF MANUFACTURING VARIABLES	
S101	965	684	5.3	0	684	5.3	1,608	585	6.0	DC-05	WET	AIR	PT	WET	AR	SIC	E-008	EVALUATION OF DEVELOPMENTAL CATALYSIS STRESS TEST	
S102	965	674	6.2	0	674	6.2	1,608	650	7.3	DC-05	WET	AIR	PT	WET	AR	SIC	E-008	EVALUATION OF DEVELOPMENTAL CATALYSIS STRESS TEST	
S103	950	685	7.0	0	685	7.0	1,608	576	11.2	DC-06	WET	AIR	PT	WET	AR	SIC	E-008	EVALUATION OF DEVELOPMENTAL CATALYSIS STRESS TEST	
S104	950	700	5.7	744	703	6.1	1,608	693	6.4	DC-06	WET	AIR	PT	WET	AR	SIC	E-008	EVALUATION OF DEVELOPMENTAL CATALYSIS STRESS TEST	
S105	935	623	8.0	432	634	10.5	1,608	591	12.5	H.T.PT	DRY	AR	PT	WET	AR	SIC	E-008	EVALUATION OF DEVELOPMENTAL CATALYSIS STRESS TEST	
S106	925	617	8.0	600	638	8.5	1,608	627	9.0	H.T.PT	DRY	AR	PT	WET	AR	SIC	E-008	EVALUATION OF DEVELOPMENTAL CATALYSIS STRESS TEST	
TH01	790	660	3.4	908	678	3.5	1,076	677	3.5	H.T.PT	DRY	AR	PT	WET	AR	MAT-1	E-003	EVALUATION OF THIN MATRIX LAYERS	
TH02	790	675	3.8	644	686	4.0	1,076	680	4.0	H.T.PT	DRY	AR	PT	WET	AR	MAT-1	E-003	EVALUATION OF THIN MATRIX LAYERS	
TH03	835	668	4.7	212	674	4.7	1,076	672	4.7	H.T.PT	DRY	AR	PT	WET	AR	MAT-1	E-003	EVALUATION OF THIN MATRIX LAYERS	
TH04	790	642	6.1	404	659	6.0	1,076	657	6.1	H.T.PT	DRY	AR	PT	WET	AR	MAT-1	E-003	EVALUATION OF THIN MATRIX LAYERS	
TH05	800	679	3.3	68	687	3.3	1,076	676	4.0	H.T.PT	DRY	AR	PT	WET	AR	SIC	E-003	EVALUATION OF THIN MATRIX LAYERS	
TH06	860	670	6.0	740	681	6.1	1,076	679	6.0	H.T.PT	DRY	AR	PT	WET	AR	SIC	E-003	EVALUATION OF THIN MATRIX LAYERS	
ECPS05	940	672	7.6	0	672	7.6	19	650	7.6	DC-05	WET	AIR	DC-03	WET	AIR	MAT-1	E-008A	ELECTRODE ENDURANCE VERIFICATION	
ECPS06	900	667	8.6	0	667	8.6	19	667	8.6	DC-06	WET	AIR	DC-03	WET	AIR	MAT-1	E-008A	ELECTRODE ENDURANCE VERIFICATION	
ECPS07	920	672	8.4	0	672	8.4	19	667	8.4	DC-06	WET	AIR	DC-03	WET	AIR	MAT-1	E-008A	ELECTRODE ENDURANCE VERIFICATION	
ECPS08	932	629	8.0	19	630	8.0	19	630	8.0	H.T.PT	DRY	AR	PT	WET	AR	MAT-1	E-008A	ELECTRODE ENDURANCE VERIFICATION	
CAS92	930	655	6.2	96	659	6.2	96	659	6.2	H.T.PT	DRY	AR	PT	DRY	AR	MAT-1	W-005	BASELINE PERFORMANCE & FACILITY COMPARISON	
CAS93	905	635	7.5	96	639	7.5	96	639	7.5	H.T.PT	DRY	AR	PT	DRY	AR	SIC	W-005	BASELINE PERFORMANCE & FACILITY COMPARISON	
CAS94	930	660	5.5	72	663	5.4	96	663	5.4	H.T.PT	DRY	AR	PT	DRY	AR	MAT-1	W-005	BASELINE PERFORMANCE & FACILITY COMPARISON	
CAS95	925	651	7.2	46	652	7.7	96	652	7.7	H.T.PT	DRY	AR	PT	DRY	AR	SIC	W-005	BASELINE PERFORMANCE & FACILITY COMPARISON	

PRESSURIZED TESTS

TEST CONDITIONS (UNLESS OTHERWISE NOTED)

TEMPERATURE : 190 C
PRESSURE : 4.8 ATM.
CURRENT DENSITY : 325 MA/CM2
FUEL : H2, 83% UTILIZATION
OXIDANT :AIR, 50% UTILIZATION

ECPS01	1000	674	6.4	121	684	5.9	121	684	5.9	DC-05	WET	AIR	DC-03	WET	AIR	SIC	E-008A	ELECTRODE ENDURANCE VERIFICATION PRESSURE TEST	02/28/84
ECPS02	990	678	8.1	0	678	8.1	121	653	8.0	DC-06	WET	AIR	DC-03	WET	AIR	SIC	E-008A	ELECTRODE ENDURANCE VERIFICATION PRESSURE TEST	02/28/84
ECPS03	980	641	12.9	0	641	12.9	121	627	13.0	DC-06	WET	AIR	DC-03	WET	AIR	SIC	E-008A	ELECTRODE ENDURANCE VERIFICATION PRESSURE TEST	02/28/84
ECPS04	990	629	12.0	0	629	12.0	121	594	12.5	H.T.PT	DRY	AR	PT	WET	AIR	SIC	E-008A	ELECTRODE ENDURANCE VERIFICATION PRESSURE TEST	02/28/84
ECPS05	---	693	6.7	0	693	6.7	1,757	652	7.0	DC-05	WET	AIR	DC-03	WET	AIR	MAT-1	E-008A	ELECTRODE ENDURANCE VERIFICATION PRESSURE TEST	
ECPS06	---	697	7.6	0	697	7.6	1,757	650	9.7	DC-06	WET	AIR	DC-03	WET	AIR	MAT-1	E-008A	ELECTRODE ENDURANCE VERIFICATION PRESSURE TEST	
ECPS07	---	696	8.0	0	696	8.0	1,757	657	9.7	DC-06	WET	AIR	DC-03	WET	AIR	MAT-1	E-008A	ELECTRODE ENDURANCE VERIFICATION PRESSURE TEST	
ECPS08	---	667	7.5	23	669	7.5	1,757	650	10.1	H.T.PT	DRY	AR	PT	WET	AIR	MAT-1	E-008A	ELECTRODE ENDURANCE VERIFICATION PRESSURE TEST	

- To provide a base for stack scaling, and
- To determine the effects of principal parameters in order to develop predictive correlations for performance scaling.

Table 3-4 shows the objectives and status of the various test plans.

3.1.2.1 Objectives and Results of Various Test Plans

TS 2X2-002, Rev. 0, 1, 2

The goal of this test plan is to determine the effect of the following parameters on electrode/cell performance.

- Two different shipments/lots of catalyst.
- Catalyst heat treatment/nonheat treatment.
- Two different heat treatment lots.
- Catalyst loading on cathode.
- Wet and dry bonding of catalyst layer to the substrate.
- Two different SiC lots.
- Thin, < 125 microns (< 5 mils), and thick SiC layers.
- SiC material Polyox 1 and Polyox 2.

Table 3-5 shows the performance and status of the cells built in this test plan with the cell voltages (terminal) reported at 200 mA/cm^2 (186 A/ft^2), 101 kPa (1 atm), 190°C (374°F), 80 percent hydrogen utilization and 20 percent air utilization.

TABLE 3-4
SUBSCALE TESTING STATUS

Test Specification		Test Results	Test Objective
TS 2X2-001	Rev. 0	Complete	Reproducibility (fabrication, assembly and test)
TS 2X2-002	Rev. 0	Complete	Five manufacturing variable effects
	Rev. 1	Retest needed	Addition of four variables
	Rev. 2	Retest needed	Replacement of inappropriate cells
TS 2X2-004	Rev. 0	Reformatted as Rev. 2	Initial baseline electrode characterization at pressure
	Rev. 2	Terminated (updated)	Rev. 0 in new format and 10 kW stack electrodes
	Rev. 3	Ongoing	Update to use new baseline electrodes
	Rev. 4	Ongoing	Additional tests required by facility problems
TS 2X2-005	Rev. 0	Reformatted as Rev. 2	Initial baseline electrode characterization
	Rev. 2	Cancelled (updated)	Rev. 0 reformattted
	Rev. 3	Ongoing	Update to use new baseline electrodes
TS 2X2-006	Rev. 0	Completed	Screening of alternate vendor catalyst
	Rev. 1	Ongoing	Addition of other catalyst and electrodes
	Rev. 2	Ongoing	Addition of other catalyst and elecrodes
	Rev. 3	Scheduled	Addition of other catalyst and electrodes
TS 2X2-007	Rev. 0	Completed	Alternate backing paper/process evaluation
	Rev. 1	Completed	Extension to screen a production wetproofing process
TS 2X2-008	Rev. 0	Completed	Electrode bonding and sintering assessment
TS 2X2-010	Rev. 0	Cancelled	10 kW stack electrode performance
TS 2X2-011	Rev. 0	Ongoing	Alternate acid transport evaluation
	Rev. 1	Scheduled	Addition of cells for Kureha 604 alternate
	Rev. 2	Scheduled	Addition of cells for 4-1/2% Teflon-MAT-1
TS 2X2-012	Rev. 0	Scheduled	Manufacturing variables evaluation, catalyst and backing paper wetproofing

TABLE 3-4
SUBSCALE TESTING STATUS (CONT'D)

Test Specification		Test Results	Test Objective
TS 2X2-013	Rev. 0	Completed	10 kW stack electrode quality verification
	Rev. 1	Ongoing	Additional batch quality verification
	Rev. 2	Ongoing	Additional batch quality verification
	Rev. 3	Ongoing	Additional batch quality verification
	Rev. 4	Scheduled	Additional tests to qualify pressurized endurance cells
TS 2X2-014	Rev. 0	Hold	Pressurized endurance demonstration
TS 2X2-015	Rev. 0	Scheduled	Screening of manufacturing variables
TS 2X2-016	Rev. 0	Ongoing	Non-electrode catalyst poison/contamination assessment

TABLE 3-5

TEST 2x2-002 REV. 0 ASSESSMENT OF FIVE ELECTRODE VARIABLES

(Status as of 5/31/84)

Test Conditions: 1 Atm, 80% H_2 Util., 20% Air Util., - 200 mA/cm^2 @ 190°C

Cell ID	Initial Resistance (mΩ)	200 Hours E cell (mV)	600 Hours E cell (mV)	1,000 Hours E cell (mV)	PRESENT TEST STATUS				CATHODE			ANODE			
					E cell (mV)	Total Hours	Off Test	Cat.	Bond.	Sint.	Cat.	Bond.	Sint.	Mat-1	Assembly and Test Comments
CAS-001	6.8	623	405	-	405	715	7/83	Std	Wet	Air	Std	Wet	Air	R	Low Pt, Thin SiC, Polyox #1
CAS-001-S1	8.8	623	626	616	566	1749	10/83	Std	Wet	Air	Std	Wet	Air	R	Low Pt, Thin SiC, Polyox #1
CAS-002	6.6	646	646	618	630	2160	9/83	HT	Wet	Air	HT	Wet	Air	R	Low Pt, Thin SiC, Polyox #2
CAS-003	3.1	626	600	528	476	1293	6/83	Std	Wet	Air	Std	Wet	Air	R	High Pt, Thin SiC, Polyox #2
CAS-004	5.8	627	625	611	594	1992	9/83	HT	Wet	Air	HT	Wet	Air	R	High Pt, Thin SiC, Polyox #1
CAS-005	-	610	-	-	490	480	7/83	Std	Dry	Air	Std	Dry	Air	R	Low Pt, Thin SiC, Polyox #2
CAS-005-S1	6.7	632	628	624	617	1221	10/83	Std	Dry	Air	Std	Dry	Air	R	Low Pt, Thin SiC, Polyox #2
CAS-006	6.9	657	655	655	563	1824	9/83	HT	Dry	Air	HT	Dry	Air	R	Low Pt, Thin SiC, Polyox #1
CAS-007	7.8	615	610	611	594	2472	9/83	Std	Dry	Air	Std	Dry	Air	R	High Pt, Thin SiC, Polyox #1
CAS-008	8.0	650	589	609	541	2160	9/83	HT	Dry	Air	HT	Dry	Air	R	High Pt, Thin SiC, Polyox #2
CAS-009	9.9	607	580	600	592	2176	9/83	Std	Wet	Air	Std	Wet	Air	R	Low Pt, Thick SiC, Polyox #2
CAS-010	6.8	641	642	639	634	1486	7/83	HT	Wet	Air	HT	Wet	Air	R	Low Pt, Thick SiC, Polyox #1
CAS-011	7.6	644	641	632	607	1733	10/83	Std	Wet	Air	Std	Wet	Air	R	High Pt, Thick SiC, Polyox #1
CAS-012	7.9	644	643	630	584	1845	10/83	HT	Wet	Air	HT	Wet	Air	R	High Pt, Thick SiC, Polyox #2
CAS-013	6.7	635	632	625	523	2376	8/83	Std	Dry	Air	Std	Dry	Air	R	Low Pt, Thick SiC, Polyox #1
CAS-014	7.4	639	637	594	296	1648	9/83	HT	Dry	Air	HT	Dry	Air	R	Low Pt, Thick SiC, Polyox #2
CAS-015	9.0	621	605	605	561	1652	9/83	Std	Dry	Air	Std	Dry	Air	R	High Pt, Thick SiC, Polyox #2
CAS-016	9.4	635	634	630	472	2520	9/83	HT	Dry	Air	HT	Dry	Air	R	High Pt, Thick SiC, Polyox #1

HT - 900°C Heat Treated Pt.

(-S1) Rebuilt identical sister cells

R - Small Batch Ross Mixed

Lot #3 Catalyst was used in all cells

TABLE 3-5

TEST 2x2-002 REV. 1 and REV. 2 ASSESSMENT OF FIVE ELECTRODE VARIABLES (CONT'D)

(Status as of 5/31/84)

Test Conditions: 1 Atm, 80% H_2 Util., 20% Air Util., - 200 mA/cm^2 @ 190°C

Cell ID	Initial Resistance (mΩ)	200 Hours E cell (mV)	600 Hours E cell (mV)	1,000 Hours E cell (mV)	PRESENT TEST STATUS E cell (mV)	PRESENT TEST STATUS Total Hours	PRESENT TEST STATUS Off Test	CATHODE Cat.	CATHODE Bond.	CATHODE Sint.	ANODE Cat.	ANODE Bond.	ANODE Sint.	Mat-1	Assembly and Test Comments
CAS-061	6.5	646	651	648	649	1288	3/84	HT	Dry	Arg	Std	Dry	Arg	S	Compares to CAS-006
CAS-062	6.9	668	671	484*	647	1120	3/84	HT	Dry	Arg	Std	Dry	Arg	S	
CAS-063	7.3	655	655	648	658	1320	3/84	HT	Dry	Arg	Std	Dry	Arg	S	
CAS-064	6.2	650	652	654	645	1341	4/84	HT	Dry	Arg	Std	Dry	Arg	S	
CAS-065	6.8	657	656	654	628	2488		HT	Dry	Arg	Std	Dry	Arg	S	
CAS-066	6.3	647	653	653	645	2488		HT	Dry	Arg	Std	Dry	Arg	S	
CAS-067	7.6	656	661	653	652	1509	4/84	HT	Dry	Arg	Std	Dry	Arg	S	
CAS-068	10.1	627	630	633	632	1341	4/84	HT	Dry	Arg	Std	Dry	Arg	S	
CAS-069	8.1	642	647	645	635	1744	5/84	HT	Dry	Arg	Std	Dry	Arg	S	
CAS-070	7.8	630	636	637	641	1509	4/84	HT	Dry	Arg	Std	Dry	Arg	S	Compares to CAS-014
CAS-071	9.0	643	-	-	647	378	3/84	HT	Dry	Arg	Std	Dry	Arg	S	
CAS-072	6.7	652	658	658	635	2848		HT	Dry	Arg	Std	Dry	Arg	S	
CAS-112	6.0	630	598	608	609	640		HT	Dry	Arg	Std	Dry	Arg	S	
CAS-113	7.6	638	632	626	633	640		HT	Dry	Arg	Std	Dry	Arg	S	Compares to CAS-008
CAS-114	8.3	634	626	615	624	640		HT	Dry	Arg	Std	Dry	Arg	S	
CAS-115	7.7	654	655	652	655	640		HT	Dry	Arg	Std	Dry	Arg	S	Compares to CAS-016

*Air line pinched for ~ 24 hours

HT - 900°C Heat Treated

S - Large Batch Schold Mixed

The results of this plan can be summarized as follows:

- The present baseline cell performance (mean of 12 cells) is 648 ± 6 mV.
- The effect of different catalyst lots (lots 2 and 3) was within the expected ± 10 mV deviation.
- Catalyst heat treatment has 10 - 25 mV advantage over non-heat treated catalyst.
- The two furnace heat treatment runs of catalyst were within the ± 10 mV expected deviation.
- The effect of catalyst loading, SiC coating thickness and manufacturing process were interactive with + 21 to -26 mV variability over mean.
- There was no significant effect of dry bonding over wet bonding on cell voltage (was within the ± 10 mV expected deviation); however, dry bonding was preferred over wet bonding due to ease of manufacturing.
- The effect of new SiC lot was within the ± 10 mV expected deviation.
- Thinner SiC coating (from 250 microns (10 mil) to 125 microns (5 mil)) provided 12 ± 6 mV benefit.

TS 2X2-004, Rev. 2, 3 and 4

The objective of this test plan was to characterize pressurized 2 x 2 subscale cells; i.e., to quantify the map of acceptable fuel cell operation and to provide data base for assessment of stack scaling effects. The approach was to assemble and test pressurized 2 x 2 cells with the following variables: catalyst heat treatment, current density, pressure, and temperature. The results and the status of these tests are given in Table 3-6.

TABLE 3-6

TEST 2x2-004 REV. 2 AND REV. 4 PRESSURIZED ELECTRODE CHARACTERIZATION

(Status as of 5/31/84)

Test Conditions: 4.8 Atm., Util. 80% H_2 (SRG), 20% Air Util.
- 200 mA/cm^2@ 190°C

Cell ID	Resistance (mΩ)	E cell (mV)	E cell (mV)	E cell (mV)	E cell (mV)	Total Hours	Off Test	Cat.	Bond.	Sint.	Cat.	Bond.	Sint.	Mat-1	Assembly and Test Comments
CPS-017	6.8	709	694	637***	643	1204	11/83	Std	Dry	Air	Std	Dry	Air	S	
CPS-018**	6.8	597*	648*	-	648*	641	9/83	Std	Dry	Air	Std	Dry	Air	S	
CPS-018-S1	6.2	708	706	-	668	860	1/84	Std	Dry	Air	Std	Dry	Air	S	
CPS-019	7.0	707	688	682	615	1204	11/83	Std	Dry	Air	Std	Dry	Air	S	
CPS-020**	6.2	578*	629*	-	629*	641	9/83	Std	Dry	Air	Std	Dry	Air	S	
CPS-020-S1	6.3	698	601	-	348	860	1/84	Std	Dry	Air	Std	Dry	Air	S	
CPS-021**	7.2	600*	336*	-	336*	641	9/83	HT	Dry	Air	HT	Dry	Air	S	
CPS-021-S1	5.9	669	689	-	607	860	1/84	HT	Dry	Air	HT	Dry	Air	S	
CPS-022	5.9	722	686	676	628	1204	11/83	HT	Dry	Air	HT	Dry	Air	S	ERC Heat Treated Catalyst
CPS-023**	5.1	542*	363*	-	363*	641	9/83	HT	Dry	Air	HT	Dry	Air	S	
CPS-023-S1	34.7	-	-	-	-	0	12/83	HT	Dry	Air	HT	Dry	Air	S	
CPS-023-S2	9.5	560	-	-	622	427	5/84	HT	Dry	Air	HT	Dry	Air	S	
CPS-024	6.7	708	699	671	624	1204	11/83	HT	Dry	Air	HT	Dry	Air	S	
CPS-045	9.1	633	-	-	612	427	5/84	Std	Dry	Air	Std	Dry	Air	S	
CPS-046	9.8	612	-	-	478	427	5/84	HT	Dry	Air	HT	Dry	Air	S	
CPS-047	7.8	686	-	-	683	427	5/84	HT	Dry	Air	HT	Dry	Air	S	

HT - 900°C Heat Treated

S - Large Batch Schold Mixed.

*Conversion from H_2 to SRG (-40 mV) based on previous test performance of these cells

**Cells terminated due to low performance. 20 hr voltages at rated conditions before hardware failures were 715 mV, 737 mV, 685 mV, and 736 mV, respectively. (-S1 or -S2) Rebuilt identical sister cells

***Cell went erratic after shift from H to SRG (680 mV performance before acid addition shutdown at 700 hrs)

TABLE 3-6

TEST 2x2-004 REV. 3 PRESSURIZED ELECTRODE CHARACTERIZATION (CONT'D)

(Status as of 5/31/84)

Test Conditions: 4.8 Atm., Util. 80% H_2 (SRG), 20% Air Util. - 200 mA/cm^2 @ 190°C

Cell ID	Initial Resistance (mΩ)	200 Hours E cell (mV)	600 Hours E cell (mV)	1,000 Hours E cell (mV)	PRESENT TEST STATUS			CATHODE			ANODE			Mat-1	Assembly and Test Comments
					E cell (mV)	Total Hours	Off Test	Cat.	Bond.	Sint.	Cat.	Bond.	Sint.		
CPS-026	7.8	692			700	221		HT	Dry	Arg	Std	Dry	Arg	S	
CPS-028	9.1	622			625	221		HT	Dry	Arg	Std	Dry	Arg	S	
CPS-029	6.8	691			699	221		HT	Dry	Arg	Std	Dry	Arg	S	
CPS-031	6.6	689			701	221		HT	Dry	Arg	Std	Dry	Arg	S	

HT - 900°C Heat Treated

S - Large Batch Schold Mixed.

*Recovery following hardware failure and depressurization

**At 325 mA/cm^2

Only preliminary results were obtained from this test plan, since there were difficulties associated with the functioning of the facility and some premature cell failures due to unknown causes.

Test Plan - TS 2X2-005, Rev. 2 and 3

The aim of this plan was to characterize the baseline performance of subscale cells by mutual exchange of cells between ERC and W. This type of "Round Robin" test also enables a comparison of the two facilities.

The approach was to fabricate and assemble eight 2 x 2 cells with the pertinent variables being the assembly facility, test facility and test cells with and without MAT-1. The test plans are shown in Table 3-7 with some preliminary results.

These tests are in progress both at ERC and W. From the preliminary data, it can be stated that W built and tested cells averaged 659 mV at 200 mA/cm^2 (186 A/ft^2) and 190°C (374°F) with 80 percent hydrogen utilization and 20 percent air utilization, whereas the ERC cells under similar conditions averaged 660 mV. Further testing, in terms of rebuilding and exchange, is in progress.

Test Plan TS 2X2-006, Rev. 0 and 1

This test plan was designed to evaluate alternate catalyst/electrode performance and also to perform an assessment of vendor manufacturing processes. The test plan for this task is shown in Table 3-8 and all the cells were evaluated under standard atmospheric conditions at 190°C (374°F) at 200 mA/cm^2 (186 A/ft^2) and 80 percent hydrogen utilization and 20 percent air utilization.

It can also be observed that Prototech (DC01) could be considered as an alternate supplier of catalyst. Giner fabricated cathodes (G82-5-10 and 7) had good initial performance which was better than the baseline, but the electrodes

TABLE 3-7

TEST x2x-005 REV. 2 & REV. 3 BASELINE PERFORMANCE AND FACILITY COMPARISON

(Status as of 5/31/84)

Test Conditions: 1 Atm., 80% H_2 Util., 20% Air Util., - 200 mA/cm^2 @ 190°C

						PRESENT TEST STATUS			CATHODE			ANODE			
Cell ID	Initial Resistance (mΩ)	200 Hours E cell (mV)	600 Hours E cell (mV)	1,000 Hours E cell (mV)	E cell (mV)	Total Hours	Off Test	Cat.	Bond.	Sint.	Cat.	Bond.	Sint.	Mat-1	Assembly and Test Comments
CAS-017	8.8	584	588	596	609	1124	10/83	HT-W	Dry	Wet	HT-W	Dry	Wet	S	Cancelled due to wet
CAS-018, -019, -020, -021, -022			-	-	-	Not Built		HT-W	Dry	Wet	HT-W	Dry	Wet	No	sinter low performance.
CAS-023	7.6	600	598	605	610	1124	10/83	HT-W	Dry	Wet	HT-W	Dry	Wet	S	Test units redefined below
CAS-024	-	-	-	-	-	Not Built		HT-W	Dry	Wet	HT-W	Dry	Wet	No	as CAS-090 thru CAS-097
CAS-090	6.3	662	658	656	655	1144		HT-W	Dry	Arg	Std	Dry	Arg	S	<u>W</u> Fab. <u>W</u> Test - Sent to ERC
	8.0	630	628	-	628	761									ERC Test
CAS-091	7.0	664	642	635	632	1144		HT-W	Dry	Arg	Std	Dry	Arg	No	<u>W</u> Fab. <u>W</u> Test - Sent to ERC
	10.8	613	592	-	584	761									ERC Test
CAS-096	9.1	637	618	608	606	1144		HT-W	Dry	Arg	Std	Dry	Arg	S	<u>W</u> Fab. <u>W</u> Test
CAS-097	7.0	667	652	650	649	1144		HT-W	Dry	Arg	Std	Dry	Arg	No	<u>W</u> Fab. <u>W</u> Test

HT-W 900°C Heat Treated, Westinghouse Fabricated

(-S1) Rebuilt identical sister cells.

S - Large Batch Schold Mixed

TABLE 3-8

TEST 2x2-006 REV. 0 ALTERNATE CATALYST COMPARISON AND ELECTRODE EVALUATION

(Status as of 5/31/84)

Test Conditions: 1 Atm., 80% H_2 Util., 20% Air Utilization, - 200 mA/cm^2 @ 190°C

Cell ID	Initial Resistance (mΩ)	200 Hours E cell (mV)	600 Hours E cell (mV)	1,000 Hours E cell (mV)	PRESENT TEST STATUS E cell (mV)	PRESENT TEST STATUS Total Hours	PRESENT TEST STATUS Off Test	CATHODE Cat.	CATHODE Bond.	CATHODE Sint.	ANODE Cat.	ANODE Bond.	ANODE Sint.	Mat-1	Assembly and Test Comments
CAS-026	7.4	644	631	632	612	2235	12/83	DC05	Wet	Air	Std	Wet	Air	S	
CAS-027	6.4	654	646	649	631	2235	12/83	DC05	Wet	Air	Std	Wet	Air	S	
CAS-028	6.3	642	638	638	632	2176	1/84	DC04	Wet	Air	Std	Wet	Air	S	
CAS-029	-	-	-	-	-	-	-	DC04							Cancelled
CAS-030	7.6	673	668	663	604	3877	2/84	DC06	Wet	Air	Std	Wet	Air	S	
CAS-031	6.6	680	682	681	592	6184		DC06	Wet	Air	Std	Wet	Air	S	
CAS-032	13.2	625	623	623	597	1966	1/84	DC07	Wet	Air	Std	Wet	Air	S	
CAS-033	8.0	672	670	672	629	5008		DC07	Wet	Air	Std	Wet	Air	S	
CAS-034	8.1	644	612	538	441	1298	11/83	DC06	NA	NA	Std	Wet	Air	S	Vendor Fabricated
CAS-035	8.2	627	545	390	251	1250	12/83	DC07	NA	NA	Std	Wet	Air	S	Vendor Fabricated
CAS-036	8.1	664	658	649	636	1316	11/83	DC06	NA	NA	Std	Wet	Air	S	Vendor Fabricated, W Backing
CAS-037	5.4	675	660	654	630	1770	1/84	DC07	NA	NA	Std	Wet	Air	S	Vendor Fabricated, W Backing
CAS-038	6.9	633	627	627	623	1772	1/84	DC01	Wet	Air	Std	Wet	Air	S	
CAS-039	5.2	537	-	-	537	139	10/83	DC02	Wet	Air	Std	Wet	Air	S	Terminated; poor performance

S - Large Batch Schold Mixed

TABLE 3-8

TEST 2x2-006 REV. 1 ALTERNATE CATALYST COMPARISON AND ELECTRODE EVALUATION (CONT'D)

(Status as of 5/31/84)

Test Conditions: 1 Atm., 80% H_2 Util., 20% Air Utilization, - 200 mA/cm^2 @ 190°C

Cell ID	Initial Resistance (mΩ)	200 Hours E cell (mV)	600 Hours E cell (mV)	1,000 Hours E cell (mV)	PRESENT TEST STATUS E cell (mV)			CATHODE Cat.			ANODE Cat.			Mat-1	Assembly and Test Comments
						Total Hours	Off-Test		Bond.	Sint.		Bond.	Sint.		
CAS-047	5.5	649	639	641	553	2134	1/84	DC05	Wet	Air	DC03	Wet	Air	S	
CAS-048	6.7	656	651	645	626	2182	1/84	DC05	Wet	Air	DC03	Wet	Air	S	
CAS-049	9.5	601	594	-	594	622	3/84	DC01	Wet	Air	DC01	Wet	Air	S	Anode load 0.45 mg/cm^2
CAS-050	-	-	-	-	-	-	-	DC02	Wet	Air	DC02	Wet	Air	S	Anode load 0.43 mg/cm^2-Cancelled
CAS-051	6.2	686	683	680	441	5026		DC06	Wet	Air	DC03	Wet	Air	S	
CAS-052	7.7	675	671	672	587	5170		DC06	Wet	Air	DC03	Wet	Air	S	
CAS-053	7.2	667	662	660	516	3784		DC07	Wet	Air	DC03	Wet	Air	S	
CAS-054	8.9	662	661	661	596	4192		DC07	Wet	Air	DC03	Wet	Air	S	
CAS-055	-	-	-	-	-	-	-	DC10	Dry	Arg	Std	Wet	Air	S	Cancelled
CAS-056	7.5	612	608	591	585	1336	4/84	DC10	Dry	Arg	Std	Wet	Air	S	
CAS-057	7.7	602	596	595	547	1336	4/84	DC10	Dry	Arg	DC03	Wet	Air	S	
CAS-058	6.0	553	555	555	522	1240	4/84	DC10	Dry	Arg	DC03	Wet	Air	S	
CAS-059	7.6	623	613	605	559	1240	4/84	DC10	Wet	Air	Std	Wet	Air	S	
CAS-060	8.3	622	616	612	625	1168	4/84	DC10	Wet	Air	Std	Wet	Air	S	
CAS-100	7.6	677	672	673	640	2056		DC06	Dry	Arg	Std	Dry	Arg	S	
CAS-101	6.8	693	683	672	585	1840		DC07	Dry	Arg	Std	Dry	Arg	No	
CAS-102	7.7	679	675	669	603	2226		DC06	Dry	Arg	Std	Dry	Arg	No	
CAS-103	7.9	670	665	663	616	2344		DC07	Dry	Arg	Std	Dry	Arg	S	
CAS-104	9.6	655	654	649	535	2104	5/84	DC07	Wet	Air	DC03	Wet	Air	S	
CAS-105	7.0	680	677	672	633	2344		DC06	Wet	Air	DC03	Wet	Air	S	
CAS-106	7.2	53	-	-	43	232	5/84	DC11	Dry	Arg	Std	Dry	Arg	S	
CAS-108	22.2	129	-	-	54	232	5/84	DC12	Dry	Arg	Std	Dry	Arg	S	

S - Large Batch Schold Mixed

TABLE 3-9

TEST 2x2-007 REV. 0 THRU REV. 2 ALTERNATE BACKING PAPER COMPARISON AND PROCESS EVALUATION

(Status as of 5/31/84)

Test Conditions: 1 Atm., 80% H_2 Util., 20% Air Utilization, - 200 mA/cm^2 @ 190°C

Cell ID	Initial Resistance (mΩ)	200 Hours E cell (mV)	600 Hours E cell (mV)	1,000 Hours E cell (mV)	PRESENT TEST STATUS E cell (mV)			CATHODE Cat.			ANODE Cat.				
					E cell (mV)	Total Hours	Off Test	Cat.	Bond.	Sint.	Cat.	Bond.	Sint.	Mat-1	Assembly and Test Comments
CAS-040	18.0	583	577	587	572	1990	1/84	Std	Wet	Air	Std	Wet	Air	S	Kureha E715, 33% TFE, Std. Process
CAS-041	12.2	592	578	585	584	1081	3/84	Std	Wet	Air	Std	Wet	Air	S	Kureha E715, 33% TFE, Paste Process
CAS-042	14.7	580	575	577	535	2018	1/84	Std	Wet	Air	Std	Wet	Air	S	Kureha E715, 42% TFE, Std. Process
CAS-043	11.1	604	598	568	555	1123	3/84	Std	Wet	Air	Std	Wet	Air	S	Kureha E715, 42% TFE, Paste Process
CAS-044	9.1	618	602	587	575	1134	2/84	Std	Wet	Air	Std	Wet	Air	S	Stackpole PC206, 39% TFE, Std. Process
CAS-045	7.5	631	633	636	633	1132	2/84	Std	Wet	Air	Std	Wet	Air	S	Stackpole PC206, 39% TFE, Paste Proc.
CAS-073	6.8	665	662	645	645	1600	5/84	HT	Dry	Arg	Std	Dry	Arg	No	
CAS-074	5.9	675	677	654	653	1600	5/84	HT	Dry	Arg	Std	Dry	Arg	No	
CAS-075	7.7	647	644	622	614	1600	5/84	HT	Dry	Arg	Std	Dry	Arg	No	Silk Screen Production Paste Process
CAS-076	6.7	669	665	639	613	1600	5/84	HT	Dry	Arg	Std	Dry	Arg	No	Silk Screen Production Paste Process

HT - 900°C Heat Treated

S - Large Batch Schold Mixed

had high decay rates. The performance of this cell is shown in Fig. 3-1. Vendor cathodes DC05 and 10 provided acceptable initial performance and DC04 also appears to be good but these electrodes need further endurance testing. Alternate catalyst materials DC-11 and DC-12 initially appear to be unacceptable. A number of these tests are being continued for up to 5000 hours and a detailed analysis of their performance will be delayed until the tests are completed. However, based on the available data, it is apparent that reliable predictions regarding the performance degradation of certain catalysts cannot be made based on test duration of less than 3000 hours.

Test Plan TS 2X2-007, Rev. 0 and 1

The objective of this plan was to assess the performance of alternate backing paper, alternate wet proofing methods and effect of changing Teflon levels in the backing paper on 2x2 subscale cells. The performance histories for various cells in this test plan are shown in Table 3-9.

One series of cells, CAS-040 through -043, was fabricated from electrodes supported by a possible alternate support layer, namely, Kureha E715 carbon paper. The backing or support layer was wet proofed to two levels of Teflon using two processes, the standard dipping process and a paste spreading process. The terminal cell voltage of these cells was 600 mV or lower and the cell resistance was high, 11 mΩ or greater (since the backing paper resistance was 50 percent higher than Stackpole paper). The poor cell performance can tentatively be attributed to the higher resistance of the cells compared to baseline cells. Additionally, the rapid degradation of the cells, approximately 12 mV in 800 hours, indicates possible flooding of the backing layer at both Teflon levels. This data indicates that the E715 paper is not an acceptable alternative or substitute for the material presently being used for electrode layer backing.

The use of the alternate "paste" wetproofing process, or "silkscreen" process, was found to be comparable to the double dip process, and average cell voltages from the two processes were similar. This indicates that the silkscreen wetproofing process is an acceptable alternate process for further study.

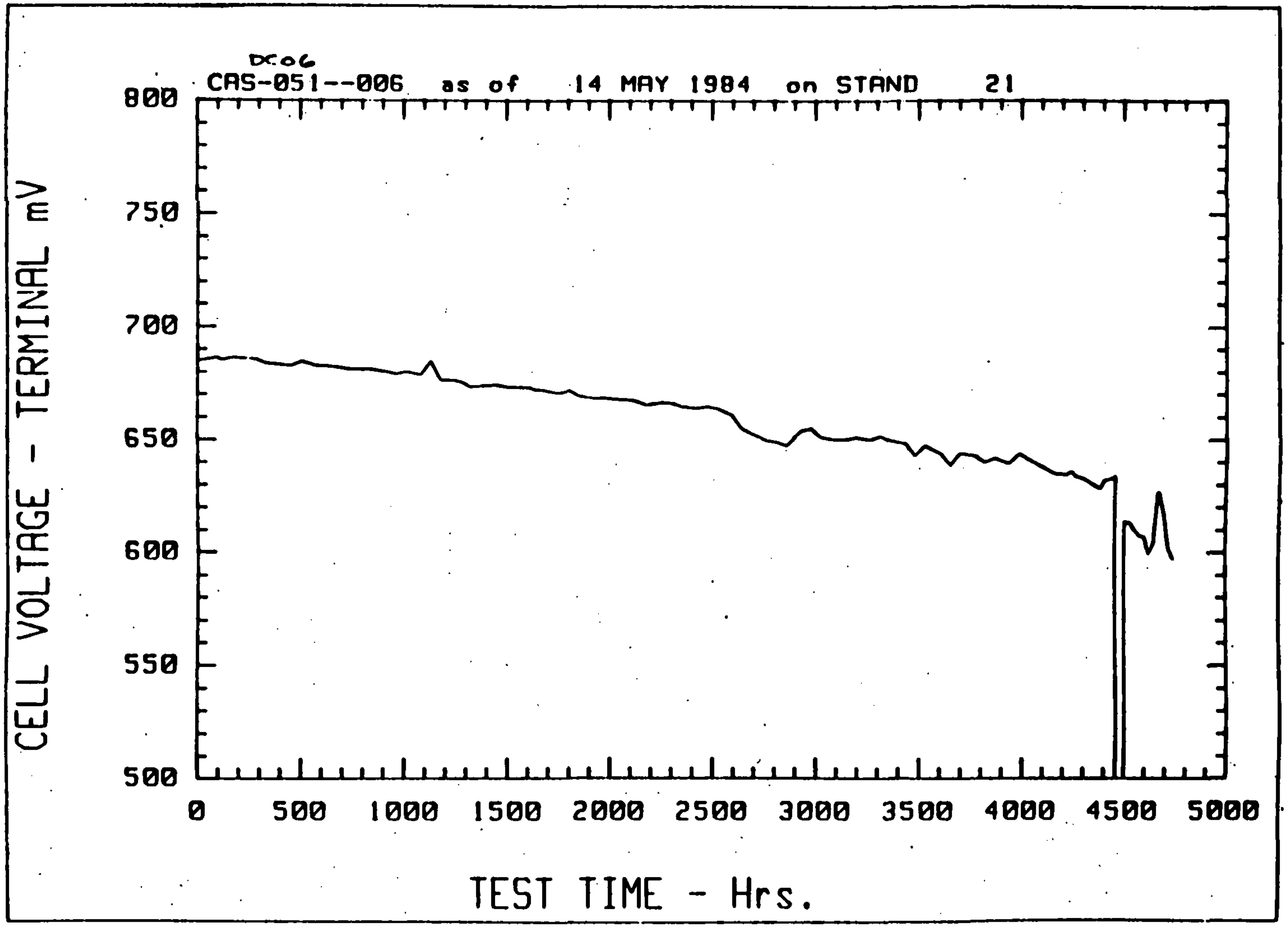

Figure 3-1. Fuel Cell Performance.

Test Plan 2X2-008, Rev. 0

A total of ten cells were built under this test plan to evaluate the effects of (1) dry and wet bonding, (2) alternate sintering environment, viz., steam, air and argon. This plan also was aimed at providing an acceptance screening of Schold Mix MAT-1 compared to Ross Mix MAT-1. The performance of the various cells is shown in Table 3-10.

The results from wet/dry lamination comparisons conclusively show that dry bonding produces an acceptable result, which was also shown earlier in TS 2x2-002. Sintering of electrodes in argon is also an acceptable process (also confirmed by ERC test plan TSE 2x2-006 results). There was no significant difference in subscale cell voltages whether Ross Mixed MAT-1 or Schold Mixed MAT-1 is used, and this clearly shows that Schold Mixed MAT-1 matrix is acceptable.

Test Plan 2X2- 010, Rev. 0

The main aim of this test plan was to verify the quality of electrodes for a 10 kW stack. Seven cells were assembled and tested to assess the variation in the performance of electrodes within a batch and batch-to-batch. During the initial phase of this plan, the baseline processing procedure was revised due to the change of electrode sintering gas to argon; hence, this test plan was cancelled.

TS 2X2-011, Rev. 0, 1 and 2

The purpose of this test plan was to study the effect of alternate acid transport medium, especially zirconium pyrophosphate insulation material, Teflon content in MAT-1 matrix, and the thickness of SiC coating. A series of tests was designed and cells were tested as described in Table 3-11.

TABLE 3-10

TEST 2x2-008 REV. 0 ELECTRODE BONDING AND SINTERING PROCESS DEVELOPMENT TESTS

(Status as of 5/31/84)

Test Conditions: 1 Atm. 80% H_2 Util., 20% Air Util., - 200 mA/cm^2 @ 190°C

Cell ID	Initial Resistance (mΩ)	200 Hours E cell (mV)	600 Hours E cell (mV)	1,000 Hours E cell (mV)	PRESENT TEST STATUS			CATHODE			ANODE				
					E cell (mV)	Total Hours	Off Test	Cat.	Bond.	Sint.	Cat.	Bond.	Sint.	Mat-1	Assembly and Test Comments
DAS-001	7.0	634	636	639	633	1586	12/83	Std	Wet	Air	Std	Wet	Air	R	Reproducibility of Standard
DAS-002	6.9	626	623	611	581	1586	12/83	Std	Wet	Air	Std	Wet	Air	S	electrode and matrix
DAS-003	6.6	623	623	625	602	1635	11/83	HT-W	Dry	Wet	HT-W	Dry	Wet	S	Same Electrode Batch as CAS 17 & 23
DAS-004	5.8	624	627	626	616	1635	11/83	HT-W	Dry	Wet	HT-W	Dry	Wet	R	Same Electrode Batch as CAS 17 & 23
DAS-005	6.9	640	641	643	643	1778	12/83	Std	Dry	Wet	Std	Dry	Wet	S	
DAS-006	6.7	657	660	657	614	3194	2/84	Std	Dry	Arg	Std	Dry	Arg	S	
DAS-007	7.1	649	646	641	635	1586	12/83	Std	Wet	Wet	Std	Wet	Wet	S	
DAS-008	6.4	657	655	653	630	2662	1/84	Std	Wet	Arg	Std	Wet	Arg	S	
DAS-009	6.9	661	664	665	646	4266	4/84	HT-W	Dry	Arg	Std	Dry	Arg	S	
DAS-010	6.3	664	664	663	642	2900	2/84	HT-W	Dry	Arg	Std	Dry	Arg	R	

HT-W Heat Treated Westinghouse Fabricated

R - Small Batch Ross Mixed

S - Large Batch Schold Mixed

TABLE 3-11

TEST 2x2-001 - REV. 0, REV. 1 AND REV. 2 - MANUFACTURING PROCESS AND ACID TRANSPORT VARIABLE EVALUATION

(Status as of 5/31/84)

Test Conditions: 1 Atm. 80% H_2 Util., 20% Air Util., - 200 mA/cm^2 @ 190°C

	Initial	200 Hours	600 Hours	1,000 Hours	PRESENT TEST STATUS				CATHODE			ANODE			
Cell ID	Resistance (mΩ)	E cell (mV)	E cell (mV)	E cell (mV)	E cell (mV)	Total Hours	Off Test		Cat.	Bond.	Sint.	Cat.	Bond.	Sint.	Mat-1Assembly and Test Comments
DAS-011	8.3	636	644	645	640	1900	2/84	HT	Dry	Arg	Std	Wet	Air	S	Std 3% Teflon MAT-1
DAS-012	7.5	658	663	653	642	1994	2/84	HT	Dry	Arg	Std	Wet	Air	No	Nominal SiC
DAS-013	-	-	-	-	-	-	-	HT	Dry	Arg	Std	Dry	Arg	No	Kureha E715 - Cancelled
DAS-014	-	-	-	-	-	-	-	HT	Dry	Arg	Std	Dry	Arg	No	Stackpole PC 206 - Cancelled
DAS-015	6.1	666	671	669	628	10554		HT	Dry	Arg	Std	Dry	Arg	S	Std 3% Teflon MAT-1
DAS-016	6.1	669	675	673	625	10554		HT	Dry	Arg	Std	Dry	Arg	No	Thin SiC
DAS-019	8.1	639	648	646	625	2116	3/84	HT	Dry	Arg	Std	Dry	Arg	S	Std 3% Teflon MAT-1
DAS-020	7.6	666	670	666	649	2140	3/84	HT	Dry	Arg	Std	Dry	Arg	No	Thick SiC
DAS-021	7.9	655	658	660	623	4168		HT	Dry	Arg	Std	Dry	Arg	S	Std 3% Teflon MAT-1
DAS-022	7.1	667	661	667	624	4168		HT	Dry	Arg	Std	Dry	Arg	No	Nominal SiC
DAS-023	11.4	613	614	617	619	1408	5/84	HT	Dry	Arg	Std	Dry	Arg	S	Zr P_2O_7 Coated Cathode
DAS-024	11.6	623	603	575	560	1408	5/84	HT	Dry	Arg	Std	Dry	Arg	No	Zr P_2O_7 Coated Cathode
DAS-047	8.2	628			628	232		HT	Dry	Arg	Std	Dry	Arg	S	4 1/2% Teflon Mat-1, Thin SiC
DAS-048	8.8	624			624	232		HT	Dry	Arg	Std	Dry	Arg	S	4 1/2% Teflon Mat-1, Nom SiC

HT - 900°C Heat Treated

S - Large Batch Schold Mixed

One of the important conclusions from this test plan is that the insulation coating from zirconium pyrophosphate is not acceptable since the cells had lower cell voltages and also 60 percent (approximately) higher resistance than silicon carbide. It can be seen once again (previously shown in TS 2X2-002) that thin SiC coating is highly desirable (also confirmed by ERC Test Plan TSE 2X2-003 results) and the measured resistance of SiC coating is about .02-.03 mΩ/micron (0.5-0.7 mΩ/mil).

The effect of MAT-1 carbon layer on cell internal resistance was assessed using subscale cells DAS-011 and DAS-012. MAT-1 was assembled in DAS-011, but omitted in DAS-012. After continuous testing at 200 mA/cm^2 (186 A/ft^2) for ∿200 hours, the polarization data and internal resistances were measured at 190°C (374°F) and ambient pressure. At the current densities of this study, no major differences were observed in the internal resistances of the two cells. Since the presence of MAT-1 increases the interelectrode distance, one would expect a higher resistance in DAS-011 than that measured in DAS-012. The additional resistance was not detected, presumably due to the electronic conductivity of the MAT-1.

Figure 3-2 shows the IR-free cell voltage vs. current density relationships for the two cells. At very low current densities, both cells exhibited similar voltages. With increased operating current density, however, the voltage difference between these cells became significant. If one plots the voltage difference as a function of current density, a linear curve is obtained, revealing that the MAT-1 in DAS-011 contributes approximately an additional 3.1 mΩ to the overall cell internal resistance. At 190°C (374°F), the measured electrical conductivity of 100 w/o H_3PO_4 is ∿ 0.5/ohm-cm. Assuming that the tortuosity factor for a loose random pore structure is $\sqrt{3}$, the calculated electrical resistance through a typical MAT-1 of thickness 0.229 mm (∿0.009 in.) is ∿3.09 mΩ. This estimated value is in good agreement with the additional internal resistance of 3.1 mΩ obtained experimentally. In conclusion, the inclusion of MAT-1 increases the cell internal resistance by ∿3 mΩ and the inferred resistance is about .012-.02 mΩ/micron (0.3-0.5 mΩ/mil). As a result, the terminal voltage of

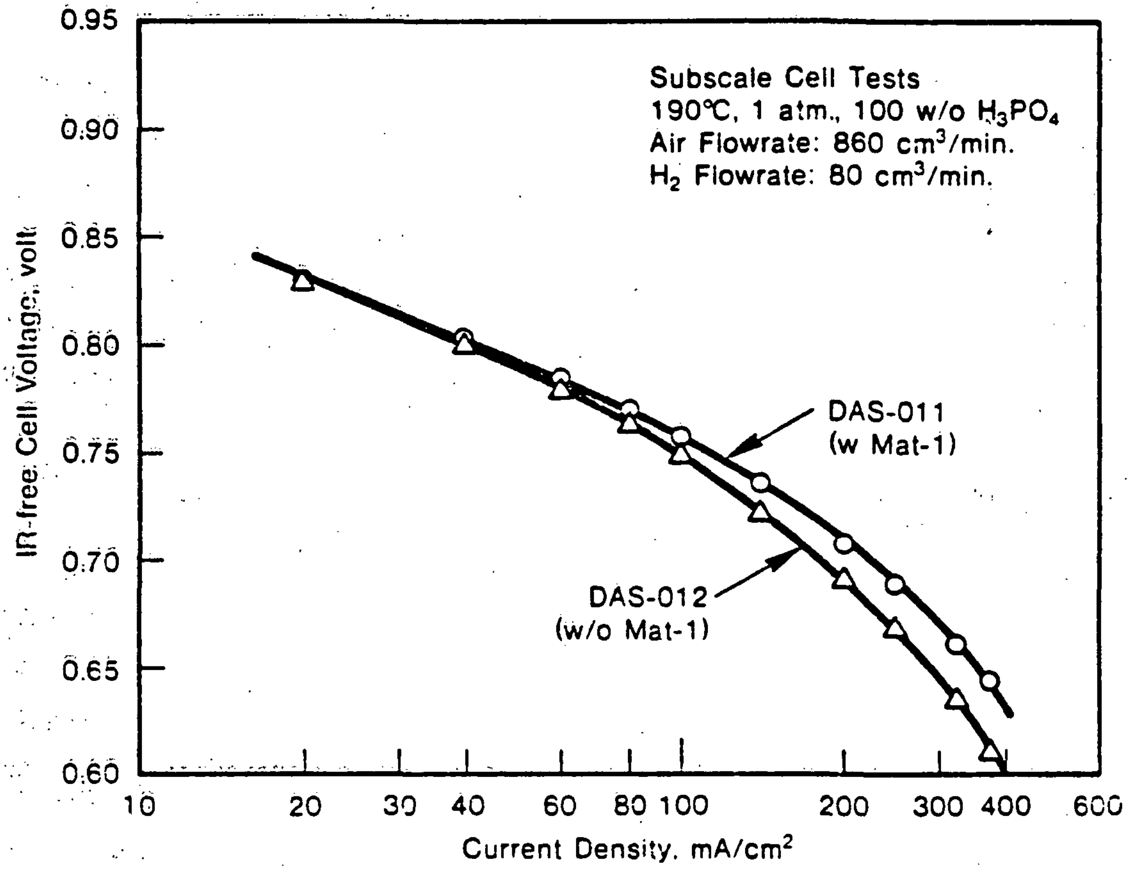

Figure 3-2. Polarization Data for Subscale Cells DAS-011 and -012.

a subscale cell without MAT-1 at 200 mA/cm^2 (186 A/ft^2) should be about 16 mV higher than the cell with MAT-1. However, additional data are required to completely define the resistance contribution of MAT-1.

TS 2X2-013, Rev. 0, 1, 2, 3 and 4

The major objective of this test plan is to verify (using subscale cells) the quality of the electrodes and cell components that are incorporated in the baseline Stacks W-009-10, W-009-11 and W-009-12. A series of 27 cells were built and testing is in progress as shown in Table 3-12.

From the tables, it can be observed that the QAS-006-009 (S1) cell voltages ranged from 635 - 652 mV with an average of 645 mV (based on 200 hour data) at the specified test conditions. The same electrodes in cells QPS-009 through -012 performed at an average voltage of 640 mV (range 627-647 mV) with SRG at 485 kPa (4.8 atm.), 80 percent H_2 (SRG), 20 percent air utilization, 325 mA/cm^2 (300 A/ft^2) at 190°C (374°F). These are the electrodes that were used in assembling in Stack W-009-10.

The electrodes that were obtained from heat treatment run No. 4 were incorporated in Stacks W-009-11 and W-044-1 and these were tested in subscale cells QAS-016 through -019, -019-S1 and -019-S2 under atmospheric pressure and in QPS-017 through -020 under pressurized conditions. The atmospheric test cells showed an average of 648 mV with a range from 624 mV to 680 mV (based on 200-hour data). The same electrodes in pressurized cell conditions with SRG exhibited 659 mV (range 647-669 for 3 cells) indicating that the effect of SRG was about -25 mV as expected with the range from -15 mV to -30 mV. These electrodes appear to be acceptable for stacks (with a minimum performance > 630 mV) and will presumably aid in understanding the data from the stack development program.

TS 2X2-014, Rev. 0 and 1

This test plan was designed to evaluate alternate catalysts in terms of endurance under pressurized conditions. During this reporting period, tests

TABLE 3-12
TEST x2x-013 REV. 0 THRU REV. 5 ELECTRODE QUALITY VERIFICATION TEST
(Status as of 5/31/84)

Test Conditions: 1 Atm., 80% H_2 Util., 20% Air Utilization, - 200 mA/cm^2 @ 190°C

Cell ID	Initial Resistance (mΩ)	200 Hours E cell (mV)	600 Hours E cell (mV)	1,000 Hours E cell (mV)	PRESENT TEST STATUS E cell (mV)			CATHODE			ANODE				
					E cell (mV)	Total Hours	Off Test	Cat.	Bond.	Sint.	Cat.	Bond.	Sint.	Mat-1	Assembly and Test Comments
QAS-006	8.3	648	644	643	645	1034	2/84	HT2	Dry	Arg	Std	Dry	Arg	No	High nominal
QAS-007	8.4	652	651	642	638	1056	2/84	HT2	Dry	Arg	Std	Dry	Arg	No	
QAS-008	9.0	646	638	600	600	1005	2/84	HT2	Dry	Arg	Std	Dry	Arg	No	
QAS-009	11.8	609	-	-	610	286	1/84	HT2	Dry	Arg	Std	Dry	Arg	No	Low nominal (hardware failure)
QAS-009-S1	8.8	635	638	632	632	1000	3/84	HT2	Dry	Arg	Std	Dry	Arg	No	
QAS-016	7.2	667	662	651	648	1312	5/84	HT4	Dry	Arg	Std	Dry	Arg	No	High nominal
QAS-017	7.2	680	643	633	620	1312	5/84	HT4	Dry	Arg	Std	Dry	Arg	No	
QAS-018	7.7	641	625	574	557	1312	5/84	HT4	Dry	Arg	Std	Dry	Arg	No	Low nominal
QAS-019	7.8	598	-	-	598	160	4/84	HT4	Dry	Arg	Std	Dry	Arg	No	
QAS-019-S1	9.3	607	-	-	597	240	5/84	HT4	Dry	Arg	Std	Dry	Arg	No	
QAS-019-S2	8.8	624	623		622	649		HT4	Dry	Arg	Std	Dry	Arg	No	
QAS-020	9.1	646			645	313		HT4	Dry	Arg	Std	Dry	Arg	No	
QAS-025	10.5	628			617	304		HT4	Dry	Arg	Std	Dry	Arg	No	Low nominal
QAS-026	8.8	650			641	304		HT4	Dry	Arg	Std	Dry	Arg	No	
QAS-027	8.2	649			653	304		HT4	Dry	Arg	Std	Dry	Arg	No	High nominal

HT - 900°C Heat Treated
(-S1 or -S2) Rebuilt identical sister cell

S - Large Batch Schold Mixed.

c-2

TABLE 3-12

TEST 2x2-013, REV. 0 THRU REV. 5, ELECTRODE QUALITY VERIFICATION TEST (CONT'D)

(Status as of 5/31/84)

Test Conditions: 4.8 Atm., 80% H_2 (SRG), 20% Air - 325 mA/cm^2 @ 190°C

Cell ID	Initial Resistance (mΩ)	200 Hours E cell (mV)	600 Hours E cell (mV)	1,000 Hours E cell (mV)	PRESENT TEST STATUS E cell (mV)	Total Hours	Off Test	Cat.	CATHODE Bond.	Sint.	Cat.	ANODE Bond.	Sint.	Mat-1	Assembly and Test Comments
QPS-009	5.5	645	670(H2)	-	0	857	3/84	HT2	Dry	Arg	Std	Dry	Arg	No	High nominal
QPS-010	4.9	642	671(H2)	-	450(H2)	857	3/84	HT2	Dry	Arg	Std	Dry	Arg	No	
QPS-011	4.6	647	0	-	0	857	3/84	HT2	Dry	Arg	Std	Dry	Arg	No	Low nominal
QPS-012	4.5	627	0	-	0	857	3/84	HT2	Dry	Arg	Std	Dry	Arg	No	
QPS-013	9.7	608(H2)	609(H2)	-	606(H2)	794	5/84	HT2	Dry	Arg	Std	Dry	Arg	S	1
QPS-014	8.0	640(H2)	639(H2)	-	635(H2)	794	5/84	HT2	Dry	Arg	Std	Dry	Arg	S	2 Pressurized loop-station
QPS-015	8.0	660(H2)	629(H2)	-	589(H2)	794	5/84	HT2	Dry	Arg	Std	Dry	Arg	S	3 (location) dependence test
QPS-016	10.0	623(H2)	621(H2)	-	602(H2)	794	5/84	HT2	Dry	Arg	Std	Dry	Arg	S	4
QPS-017	6.1	659		-	679(H2)*	256		HT4	Dry	Arg	Std	Dry	Arg	S	High nominal
QPS-018	6.9	638		-	673(H2)*	256		HT4	Dry	Arg	Std	Dry	Arg	S	
QPS-019	5.9	667		-	679(H2)*	256		HT4	Dry	Arg	Std	Dry	Arg	S	Low nominal
QPS-020	10.6	522		-	561(H2)*	256		HT4	Dry	Arg	Std	Dry	Arg	S	

HTx - 900°C Heat Treated Pt, Furnace Run X

S - Large Batch Schold Mixed.

* low (∿ 50%) H_2 utilization

were initiated with an alternate catalyst, DC-06, in two cells, along with two Westinghouse baseline cells (CPS-033 through -036) as shown in Table 3-13. Further tests are planned in this area with various types of catalysts.

The preliminary tests in this test plan were performed with gold-plated hardware (plated bipolar plates). The initial results showed a poor performance with an average of 580 mV under pressurized conditions which indicates that gold plated hardware may not be acceptable.

Test Plan TS 2X2-016

The objective of this test plan was to evaluate the effects of various nonelectrode related poisons such as by-product materials dissolution at various temperatures. Two sealing materials, viz., Viton and Teflon were assessed at 190° and 200°C (374° and 392°F) temperatures with and without MAT-1. An attempt was also made to evaluate the effect of alternate end plates. Testing of the cells built in this plan is in progress and preliminary results are shown in Table 3-14.

Although the initial performance data on cells CAS-116 through -121 exhibit a scatter, it is safe to conclude that Teflon is an acceptable sealant. Further re-building and re-testing is required to obtain any endurance data and/or other conclusions.

EFFECT OF VARIATIONS IN KEY OPERATIONAL PARAMETERS ON UNPRESSURIZED CELL PERFORMANCE

To normalize the experimental data for unpressurized subscale tests, the effects of minor variations in test temperature and current density on cell performance were investigated using cells DAS-019 and -021. Both cells were assembled using dry bonded argon sintered cathodes made using Lot No. 3 heat treated catalyst, dry bonded argon sintered anodes made using as-received catalyst and carbon layer (MAT-1). Tests were performed at 80 percent hydrogen utilization, 25 percent air utilization at 200 mA/cm^2 (186 A/ft^2) (5.13 amps).

TABLE 3-13

TEST 2x2-014 REV. 0 AND REV. 1 PRESSURIZED ELECTRODE ENDURANCE VERIFICATION

(Status as of 5/31/84)

Test Conditions: 4.8 Atm., Util. 80% H_2 (SRG), 20% Air Util. - 325 mA/cm^2 @ 190°C

Cell ID	Initial Resistance (mΩ)	200 Hours E cell (mV)	600 Hours E cell (mV)	1,000 Hours E cell (mV)	PRESENT TEST STATUS E cell (mV)	PRESENT TEST STATUS Total Hours	PRESENT TEST STATUS Off Test	CATHODE Cat.	CATHODE Bond.	CATHODE Sint.	ANODE Cat.	ANODE Bond.	ANODE Sint.	Mat-1	Assembly and Test Comments
CPS-033	-	-	-	-	516(H_2)	0	4/84	DC06	Dry	Arg	Std	Dry	Arg	S	
CPS-034	-	-	-	-	612(H_2)	0	4/84	DC06	Dry	Arg	Std	Dry	Arg	S	Preliminary tests with Gold Plated Hardware
CPS-035	-	-	-	-	570(H_2)	0	4/84	Std	Dry	Arg	Std	Dry	Arg	S	
CPS-036	-	-	-	-	573(H_2)	0	4/84	Std	Dry	Arg	Std	Dry	Arg	S	

HT - 900°C Heat Treated

S - Large Batch Schold Mixed.

TABLE 3-14

TEST 2x2-016 NON-ELECTRODE RELATED CATALYST POISONS

(Status as of 5/31/84)

Test Conditions: 1 Atm., Util. 80% H_2, 20% Air Util. - 200 mA/cm^2 @ 190°C

Cell ID	Initial Resistance (mΩ)	200 Hours E cell (mV)	600 Hours E cell (mV)	1,000 Hours E cell (mV)	PRESENT TEST STATUS E cell (mV)	PRESENT TEST STATUS Total Hours	PRESENT TEST STATUS Off Test	CATHODE Cat.	CATHODE Bond.	CATHODE Sint.	ANODE Cat.	ANODE Bond.	ANODE Sint.	Mat-1	Assembly and Test Comments
CAS-116	6.7	664			667	592		HT	Dry	Arg	Std	Dry	Arg	S	Viton seal
CAS-117	10.5	644	643		642	736		HT	Dry	Arg	Std	Dry	Arg	No	Viton seal
CAS-118	7.0	677			676	592		HT	Dry	Arg	Std	Dry	Arg	No	Teflon seal
CAS-119	11.6	589			635	328		HT	Dry	Arg	Std	Dry	Arg	S	Teflon seal
CAS-120	6.8	666	668		669	736		HT	Dry	Arg	Std	Dry	Arg	S	Viton seal, Alt. end plates
CAS-121	7.6	657	649		647	736		HT	Dry	Arg	Std	Dry	Arg	S	Teflon seal, Alt. end plates

HT - 900°C Heat Treated

S - Large Batch Schold Mixed.

Figures 3-3 and 3-4 show the effect of varying cell current between 4.5 and 5.5 amperes on cell voltage at 185° and 190°C (365° and 374°F). Both cells varied approximately 2.9 mV per 0.1 amps at 190°C (374°F) and between 2.7 and 3.0 mV per 0.1 amp at 185°C (365°F).

Cell voltage as a function of temperature is plotted in Figure 3-5. Over the range of temperatures examined, the cells vary 1.2 mV/°C (.7 mV/°F) (DAS-019) and 1.1 mV/°C (.6 mV/°F) (DAS-021).

Similar data was previously determined for wet bonded, non-heat treated catalyst electrodes. The agreement between the sets of data indicates very little effect of process changes. The new data was utilized in the data acquisition programming to perform the normalization of actual test values.

3.1.2.2 Performance Improvement From Pressurization

The effect of operating pressure on performance of subscale fuel cells continued to be studied. This work was initiated in the First Logical Unit. Test cells were wet assembled using 93 w/o H_3PO_4 and measurements made at 190°C (374°F) over the pressure range of 101-687 kPa (1 - 6.8 atms). The cells were operated for over 300 hours at pressure to stabilize the electrode performance and improve the reproducibility of the results prior to taking the measurements for pressurization effects. Polarization data was obtained at each pressure and the cells were equilibrated at each current level for approximately ten minutes before data was taken. Cell internal resistance was measured using an in-situ technique with an AC milliohmeter (Hewlett-Packard Model 4328A).

Typical cathode potential-current density relationships at pressures of 101, 240, and 480 kPa (1.0, 2.4, and 4.8 atms) are given in Figure 3-6. Linear Tafel regions were observed at current densities below 150 mA/cm^2 (140 A/ft^2), the measured slopes ranging from 106 to 109 mV/decade and independent of operating pressure. Increased pressure did not affect the mechanism of the oxygen reduction reaction. Based on the assumption that pressure effects on

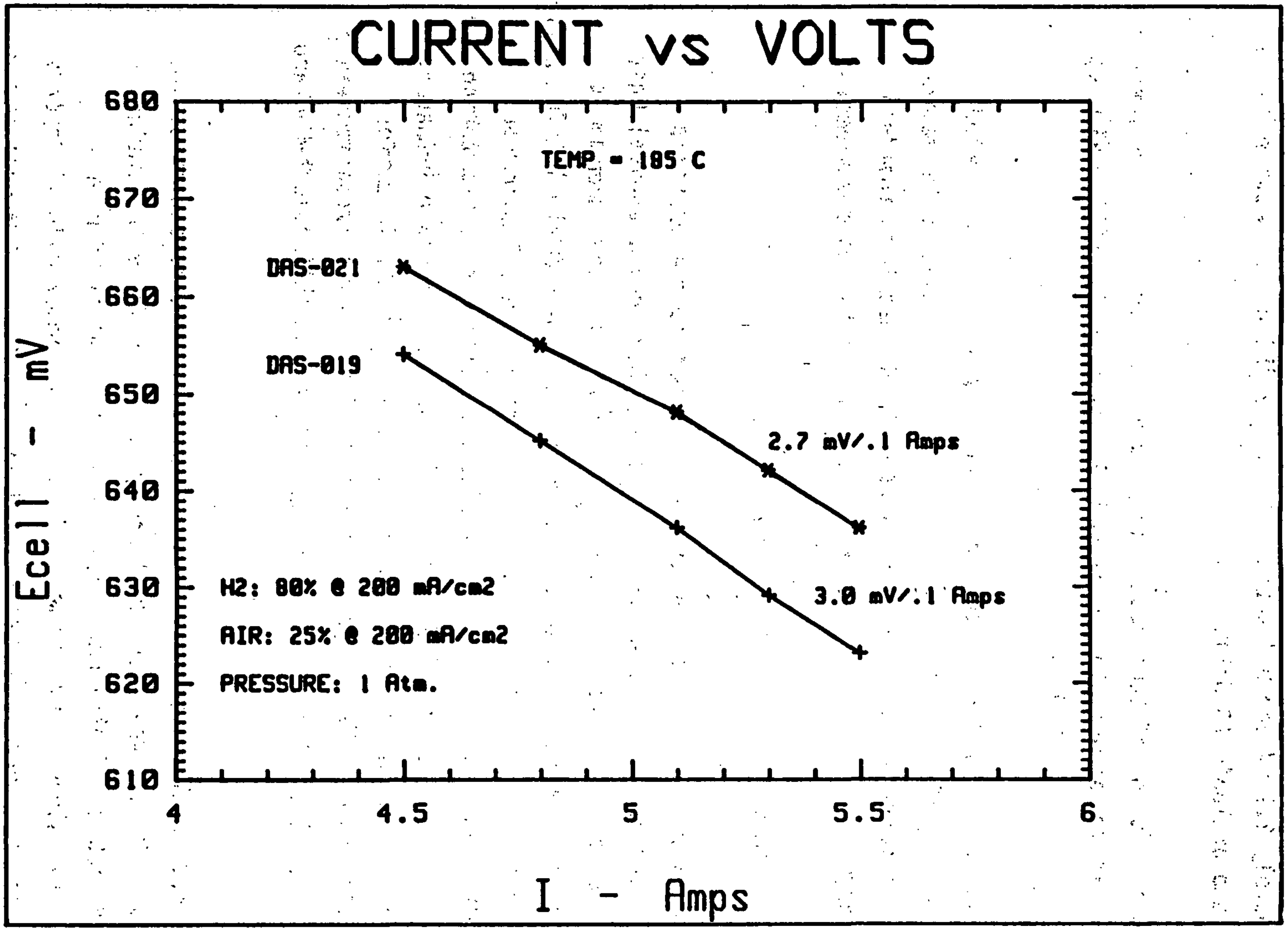

Figure 3-3. Cell Voltage as a Function of Current at 185°C

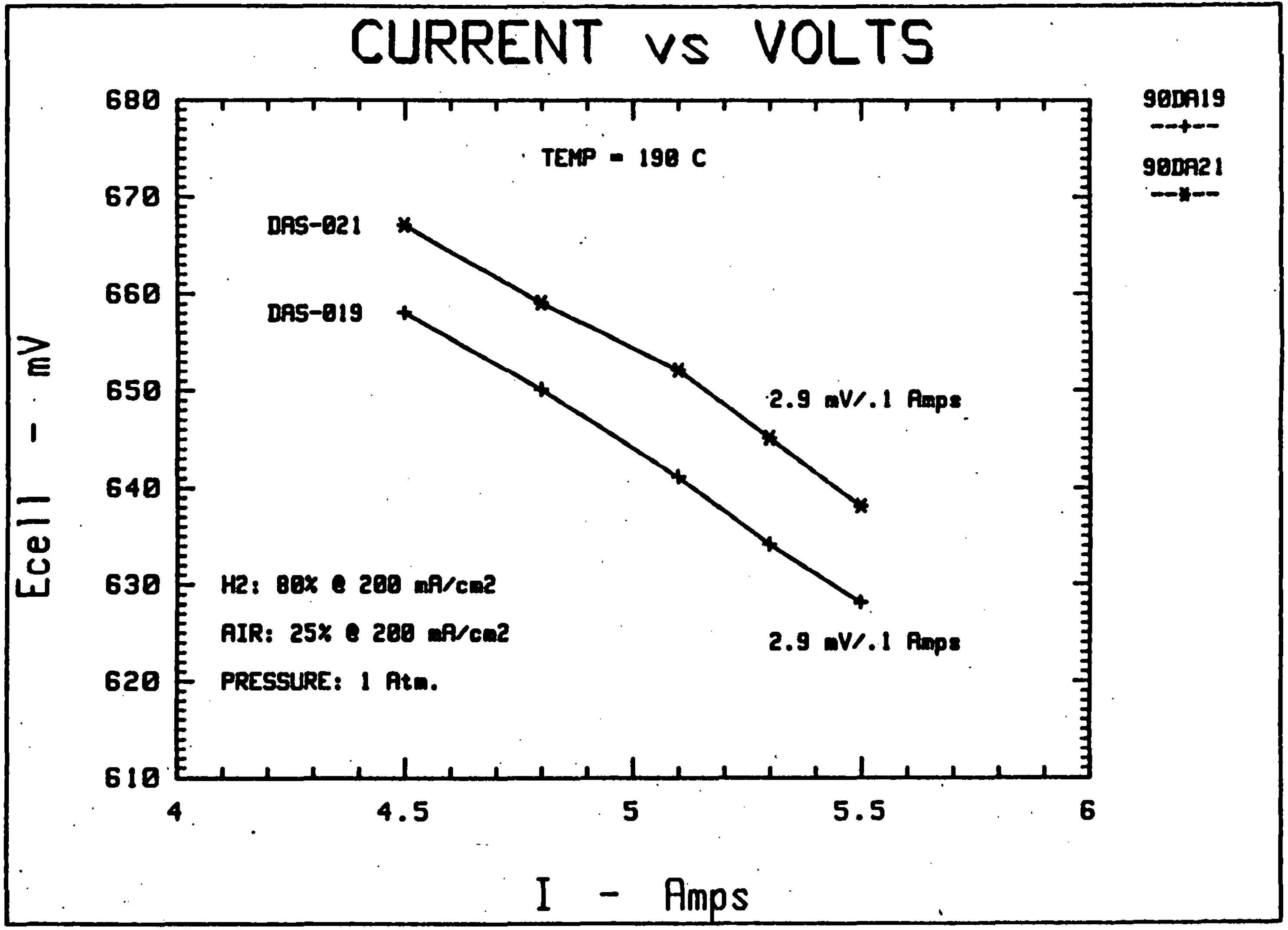

Figure 3-4. Cell Voltage as a Function of Current at 190°C

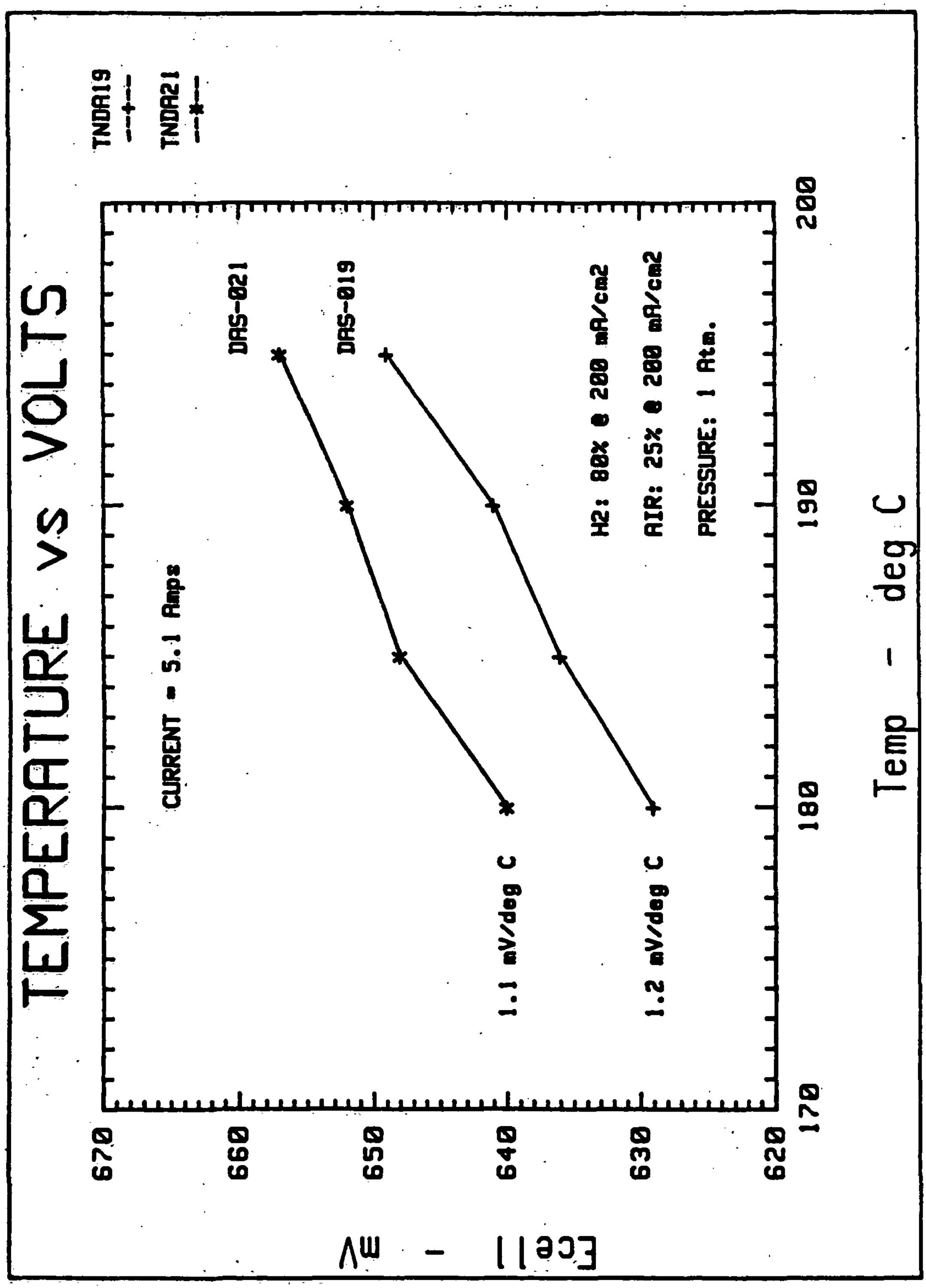

Figure 3-5. Cell Voltage as a Function of Temperature

the activation and concentration overpotentials of the hydrogen electrode are small and can be neglected, the mathematical equation for predicting voltage increase resulting from pressurization was re-examined. At low current densities, where the concentration overpotentials of air electrodes are small, the expected voltage gain is given by:

$$\Delta Ep = [2.3\ RT\ (2 + 4/\alpha_c)/4F)]\cdot\log P \qquad [1]$$

where P is the operating pressure in atmospheres, α_c denotes the apparent transfer coefficient for oxygen reduction, and F is Faraday's constant. In practice, α_c is obtained from the measured Tafel slope b_c using the expression:

$$\alpha_c = 2.3\ RT/(b_cF) \qquad [2]$$

Using an average Tafel slope of 108 mV/decade, the cell voltage gains at various pressures were calculated using equation [1] and the solid line in Figure 3-7 shows this gain. The experimental voltage gains at current densities of 100, 200 and 325 mA/cm^2 are presented in Figure 3-8. At both 100 and 200 mA/cm^2 (93 and 186 A/ft^2), the observed voltage gains are in excellent agreement with those predicted by equation [1]. Thus indicating that, in the operating current density range where cell voltage losses are mainly due to the activation overpotentials at the cathode, Eq. [1] predicts the gains from pressurization.

As shown in Figure 3-8, the voltage gains at 325 mA/cm^2 (300 A/ft^2) are slightly higher than predicted by Eq. [1]. Pressurization results in increased oxygen solubility which, in turn, reduces the concentration overpotential. Thus, the additional voltage gains at higher current densities are presumably attributed to the reduction of concentration overpotentials at the cathode.

The influence of operating pressure on cell internal resistance is given in Figure 3-9. Increasing pressure from 101 kPa to 240 kPa (1 atm to 2.4 atms)

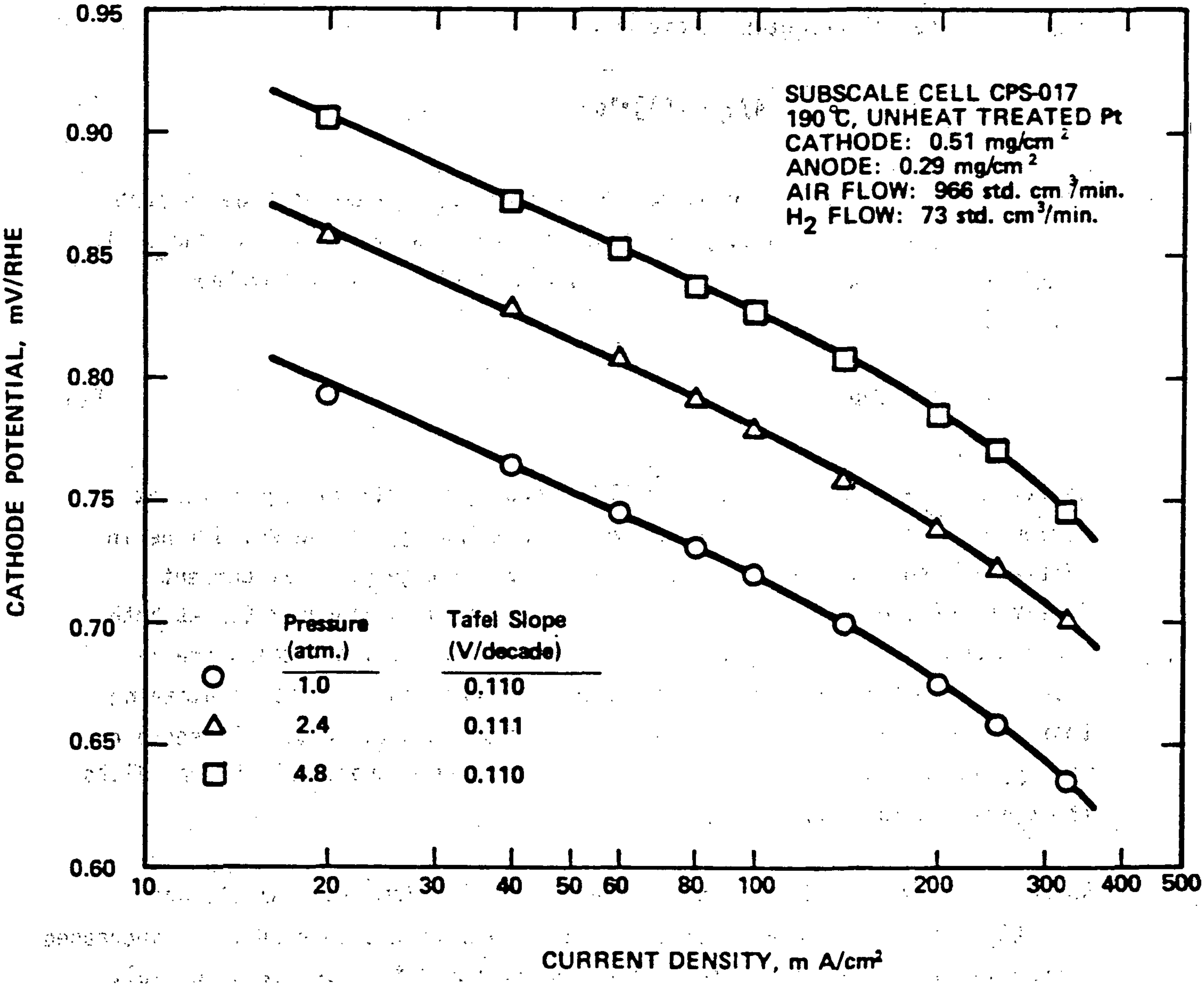

Figure 3-6. Tafel Plots for Oxygen Reduction on a Fuel Cell Cathode at 1.0, 2.4, and 4.8 atm

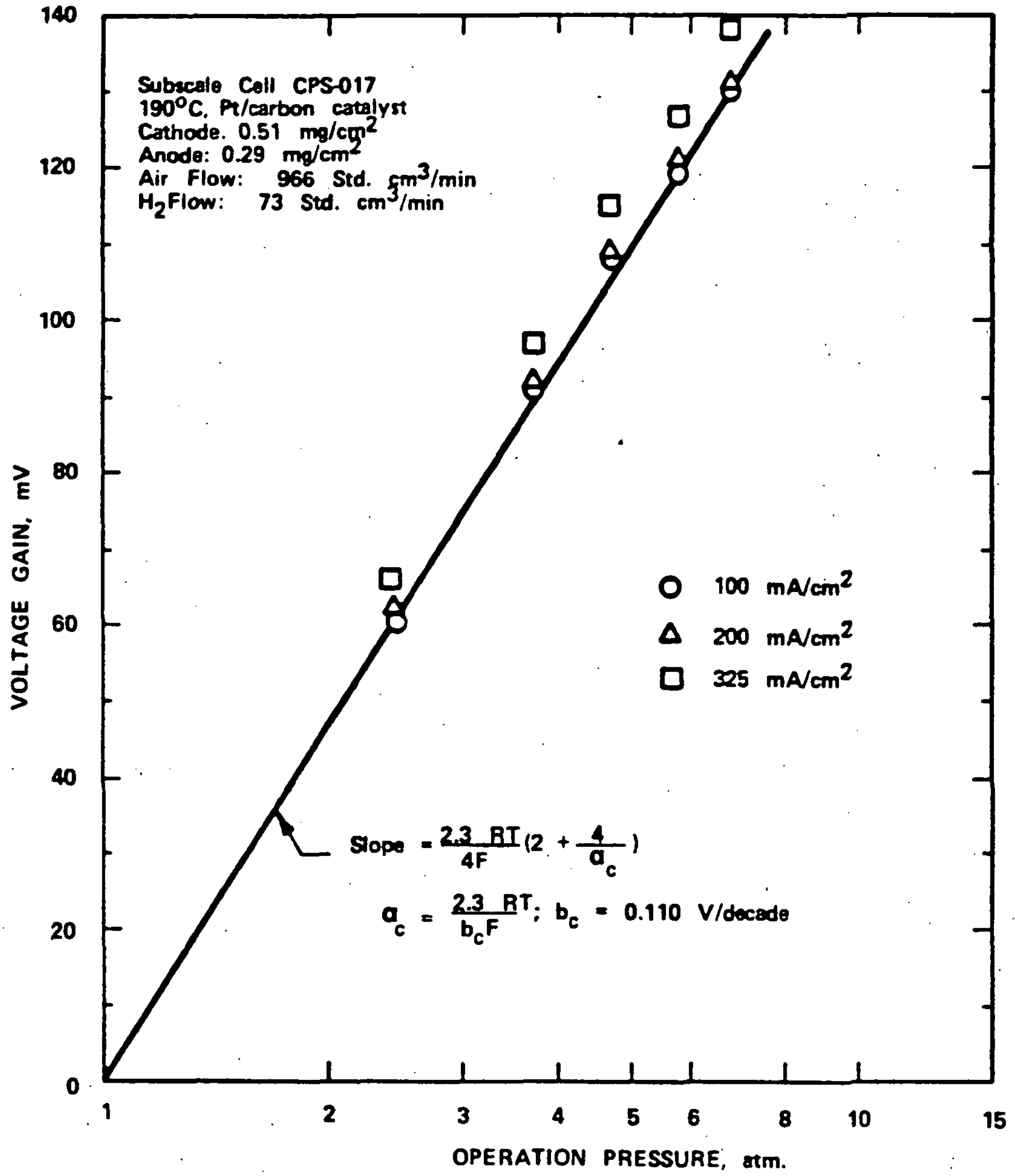

Figure 3-7. Variation of the Measured and Predicted Cell Voltage Gains with Operating Pressure

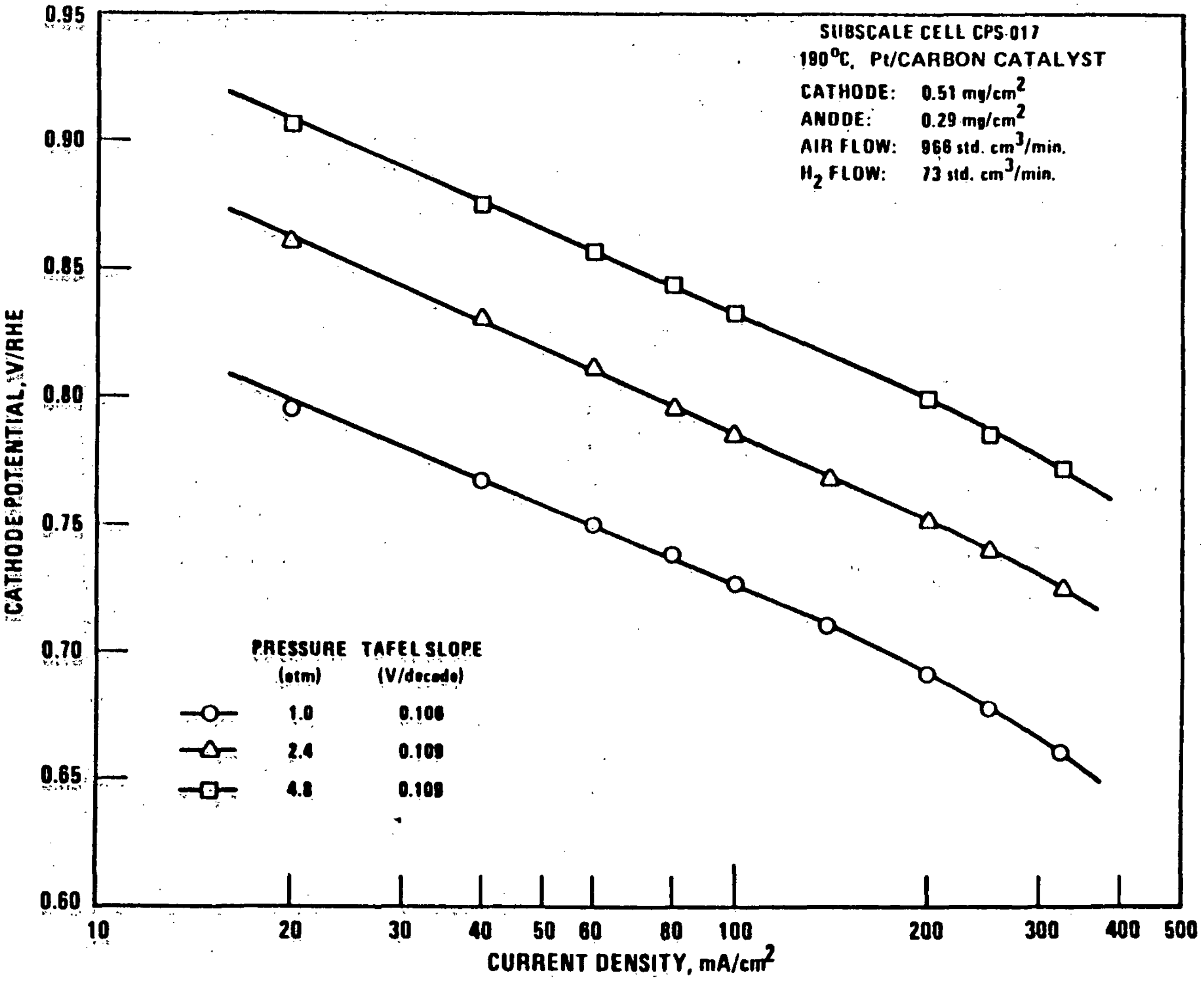

Figure 3-8. Effect of Pressure on Tafel Slopes

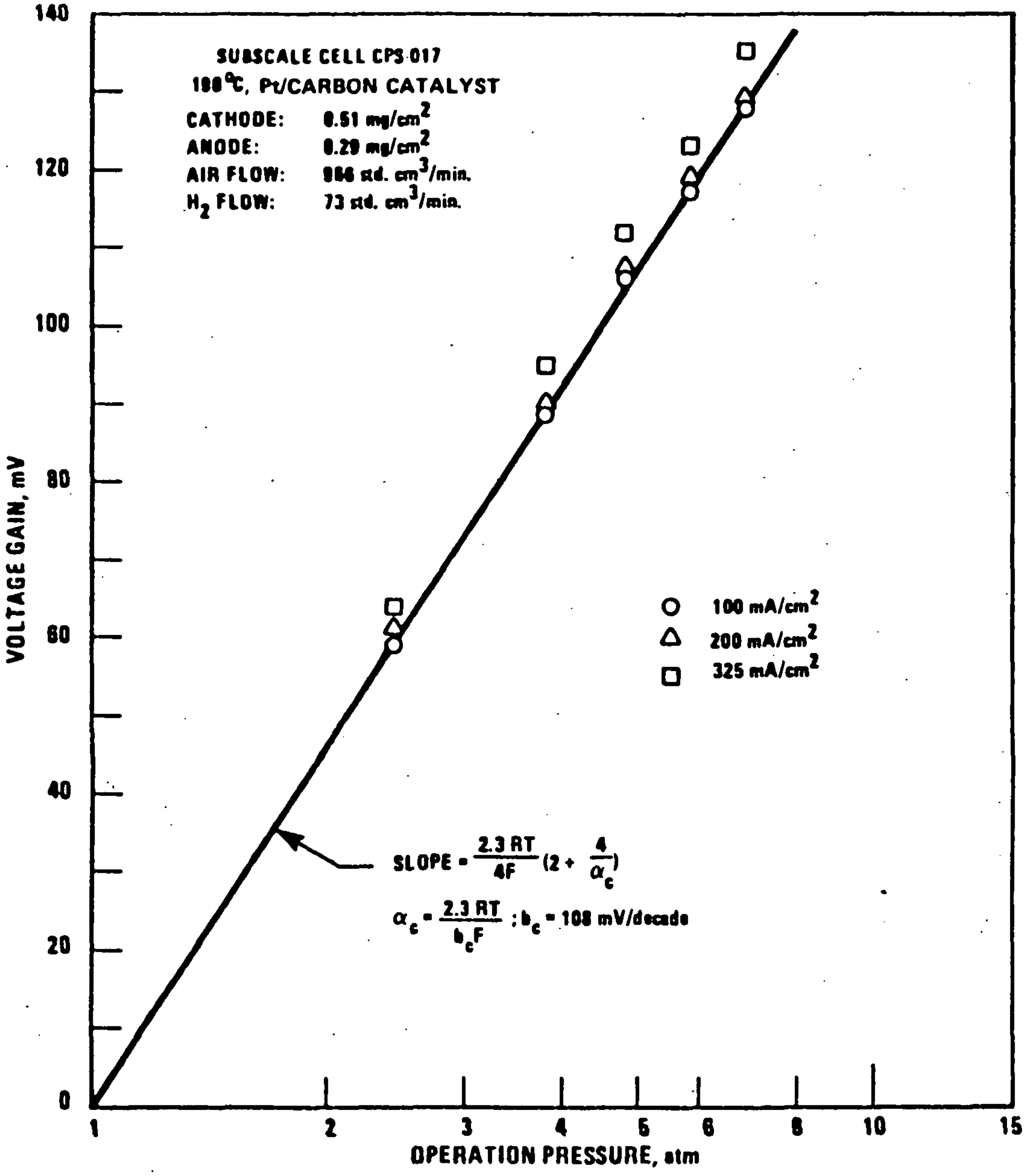

Figure 3-9. Voltage Gain at Various Pressures

results in a relatively significant decrease in cell resistance. At 100 mA/cm^2 (93 A/ft^2), for example, the resistance drops from about 10.5 mΩ to 9.0 mΩ, while above 303 kPa (3 atms), the measured resistance is relatively independent of pressure. This behavior is related to the acid concentration decreasing with increased pressure, essentially due to increased partial pressure of water vapor at higher pressures. As has been well documented, the electrical conductivity of H_3PO_4 increases with decreasing concentration in the range of 86-102 w/o. Under pressurization, the decreased cell internal resistance is primarily associated with decreased acid concentration.

At higher current densities from 200 - 400 mA/cm^2 (186-372 A/ft^2) and pressures above 240 kPa (2.4 atm), an empirical equation for total cell voltage gain from pressurization was derived by taking into consideration the combined effect of pressure on the Nernst potential, cell internal resistance, and both activation and concentration overpotentials at the cathode, namely:

$$\Delta E_{cell} = (2.3\ RT/4F)\cdot(2 + 4\ \alpha_c)\log P + 1.22 \times 10^{-4}\ i + 4.8 \times 10^{-3}\ P - 1.93 \times 10^{-5}\ iP - 1.95 \times 10^{-2} \qquad [3]$$

where i is the current density in mA/cm^2 and P is the operating pressure in atms.

For the apparent average transfer coefficient of 0.85, Table 3-15 compares the measured voltage gains with the cell voltages predicted by both Eqs. [1] and [3]. At 485 kPa (4.8 atm), the observed voltage gains are higher than predicted by Eq. [1] which accounts for voltage gains in reversible potential and activation overpotentials of the cathode. As shown in Table 3-16, the total cell voltage gains given by Eq. [3] are in excellent agreement with the measured values, the gains predicted by Eq. [3] being within ± 2 percent of the measured gains.

TABLE 3-15

COMPARISON OF MEASURED AND PREDICTED CELL VOLTAGE GAINS FROM PRESSURIZATION(1)

Pressure (atm)	Current Density (mA/cm^2)	Measured Cell Voltage gain (mV)	$\Delta E_r + \lvert \Delta \eta_{c,act} \rvert$(2) by Eq. [1] (mV)	Predicted Voltage Gain by Eq. [3] (mV)	Deviation(3) (%)
4.8	100	111	105	111	0.0
4.8	200	115	105	114	-0.9
4.8	325	120	105	118	-1.7
2.4	200	67	58	67	0.0
3.7	200	98	87	96	-2.0
5.8	200	127	117	128	+0.8
6.8	200	137	128	139	+1.5

---

(1) At 190°C, the apparent transfer coefficient $\alpha_c = 0.85$.

(2) $\Delta E_r + \lvert \Delta \eta_{c,act} \rvert$ = the cell voltage gains arising from improvements in Nernst potential and activation overpotentials at the cathode.

(3) Deviation = (predicted voltage gain - measured voltage gain)/(measured voltage gain)

3.1.2.3 Correlation of Performance Decay with Cell Voltage

Electrochemical investigations were completed on the correlation between performance deterioration and cell voltage at ambient pressure, 190°C (374°F), 20 percent air utilization and 80 percent hydrogen utilization. After reproducibility testing at 200 mA/cm^2 (186 A/ft^2) for approximately 1600 hours, three subscale cells SC-037, SC-038 and SC-039 were operated at 80, 100, and 200 mA/cm^2 (75, 93, and 186 A/ft^2), respectively, so that their initial IR-free cell voltages were in the range of 700-800 mV, above 800 mV and below 700 mV. In the course of testing these cells, 100 w/o H_3PO_4 was added twice to the cell acid reservoirs. Electrode flooding was found in SC-039 after ∿1850 hours of continuous operation. The IR-free cell voltages and internal resistances are depicted as a function of time (up to ∿2400 hours) in Figures 3-10 and 3-11, respectively.

With an initial IR-free cell voltage above 800 mV, subscale cell SC-037 exhibited a performance deterioration rate as high as 6.0 mV/1000 hours (see Figure 3-10). At 80 mA/cm^2 (75 A/ft^2), the IR-free cell voltage of SC-038 decreased with time at ∿2.1 mV/1000 hour. Prior to electrode flooding, however, the performance deterioration rate of SC-039 operating at 200 mA/cm^2 (186 A/ft^2) was only ∿1.6 mV/1000 hour.

As shown in Figure 3-11, the in-test addition of phosphoric acid resulted in no beneficial effect on the internal resistances of SC-037 and SC-038. After refilling the acid reservoirs with H_3PO_4, the internal resistance of SC-039 decreased ∿0.5 mΩ, indicating that electrolyte dryout may have occurred in this cell. As seen in Figure 3-11, however, the measured internal resistance of SC-069 continued to increase with time.

3.1.2.4 Dependence of Cell Performance on Hydrogen Utilization

The effect of hydrogen utilization on cell performance was re-examined in subscale cells ERC-3036 and CPS-023. [Note that cell ERC-3036 was previously tested at Energy Research Corporation for about 700 hours and was transferred

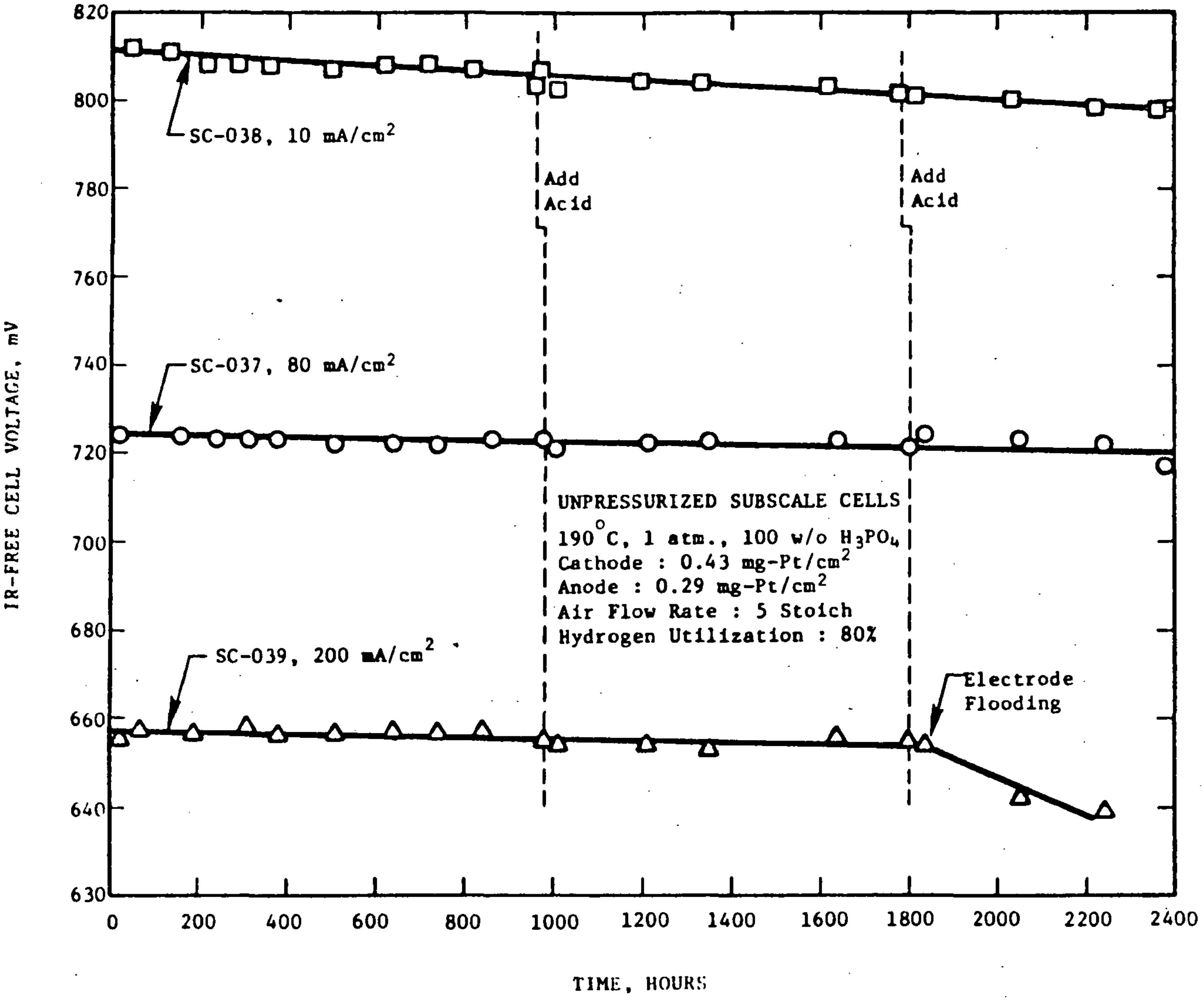

Figure 3-10. Variation of IR-Free Cell Voltage With Time

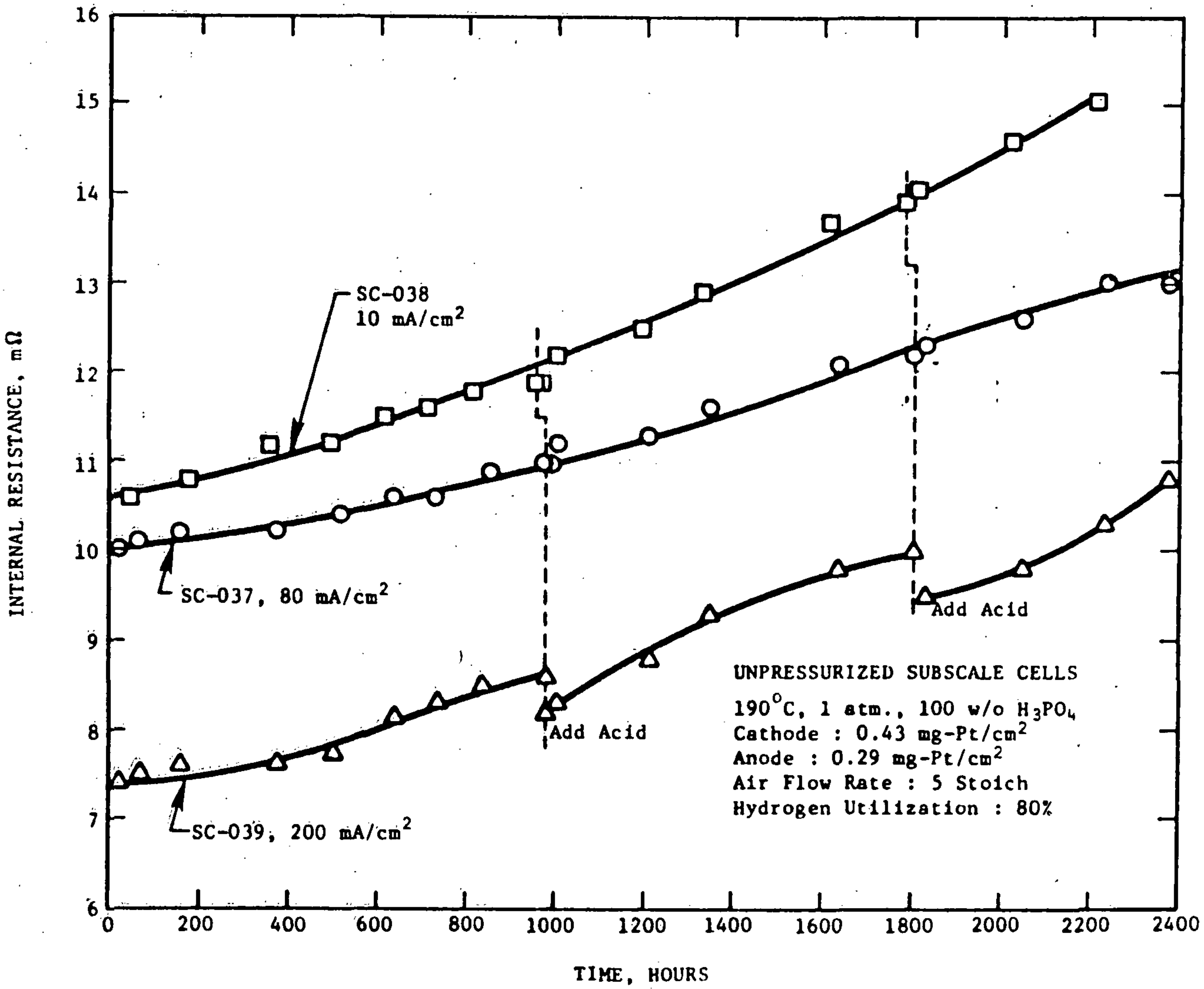

Figure 3-11. Variation of Internal Resistances With Time

to WAESD for testing.] At a constant current density of 200 mA/cm^2 (186 A/ft^2) and air flow rate of 32.8 cm^3/min (2 in^3/min) (25 percent utilization), experiments were performed using hydrogen and SRG (simulated reformer gas containing 74 percent hydrogen, 25 percent CO_2 and 1 percent CO). With hydrogen as fuel, the cell voltage remained constant with increasing utilization up to 90 percent, but it started to drop significantly for a utilization of 92 percent. In the case of SRG fuel, the cell voltage decreased linearly at approximately 1 mV per each 10 percent increase in hydrogen utilization over the range 20 - 70 percent utilization. Above 70 percent utilization, cell voltage decreased more rapidly with increasing utilization, presumably due to the CO blocking and/or poisoning effects on the platinum catalyst.

3.2 Nine Cell Stack Development (WBS 1103-02)

3.2.1 Design Developments

In accordance with the performance goals established for the prototype powerplant, the primary objectives of the nine cell stack developmental effort were to:

- establish startup and operating procedures for pressurized stack testing
- establish baseline performance, reproducibility and endurance at rated power operating conditions
- increase stack average cell performance to 680 mV at operating conditions of 480 kPa (70 psia), 190°C (374°F), 325 mA/cm^2 (300 A/ft^2), 83 percent fuel (SRG) and 50 percent air utilizations with a maximum degradation rate of 2 mV/1000 hours of operation.

The nine cell stack design, developed during the First Logical Unit of Work, was refined and developed further. The refinements were primarily in the areas of electrode edge seal improvements, acid transport improvements within the cells, and manifold sealing. Additionally, some minor changes were incorporated into the design to address performance problems primarily affecting end cells of numerous stacks.

3.2.1.1 Nine Cell Stack Elastomer Edge Seal Development

The initial nine cell stack design incorporated elastomer cell edge seals of a single thickness at each edge of the electrode pair. The seal thickness exceeded the thickness of the electrode pair to provide a compressed edge seal. The seals provided edge sealing only and did not prevent internal crossleaks within the seal boundary at the edge of the electrode pair. Edge crossleaks were to be prevented by application of a sealant material along the edges of each electrode. Problems with obtaining an effective edge sealant application caused this design to be abandoned after testing only one stack during the First Logical Unit of Work.

The elastomer cell edge seal design was revised to address the problem of internal crossleak at the edge of the electrode pair. The single thickness edge seal was replaced by a double layer seal. The thickness of each layer was sized to the thickness of the corresponding cell component (electrode or electrode and MAT-1). One seal was made wider than the other for the seal to overlap the edge of the electrode to block crossleak at the edge of the electrode. Figure 3-12C illustrates a typical section through a cell with the overlapped double Viton seal as compared to Figure 3-12A, which illustrates the standard Teflon and MAT-1 seal arrangement, and Figure 3-12B, which illustrates the single thickness Viton seal.

A 10 cm by 10 cm (4 in. by 4 in.) single cell was built to assess the sealability of the overlap design against crossleak before the nine cell stack design was revised. For this test, the proposed overlap condition was duplicated on all four sides of the electrode pair, which was assembled with acid-wetted MAT-1. Pressurized helium gas was then introduced to one side of

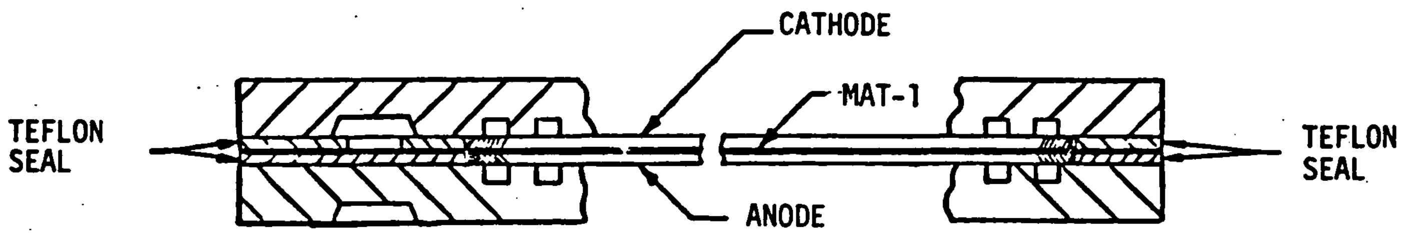

A. TEFLON DESIGN - STACKS W009-01, 02, & 04 THRU 07.

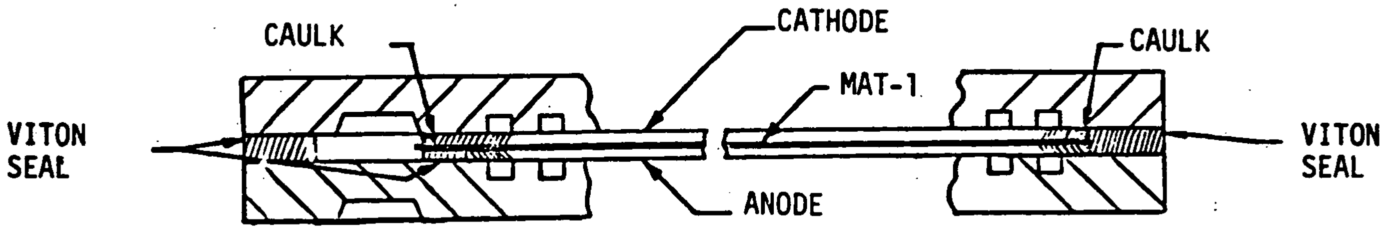

B. VITON DESIGN - STACK W009-03.

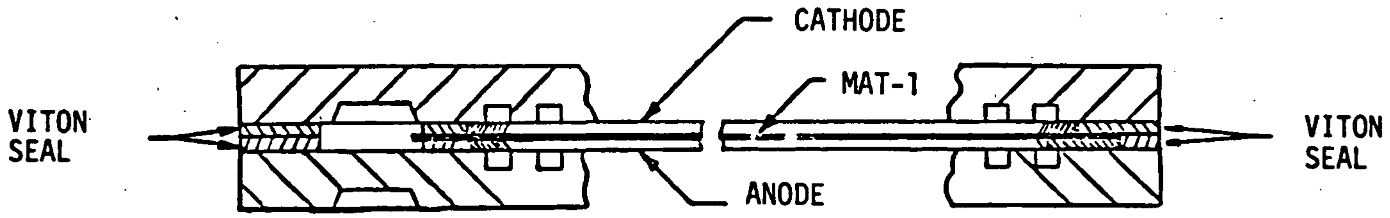

C. VITON DESIGN - STACKS W009-08.

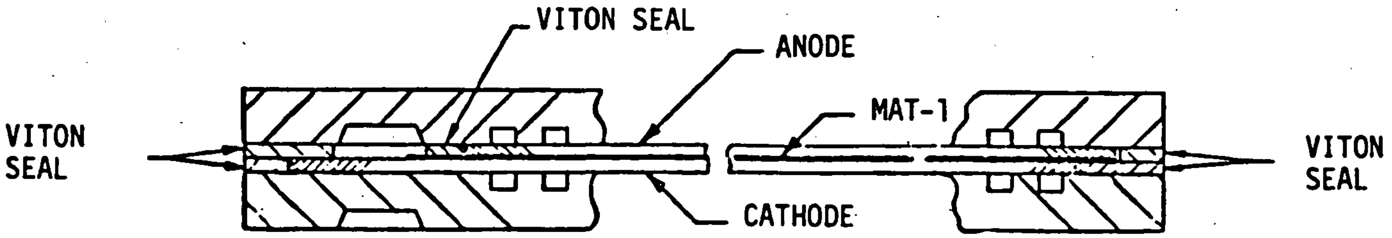

D. VITON DESIGN - STACKS W009-10 AND 11.

Figure 3-12. Nine Cell Stack Cell Edge Seal Configurations the cell with the other side connected to a manometer. The helium source and manometer were then interchanged and the test repeated. For both tests, the cell and seal withstood a maximum 6.9 kPa (10 psi) differential with no observable leakage. Tests were performed at room temperature only.

Following the success of the single cell test, a five cell engineering stack was built to develop the manufacturing techniques and to test a multi-cell stack which had acid applied with the standard syringe technique. This technique was considered to provide less uniform acid wetting than that used for the 10 cm by 10 cm (4 in. by 4 in.) test assembly in which the MAT-1 was floated on acid for uniform wetting. Helium leak testing was performed on the five cell stack using the same methods as applied to all previous nine-cell stacks. At helium pressures up to 356 mm (14 in.) of water, crossleaks of less than 20 cm^3/min (72 ft^3/h) were measured. This was considered quite satisfactory in comparison to crossleak results obtained with previous stacks built with the standard Teflon and MAT-1 edge seal design. The nine cell stack drawings were revised to reflect the double layer Viton seal. The first application of the design to an operating nine cell stack was W009-08.

A second major change to the basic cell design is illustrated in Figures 3-12, 3-13, and 3-14. The cell assembly (anode, MAT-1, cathode) between the bipolar plates was inverted and the cathode was extended below the acid channel in the upper plate. Thus, the acid supplied through the acid channel directly contacts the silicon carbide layer of the cathode. The silicon carbide layer serves as the primary acid transport member for the cell and addition of acid to an assembled cell is significantly improved by this change. As shown in Figure 3-12, all previous cell designs suffered from poor lateral acid transport because the acid had to first move laterally through a length of MAT-1 until contact with the silicon carbide layer was made. Independent tests to assess lateral acid transport rates associated with both MAT-1 and silicon carbide have shown that the MAT-1 has a slower rate. As shown in Figure 3-14, the feature of MAT-1 extending beneath the seal inboard of the acid channel has been retained in the revised design. The MAT-1 serves as the

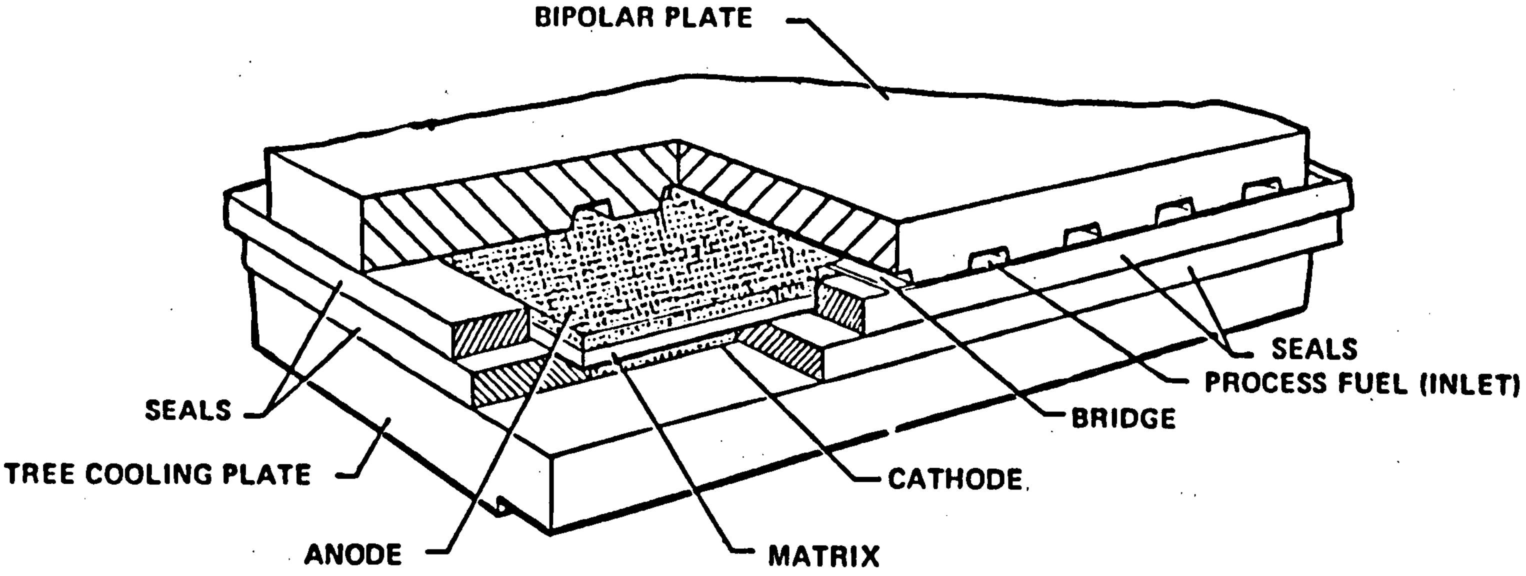

Figure 3-13. Fuel Cell Resilient Seal Arrangement

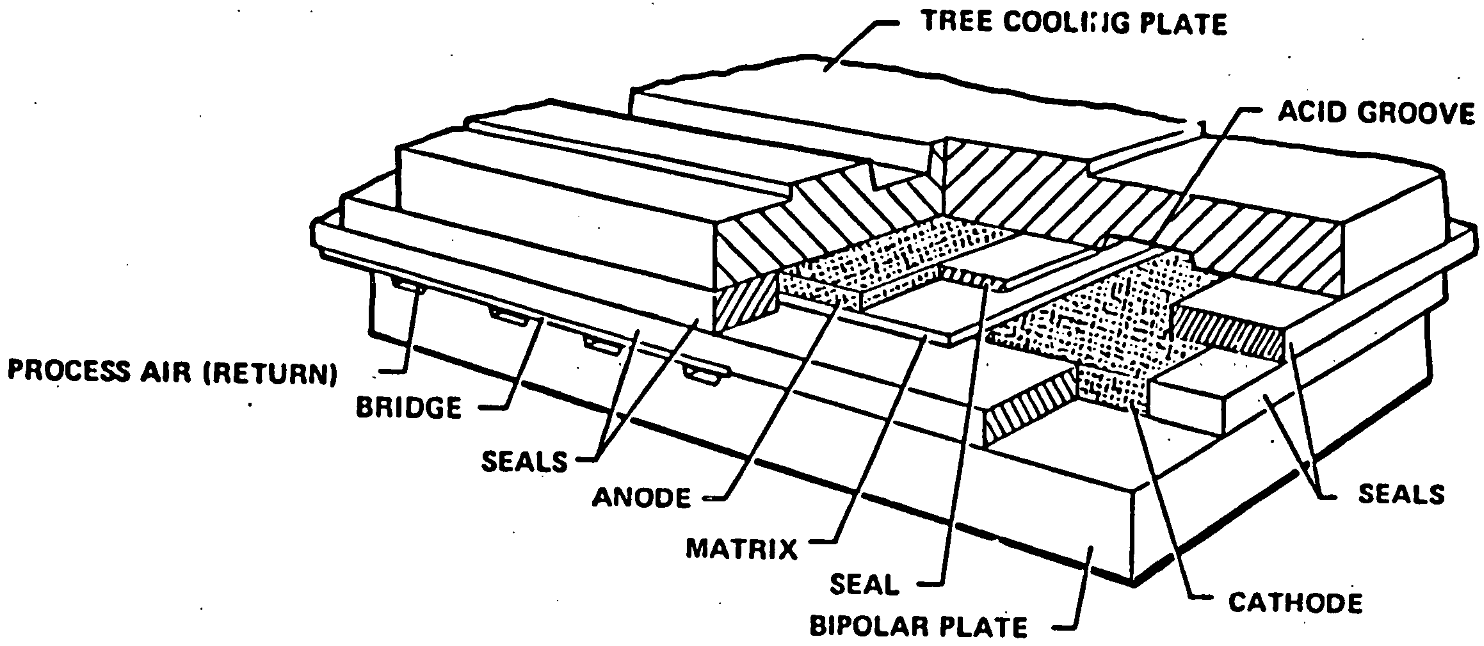

Figure 3-14. Fuel Cell Resilient Seal Arrangement at Acid Groove

main barrier to anode/cathode crossleak at the joint between anode and seal, and it also cushions and prevents damage to the silicon carbide layer of the cathode caused by seal edge shearing effects.

The inverted cell design has been used in three stacks built to date; Stacks W009-09, -10, and -11. However, only Stacks W009-10 and -11 employed a MAT-1 layer as shown in Figure 3-14. Stack W009-09 was assembled without MAT-1, but with a thicker silicon carbide layer, to test the feasibility of stack operation without MAT-1. Acid additions to these stacks after assembly have been successfully performed within much shorter time periods, whereas for prior stacks, acid additions were difficult to perform in a reasonable time period. The acid addition data for individual stacks is provided in Table 3-16.

3.2.1.2 Nine Cell Stack Manifold Seal

Limited process gas manifold seal tests were performed in the dry room on Stack W009-09 after initial performance tests. The purpose of these tests was to begin building seal leak test experience on a relatively inexpensive test bed and to identify seal configurations for further development on the 10 kW "Metal Stack" (Section 3.3.1). Seals of Viton elastomer (both O-rings and flat gaskets) and expanded Teflon ("Gore-Tex" joint sealant) were tested. To test O-rings, a special gasket/frame (Figure 3-15) was made with standard O-ring grooves on both sides to seal between the stack to frame and frame to manifold. Prior to starting the tests, the frame to flat aluminum manifold joint was proven to be leak tight. The "Gore-Tex" and flat gaskets were applied directly to the manifold. Tests were performed at 150°C to insure that the standard gaskets (uncured Viton sheets) on the end not being tested would remain leak tight. The test results are summarized on Table 3-17. These tests show that flat, cured Viton 0.32 cm (.125 in.) thick by 0.64 cm (.25 in.) wide produces a good seal, two layers of 0.48 cm (.189 in.) "Gore-Tex" shows some promise, and 75 durometer O-rings with standard compression (25 percent) is not an acceptable seal. These test results were further verified by the "Metal Stack" tests (Section 3.3.1).

TABLE 3-16

STACK ASSEMBLY COMPARISON

	UNITS	W009-01	W009-02	W009-03	W009-04	W009-05	W009-06	W009-07	W009-08	W009-09	W009-10	W009-11
BIPOLAR PLATES												
Material		A99	→	→	→	→	→	→	A99 Regrind	→	→	→
Manufacturing Type		Machined	→	→	→	→	→	→	Molded Z/Molded Z	→	→	→
Heat Treatment Temp	°C	900	→	→	→	→	→	→	900	→	→	→
Nominal Thickness Range	cm	-	.310/.330	.318/.368	.309/.323	.292/.319	.318/.328	.318/.333	.324/.328	.323/.340	.318/.330	.328/.335
Nominal Active Area	cm²	1080	→	→	→	→	→	→	1045	→	→	→
Graphite Bridges		No	No	Yes	→	→	→	→	→	→	→	→
Recessed Zee or Flat	R or F	R	R	F	→	→	→	→	→	→	→	→
COOLING PLATES												
Material		A99	→	→	→	→	→	→	A99 Regrind	→	→	→
Manufacturing Type		Machined	→	→	→	→	→	→	Molded Z/Machined Tree	→	→	→
Heat Treatment Temp	°C	900	→	→	→	→	→	→	900	→	→	→
Nominal Thickness Range	cm	-	.467/.480	.467/.478	.398/.443	.376/.384	.401/.414	.391/.406	.403/.409	.406/.411	.404/.417	.409/.439
Nominal Active Area	cm²	1080	→	→	→	→	→	→	1045	→	→	→
Graphite Bridges		No	No	Yes	→	→	→	→	→	→	→	→
Recessed Zee or Flat	R or F	R	R	F	→	→	→	→	→	→	→	→
END PLATES												
Material		A99	→	→	→	→	→	→	A99 Regrind	→	→	→
Manufacturing Type		Machined	→	→	→	→	→	→	Molded Z/Machined Tree	→	→	→
Heat Treatment Temp	°C	900	→	→	→	→	→	→	900	→	→	→
Nominal Thickness Range	cm	-	.485/.490	.495/.498	.406/.419	.400/.410	.406/.411	.411/.414	.401/.408	.422/.424	.406/.409	.406
Nominal Active Area	cm²	1080	→	→	→	→	→	→	1045	→	→	→
Graphite Bridges		No	No	Yes	→	→	→	→	→	→	→	→
Recessed Zee or Flat	R or F	R	R	F	→	→	→	→	→	→	→	→
CELL EDGE SEALS												
Material		Teflon TFE	→	Viton	Teflon TFE	→	→	→	Viton	→	→	→
Design (See Fig. 3-12)		(1)	(1)	B	A	→	→	→	C	(2)	D	D
Thickness - Anode (3)	mils	2/3	5	-	17	17	17	17	31/33 C	19/21 P	32/34 P	
- Inboard Acid Groove (3)	mils									19/21 P		19/21 P
- Cathode (3)	mils	10	11	-	27	26	30	29	31/33 C	36/38 M	32/34 P	
Bonding Material		Viton Cement	→	→	→	→	3M 1300 L	Viton Cement	→	→	→	→
ANODES												
Catalyst		10% Pt on XC72	→	→	→	→	→	→	→	10% Pt on XC72	→	→
Catalyst Heat Treatment	°C	None	→	→	→	→	→	→	→	None	→	→
Backing Paper		Stackpole PC206	→	→	→	→	→	→	→	Stackpole PC206	→	→
Wet Proofing Method		FEP Double Dip	→	→	→	→	→	→	→	FEP Double Dip	→	→
Lamination Method/Press.	Ton	Wet @ 30	→	→	→	→	→	→	→	Wet @ 30	→	→
Sinter Atmosphere & Temp	°C	Air @ 360	→	→	→	→	→	→	→	Argon @ 360	→	→
Final Thickness Range	mils	19/21	19/20	18/20	18/20	18/21	19/22	19/20	19/23	19/21	20/22	19/20

(1) Design similar to Figure 3-12A, but edges of plates raised. Thus, thinner seals were required.
(2) Design similar to Figure 3-12D, but without MAT-1. Thus, seal thickness adjusted.
(3) P = Pelmor Viton; M = Mosites Viton; C = Commercial Grade Viton.

TABLE 3-16

STACK ASSEMBLY COMPARISON (CONT'D)

	UNITS	W009-01	W009-02	W009-03	W009-04	W009-05	W009-06	W009-07	W009-08	W009-09	W009-10	W009-11
CATHODES												
Catalyst		10% Pt on XC72	→	→	→	→	→	→	→	10% Pt on XC72	→	→
Catalyst Heat Treatment	°C	None	→	→	→	→	→	→	→	900	→	→
Backing Paper		Stackpole PC206	→	→	→	→	→	→	→	Stackpole PC206	→	→
Wet Proofing Method		FEP Double Dip	→	→	→	→	→	→	→	FEP Double Dip	→	→
Lamination Method/Pressure	Ton	Wet @ 30	→	→	→	→	→	→	→	Dry @ 30	→	→
Sinter Atmosphere & Temp	°C	Air @ 360	→	→	→	→	→	→	→	Argon @ 360	→	→
Final Thickness Range	mils	29/32	30/32	30/33	28/31	28/30	30/32	28/31	27/30	31/34	30/33	28/29
SiC Thickness Range	mils	5/6	→	→	→	→	→	→	→	7/9	8	5/6
MAT-1												
Manufacturing Type		Ross Blender	→	Expmt'l. Schold Mixer	→	→	→	→	→	-	Schold	→
Teflon Percent	%	3	→	→	→	→	→	→	→	-	3	→
Final Thickness Range	mils	9/12	-	10/11	10/11	10/11	10/11	9/10	11	-	10/11	9/10
ACID LOADING												
Anode Application	cm^3	0	→	→	→	→	→	→	→	→	→	→
Cathode (SiC) Application	cm^3	15	13	13	10	10	13	10	10	27	15	→
Matrix (MAT-1) Application	cm^3	24.5	35	33	32	35	35	35	32	-	30	→
Acid Groove Application	cm^3	2	2	2	0	1.5	2	1.5	0	0	0	→
Total Cell Application	cm^3	41.5	50	48	42	46.5	50	46.5	42	27	45	→
Acid Concentration	wt. %	94	97	97	93	93	97.3	92.7	92.5	98.4	98	97.8
Acid Supplier		Fisher	→	→	Baker	→	→	→	→	→	→	→
Dry Rm Humidity Range(1)	%	5/7S	→	→	→	13/17S	5/7S	13/17S	13/17S	3.5/6.5	5.5/6.0	5.0/6.5
Added & Retained Before Testing	cm^3	Acid Transport Ineffective	→	→	→	→	→	→	0(3)	5	27	~30
STACK CONDITIONING												
Stack Temperature(1)	°F	180	150	180S	150	128	162	130	130	130	120	130
Conditioning Period	hrs	19	18	~18	19	21	18	16	20	21	20	18
Dry Rm Humidity Range(1)	%	5/7S	→	→	→	13/17S	5/7S	13/17S	13/17S	6.0/12	5.5/6.0	5.0/6.0
STACK COMPRESSION												
Avg. Compression Applied	PSI	50	60	55	50	45	55	55	50	30	40	11
No. Compression Cycles		3	1	→	→	→	→	→	3(2)	2	1	1
Stack Temperature	°F	176	143	178	108	127	168	130	130	130	130	130
Compressed Stack Resist.	mΩ	9.5	~8.5	-	9.9	8.2	7.8	8.6	6.5	24.0	10.0	13.2
Pre-Test Stack Resist.	mΩ	-	6.5	-	6.8	6.5	6.5	7.0	5.5	16.0	8.2	9.2

(1) S = Specification requirement, not actual measurement.
(2) 1st cycle to 15 psi, 2nd from 15 to 30 psi, and 3rd from 30 to 50 psi.
(3) Stack W009-08 expelled 50 cm^3 acid after assembly. Acid added and retained was 50 cm^3 from 0 net addition.

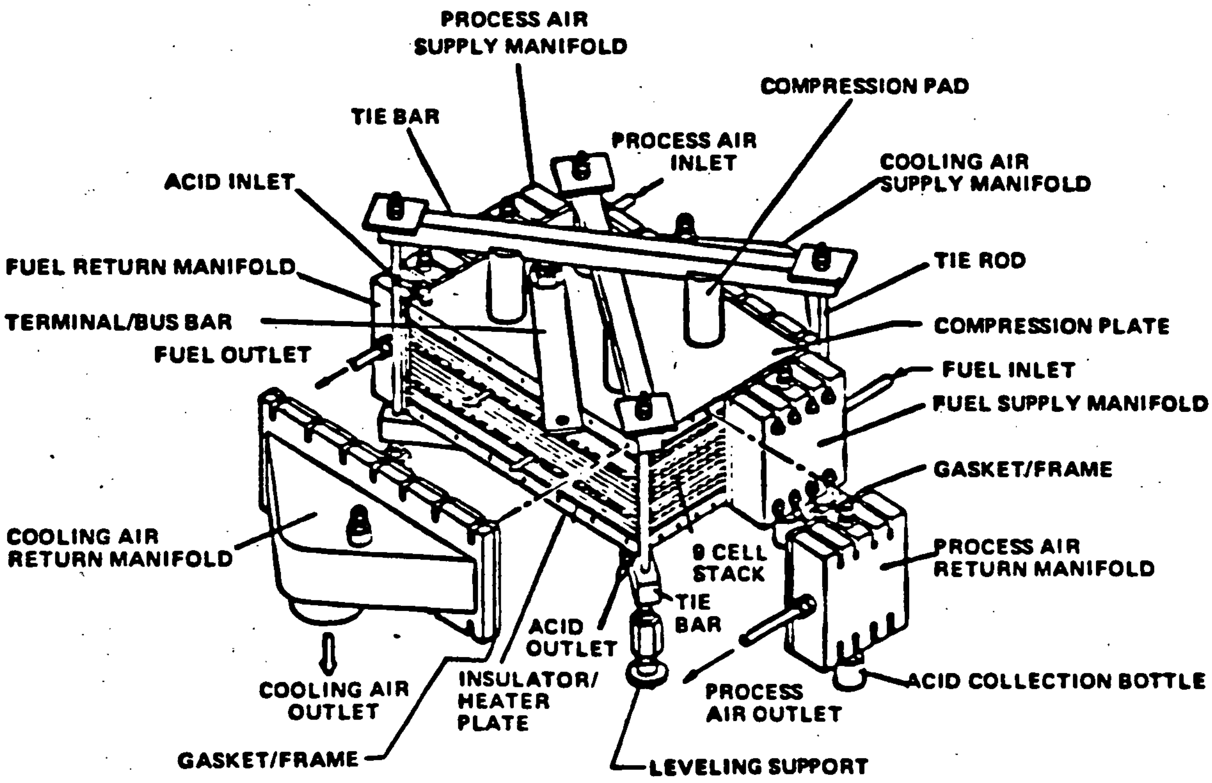

Figure 3-15. Nine Cell Stack Assembly

TABLE 3-17
NINE CELL STACK MANIFOLD SEAL TEST SUMMARY

		External Leakage
1) GORE-TEX 0.32 cm (1/8 in.)		∿< 400 cm^3/min
o Final Manifold to Stack Gap	∿ 0.013 cm (.005 in)	
o Average Seal Width	∿ 0.51 cm (.20 in)	
2) O-RINGS (75 Durometer, 0.53 cm [3/16 in])		∿ 60 cm^3/min
o Standard Compression	∿ 28 percent	
3) GORE-TEX (2 Layers of 0.48 cm (3/16"))		∿ 9 cm^3/min
o Final Manifold to Stack Gap	∿ 0.11 cm (.045 in)	
o Average Seal Width	∿ 0.64 cm (.25 in)	
4) FLAT CURED VITON (2 Layers at 0.16 cm (1/16 in.) Thick by 0.64 cm (1/4 in.), ∿ 50 Durometer		∿ 0 cm^3/min
o Compressed	∿ 40 percent	

NOTE: 1) Extruded edge seal gaskets cut flush with razor blade for all tests.
2) All data at 150°C (300°F).

3.2.1.3 Plate Cracking

Other refinements were made to the nine cell stack design to address performance problems primarily affecting end cells. Cracks were observed in both end plates and cooler plates on a majority of the stacks that had been disassembled following testing. In most cases the cracks were located at the process ends of the plates in the nonfunctional grooves that are there to reduce material thickness for heat treatment purposes. The design of these grooves was modified to reduce the depth and gussets added. Both of these changes are designed to improve the bending capability of the plates near the edges, which are subject to bending moments resulting from gasket loads. The revised design (Figure 3-16) was incorporated into the cooler dies and molded plates will be tested in Stack W009-12 (Third Logical Unit of Work).

In parallel with the above plate design modification, a thicker insulator plate was incorporated in the stack design between each end of the stack and the stack heaters. The thickness was increased as much as practical within the height limits, which are controlled by existing manifolds. The insulation plates were made 3/8 in. thicker at each end. The purpose of this change was to provide more uniform load distribution to the repeating stack components by providing a stiffer member between the stack and the flexible heaters, which do not react well to loading. Also, a single layer of carbon paper was placed between the copper current collector plate and the carbon end plate at each end of the stack. The compressibility of the carbon paper compensates for variations associated with thickness matchup between terminal post foot and the pocket stamped into the collector plate.

3.2.1.4 Stack Assembly Status

During this period of time, five additional nine cell stacks were assembled and tested. Table 3-16 provides a summary of the characteristics for each new stack and also provides a summary for previous stacks to allow comparison.

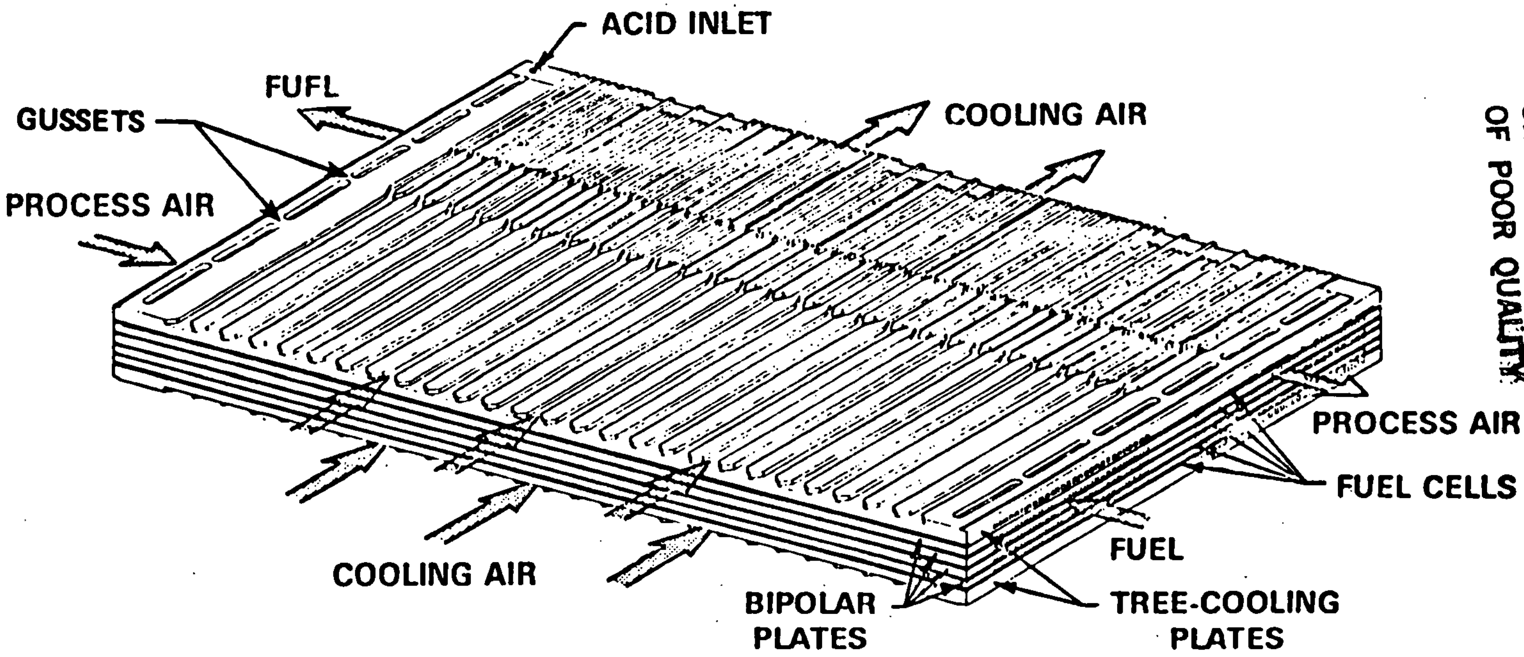

Figure 3-16. Phosphoric Acid Fuel Cell Five Cell Stack

3.2.2 Acid Transport Test Fixture

The Acid Transport Test Fixture was developed to provide a technique for measuring wicking rates and wicking capabilities of various candidate fuel cell matrices. The initial design of the Acid Transport Test Fixture is shown in Figure 3-17.

The test fixture consists, basically, of a single cell combined with the nine cell assembly non-repeating hardware. The anode and cathode end plates were modified to include nine resistance measuring contacts recessed in each of the "A" and "B" faces of the ends plates. The Viton insulations located in the recesses of the plates provide a small spring force to maintain contact between the resistance measuring contacts and the electrodes and insulate the contacts from the end plate. The resistance measuring terminal wires are cemented within the end plate grooves and routed out to a rotary switch. The rotary switch is used to connect the individual pairs of contacts to a milliohmmeter.

An acid level indicator tube is provided at the anode end plate near the acid inlet to monitor the inlet acid head. Three acid level indicator tubes are provided at the cathode end plate in a location opposite to the acid groove to monitor the acid that moves across the cell from the acid groove. The stack assembly heaters are included in the fixture so the wicking process can be observed with the cell at the desired temperature (presently 54°C (130°F)).

The first test was conducted to determine the sensitivity of the technique used to measure the wicking rate and to establish improved techniques for future tests. The test results indicated that the wicking rate measurement technique could be improved by insulating the contacts in the anode end plate from the anode backing paper. This can be achieved by providing an anode with nine 1.3 cm (0.50 in.) diameter cut-outs at the anode resistance measuring contact locations. The cut-outs could be replaced with blotter paper or silicon carbide. Since the cathode backing paper and cathode end plate are both good conductors and make contact with each other, the only resistance measuring connection needed on the cathode side of the fuel cell is to the cathode end plate.

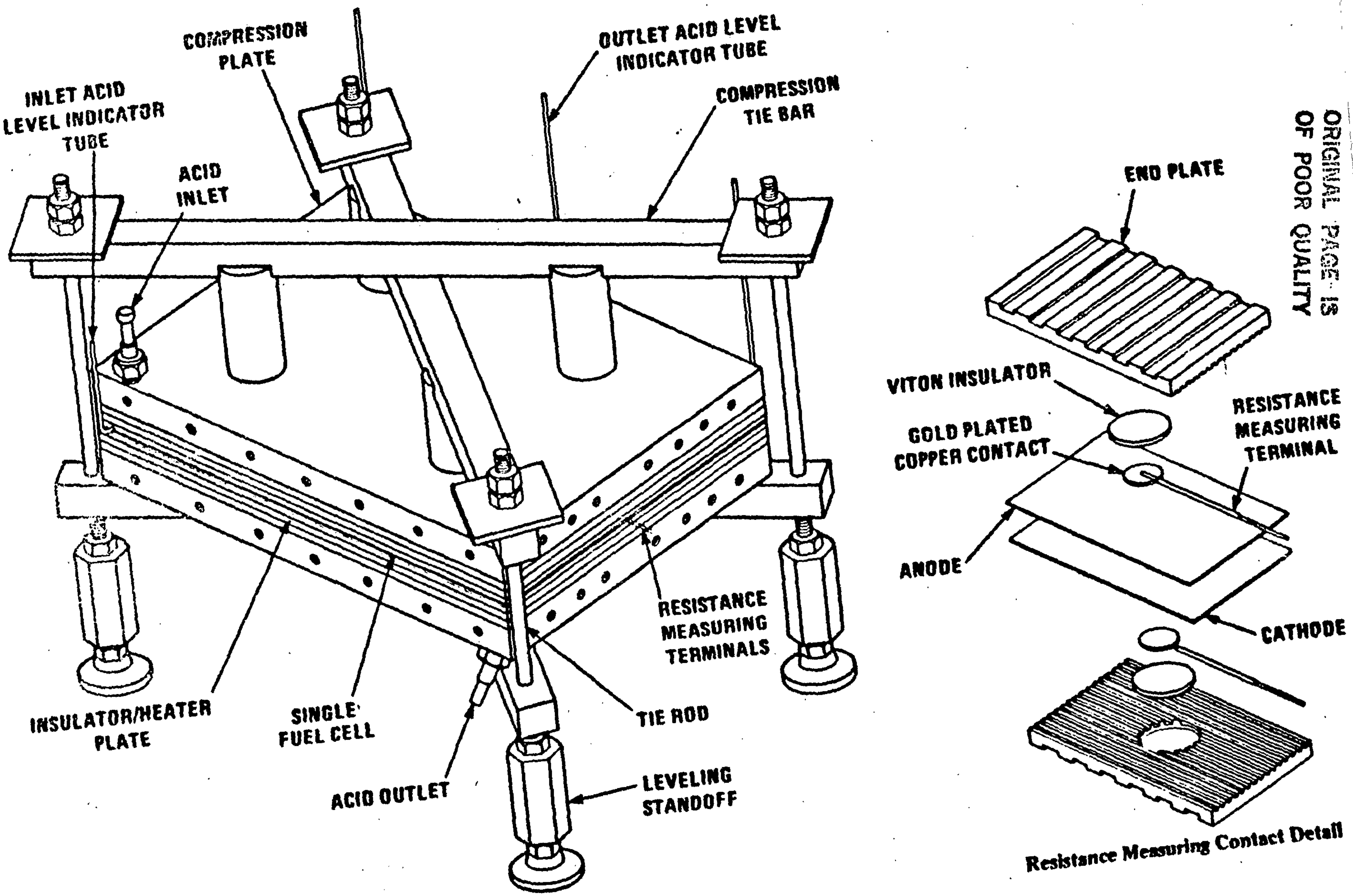

Figure 3-17. Acid Transport Test Fixture

The test results indicated that in a single cell with no MAT-1 the cell resistance after adding acid reduced from 85 mΩ to 10 mΩ in 24 hours. The test results also indicated that with an acid inlet head up to 10 cm (4 in.) and the acid outlet closed off no acid could be forced horizontally out of the opposite edge of the cathode in a 24 hour period. The post test examination after disassembly of the fixture revealed that the acid wicking in the silicon carbide layer of the cathode progressed approximately 2/3 of the distance across the cell.

3.2.3 Acid Delivery System

An Acid Delivery System (Figure 3-18) was designed for bench-top testing in order to obtain design and operational information. The bench-top design was modified to include in-vessel testing in conjunction with a phosphoric acid fuel cell stack and provide startup and operational information for the final design of the acid pumping system.

The pump selected for the bench-top testing is a pneumatically driven commercial metering pump made of PVC material. Although the pump has an adjustable stroke, the volume of fluid delivered (with the shortest stroke possible) is much greater than required for addition to an operating stack. An overflow line from the acid reservoir on top of the stack returns the excess acid to the pump sump outside of the pressure vessel. A metering valve was added between the acid reservoir and the inlet connection on the stack to restrict the flow of acid and allow sufficient time for the excess to flow through the overflow line.

3.2.4 Nine Cell Stack Testing

The overall performance results in the nine cell stack testing activity at Westinghouse are summarized in Table 3-18 and Figure 3-19. Note that Table 3-18 is cumulative from the start of the stack testing program. Details regarding the performance of each nine cell stack tested are given in the sections which follow.

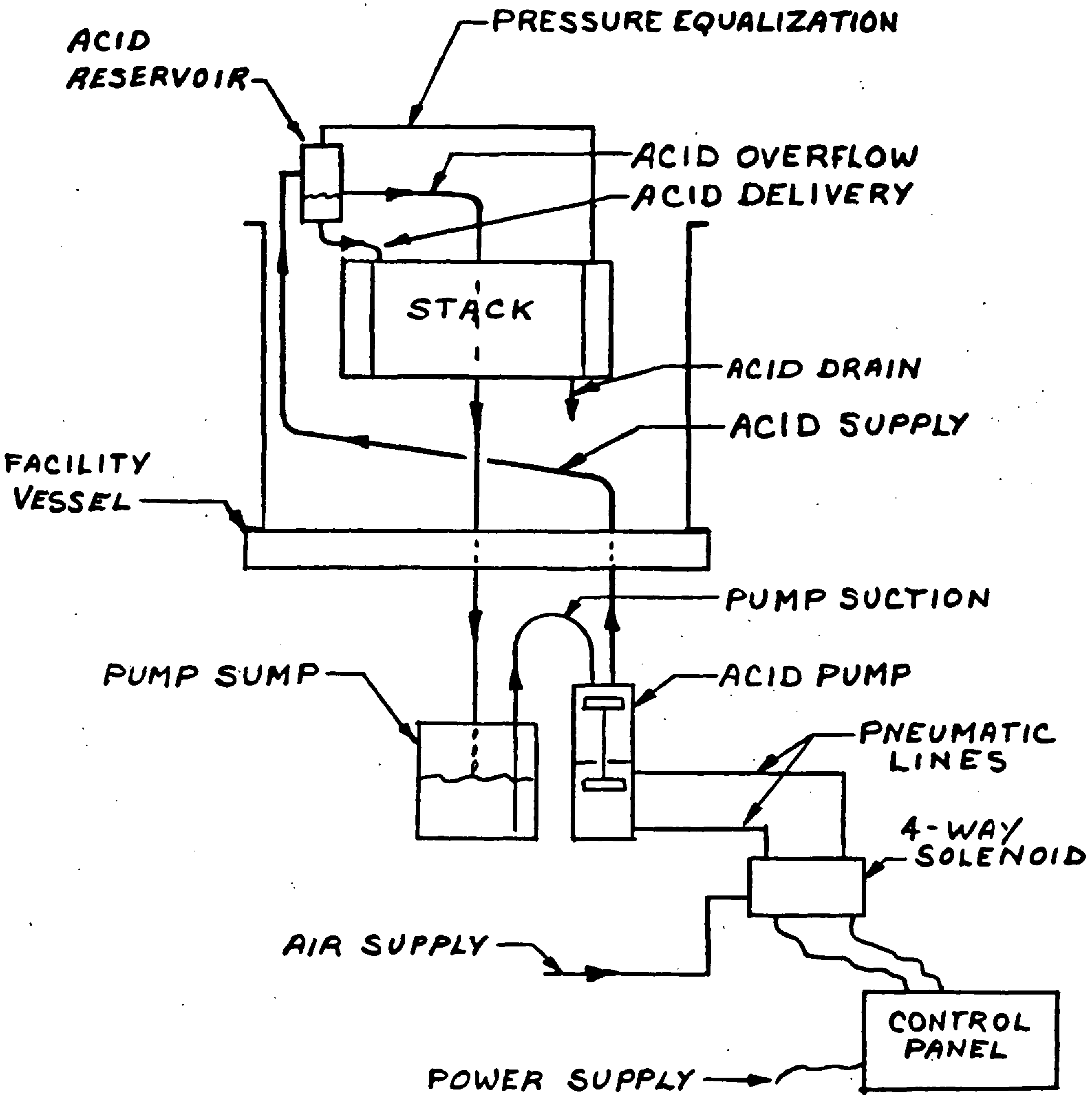

Figure 3-18. Acid Delivery System - Nine Cell System

TABLE 3-18

SUMMARY OF NINE CELL STACK PERFORMANCE

Stack No.	Performance Range @ 1 atm (H_2), mV	Performance Range @ 4.8 atm (SRG), mV	Avg. of 5 center cells 4.8 atm (SRG), mV	Test Time (Hrs) @ 1 atm (H_2)	Test Time (Hrs) @ 4.8 atm (SRG)	Total Oper. Hours	Stack Resistance, mΩ @ Full Power 6 hrs	Stack Resistance, mΩ @ Full Power End	Cell Resistance, mΩ @ Full Power 6 hrs	Cell Resistance, mΩ @ Full Power End
W009-01	459/711(4)	88/706(2)	634(2)	2	2(2)	48	N/A	N/A	N/A	N/A
W009-02	664/706	(512/642)*	587*	118	35*	570	2.95/2.7	3.3	0.21	0.27
W009-03	Did not Test Stack									
W009-04	745/774	486/633	620	30	470	830	1.91	2.3	0.19	0.19
W009-05-1st	515/684(3)	(542/652)*	631*	110	30*	140	N/A	N/A	N/A	N/A
-2nd	667/699	(518/647)*	627*	39	21*	60	2.8	7.0	0.22	0.62
		(598/633)(6)	614		< 1hr		N/A	N/A	N/A	N/A
-3rd	669/684	(579/652)*	632*	67	33*	100	1.77	1.85	0.17	0.21
W009-06	730/743	(606/655)*	608*	48	23*	80	2.17	3.2	0.20	0.31
W009-07	500/664	482/586	530	60	376	778	3.70	4.5	N/A	N/A
W009-08										
I (9/22/83)	625/669	(303/557)*	382*	32	63*	101	6.3*	7.1*	0.59*	0.7*
II (11/21/83)	664/694	369/657	634	30	1	57	N/A	N/A	N/A	N/A
III (12/14/83)	645/696	303/657	645	8	153	178	2.23	2.3	0.145	0.136
IV (1/3/84)	642/708	59/664	650	10	23	128	2.3	3.0	0.143	0.203
V (1/24/84)	508/733	(49/660)*	654*	23	25*	90	N/A	N/A	N/A	N/A
W009-09	625/699	66/681(5)	667(5)	138	5	186	3.5	3.5	0.3	0.3
W009-10	484/691	403/655	630	117	254	1007	2.5	2.9	0.17	0.2
W009-11	467/655*	542/601*	558*	37	115	152	3.0	3.4	0.28	0.28

*H_2 Fueled
**Cells 1 & 2 were excluded from the selection because of voltage sharing problem.

<u>Notes</u> (1) All testing @ 1 atm @ 47 mA/cm^2 unless otherwise indicated; all testing @ 4.7 atm @ 325 mA/cm^2, SRG/Air unless otherwise indicated
(2) 200 Amps on SRG
(3) Cell #3 not included
(4) 90 Amps on H_2
(5) Cell 7 not included
(6) 5 center cells range

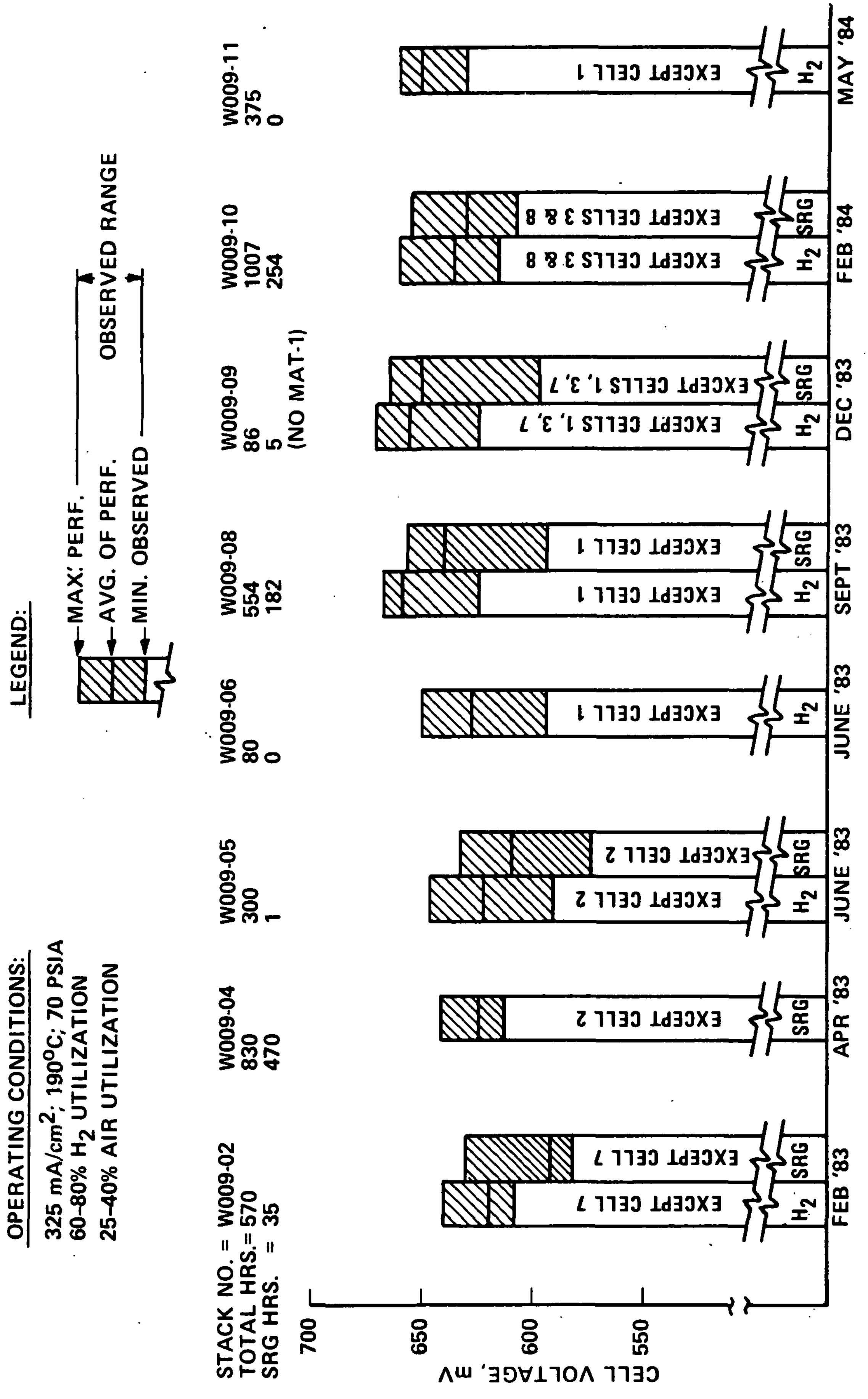

Figure 3-19. Westinghouse Nine Cell Stack Performance-1983

Additional stack testing at ERC established an initial performance baseline using pure hydrogen fuel in Stack E-009-02. The performance level of Cells 1 thru 5 was 624 mV at the following operating conditions: 480 kPa (70 psia), 190°C (374°F), 325 mA/cm^2 (300 A/ft^2), 80-83 percent fuel utilization, 40-50 percent oxidant utilization. A new performance baseline was established in Cells 1 thru 5 of Stack E-009-04. This new baseline is 672 mV at the same operating conditions mentioned previously. The 48 mV increase is attributed mainly to the increased inlet gas temperatures of the new test facility, new startup procedures and new manufacturing procedures may have contributed to this increase. A quantitative separation of the individual contributions cannot be made from the existing data. Factors which will provide additional improvements in performance were demonstrated by comparing the resistance of cells with 175 microns (7 mil) and 75 microns (3 mil) silicon carbide layers (.12 mΩ and .09 mΩ, respectively), and then comparing performance of cells with the standard 250 microns (10 mil) carbon plus 175 microns (7 mil) silicon carbide with the thin, 150 microns (6 mil) carbon plus 75 microns (3 mil) silicon carbide (624 mV and 654 mV, respectively). These thinner matrices are projected to result in a 30 mV improvement over the present 672 mV baseline and thus meet the goal of 700 mV. Future stacks which incorporate both matrix improvements and operating procedure improvements are required to confirm this expectation. Reproducibility will also be demonstrated in future stacks.

The goal of 500 hours of continuous operation at 480 kPa (70 psia) was achieved in Stack E-009-04, but there was significant performance decay due to a resistance increase. The longest stable performance was achieved in Stack E-009-02. Over a period of 359 hours (between the peak and final performance) there was an average loss of 8 mV/cell. A number of factors have limited the achievement of long term endurance. These factors include facility upsets in Δp, power failure to controls, cell assembly defects, cross leaks and acid management problems. Procedures have been identified to improve each of these factors in future stacks.

Though the factors mentioned above were present, some limited data was obtained using SRG containing 75 percent hydrogen, 24 percent CO_2, and 1 percent CO from cylinders of premixed gases. The expected performance loss on SRG is 20 mV. Stack E-009-04, which was tested after revising the operating procedures, showed a 20-30 mV SRG loss. Higher losses were observed in those cells which were diagnosed to have cross leaks and poor temperature distribution. Higher than expected SRG losses are suspected to be caused by the following factors:

- cross leaks
- fuel maldistribution
- inaccurate flow measurement
- poor cell temperature distribution caused by low coolant and process gas inlet temperatures.

Steps have been identified to improve test facility and cell design to correct the problems mentioned above.

Stack W-009-06

Test and disassembly data were developed for a pressurized nine cell stack (W-009-06) tested at Westinghouse and ERC. The stack was operated for over 500 hours, of which 325 were at 480 kPa (70 psia). Average stack performance for the center five cell group at 140 mA/cm^2 (130 A/ft^2) was approximately 718 mV/cell (190°C (374°F), 480 kPa (70 psia), 70 percent hydrogen utilization, 40 percent air utilization).

The following is a summary of important observations/conclusions:

- The final average stack performance of the center five cell group at 480 kPa (70 psia) at Westinghouse was within approximately 6 mV/cell of the initial average stack performance at 480 kPa (70 psia) at ERC.

- Initial OCV testing at ERC indicated possible problems with Cells 1 and 9. Throughout the testing, Cells 1 and 9 were substantially below the stack average. Eliminating these two cells from the average showed this stack performance approximately equaled Stack E-009-01 performance, 725 mV/cell and 721 mV/cell respectively at 140 mA/cm^2 (130 A/ft^2). These two cells (1 and 9) were found to be corroded upon disassembly of the stack.

- Cathode plate and backing paper corrosion was found in Cells 1, 3, 6 and 9.
  - Cell 1 oxidant inlet area and acid channel area
  - Cell 3 fuel outlet area of the cathode plate
  - Cell 6 fuel outlet area of the cathode plate
  - Cell 9 oxidant inlet area
- Low performance of Cells 1 and 9 made it necessary to test the stack at a reduced current.

Stack W-009-07

Stack W-009-07 underwent testing in two phases of operation which totaled 778 hours.

Major results during each phase of testing are given in Tables 3-19 and 3-20 and noted below:

Phase I

Total Phase I test time was 385 hours which includes 262 hours at atmospheric conditions and 123 hours at pressure. Testing included OCV tests, polarization tests at 143kPa (20.7 psia) and 480 kPa (70 psia), and process gas utilization tests for the anode and cathode. The desired full power hold was not achieved due to problems with the cathode air flow.

TABLE 3-19

CELL VOLTAGE AND RESISTANCES AT RATED POWER (SRG FLOW)

	Phase I				Phase II				
	Beginning		End		Beginning		(H_2 Fueled)	End	
Date, Time	7/31, 0:27:51		8/9, 5:00:02		10/17, 8:20:15		10/18, 8:55:51	10/25, 10:11:13	
Current, A	351.7		350.5		351.2		351	351	
Temp, °C	189.6 (373°F)		195.7 (384°F)		193.8 (381°F)		191 (376°F)	191.2 (376°F)	
Pressure, kPa	480 (70 psia)		480 (70 psia)		480 (70 psia)		480 (70 psia)	480 (70 psia)	
% H_2	83		83		70		70	70	
% O_2	40		50		51		50	51	
Cell #	Voltage, mV	Res, mΩ	Voltage, mV	Res, mΩ	Voltage, mV	Res, mΩ	Voltage, mV	Voltage, mV	Res, mΩ
1	574	0.285	540	0.34	567	0.27	576	535	0.32
2	576	0.24	552	0.28	601	0.19	608	579	0.20
3	479	0.335	489	0.35	542	0.29	545	520	0.285
4	471	0.435	354	0.70	432	0.52	427	266	0.85
5	557	0.280	440	0.49	511	0.29	520	459	0.40
6	503	0.370	410	0.56	496	0.36	506	467	0.40
7	508	0.355	467	0.40	606	0.17	608	586	0.16
8	569	0.240	293	0.71	537	0.31	550	513	0.295
9	493	0.390	230	0.895	547	0.29	557	515	0.30
AVERAGE	525		419		538		544	493	
STACK	4.514V	3.6 mΩ	3.56V	5.45 mΩ	4.77V	2.69 mΩ	4.83V	4.38V	3.8 mΩ

TABLE 3-20
STEADY STATE PERFORMANCE AT QUARTER POWER POINT

Date, Time	7/29/83, 14:01:14	7/29, 16:17:29	8/1, 23:07:53	8/1, 23:15:38 (after depressurization due to loss of power)
Fuel	H_2	SRG	H_2	SRG
Current, A	94.3	92.3	93.5	93.6
Temp, °C	190 (374°F)	190 (374°F)	191 (376°F)	191 (376°F)
Pressure, kPa	276 (40 psia)	276 (40 psia)	276 (40 psia)	276 (40 psia)
% H_2	70-85	90.5	86	87
% O_2	40	42	42	42

Cell #	Voltage, mV	Res, mΩ	Voltage, mV	Res, mΩ	Voltage, mV	Res, mΩ	Voltage, mV	Res, mΩ
1	723	0.45	713	0.49	728	0.51	725	0.54
2	716	0.48	701	0.52	708	0.63	706	0.67
3	669	0.57	657	0.60	686	0.54	686	0.55
4	674	0.69	662	0.75	660	0.85	657	0.90
5	703	0.45	691	0.49	691	0.56	689	0.58
6	679	0.73	662	0.83	667	0.72	662	0.77
7	686	0.55	679	0.59	686	0.59	684	0.61
8	733	0.38	718	0.40	728	0.46	725	0.46
9	699	0.66	681	0.70	694	0.67	689	0.70
AVERAGE	698		685		694		691	
STACK	6.20V	6.0 mΩ	6.1V	6.3 mΩ	6.18V		6.145V	6.6 mΩ

TABLE 3-20

STEADY STATE PERFORMANCE AT QUARTER POWER POINT (CONT'D)

Date, Time	8/2, 19:28:31	8/2, 19:43:20	8/6, 0:20:26	8/6, 0:33:55
Fuel	H_2	SRG	H_2	SRG
Current, A	93.6	92	90.4	88.9
Temp, °C	190 (374°F)	190 (374°F)	191 (376°F)	189.9 (374°F)
Pressure, kPa	480 (70 psia)	480 (70 psia)	276 (40 psia)	276 (40 psia)
% H_2	84	86	93	73
% O_2	42	42	40	40

Cell #	Voltage, mV	Res, mΩ	Voltage, mV	Res, mΩ	Voltage, mV	Res, mΩ	Voltage, mV	Res, mΩ
1	728	0.51	716	0.54	718	0.58	711	0.615
2	708	0.64	696	0.68	686	0.84	672	0.925
3	689	0.54	681	0.56	686	0.63	677	0.66
4	662	0.86	647	0.91	623	1.22	608	1.32
5	689	0.58	679	0.61	657	0.83	645	0.90
6	655	0.76	650	0.84	623	1.0	623	1.10
7	689	0.58	674	0.61	689	0.62	672	0.645
8	723	0.51	711	0.52	691	0.82	677	0.84
9	691	0.66	674	0.70	664	0.96	650	1.05
AVERAGE	693		681		671		649	
STACK	6.165V	6.6 mΩ	6.057V	6.9 mΩ	5.964V	8.4 mΩ	5.867V	8.95 mΩ

TABLE 3-20
STEADY STATE PERFORMANCE AT QUARTER POWER POINT (CONT'D)

Date, Time	8/9, 10:37:05	8/9, 10:54:02	10/13, 2:04:24
Fuel	SRG	H_2	H_2
Current, A	89.6	90.9	89.6
Temp, C	191.5 (377°F)	191.7 (377°F)	189.5 (373°F)
Pressure, kPa	276 (40 psia)	276 (40 psia)	480 (70 psia)
% H_2	70	84	50
% O_2	45	47.5	30

Cell #	Voltage, mV	Res, mΩ	Voltage, mV	Res, mΩ	Voltage, mV
1	701	0.57	708	0.56	767
2	674	0.80	681	0.78	772
3	664	0.65	674	0.64	757
4	567	1.59	572	1.52	730
5	611	1.50	618	1.00	733
6	584	1.36	594	1.32	733
7	660	0.60	669	0.59	779
8	520	1.85	528	1.90	750
9	576	1.50	596	1.42	750
AVERAGE	617		627		752
STACK	5.495V	10.9 mΩ	5.569V	10.8 mΩ	6.741V

Phase II

Acid additions in the dry room between testing phases recovered cell voltage degradation. Average cell voltage increased 119 mV from the end of Phase I to the start of Phase II. Total test time was 393 hours with 99 hours under atmospheric conditions and 294 hours at pressure. The stack was operated 125 hours at the full power condition: 325 mA/cm^2 (300 A/ft^2), 190°C (374°F), 50 percent cathode air utilization, 70 percent hydrogen utilization.

Stack W-009-08

Stack W-009-08 was tested a total of 567 hours which included 103 hours under atmospheric conditions and 464 hours at pressurized conditions. During pressurized operation, hydrogen fuel testing at full power conditions ran for 173 hours while SRG fuel testing lasted 177 hours.

Testing was accomplished in five different phases of operation. Open circuit voltage tests were conducted. Hydrogen utilization tests occurred during Phase V. Table 3-21 lists the various conditions and test times for the five phases of testing. Performance of this stack is indicated in Table 3-22 for each phase. These data indicated no voltage penalty from power or pressure cycling for cells with stable performance. Acid addition helped recover performance and enhance performance of several cells.

Stack W-009-09

Test operations lasted a total of 157 hours, which included 60 hours at atmospheric conditions and 97 hours at pressure. This stack was the first of the inverted design with anode on top and cathode on the bottom. No MAT-1 matrix was used and the silicon carbide layer on the cathode was increased nominally by 50 microns (2 mils) to improve acid transport. Dry laminated electrodes were also used for the first time in a full size stack.

TABLE 3-21

TEST TIMES FOR STACK W-009-08

Phase	Total Operating Time	Atmospheric Operation	Pressurized Operation	Full Power Operation with H_2	Full Power Operation with SRG
I	110 hrs	32 hrs	78 hrs	63 hrs	0 hrs
II	54	30	24	3	1
III	181	8	173	2	153
IV	130	10	120	80	23
V	92	23	69	25	0
Totals:	567	103	464	173	177

TABLE 3-22

SUMMARY OF STACK W009-08 DATA

Cell No.	Electrodes		Resistances in Dry Room @ Before Transferred to FCTF	Performance @ FP w/H_2, 50% H_2, 40% O_2		Electrodes		@ 130°F Resistances in Dry Room Before Transferred to FCTF (mΩ)
1	C159-4	A163-6	0.43	557	(0.25)			0.52
2	C161-6	A162-7	0.46	523	(0.28)			0.57
3	C159-1	A162-5	0.45	471	(0.43)			0.66
4	C160-5	A164-1	0.50	386	(0.65)			0.64
5	C161-5	A162-6	0.44	371	(0.53)			0.67
6	C160-1	A164-5	0.50	315	(0.85)			0.63
7	C160-2	A164-4	0.51	369	(0.65)			0.62
8	C159-7	A163-2	0.71	418	(0.50)	C160-6	A163-6	0.76
9	C160-3	A162-8	0.46	303	(0.86)	C161-2	A163-8	0.74
			Sk = 5.6 mΩ	3.45	(6.4)			7.7

Note:

(1) Added acid (93% and 16% RH) spec/cell - loss 50 cm^3 (total) during assembly. Wicked in 150 cm^3, retained 56 cm^3.

(2) External leak ∿ 30 cm^3/min - No cross leak.

(3) Before phase 2 operation, cells 8 & 9 was added ints 98 wt% acid, 6% RH. Wick in 190 cm^3 acid (98%) retained 120 cm^3.

(4) Total test hours of Phase I = 100 hrs, 76 hrs at pressure.

TABLE 3-22

SUMMARY OF STACK W009-08 DATA (CONT'D)

Cell No.	Phase II (18:30, 11/23)	Phase III (8:30, 12/16)	Phase IV (22:06, 1/4)	Electrodes	Resistance in DR Before Transferred to FCTF (mΩ)	Phase V (13:00, 1/25)	(11:00, 1/29)
	Performance @ FP W/SRG, 50% H_2, 33% O_2					Performance @ FP w/H_2 50% H_2, 40% O_2	
	Beginning	Peak	End (3)			Beginning	End
1	547	603 (0.2)	59 (0.19)	C201-8 A207-8	2.72	271	230
2	598	672 (0.16)	721 (0.15)	C204-6 A207-1	0.64	623	657
3	608	652 (0.14)	667 (0.14)		0.70	635	660
4	657	657 (0.12)	660 (0.12)		0.70	655	664
5	642	655 (0.13)	657 (0.14)		0.74	660	664
6	650	650 (0.11)	655 (0.12)		0.71	655	655
7	608	613 (0.13)	616 (0.14)		0.67	650	642
8	410	594 (0.13)	596 (0.16)		0.80	642	635
9	591	635 (0.14)	650 (0.13)		0.74	650	647
	5.20 V	5.25 V (2.2 mΩ)	5.10 (2.3)		9.40	5.37 V	4.91 V
		acid added				shutdown because of cell 1 perf.	

Note:

(1) Total test time of Phase 2 + 3 + 4 = 363 hrs, at pressure = 315 hrs, w/SRG at press = 182 hrs.

(2) Total test time of Phase V = 90 hrs, at press = 69 hrs.

(3) Shutdown, replaced Cells 1 and 2. Total acid added - 150 cm^3; total acid retained - 88 cm^3.

Testing was conducted in two phases. During Phase I, the stack ran for one hour at atmospheric conditions when an emergency shutdown occurred due to extremely high temperatures. Phase II testing lasted 156 hours. Atmospheric pressure tests ran for 59 hours. The remaining test time included 36 hours at full power conditions with hydrogen fuel and nine hours at full power using SRG. OCV and utilization tests were conducted.

The stack exhibited an improved ability to wick acid due to the design change which provided partial surface exposure of the acid transport member (SiC) to the acid groove. Stack resistance was higher than noted in previous stacks, partly due to the thicker silicon carbide layer. However, Cell 1 was the single largest contributor to the increased resistance.

After the high temperature excursion in Phase I, the stack was returned to the dry room and examined. No visible damage was apparent but cross leaks were much higher than before testing. Additional tests showed that the stack retained acceptable bubble pressure.

Significant accomplishments achieved with this stack included:

- Recovery of stack performance after an over-temperature excursion of nearly 56°C (100°F) was experienced.
- Completion of a full startup on SRG.
- Demonstration of an emergency shutdown from rated full power.
- Mapping of 100°C (212°F) shutdown from two atmospheres with SRG.
- Performance of numerous startup and pressurizing cycles that verified the results obtained from stack W-009-08 (indicating no performance penalty resulting from pressure cycling).

- Acid addition in the test loop to recover cell performance after apparent electrolyte loss.

This stack provided a number of diagnostic data including effects of:

- Oxygen gain of 80-85 mV at atmospheric test conditions.
- Negative voltage condition startup.
- No apparent enhancement from the reversal of process gases to electrodes (exchange of anode for cathode, and vice versa).
- Current step and flow interruption cell voltage and response characteristics.

Stack W009-10

The stack accumulated 1007 hours of test operation with 117 hours at atmospheric conditions and 890 hours at pressure. During pressure testing the stack ran 290 hours on SRG with 254 hours at rated conditions.

The stack design is similar to Stack W009-09 except that MAT-1 was included in the matrix. Minor design changes involved increased thickness of the insulator plates between the end heaters and current collectors to more uniformly redistribute the load transferred through the flexible heater elements to the end plates. A sheet of carbon paper was also placed between the current collector and end plate at each end of the stack to cushion any high load points caused by the interface of the terminal point base in the collector plate and the end plate.

Test Results

Table 3-23 summarizes steady state performance at full power condition with SRG. At peak performance, which occurred after 45 hours in the SRG endurance run, the center four cell average was 630 mV.

TABLE 3-23

STACK W-009-10 STEADY STATE PERFORMANCE AT FULL POWER POINT WITH SRG

	Phase 1b		Phase 1c	
	1st FP data pt	1st FP Data	Peak	Last FP Data
Date, Time	3/19, 9:24	4/4, 3:00	4/6, 10:00	4/6, 16:00
Time on Test (at pressure)	428 hours	597 hours	652 hours	890 hours
Current	322A	338A	336A	341A
Temperature	192°C	190°C	193°C	192°C
Pressure	70 psia	70 psia	70 psia	70 psia
% H_2 Util.	70%	70%	70%	70%
% O_2 Util.	31%	40%	33%	33%
Cell Voltage				
Cell 1, mV (Res, mΩ)	547 (0.23)	616 (0.17)	618 (0.18)	611 (0.19)
Cell 2, mV (Res, mΩ)	442 (0.19)	611 (0.16-0.18)	620 (0.17)	572 (0.08-0.12)
Cell 3, mV (Res, mΩ)	486 (0.24)	515 (0.23)	508 (0.26)	447 (0.33)
Cell 4, mV (Res, mΩ)	611 (0.21)	620 (0.19)	628 (0.19)	623 (0.21)
Cell 5, mV (Res, mΩ)	635 (0.16)	647 (0.16)	655 (0.16)	647 (0.18)
Cell 6, mV (Res, mΩ)	591 (0.20)	594 (0.18)	608 (0.18)	576 (0.21)
Cell 7, mV (Res, mΩ)	589 (0.21)	608 (0.15)	630 (0.17)	596 (0.22)
Cell 8, mV (Res, mΩ)	349 (0.15)	544 (0.15)	403 (0.165)	550 (0.20)
Cell 9, mV (Res, mΩ)	620 (0.16)	623 (0.15)	667 (0.15)	620 (0.16)
Stack Voltage, V	4.704	5.158	5.124	4.922
(Stack Resistance, mΩ)	(2.60)	(2.50)	(2.50)	(2.90)

Effects of humidification were studied during Phase 1b operation. The design levels of moisture were chosen for the anode and cathode stream, which were 4.4 percent and 1 percent by mole, respectively, for the anode and cathode. Table 3-24 presents the results of the tests. For the anode fuel, moisture was added to hydrogen first and then to hydrogen with CO_2 later. About 5 mV gain per cell was observed in both cases with humidified anodes. For humidified cathodes, an average of 5 mV increase in cell voltage was also observed. However, an endurance run with the humidified hydrogen with CO_2 fuel was conducted but cell 1 dropped 47 mV from 611 mV to 564 mV. The stack was then returned to dry fuel.

Polarization test data are shown in Figures 3-20 thru 3-24. The first figure is for the polarization test with hydrogen and the following four with SRG. The SRG tests were conducted at the beginning and end of Phase 1c. The hydrogen polarization curve shows an average 20 mV higher than that of the first SRG curve.

Before the stack was depressurized, 13 mapping points were conducted. Table 3-25 shows the results and cases used in the tabulation. In summary, the good cells of stack 10 showed higher voltage gain, due to increase in pressure than the theoretical value. The temperature gain, effect 1.5 mV/1°C (.8 mV/1°F), was considered to be high at 166A and 325 kPa (47 psia). The current effect varied with pressure operating level. A high pressure, 690 kPa (100 psia), the current effect rate was -0.57 mV per ampere increase.

Stack W-009-11

Stack W-009-11 was of the same cell arrangement as stack W009-10. At assembly, the stack was lightly loaded at an average stack pressure of 55 kPa (8 psi) and an average cell strain of 6 percent based on 190°C (374°F). The objectives of the test were: (1) to determine the minimum initial cell compressive load and strain for acceptable cell performance, (2) to determine stack and cell operating characteristics over limited operating map including startup and shutdown

TABLE 3-24

STACK W-009-10 EFFECT OF HUMIDIFICATION ON CELL PERFORMANCE (PHASE 1b)

Stack Operating Conditions						
Date, Time	3/12, 18:00	3/12, 20:00	3/13, 12:00	3/13, 16:00	3/13, 1:00	3/13, 3:00
Current, A	339A	340A	339A	339A	340A	341A
Temp, °C	190°C	190°C	192°C	192°C	189°C	191°C
Pressure, psia	70 psia	70 psia	70 psia	70 psia	70 psia	70 psia
Anode Content	H_2 only	H_2 & H_2O 4.4% by mole	H_2 and CO_2	H_2 + CO_2 & H_2O 4.4% by mole	H_2 only	H_2 only
Cathode Content	Air Only	Air Only	Air Only	Air Only	Air Only	Air & H_2O 1% by mole
% H_2 Util.	51%	51%	51%	49%	84%	84%
% O_2 Util.	40%	40%	40%	40%	33%	33%
Cell 1 mV	625	620	603	611	628	630
Cell 2 mV	635	640	623	633	640	642
Cell 3 mV	630	630	613	620	630	633
Cell 4 mV	623	628	620	623	628	633
Cell 5 mV	652	650	645	647	655	657
Cell 6 mV	613	618	608	613	620	620
Cell 7 mV	601	606	598	611	611	613
Cell 8 mV	606	608	545	547	598	603
Cell 9 mV	635	640	647	642	625	625
Stack Voltage, Volts	5.412	5.437	5.310	5.339	5.432	5.451

(with H_2) - Phase 1b

Date: 3/21

Time: 20:00

Temp: 190°C

Press: 70 psia

% H_2: 83%

% O_2: 40%

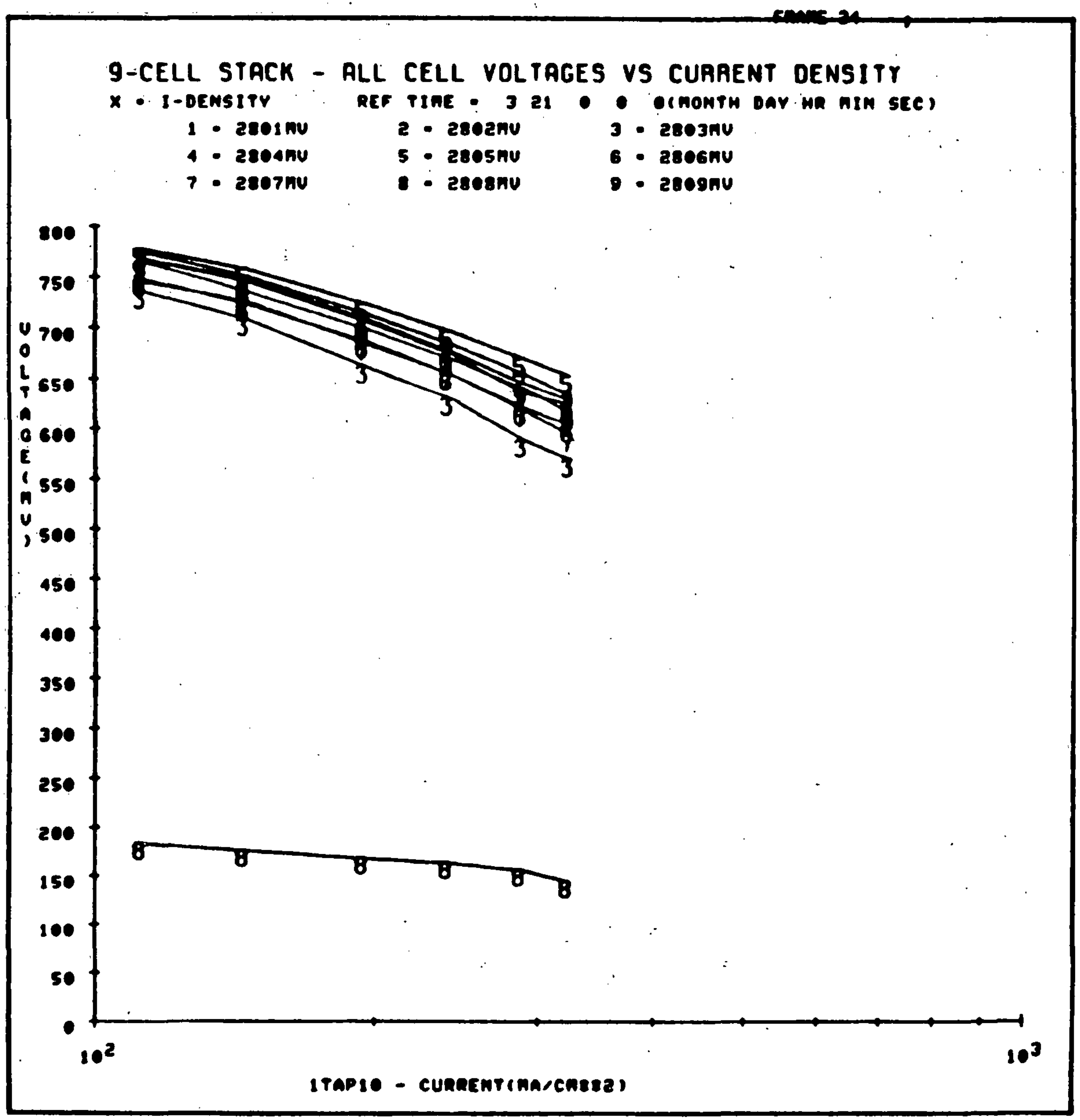

Figure 3-20. Stack W-009-10 Polarization, All Cells

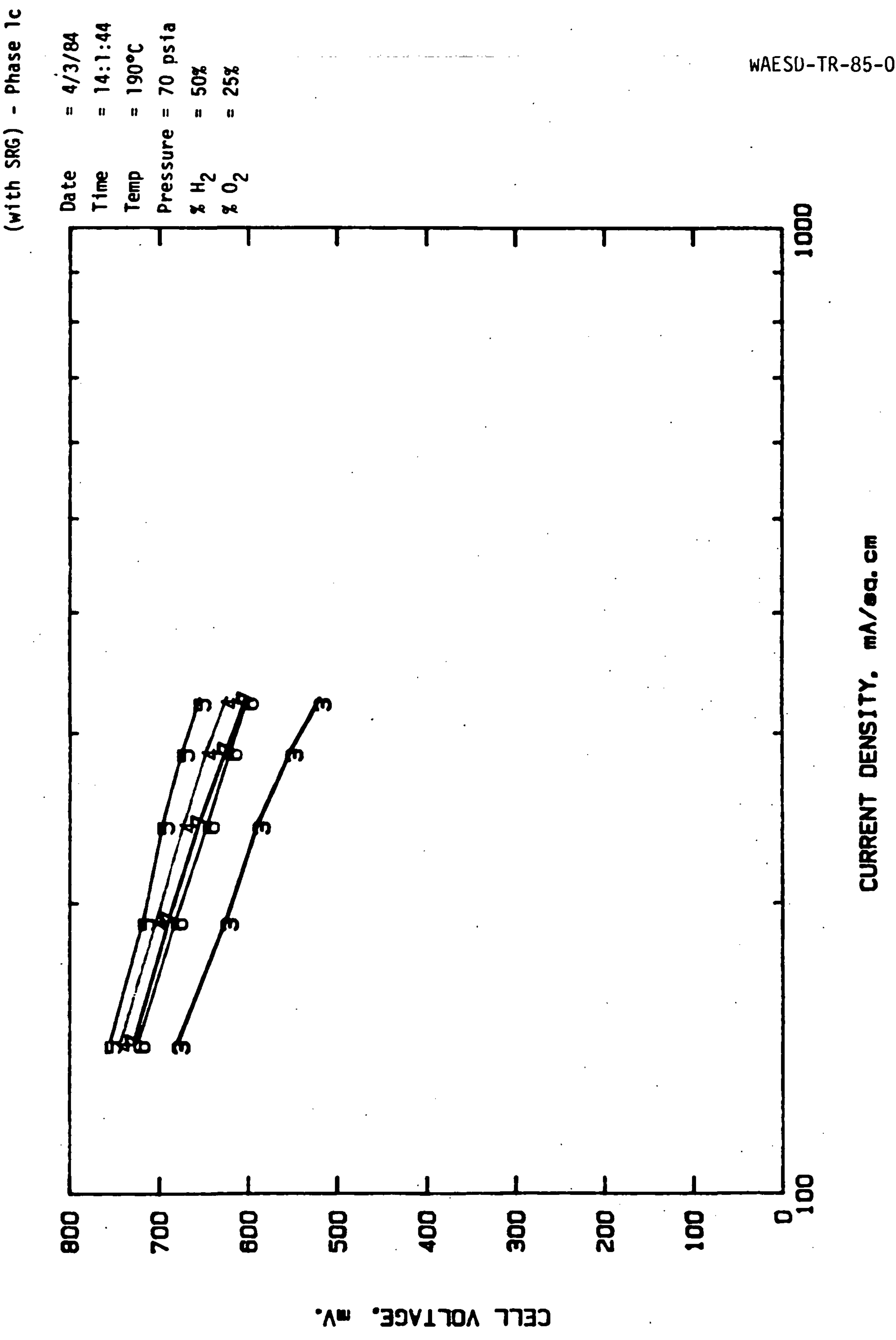

Figure 3-21. Stack W-009-10 Polarization at Beginning of Phase 1c, Five Center Cells

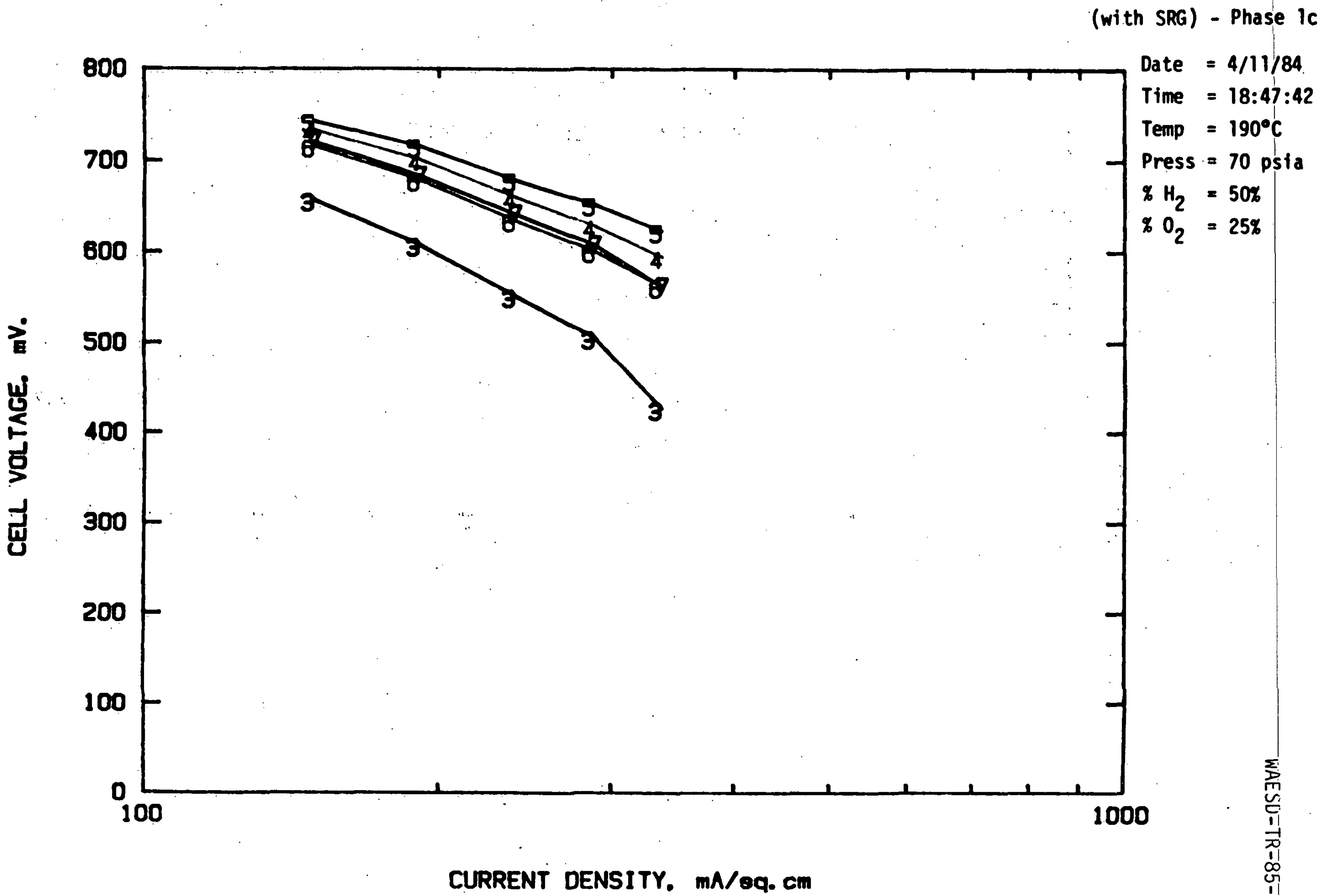

Figure 3-22. Stack W-009-10 Polarization at End of Phase 1c, Five Center Cells

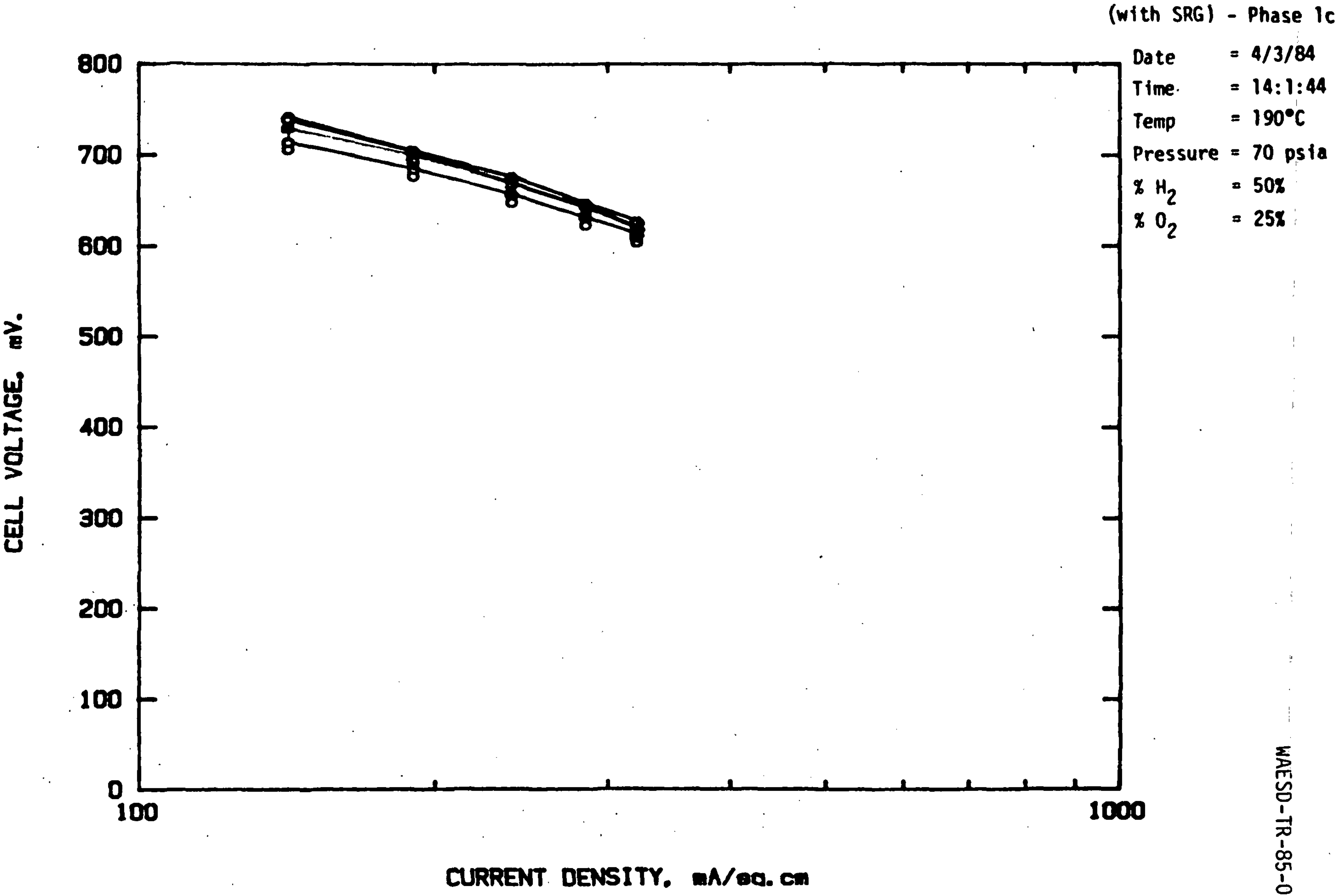

Figure 3-23. Stack W-009-10 Polarization at Beginning of Phase 1c, Four Outer Cells

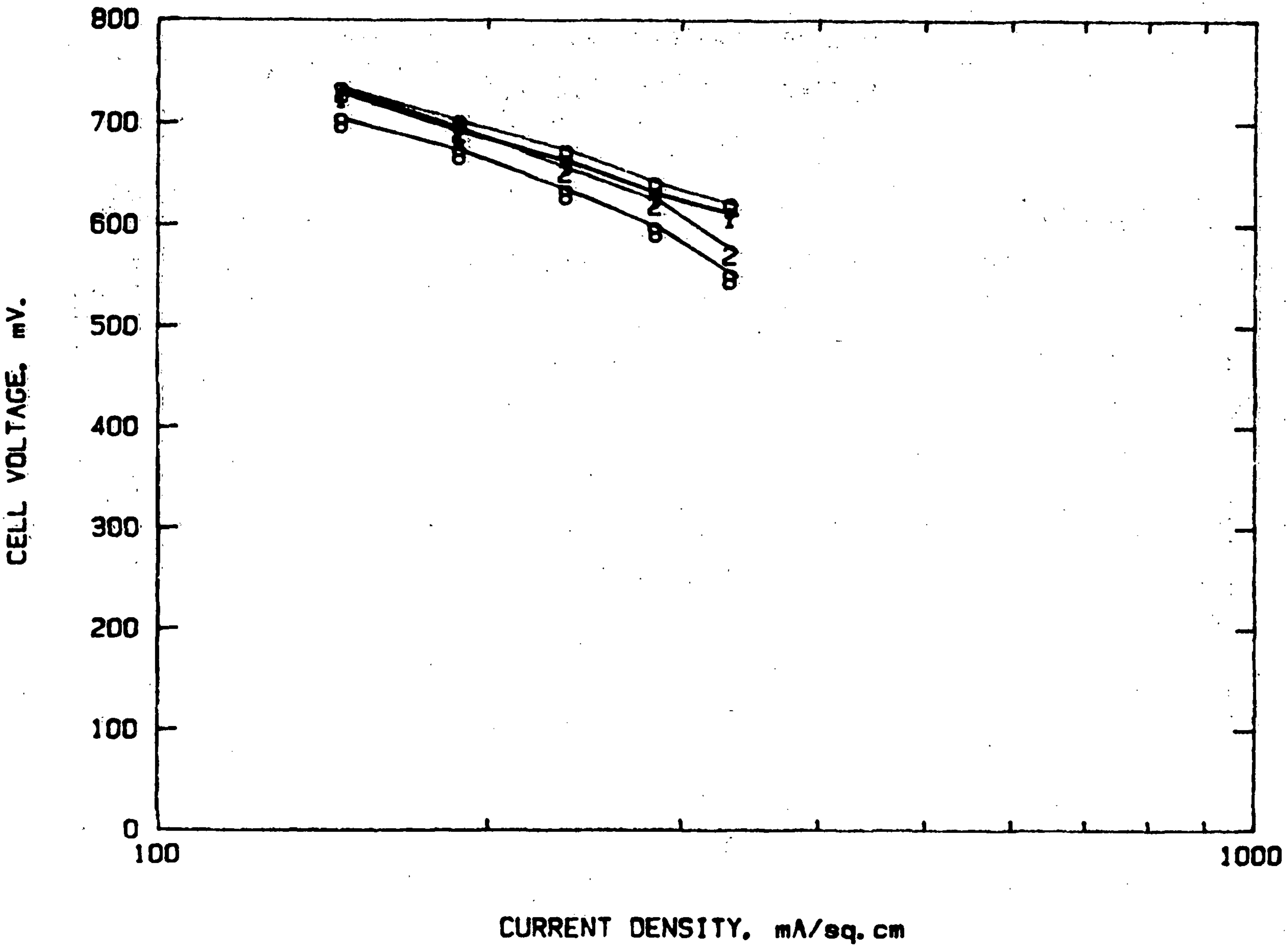

Phase 1c

with SRG

Date = 4/11/84
Time = 18:47:42
Temp = 190°C
Press = 70 psia
% H_2 = 50%
% O_2 = 25%

Figure 3-24. Stack W-009-10 Polarization at End of Phase 1c, Four Outer Cells

TABLE 3-25
STACK W-009-10 TABULATION OF MAPPING RESULTS

Cases Used	Variable Effect	Range of Variable	Experimental Value	Theoretical Value
8 and 9	Current @ 30 psia	80-160A	0.90 mV/amp	
2 and 11	Current @ 40 psia	160-340A	0.85 mV/amp	
3 and 4a	Current @ 100 psia	160-420A	0.57 mV/amp	
6 and 7	Pressure @ 165A	30-47 psia	38 mV	26 mV
3 and 5a	Pressure @ 165A	40-100 psia	77 mV	54 mV
7 and 10	Temperature @ 166A, 47 psia	170-190°C	1.5 mV/1°C	∿1.2 to 1.3 mV/1°C*
8 and 12	Temperature @ 166A, 47 psia	170-190°C	1.5 mV/1°C	∿1.2 to 1.3 mV/1°C*

*2 x 2 data

procedures, and (3) to continue verifying stack and cell performance with components to be used in the 10 kW stack and with the inverted cell stack configuration.

Only the first of the three testing phases (Phase 1a) totalling 159 hours was completed by the end of this report period. Table 3-26 summarizes the results.

3.3 10 kW Fuel Cell Stack Development (WBS 1103-03)

3.3.1 Development Status

Design modifications were made to account for the larger shrinkage (5.2 percent) incurred with the A4421 regrind plate material. Molded, heat treated plates were inspected and statistically analyzed to establish the appropriate dimensions. All drawings affected by plate shrinkage were revised and released. The instrumentation drawing was also completed and released. Based on nine cell work, the electrode configuration was re-evaluated and re-designed in an inverted configuration with the cathode on the bottom to provide better acid transport. Assembly, process gas piping, and instrumentation drawings were revised as necessary to incorporate the "inverted" cell configuration.

Plate/electrode subassembly and final stack assembly procedures were also revised for the inverted cell design. Fabrication of all non-repeating hardware was completed and plate subassembly initiated.

Samples of polyethersulfone (PES) process gas manifold material were tested in hot acid for compatibility. Some surface attack was observed (primarily in the outer glass fibers) but does not warrant a special surface coating for short term testing. This subject will be reconsidered following completion of this test. Flatness was difficult to maintain when machining the manifolds from extruded slab material. This was overcome by making light cuts and reclamping frequently without bending against the machine table.

TABLE 3-26

STACK W-009-11 STEADY STATE PERFORMANCE AT FULL POWER POINT WITH H_2

Operating Conditions	Phase 1a		
	Beginning	Peak	End
Date, Time	5/14, 12:00	5/14, 18:00	5/17, 10:00
Time on Test, hrs	78 hrs	84 hrs	148 hrs
Current, A	345 A	345 A	336 A
Temperature, °C	190°C	188°C	193°C
Pressure, psia	70 psia	70 psia	70 psia
ΔLoad, psi	0	0	0
%H_2 Utilization	70%	72%	70%
%O_2 Utilization	33%	33%	33%
Cell 1, mV (mΩ)	169 (0.25)	181 (0.28)	100 (0.65)
Cell 2, mV (mΩ)	594 (0.25)	601 (0.29)	594 (0.26)
Cell 3, mV (mΩ)	554 (0.25)	557 (0.25)	557 (0.25)
Cell 4, mV (mΩ)	591 (0.19)	601 (0.20)	596 (0.20)
Cell 5, mV (mΩ)	574 (0.23)	586 (0.23)	576 (0.24)
Cell 6, mV (mΩ)	586 (0.19)	594 (0.18)	589 (0.20)
Cell 7, mV (mΩ)	542 (0.24)	550 (0.24)	550 (0.25)
Cell 8, mV (mΩ)	562 (0.20)	574 (0.20)	569 (0.22)
Cell 9, mV (mΩ)	581 (0.22)	591 (0.22)	586 (0.24)
Stack Volt V (mΩ)	4.53 (3.0)	4.62 (3.0)	4.49 (3.4)

A prototype metal stack was designed and assembled according to test procedures using aluminum plates in place of graphite plates and prototypic edge seal gaskets. The primary purpose of this prototype was to develop a manifold seal system. It also provided experience in building a larger stack and an opportunity to evaluate the stacking assembly fixture as shown in Figure 3-25. Based on manifold seal tests on a nine cell stack, five different seal configurations were tested on this metal stack with plates aligned as well as possible. Since the aluminum plates had no flow channels, only one manifold was required and only one end of the stack was involved in the leak test. Two different manifolds were used for these tests. A PES manifold with O-ring grooves was used to test O-ring seals 0.48 cm (0.19 in.) dia. of 50 durometer and 75 durometer Viton. Based on nine cell stack tests, the grooves were reduced in depth to allow greater squeeze on the O-ring. An aluminum manifold with a flat seal surface was used to test flat cured Viton 0.32 cm (0.13 in.) by 0.64 cm (0.25 in.) of 50 durometer and "Gore-Tex" joint sealant 0.48 cm (0.19 in.) size. Table 3-27 summarizes these tests. The leakage data is reported for both chambers (anode and cathode) in the manifold and for two differential pressures 1.7 kPa and 34.5 kPa (0.25 psi and 5.0 psi). These tests show that the flat 0.32 cm Viton gasket is the best, followed by one layer of "Gore-Tex" on flat Viton, then the 50 durometer O-ring or two layers of "Gore-Tex", and finally the 75 durometer O-ring. Future tests will evaluate the best of these on a misaligned stack.

3.3.2 10 kW Stack Design Description

The 10 kW stack mounted in the test loop pressure vessel is shown in Figure 3-26. The stack contains 44 cells in eight groups of five with two cells at each end. Each group of five cells is separated by cooling plates. The remaining cell components in the five cell group are separated by bipolar plates. The nine cell stack discussion relative to the "zee" and "tree" pattern bipolar and cooling plates, respectively, is applicable for this stack and is, therefore, not repeated herein. Additional design details were previously described in the "Final Report for the First Logical Unit of Work."

ORIGINAL PAGE IS
OF POOR QUALITY

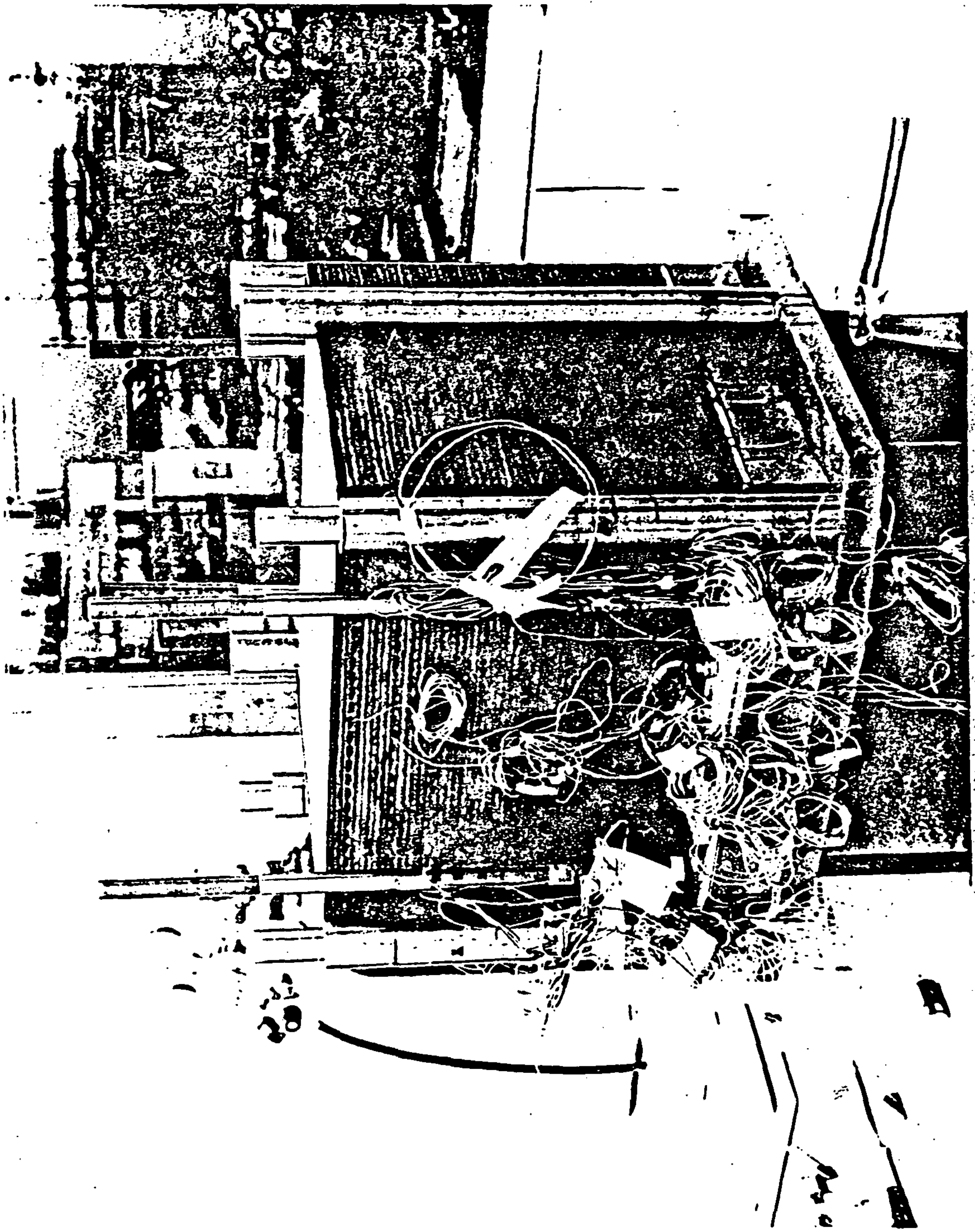

Figure 3-25. Stack Assembly Fixture

TABLE 3-27
10 kW METAL STACK MANIFOLD SEAL TEST RESULTS
(ALIGNED STACK)

	Compression (Percent)	Leakage(2) cm^2/min	
		0.172 kPa (0.25 psi)	3.45 kPa (5 psi)
Aluminum Manifold Tests(1)			
• Flat Cured Viton 0.32 cm (1/8 in.) Thick by 0.64 cm (1/4 in.) Wide	32	0/0	0/0
• Gore-Tex 2 Layers of 0.48 cm (3/16 in.)	(0.045 gap)	0/5	19/53
• Gore-Tex 0.48 cm (3/16 in.) on Top of Flat Viton 0.32 cm (1/8 in.)	(0.10 gap)	0/0	6/12
Polyethersulfone (PES) Manifold Test(3)			
• Viton O-Rings (0.53 cm (0.210 in.), 75 Durometer)	43	19/24	High
• Viton O-Rings (0.48 cm (0.187 in.), 50 Durometer	41	0/5	11/82

---

(1) Flat face sealing flange.

(2) Leakage data given for each half of one manifold.

(3) Reduced depth O-ring groove 0.25 cm (0.100 in.) vs. 0.38 cm (0.150 in.).

(4) All tests at room temperature.

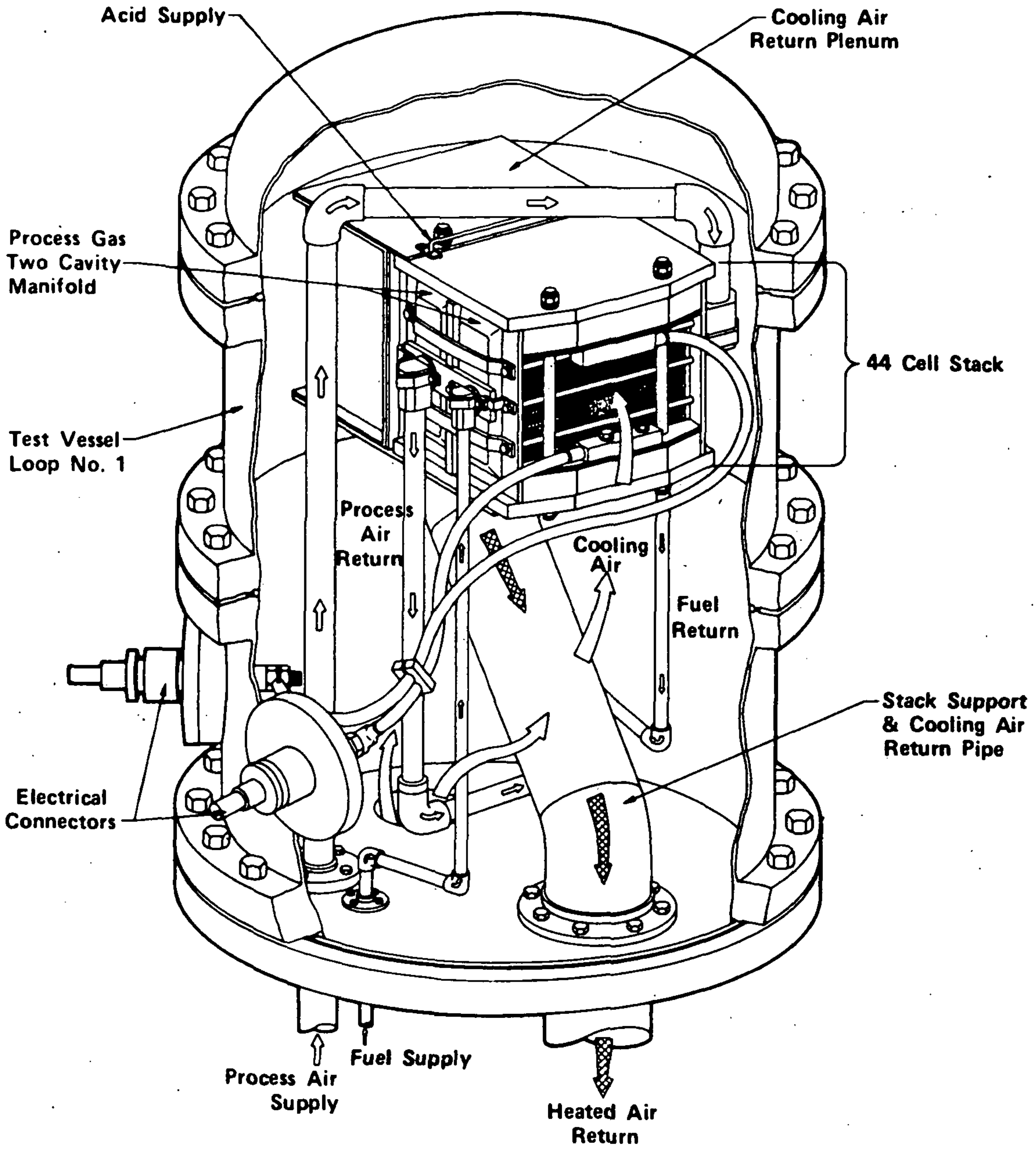

Figure 3-26. PAFC 10 kW Stack Test Assembly
(Non-Inverted Arrangement Shown)

3.4 25 kW Short Stack Development (WBS 1103-05)

3.4.1 Development Status

Consistent with the 10 kW stack, this stack was re-designed for an inverted cell with the cathode on the bottom and the anode on the top. This provides better acid transport since the acid must now run over the cathode in the acid groove area which insures good contact with the acid supply. Detail and assembly drawings were revised as required.

3.4.2 25 kW Stack Design Description

The 25 kW stack mounted in the test facility pressure vessel is illustrated in Figure 3-27, which has not been revised for the inverted cell design. The major difference would be to move the process gas connections from left to right and vice versa. The stack assembly is supported from a carbon steel lower support plate which is mounted on the cooling air outlet pipe and two support columns. Many of the 10 kW stack design features described in Section 3.3.2 are applicable to the 25 kW stack and are not repeated here.

The 25 kW stack contains 104 cells in 20 groups of five with two cells at each end of the stack. Each group of five cells is separated by cooling channels with the design identical to that used for 10 kW stacks.

3.5 100 kW Full Stack Development (WBS 1103-06)

3.5.1 Development Status

The 100 kW Stack Preliminary Design was updated to include the most current stack design features. The major revisions included in the update were as follows:

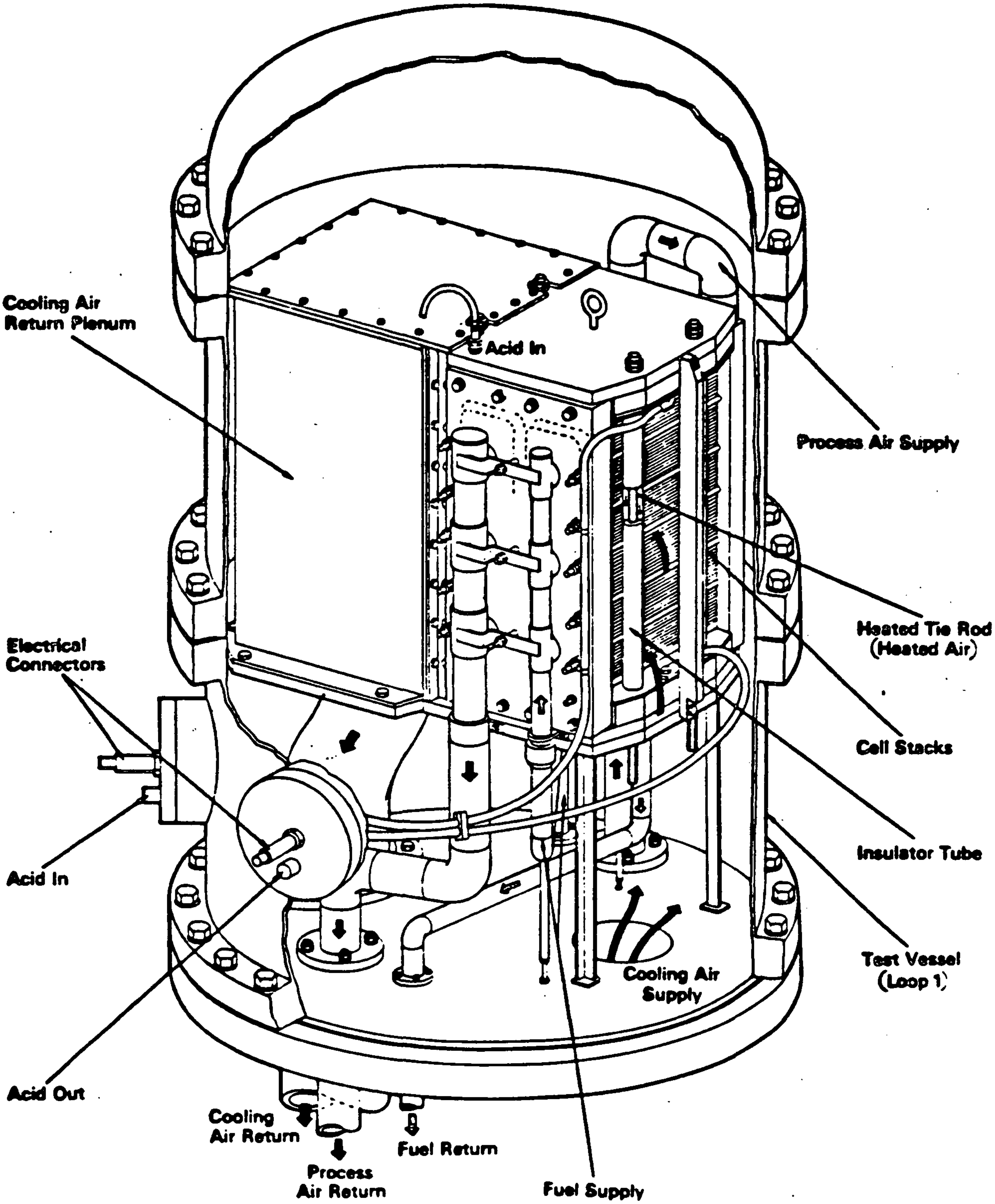

Figure 3-27. 25 kW Stack Design (Non-Inverted)

- Revision of the stack and process gas supply lines to reflect the inverted cell arrangement, i.e., the inversion of the anode and cathode. Gas supply line connections to the vessel and stack manifolds were repositioned.

- Stack related provisions for a continuous acid pumping system were added. This included an acid distribution box at the top of the cooling air plenum and designated acid and vent line routings with appropriate vessel penetrations.

- The process gas manifolds were modified from a two piece design to a molded four piece design. The shorter sections should be more suitable for injection molding than the half-height components.

- Other minor changes were incorporated. In addition, the 100 kW Stack Preliminary Design Description was revised to reflect the changes made to the 100 kW Stack Design.

3.5.2 100 kW Stack Design Description

The 100 kW Stack Preliminary Design (inverted) was developed in detail for the stack mounted in the Westinghouse-provided test facility Loop 1 pressure vessel and the stack in the prototypical 375 kW module pressure vessel. Except for test assembly differences, the basic stack design is essentially identical for these two test configurations.

The facility vessel test assembly is very similar in concept to the 25 kW stack design and employs identical support structure and piping components where possible. The main differences are the longer stack, cooling air outlet plenum box, electrical power take-off wires, acid lines, and pressure vessel. In addition, process air in the 100 kW stack is piped directly from the cooling air outlet plenum box (as in the 375 kW module design) instead of via a separate vessel penetration provided in the 25 kW stack.

The module vessel test assembly incorporates maximum component commonality with the Loop 1 test assembly configuration and the 375 kW module design (see Section 3.6). In this arrangement, the 100 kW stack and its cooling air outlet plenum box interface with the module designed internal support structure. Process air is supplied from the cooling air outlet plenum box. A departure was made from the prototypical module piping manifold arrangement on the vessel lower head, to avoid the need for blanking off and, possibly, bleeding the piping legs for the three missing stacks.

The 100 kW stack preliminary design contains 419 cells in 83 groups of five with two cells at each end of the stack. Each group of five cells is separated by cooling channels and is of a design configuration identical to that described for the 10 kW stack. Many of the 10 and 25 kW stack design features as described in Sections 3.3 and 3.4 are applicable to the 100 kW stack, and thus are not reported herein. Additional design details were previously described in the "Final Report for the First Logical Unit of Work."

3.6 375 kW Module Development (WBS 1103-07)

3.6.1 Development Status

The fuel cell module preliminary design was completed and is illustrated in Figure 3-28 and described in Section 3.6.2. The nominal design parameters of the module preliminary design are presented in Table 3-28 at beginning of use of the plant. The major changes made were:

1. Inversion of cell components (anode and cathode) and relocation of process piping to accommodate the anode-over-cathode configuration.

2. Addition of electric resistance heaters into the cooling air outlet plenum to maintain module internals temperature above 38°C (100°F) to prevent crystallization of the phosphoric acid.

3. Addition of a continuous acid supply system.

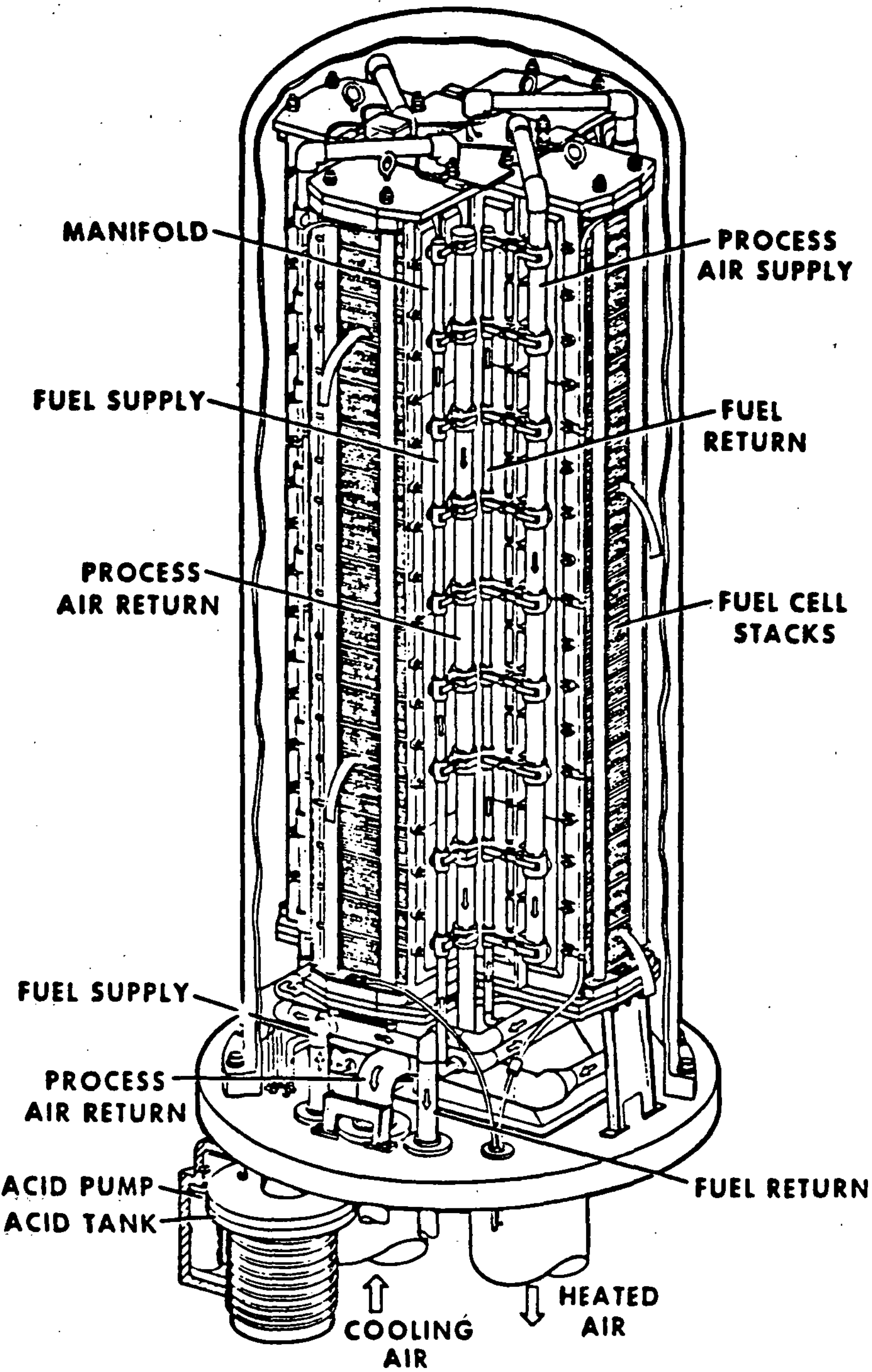

Figure 3-28. Fuel Cell Module

TABLE 3-28

FUEL CELL MODULE DESIGN PARAMETERS

PARAMETER	UNITS	NOMINAL
POWER	kW_{DC}	375
TEMPERATURE	°C(°F)	
Oxidant Inlet*		186 (366)
Coolant Inlet		147 (297)
Fuel Inlet		191 (376)
Plate Avg.		191 (376)
*Same as coolant outlet.		
PRESSURE	kPa (psia)	483 (70)
FLOW	kg/h (lb/h)	
Fuel		181 (398)
Oxidant (air)		1400 (3086)
Coolant (air)		27,842 (61,380)
CELL VOLTAGE	mV	
Open Circuit		920
Operating Limit		800
Operating Point		690
CELL CURRENT DENSITY	mA/cm^2 (A/ft^2)	300 (280)
MODULE VOLTAGE	Volts	
Open Circuit		1540
Operating Limit		1340
Operating Point		1156
MODULE CURRENT	Amps	324

A stress analysis of the module preliminary design was completed and documented. The analysis indicates that the module structural design satisfies ASME Code requirements and is adequate to withstand the loads expected during transportation, operation, and maintenance.

A preliminary maintenance assessment of the module installed in the Fuel Cell System was performed. The most important maintenance considerations were determined to be the monitoring and replenishment of the phosphoric acid and the periodic replacement of the fuel cell cartridge at approximately 5 year intervals during the 30 year life of the plant. (The fuel cell "cartridge" is the assembly of four 100 kW stacks and associated hardware that fit inside the pressure dome.) These maintenance considerations are discussed in more detail in Sections 3.6.3 and 3.6.4.

3.6.2 Module Preliminary Design Description

The fuel cell module is illustrated pictorially in Figure 3-28. The module consists of four stacks of fuel cells supported inside a containment vessel with their cooling air outlet passages discharging into the space formed between the stacks. Cooling air is admitted to the pressure vessel cavity, surrounding the stack assembly, and flows through the stack cooling air passages to the space between the stacks. Corner seals, provided between the adjacent stack inner corners, minimize the leakage of coolant air into the exhaust plenum. The cooling air enters and leaves the vessel through the lower head, allowing the vessel cylinder and upper head to be easily removed for rapid replacement of the fuel cell stacks without disturbing the external piping. Process air is piped to the stacks from the cooling air outlet cavity between the stacks through holes in the top plate which separates the inlet and outlet cooling air cavities. Fuel is piped to the stacks from a stainless steel piping assembly in the lower region of the pressure vessel which is fed, in turn, from a penetration in the lower vessel head. The fuel and process air return lines from the stacks are led to similar piping assemblies and penetrations at the lower vessel head. Figure 3-29 illustrates all of the above flow paths in a schematic illustration of the module.

ORIGINAL PAGE IS
OF POOR QUALITY

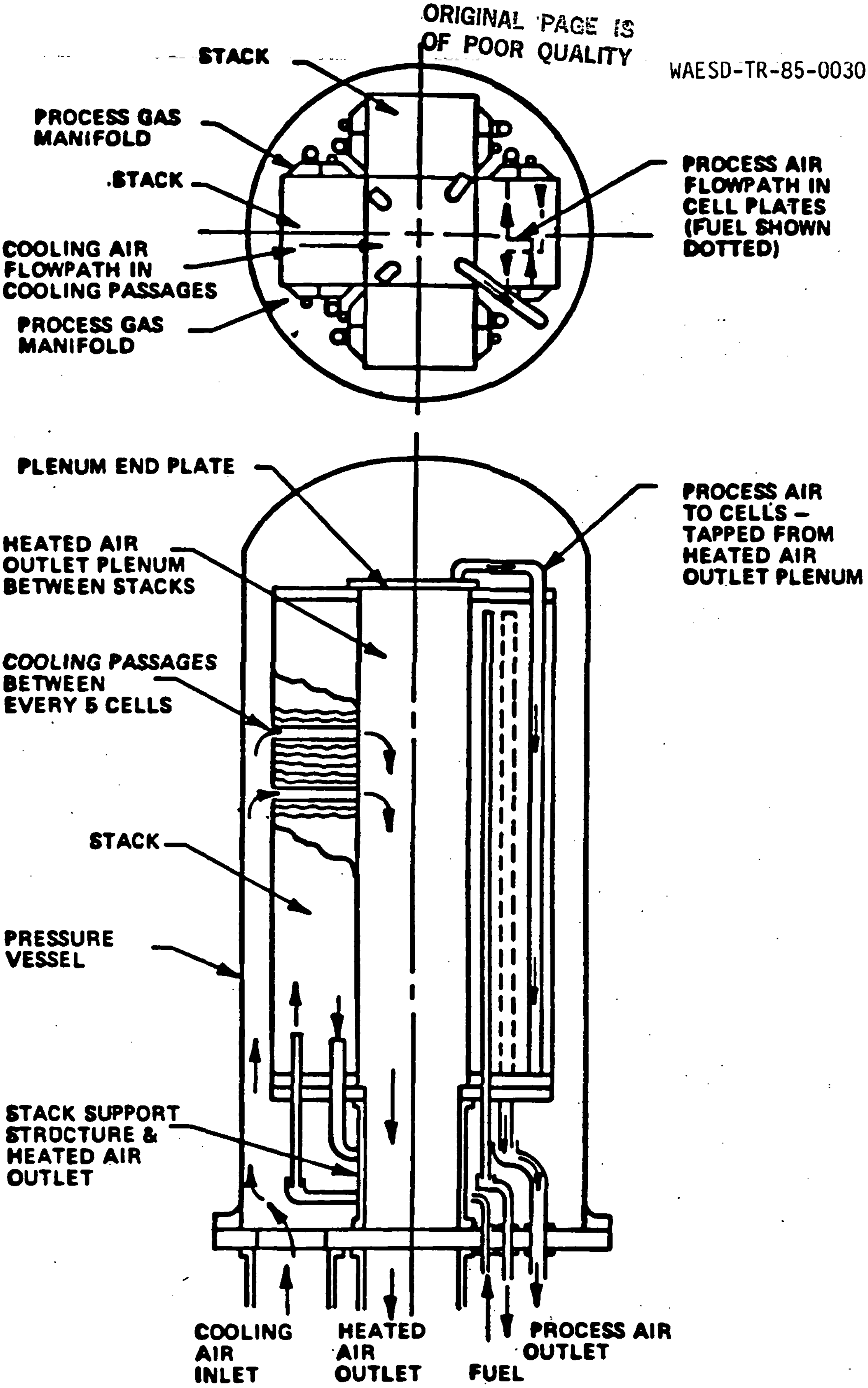

Figure 3-29. Module Flowpaths

Electric resistance heaters are installed inside the cartridge cooling air outlet plenum for use in preventing crystallization of the phosphoric acid during transportation, storage, and plant shutdown. The heaters are energized from an external source of power and are controlled to maintain a minimum temperature of 38°C (100°F) at the fuel cells. Explosion-proof temperature switches mounted outside the module pressure vessel, (or cartridge shipping container) monitor the cell temperature via a sensor bulb in the cartridge support plate and capillary tubing. The electrical leads from the switches to the heaters and the capillary tubing penetrate the lower vessel head via sealing bushings.

The electrical connections at the stack consist of copper connectors clamped to the copper collector plates with bolts and supported from the insulator plates. 4/0 nickel-coated TFE insulated cable is swaged to the copper connectors and led to the appropriate connectors on the adjacent stacks and a sealing bushing at the pressure vessel penetration. The cables are supported at intervals along their lengths to prevent whipping under short circuit fault conditions.

Two 6 in. diameter penetrations are provided in the vessel lower head to accommodate instrumentation. Each penetration has the capability of accommodating several multiple lead compression fittings. It is expected that the need for instrumentation will progressively reduce with time as the full stack and module test program proceeds.

Support for the fuel cell stack cartridge against seismic loads in the horizontal direction is provided by four adjustable support screws on a 90° spacing around the upper circumference of the pressure vessel. The supports are individually adjustable to suit the particular dimensions of initial or replacement cartridges following installation of the pressure vessel. Four guide bars supported between the stack compression plates protect the cartridge from damage during installation of the vessel.

The major physical characteristics of the module are listed in Table 3-29. The module external interfaces are listed in Table 3-30.

TABLE 3-29
MODULE PHYSICAL CHARACTERISTICS

Vessel Height	3.5 m (11 ft, 6 in)
Vessel Diameter	1.37 m (4 ft, 6 in)
Base Plate Diameter	1.68 m (5 ft, 6 in)
Weight	5400 kg (6 tons)
Module Contains 4 Stacks of 419 Cells	83 5-cell groups 2 2-cell groups
Cell Plate Dimensions (machined)	0.419 m x 0.3 m (16.5 x 11.75 in)
Stack Height	2.44 m (8 ft) (approximately)
Stack Weight	621 kg (1370 lb)
Vessel Cylinder Weight	1088 kg (2400 lb)

Automatic Disconnection of Process Fluid lines during cartridge replacement

Pressure Vessel - Carbon Steel to ASME Section VIII Division 1 for 586 kPa (85 psia) and 204°C (400°F) capability

TABLE 3-30
MODULE EXTERNAL INTERFACES

	Pipe Size	Pressure (psia)	Pressure (kPa)	Temperature (°F)	Temperature (°C)	Flow Rate (lb/hr)	Flow Rate (kg/hr)
Cooling Air - In	16" Flanged (150 lb)	70	(483)	297	(147)	61,380	(27,842)
Cooling Air - Out	16" Flanged (150 lb)	69	(476)	366	(186)	58,294	(26,442)
Process Air - Out	4" Flanged (150 lb)	69	(476)	379	(193)	3,110	(1,410)
Fuel - In	2" Flanged (150 lb)	70	(483)	376	(191)	398	(181)
Fuel - Out	2" Flanged (150 lb)	69	(476)	385	(196)	373	(169)
Acid - In	TBD	N/A		N/A			

Electric Connections	o Vessel feedthrough, two wire sealing bushing (O-Z Gedney Type CSBG) o Wire size, 4/0 avg stranded nickel-coated copper conductor (TFE insulated)
Module Voltage	1156 (Operating) 1340 (Operating Limit) 1540 (Open Circuit)
Module Current	324 amps
Module Power	375 kW
Module Heat Rate	7340 BTU/kWh

3.6.3 Acid Supply System

A continuous acid supply system has been incorporated. Phosphoric acid is supplied to the stacks through Teflon tubes clamped to connectors in the stack. The supply lines to the stacks receive acid from a distribution box attached to the cover plate of the cooling air outlet plenum.

The acid pump consists of a piston, cylinder, and check valve assembly. The piston rod of the pump extends through a sealing gland into a double-acting air cylinder. All of the pump parts exposed to acid are made of Teflon. In operation, compressed air is admitted to the piston rod side of the air cylinder causing the acid pump to withdraw acid from the reservoir. The compressed air supply is then valved to the opposite side of the air piston and the piston rod side is allowed to exhaust, causing the acid pump to discharge the swept volume of acid into the supply line to the acid distribution box at the upper end of the fuel cell cartridge.

The acid pump is mounted from the acid tank, which is suspended below the module vessel lower head, clear of the vessel thermal insulation. Under normal operating conditions the acid tank and pump are maintained at a temperature below 65°C (150°F). Heat conducted into the tank from the module pressure vessel is removed from the tank by free convection. Under low temperature ambient air conditions heater coils around the tank and pump are energized to maintain a minimum temperature of 38°C (100°F). Explosion-proof temperature switches mounted on the acid tank monitor the tank temperature and control the electrical supply to the heaters. Provision is made for monitoring the acid level in the tank and for manually replenishing the acid supply when required. Monitoring may be visual, by means of a translucent Teflon sight gauge affixed to the tank. Final details of the selected approach will be verified in testing prior to being applied to the module. Provision for filtering the acid supply from the pump and for minimizing the recirculation of corrosion products and debris may also be incorporated if testing experience shows such provisions to be necessary.

3.6.4 Module Maintenance

The only consumable, apart from the fuel and air supplies, requiring periodic attention is the phosphoric acid supply. Nominal module acid consumption is expected to be in the region of 1.2 cm^3 per hour (approximately 0.25 gallon per month). However, consumption conservatively could be four times this value, or 4.8 cm^3 per hour (1 gallon per month).

The acid reservoir suspended below the module pressure vessel has a capacity of approximately 15 liters (4 gallons) with, perhaps, 11 liters (3 gallons) effectively available to the pump. This volume is sufficient for one year of operation under expected nominal consumption conditions or, conservatively, under maximum conceivable consumption conditions, three months. Therefore, acid replenishment is not expected to be necessary more frequently than every three months. Acid level monitoring and logging of acid tank levels (possibly once a month) will be required in the early operational phases. These may be relaxed later as consumption rates are more accurately characterized. It is also conceivable, depending on the rate of contamination of the acid experienced in operation, that periodic removal of the tank for complete draining, cleaning, and replacement of the acid may be required. This would be performed during a scheduled shutdown period during the module life. Possibly, operational experience may show this to be unnecessary during the five year life of the module, in which case tank removal and cleaning would be performed only during the cartridge replacement shutdown period.

3.6.5 Cartridge Replacement

Cartridge replacement is expected to be required at five year intervals. The cartridge and pressure vessel dome must be removed together to satisfy lifting height limitations and protect the cartridge from the elements. The cartridge removal and replacement procedure outlined below satisfies these requirements and avoids disturbing the external piping connections to the module lower pressure vessel head. After removal, cartridges will be transported to an assembly area for packaging in a shipping container prior to being returned to the factory for refurbishment.

Replacement cartridges will be shipped from the factory in special shipping containers equipped with heaters and designed to maintain the requisite fuel cell environment. Assembly of a replacement cartridge into the power plant will follow the reverse of the procedure described below.

Replacement of a fuel cell module cartridge requires, first of all, that the power plant be shutdown, depressurized, and cooled. Following a sufficient period of cooling, the insulation segments at the pressure vessel bolting flange and the bolts can be removed. The pressure vessel dome can then be lifted, using a crane, until its lower flange is level with the cartridge lower support plate, a distance of 44.5 cm (17.5 inches).

While continuing to support the vessel dome from the crane, temporary bracing is deployed to ensure safe working conditions while lifting fixtures attaching the vessel lower flange to the cartridge lower support plate are bolted into position. After the vessel dome is securely bolted to the cartridge, the temporary bracing can be removed and work started to separate the cartridge from its connections to the module lower pressure vessel head. This requires the separation of electrical power takeoff leads, acid feed, drain and vent lines, heater power supply leads, temperature monitors, and cartridge holddown bolts. Any diagnostic or control instrumentation provided in the module must also be disconnected. The cartridge and vessel dome assembly can then be removed and transferred to an assembly/disassembly room for preparation for shipment to the factory. During transfer from the plant to the assembly/disassembly room, cartridge heating can be maintained, if required, by the use of a transportable power source with temporary heater power and temperature monitor connections.

In the assembly/disassembly room, preparation for shipment to the factory will normally involve removing the pressure vessel dome from the cartridge and transferring it, together with its lifting fixtures, to the replacement cartridge. The spent cartridge is then placed in a shipping container for transportation by truck. (The replacement cartridge will have been delivered to the plant site in such a shipping container.) Transfer of the replacement cartridge and pressure vessel dome from the assembly/disassembly room to the plant follows the reverse of the procedure described above.

The shipping container envisaged for use in shipping cartridges to and from the power plant has not yet been designed. The design of the shipping container must allow the cartridge to be heated and maintained in a suitably "inert" environment during shipment. In addition, the shipping container must protect the cartridge from handling damage during shipment and must be designed to minimize the volume and weight of the shipment.

3.7 <u>Fuel Cell Materials and Component Characterization and Testing</u> (WBS 1103-04)

This section addresses the characterization of the various raw materials utilized in the manufacture of repeating cell components, as well as the characterization of repeating cell components, including chemical, physical, mechanical, electrical and corrosion behavior.

3.7.1 Raw Material Specifications

The Purchasing Department Specifications (PDS) previously prepared were utilized for the procurement of raw materials for repeating component manufacture. Additional data were accumulated and will be utilized in future revisions of the PDSs as required.

3.7.2 Plate Materials

This section summarizes the characterization effort devoted to bipolar and cooling plates and the raw materials used in their formulation.

3.7.2.1 Plate Evaluation

Emphasis was placed on the evaluation of "Zee-Zee" bipolar plates produced primarily from graphite or carbon powders exhibiting approximately equiaxed particle shapes, namely Asbury Regrind A99, Asbury Regrind 4421 and Stackpole

MF958 powder. These three materials produce plates which are generally flat to within less than 0.8 mm (0.030 inch).

Plates were heat treated to 900°C (1650°F) and those evaluated are identified in Table 3-31.

The in-plane electrical resistivity and mercury porosimetry for a number of these plates are given in Tables 3-32 and 3-33.

Based on the corrosion data obtained by ERC, it was concluded that additional heat treatment to higher temperatures would be required for adequate pressurized cell performance. Sections of larger plates previously heat treated to 900°C (1650°F) were heat treated to both 1500°C and 2700°C (2732°F and 4900°F) for evaluation of selected mechanical and physical properties and for autoclave corrosion studies. Typical mercury porosimetry data for the two regrind type materials and Stackpole MF958 powder plate sections are given in Table 3-34. It is to be noted that the porosity of the three materials increased from 3.6 to 5.0 percent after 900°C (1650°F) heat treatment to between 11.0 and 14.7 percent after 2700°C (4900°F) heat treatment.

Weight loss data for ZFA64, TZA27 and TZA30 resulting from the second heat treatment cycle to 2700°C (4900°F) were determined. The data indicate a weight loss ranging from 1.2 to 3.2 w/o.

Flexural strengths at room temperature were determined for the three materials after heat treatment at 900, 1500, and 2700°C (1650, 2732, and 4900°F). The average data are plotted in Figure 3-30, together with reference data on A99 (33 w/o resin) material. After the 900°C (1650°F) heat treatment, the regrind A99 material had the lowest flexural strength while the Stackpole MF958 (33 w/o resin, dry mix) plate material had the highest. Heat treatment at 1500°C (2732°F) resulted in a small strength increase in the three materials while 2700°C (4900°F) heat treatment resulted in a strength decrease, particularly for the MF958 powder plate material.

TABLE 3-31
DEVELOPMENTAL PLATE COMPOSITIONS

Plate No.	Type Graphite	Mix	Comments
ZZ293	Poco PXB-5Q-325	Dry	
ZZ299	Airco Speer Texaco Wilmington	Dry	
ZZ300	Stackpole MF958	Dry	
ZZ302	A99 Regrind (-40)	Dry	
ZZ330	A99 Regrind	Dry	Regrind prepared from cold pressed material.
ZZ332	A99	Dry	
ZZ341	Stackpole MF958	Dry	
ZZ346	A99/MF958	Dry	50 w/o of each powder.
ZZ367	A99 Regrind (-40)	Dry	
ZZ404	Stackpole MF1001	Dry	
ZZ405	Desulco 9026	Dry	
ZZ411	A99	Dry	
ZZ414	A99	Dry	
ZZ419	Asbury 4421	Dry	
ZZ464	Asbury 4421 Regrind	Dry	5.7 day heat treatment.
ZZ465	Asbury 4421 Regrind	Dry	10.7 day heat treatment.
ZFA64	Asbury 4421 Regrind	Dry	
TZA27	Stackpole MF958 (Lot 1)	Dry	First powder lot.
TZA30	A99 Regrind	Dry	
ZZ539	Stackpole MF958	Dry	Second powder lot.
ZZ597	Stackpole MF958	Dry	Second powder lot.
ZZ608	Stackpole MF958	Dry	Second powder lot.
ZZ612	Stackpole MF958	Dry	Second powder lot.
ZZ642	Stackpole MF958	Wet	Second powder lot.
ZZ643	Stackpole MF958	Wet	Second powder lot.
ZZ650	Regrind A99	Dry	-40 mesh.
ZZ660	Regrind A99	Dry	-40 mesh.
ZZ660	Regrind A99	Dry	-40 mesh.

TABLE 3-32
IN-PLANE ELECTRICAL RESISTIVITY OF DEVELOPMENT PLATES AFTER 900°C HEAT TREATMENT

Plate No.(1)	Resistivity ρ Plane (mΩ-cm)	Resistivity(2) ρ Thickness (mΩ-cm)	Ratio(2) ρ_p/ρ_t
ZZ293	2.98	-	-
ZZ299	2.01	-	-
ZZ300	2.12	-	-
ZZ302	3.42	-	-
ZZ330	3.07	-	-
ZZ332	1.53	-	-
ZZ341	2.00	-	-
ZZ346	1.78	-	-
ZZ367	3.26	-	-
ZZ404	1.69	-	-
ZZ405	2.37	-	-

---

(1) See Table 3-31 for compositions, etc.
(2) Data to be collected.

TABLE 3-33

MERCURY POROSIMETRY DATA FOR DEVELOPMENT PLATES HEAT TREATED TO 900°C

Plate No.(1)	Skeletal Density (g/cm^3)	Bulk Density (g/cm^3)	Specific Pore Volume (cm^3/g)	Specific Pore Surface (m^2/g)	Porosity (Percent)
ZZ293	2.15	2.11	0.010	4.7	2.1
ZZ299	2.18	2.11	0.014	7.1	2.9
ZZ300	2.18	2.10	0.016	8.9	3.4
ZZ302	2.10	1.94	0.039	17.6	7.5
ZZ330	2.08	1.91	0.042	21.6	8.0
ZZ332	2.24	2.11	0.027	14.4	5.7
ZZ341	2.23	2.13	0.021	10.9	4.4
ZZ346	2.23	2.11	0.026	14.1	5.5
ZZ367	2.08	1.98	0.025	12.7	5.0
ZZ404	2.25	2.06	0.040	20.6	8.3
ZZ405	2.10	1.78	0.084	23.5	15.0
ZZ411	1.95	1.87	0.024	11.4	4.5
ZZ414	1.97	1.86	0.030	14.3	5.6
ZZ419	1.97	1.91	0.017	7.8	3.2
ZZ464	1.83	1.76	0.022	11.9	4.1
ZZ465	1.83	1.77	0.020	10.8	3.6

---

(1)See Table 3-31 for compositions, etc.

TABLE 3-34

MERCURY POROSIMETRY DATA FOR SELECTED DEVELOPMENTAL PLATES HEAT TREATED TO 2700°C

Plate No.[1] Percent	Skeletal Density (g/cm^3)	Bulk Density (g/cm^3)	Specific Pore Volume (cm^3/g)	Specific Pore Surface (m^2/g)	Porosity
ZZ341	2.10	1.87	0.059	25.3	11.0
ZZ367	2.09	1.83	0.069	24.4	12.6
ZZ465	2.07	1.76	0.083	33.3	14.7
Subscale End Plate (A99 Graphite + 33% Resin)	2.14	1.73	0.109	27.3	18.9

---

(1)See Table 3-31 for composition, etc.

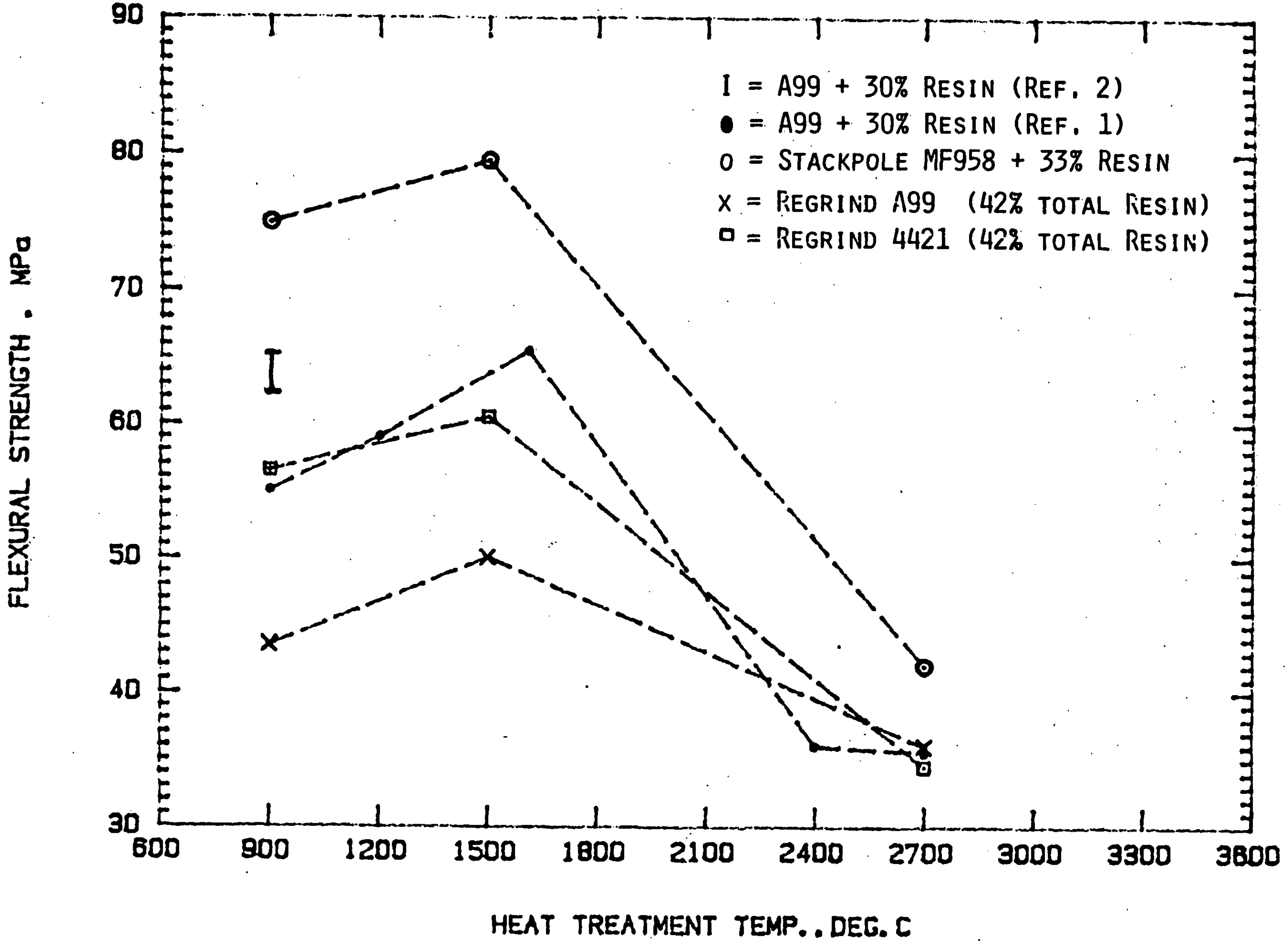

Figure 3-30. Flexural Strength Vs. Heat Treatment Temperature

The in-plane electrical resistivity of the three materials was determined and is provided in Figure 3-31. As would be expected, the resistivity decreased with increased heat treatment temperature.

Shrinkage data were obtained on small samples of Stackpole MF958 plate material heat treated to 2700°C (4900°F) and ranged from 0.5 to 0.8 percent. The accuracy of these measurements is limited and more reliable data will be obtained from full size 2700°C (4900°F) heat treated plates.

Helium permeability testing performed on small (4.5 cm (1.8 in.) diameter) samples of Zee-Zee plates heat treated to both 900°C and 2700°C (1650°F and 4900°F) indicated a very low permeability of 8 x 10^{-8} cm^3/sec (0.48 x 10^{-8} $in.^3$/sec) or less for Stackpole MF958 material, while the regrind A99 material gave values of about 6 x 10^{-6} cm^3/sec (0.36 x 10^{-6} $in.^3$/sec).

Based on the screening tests performed to date, the most promising graphite powder for production of large flat as-pressed plates is Stackpole MF958. Additional samples of this material were heat treated to 900°C and 2700°C (1650°F and 4900°F) for flexural and electrical resistivity measurements. The data obtained are given in Tables 3-35 and 3-36 and are in relatively good agreement with the screening data presented earlier.

The backup to this material will most likely be the Asbury Regrind A99 plate material. Several additional plate samples were evaluated after 900°C (1650°F) heat treatment (ZZ650, 660 and 666). The average flexural strength was 53.2 MPa (7,700 psi) and ranged from 48.5 to 55.6 MPa (7,000 to 8,100 psi), while the in-plane electrical resistance for the same samples ranged from 2.99 to 3.17 mΩ; the average was 3.08 mΩ.

3.7.2.2 Plate Corrosion

Autoclave corrosion testing of the three principal candidate plate materials, Stackpole MF958 (33 w/o resin), Asbury Regrind A99 (∿49 w/o resin) and Asbury Regrind 4421 (∿49 w/o resin) was performed in 97 w/o H_3PO_4 at

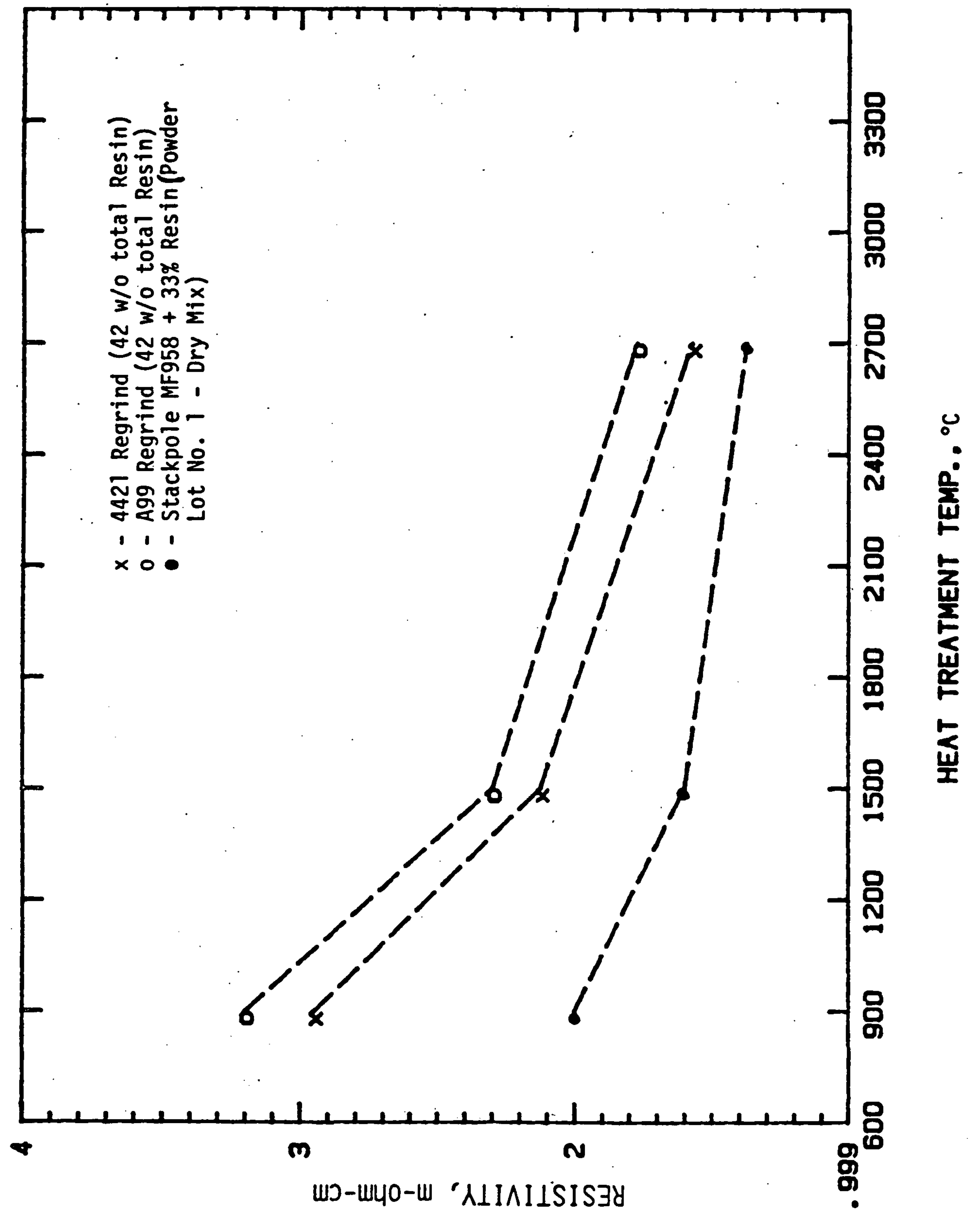

Figure 3-31. Electrical Resistivity Vs. Heat Treatment Temperature (In-Plane)

TABLE 3-35

FLEXURAL STRENGTH OF BIPOLAR PLATE MATERIAL

Material (Plate Nos.)	Heat Treatment (°C)	Average Flexural Strength		Range of Flexural Strength	
		MPa	Psi	MPa	Psi
MF958 (new powder lot) 33 w/o Resin, Dry Mixed (ZZ 589, 597)	900	77.2	11,200	75.8 to 78.9	11,000 to 11,450
	2700	47.5	6,900	36.5 to 54.8	5,300 to 7,950
MF958 (new powder lot) 36 w/o Resin, Dry Mixed (ZZ 608, 612)	900	74.4	10,800	69.6 to 83.4	10,100 to 12,100
	2700	52.4	7,600	49.3 to 55.1	7,150 to 8,000
MF958 (new powder lot) 33 w/o Resin, Wet Mixed (ZZ 642, 643)	900	68.9	10,000	59.9 to 74.4	8,700 to 10,800
	2700	45.1	6,550	39.9 to 52.0	5,800 to 7,550

TABLE 3-36

IN-PLANE ELECTRICAL RESISTIVITY OF BIPOLAR PLATE MATERIALS

Material (Plate Nos.)	Heat Treatment (°C)	Average Resistivity (mΩ-cm)
MF958 (new powder lot) 33 w/o Resin Dry Mixed (ZZ 589, 597)	900	1.90
	2700	1.34
MF958 (new powder lot) 36 w/o Resin, Dry Mixed (ZZ 608, 612)	900	2.01
	2700	1.36
MF958 (new powder lot) 33 w/o Resin, Wet Mixed (ZZ 642, 643)	900	1.98
	2700	1.47

190°C (374°F) and 485 kPa (4.8 atms) after heat treatment at 900, 1500, and 2700°C (1650, 2732, and 4900°F). The dynamic hydrogen electrode (DHE), used as a reference electrode, was polarized at 0.1 mA/cm^2 (0.09 A/ft^2) and exhibited a stable potential of approximately 22 mV below the reversible hydrogen electrode (RHE). After each corrosion test, the density of the acid was determined and showed a change of less than 0.5 w/o.

The corrosion potential-current density relationships (using one side of specimen geometric surface area) for the 900°C and 2700°C (1650°F and 4900°F) heat treated samples are shown in Figure 3-32. Relatively linear Tafel slope regions over two to three decades were observed for the samples tested. The 2700°C (4900°F) heat treated samples exhibited slopes of from 57 to 85 mV/decade which were somewhat lower than those of the 900°C (1650°F) material which gave slopes of from 116 to 145 mV/decade.

Table 3-37 summarizes the corrosion data at 0.8 and 0.9 volts versus RHE. At similar test conditions, the 900°C (1650°F) heat treated plate material made from Stackpole MF958 powder (33 w/o resin) gave a slightly lower corrosion current density than the two regrind materials (∿42 w/o resin), presumably due to the lower resin content of the former. At 0.8 V versus RHE, the 2700°C (4900°F) heat treated materials exhibited corrosion currents of 0.0017 mA/cm^2 (0.0015 A/ft^2) or lower while for the 900°C (1650°F) material, corrosion currents ranged from 0.17 to 0.77 mA/cm^2 (0.7 A/ft^2). Increasing the heat treatment temperature from 900°C to 2700°C (1650°F to 4900°F) thus reduced the corrosion current density at 0.8 V versus RHE by at least two orders of magnitude while the 1500°C (2732°F) heat treated material showed only about a factor of two reduction.

After corrosion testing, samples were gently washed in hot water to remove acid residue, vacuum dried, mounted and polished for optical microscopic examination. Microstructures of the corrosion surface cross section are shown in Figure 3-33 for the Stackpole MF958 plate material. It is noted that the carbon phase resulting from pyrolysis of the resin binder was selectively and severely corroded in the 900°C (1650°F) heat treated plate resulting in a

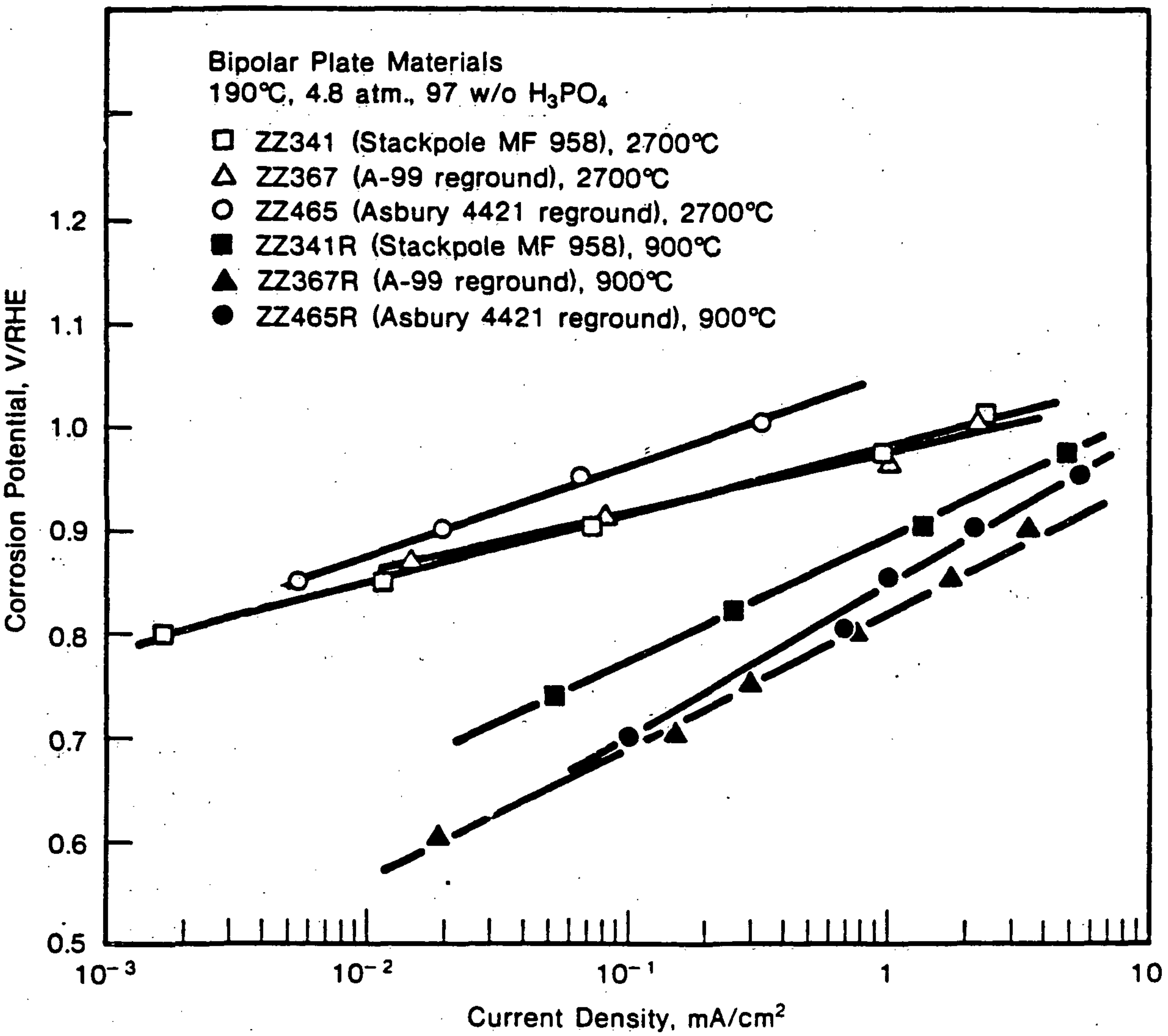

Figure 3-32. Corrosion Current Vs. Corrosion Potential for Heat Treated Plate Materials

TABLE 3-37
CORROSION RATE OF CANDIDATE BIPOLAR PLATE MATERIALS

(Experimental Conditions: 190°C, 4.8 atm, 97 w/o H_3PO_4)

Raw Materials	Sample ID	Heat Treatment Temperature, °C	Corrosion Current at 0.8 V, mA/cm^2	Corrosion Current at 0.9 V, mA/cm^2
A-99 Regrind	ZZ367R	900	0.77	3.6
A-99 Regrind	TZA-30	1500	0.34	1.06
A-99 Regrind	ZZ367	2700	0.0010*	0.057
Stackpole MF958	ZZ341R	900	0.17	1.4
Stackpole MF958	TZA-27	1500	0.12	0.66
Stackpole MF958	ZZ341	2700	0.0017	0.064
Asbury 4421 Regrind	ZZ465R	900	0.70	2.2
Asbury 4421 Regrind	ZFA-64	1500	0.30	1.26
Asbury 4421 Regrind	ZZ465	2700	0.0015*	0.020

---

*No anodic corrosion current was observed at 0.8 V. Value obtained by extrapolation of higher voltage data to 0.8 V.

BIPOLAR PLATE MATERIALS AFTER CORROSION TESTING

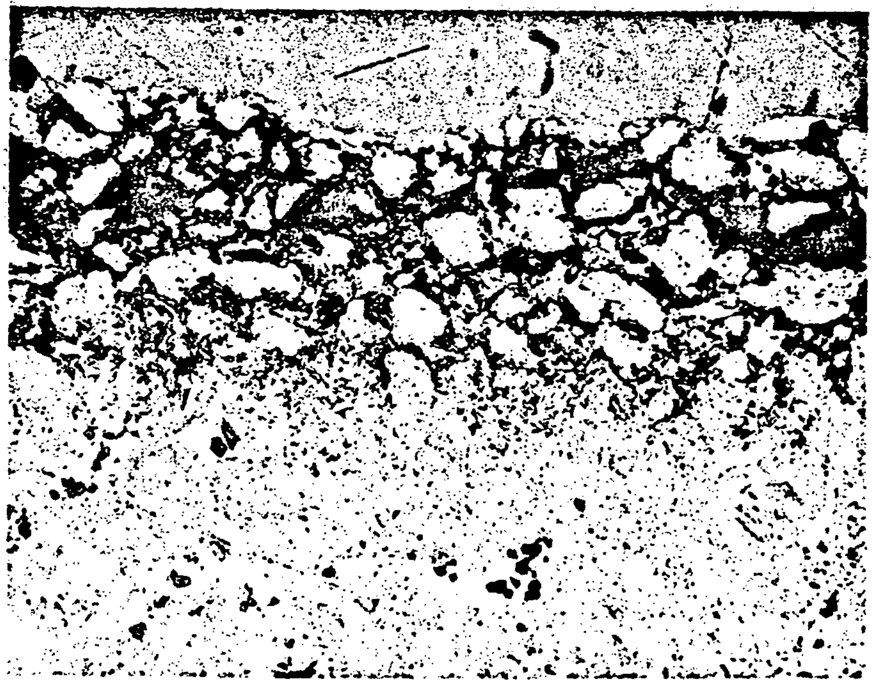

Stackpole MF958
Graphite, 900°C
Heat Treatment

200X

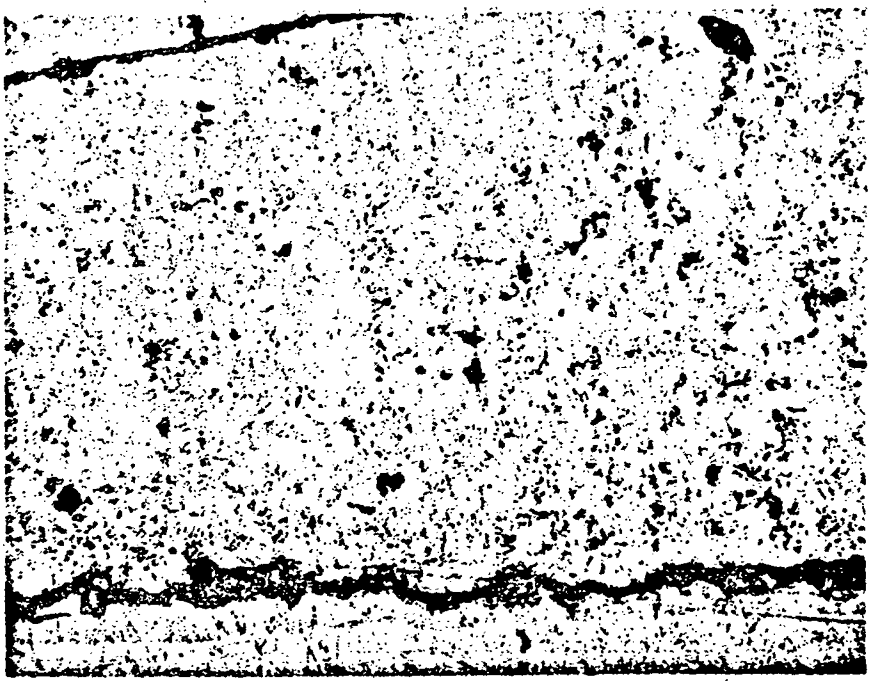

Stackpole MF958
Graphite, 2700°C
Heat Treatment

200X

Figure 3-33. Microstructures of Stackpole MF958 Plate Material after Corrosion Testing.

surface layer of relatively large loose particles similar to the Stackpole MF958 graphite powder used in preparation of these plates. The 2700°C (4900°F) heat treated sample shows relatively uniform surface attack with little or no selective attack of the carbon binder phase apparent. Metallography of the Asbury Regrind A99 and Asbury Regrind 4421 samples revealed similar corrosion behavior. The appearance of the 900°C (1650°F) samples agrees with the observations made previously on samples of plate corrosion from pressure-tested stacks and subscale tests - namely, that the resin carbon phase of the 900°C (1650°F) heat treated bipolar plates seems to be selectively corroded while the graphite powder particle shows very little attack.

Limited autoclave corrosion data were obtained on bipolar plate materials in 93 w/o phosphoric acid at 190°C (374°F) and 690 kPa (100 psia). Plate samples were heat treated for times up to 100 hours at 900, 1100, and 1200°C (1650, 2000, and 2200°F). These tests indicate that no improvement in corrosion behavior was obtained from longer heat treatment times at 900°C (1650°F) (4 versus 100 hours) and that only limited improvement is achieved at temperatures of 1100°C and 1200°C (2000°F and 2200°F) for 100 hours (see Figure 3-34). These tests confirm the conclusion that heat treatment temperature has the major impact on corrosion behavior, while longer times at temperature result in relatively little or no improvement at the lower temperatures examined.

3.7.2.3 Plate Raw Materials

Particle size distribution for a number of graphite powders utilized in plate production, including as-received samples of A99, 4421, PXB-5Q and MF958 (two lots) as well as reground A99 (-40 mesh) and reground 4421, was determined.

Samples of Varcum 29-703 were heat treated to 900, 1500, and 2700°C (1650, 2732, and 4900°F) to provide samples of the binder resin carbon for X-ray diffraction analysis. X-ray diffraction profiles show a contraction in the C direction (002) from 3.885 to 3.472 Å coupled with an increase of about

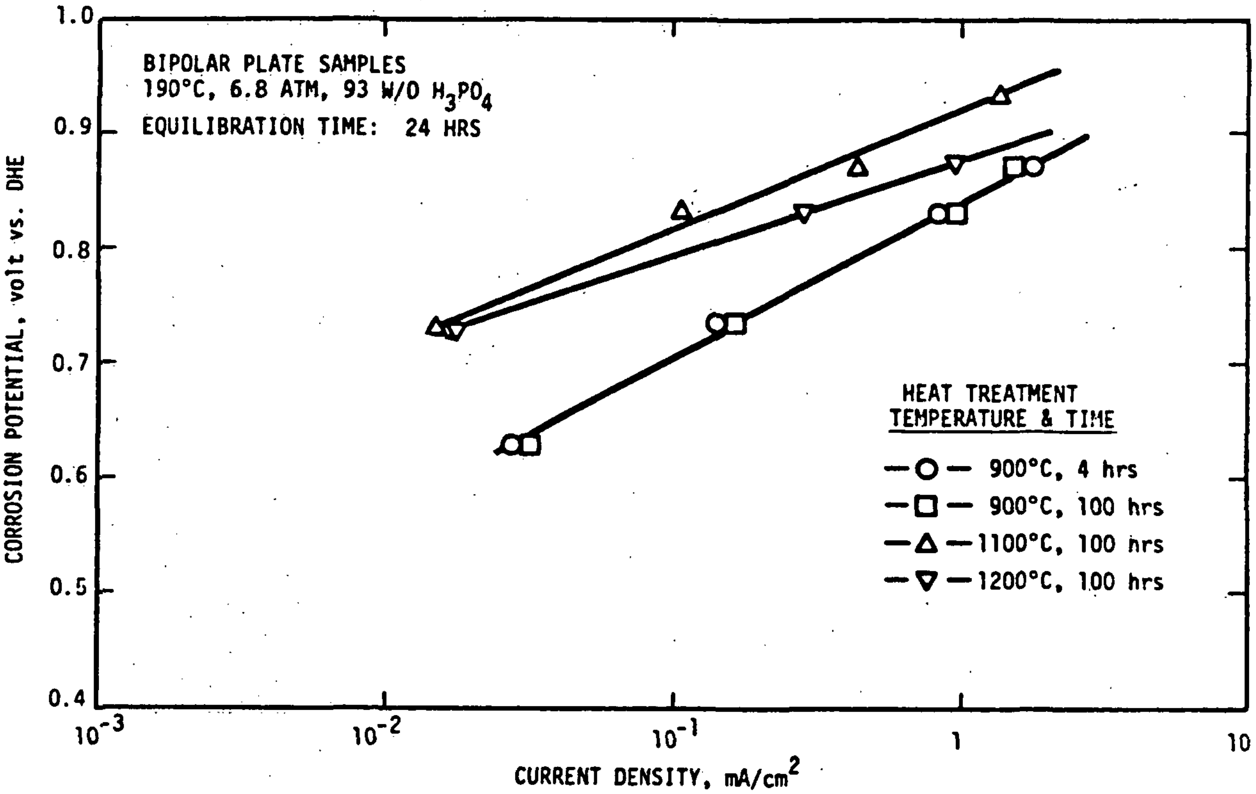

Figure 3-34. Corrosion Tafel Plots for Heat Treated Bipolar Plate Materials.

2 times in the L002 crystallite size as a result of the 2700°C (4900°F) heat treatment, see Table 3-38. Typical diffraction profiles at 900, 1500, and 2700°C (1650, 2237, and 4900°F) are shown in Figure 3-35. Selected samples were used for determination of resin carbon weight loss resulting from additional heat treatments to temperatures above 900°C (1650°F); at 1600°C (2900°C) the loss was 1.3 w/o while at 2700°C (4900°F) it was 1.6 w/o.

3.7.3 Seal Materials

The stack design relies on effective edge cell-to-cell seals as well as manifold-to-stack seals. Seal tests were conducted to simulate the seal configuration planned for the 10 and 25 kW stacks. Selection of the materials tested was based on several specific parameters such as gas sealability, structural stiffness, acid corrosion resistance, compression set, and stability at 200°C (392°F). The commercial availability of stock sheet forms is an important consideration; therefore, the thickness of samples tested are not necessarily the thickness for the stack application. Generally, gas sealability, structural stiffness, short-term compression set, and operating temperature stability parameters are exhibited via a sealing test at ambient temperature and 200°C (392°F) . The general seal test configuration is shown on Figure 3-36. A flowmeter capable of detecting flow rates as low as 0.003 cm^3/min (0.011 $in.^3$/h) air is placed in series with the gas inlet to provide a more quantitative measure of seal leakage. The testing was done on a stack of five or six picture frame seals attached to heat treated 10 x 10 cm (4 x 4 in.) graphite/resin plates on one surface with Viton cement. A linear variable displacement transducer (LVDT) is used to define the seal displacement as a function of time. The load and displacement values are recorded continuously on a strip recorder to evaluate the structural characteristics. Dry nitrogen gas was used to internally pressurize the seal stack to either 108 kPa (1 psig) or 135.5 kPa (5 psig). Usually, two stacks were used to evaluate the ambient temperature and operating temperature, 200°C (392°F), conditions.

The perfluoroelastomer Kalrez was tested at both ambient and operating temperatures. This material was tested in the standard dry seal configuration

TABLE 3-38
CRYSTALLITE SIZES AND LATTICE SPACINGS OF HEAT TREATED VARCUM 29-703 RESIN

H.T. Temperature °C	d_{002}/Å	d_{100}/Å	L_{002}/Å	L_{100}/Å
900	3.885	2.06	9	18
1500	3.667	2.08	11	27
1800	3.645	2.08	13	28
2200	3.535	2.08	15	34
2700	3.472	2.10	20	48

C-3

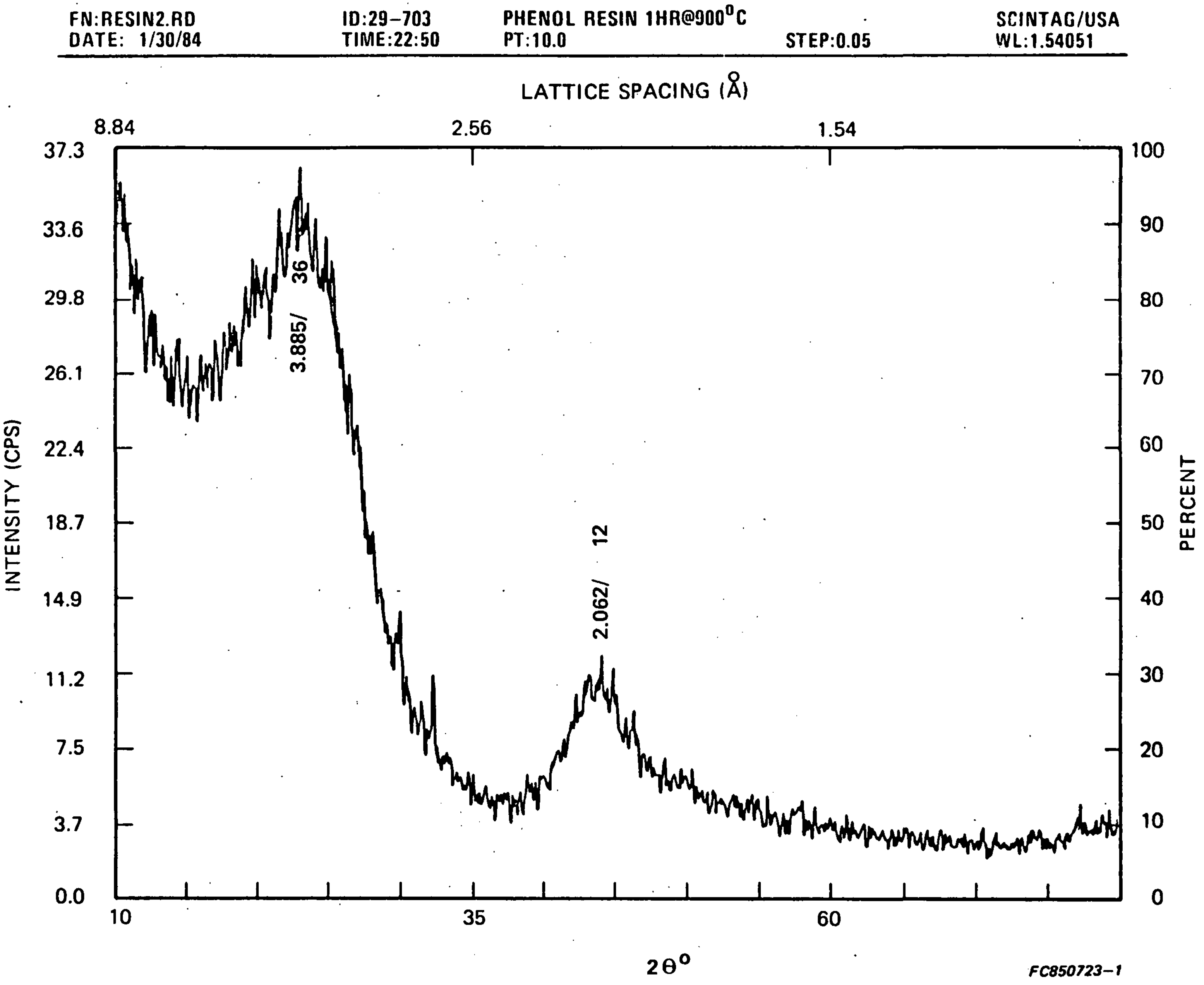

Figure 3-35. X-ray Diffraction Profile of Resin 29-703 Heat Treated at Temperatures Indicated

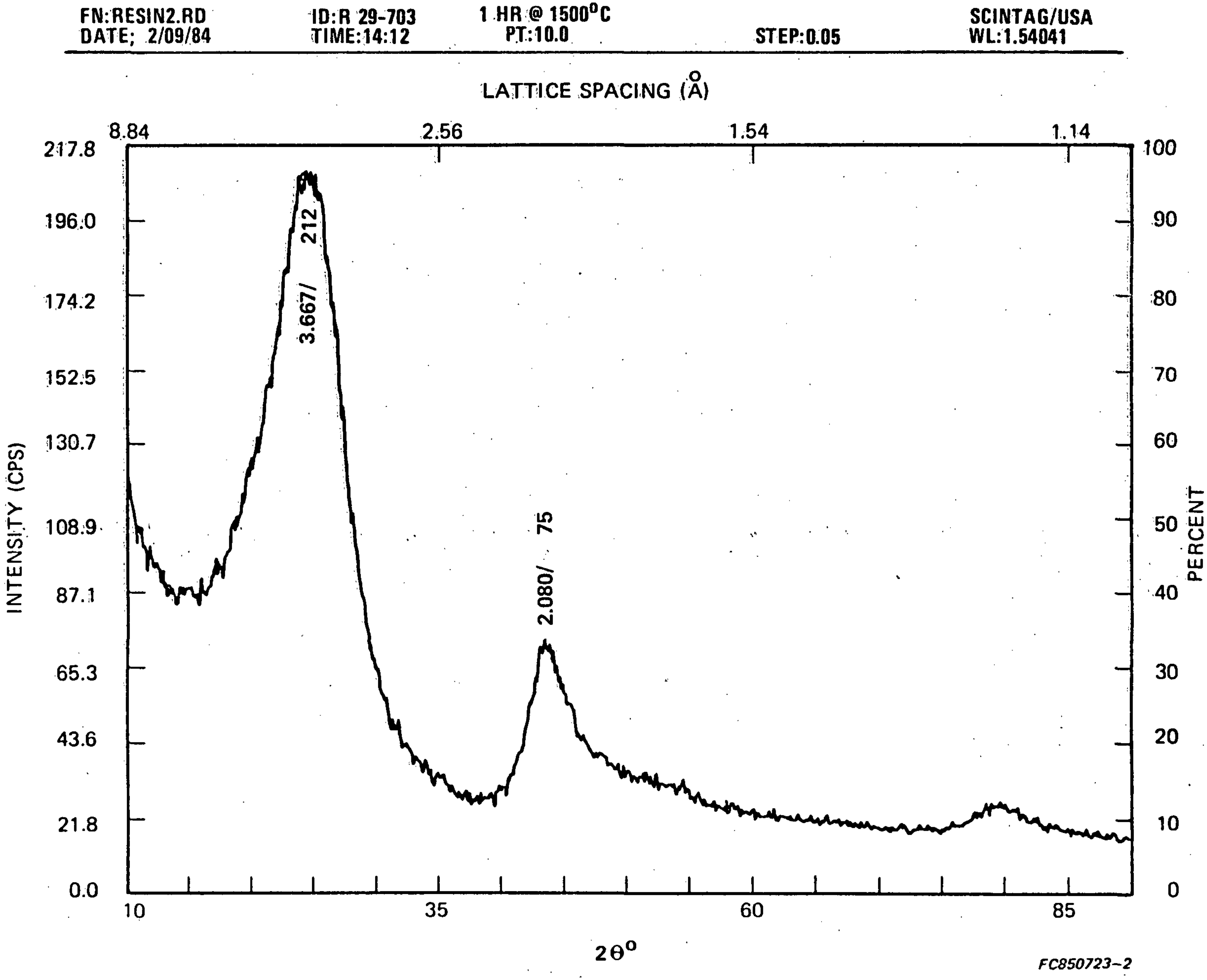

Figure 3-35. X-ray Diffraction Profile of Resin 29-703 Heat Treated at Temperatures Indicated (CONT'D)

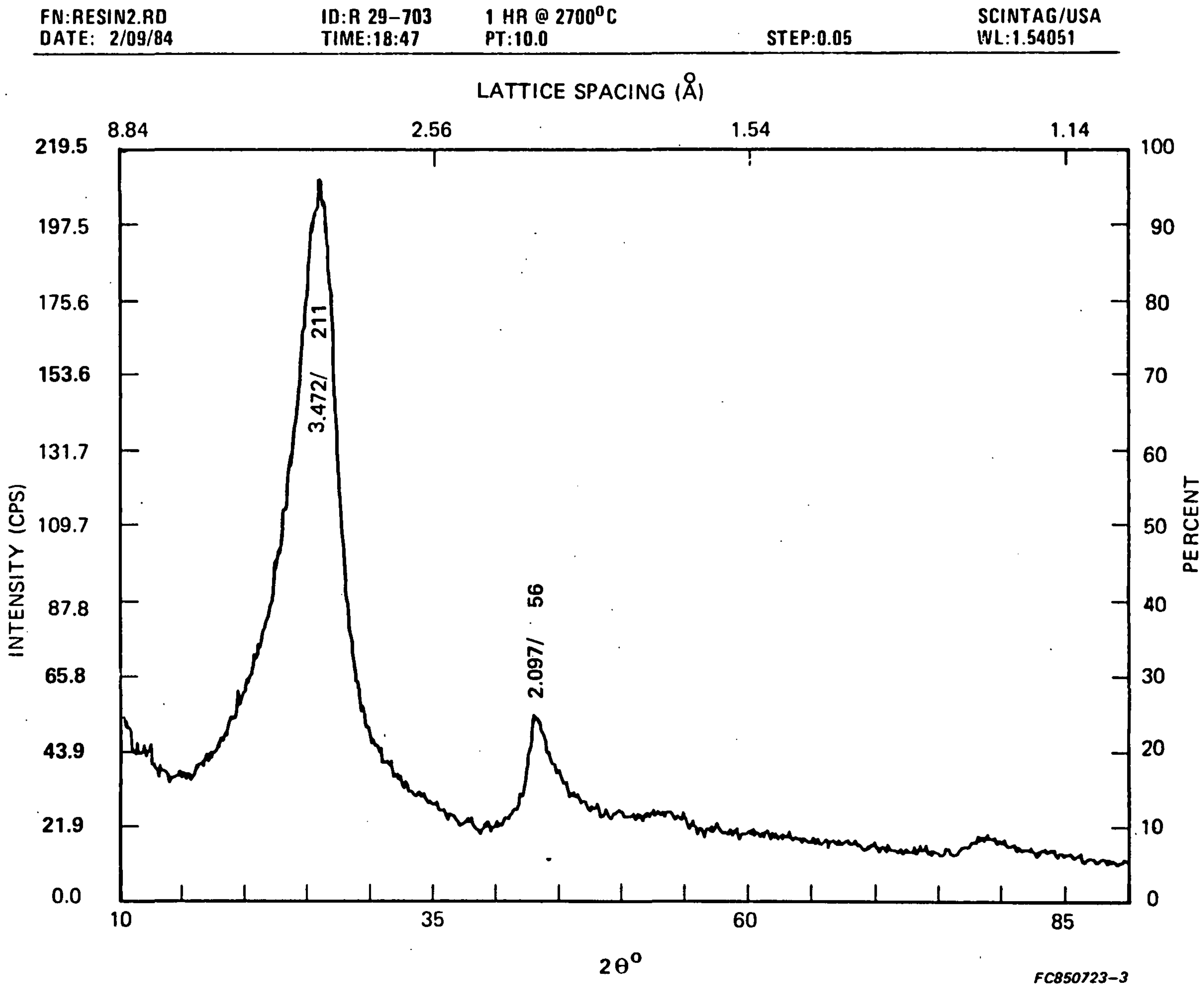

Figure 3-35. X-ray Diffraction Profile of Resin 29-703 Heat Treated at Temperatures Indicated (CONT'D)

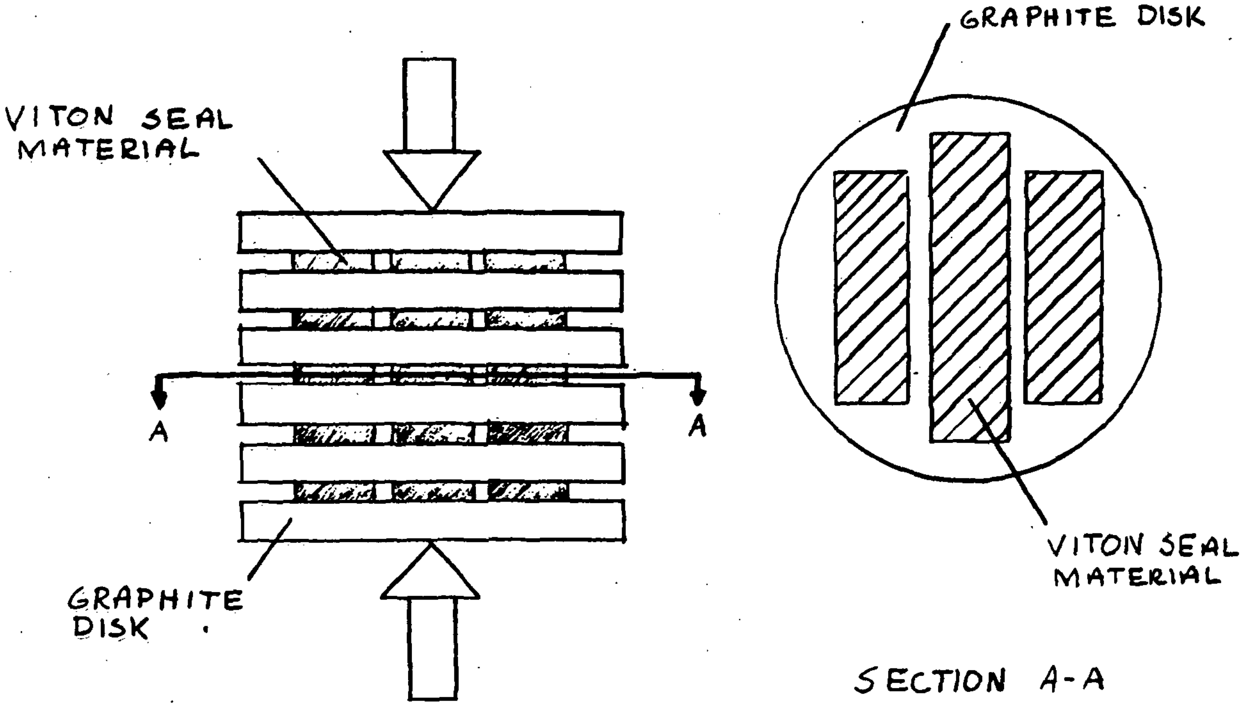

Figure 3-36. Creep Test Configuration

using no acid. The Kalrez tested, Compound 1-58, was 60 durometer Shore hardness. The Kalrez seal stack was cycled four times at ambient temperature to compressive strains of 10.3 to 28.9 percent producing tangent elastic moduli values of 9.85 MPa (1428.6 psi) to 16.01 MPa (2321.4 psi). During the first cycle, the seal stack was leak tested at 10.5 percent strain. The result was corner leakage at a pressure differential of 108 kPa (1.0 psig) of nitrogen gas. On succeeding cycles, the seal stack was compressed to progressively higher strains and the corner leak became nonexistent even at an internal pressurization of 446 kPa (50 psig) of nitrogen gas.

Ambient temperature stress-vs-strain cycle data indicate a good strain range, 0-22 percent, with a maximum seal compression pressure of 1.67 MPa (240 psi) with relatively linear behavior beyond the 3 percent strain value. The modulus of elasticity values for Kalrez is similar to Viton with tangent values equivalent to 10.4 MPa (1500 psi). A summary of these modulus of elasticity values is shown on Table 3-39 for the various loading cycles. This table also provides a comparison between the Kalrez and the Viton values for similar conditions.

The operating temperature test cycles are shown on Figure 3-37. These cycles indicate a consistent tangent modulus of elasticity of 6.894 MPa (1000 psi) over the seal strain range of 4 to 20 percent. This also indicates that the material becomes softer at temperature. Again the modulus of elasticity values are linear and repeatable.

No evidence of seal leakage could be detected for an internal nitrogen pressurization of 135.5 kPa (5.0 psig) at both test temperatures. The minimum seal contact pressure during these leak tests was 1.554 MPa (225.4 psi) at ambient temperature and 815.6 kPa (118.3 psi) at operating temperature. Kalrez seals also demonstrated the ability to withstand internal pressurizations of up to 446 kPa (50 psig) at both ambient and operating temperature with no leakage.

TABLE 3-39

SUMMARY OF LOAD VS. DEFORMATION COMPRESSION TEST DATA

Seal Material	Stack No.	Test Description	Contact Surface	Area Nominal cm^2 (in^2)	Maximum Stress Applied Load Newtons (lb)	$\nu = \frac{Load}{Area}$ KPa (psi)	N Specimens per Test Article	L[1] Height of Test Article cm (in)	ΔL Change in Length cm (in)	$E = \frac{\Delta L}{L}$ Total Strain (cm/cm or in/in)	Temp. of Test °C (°F)	$E = \nu/\epsilon$ Tangent Modulus of Elasticity MPa (psi)x10^3	$E=\nu/\epsilon$ Chord Modulus of Elasticity MPa (psi)x10^3
Kalrez	1	Cycle 1	Flat	14.45 (2.24)	1189.9 (267.5)	823.37 (119.42)	4	.620 (.244)	.0635 (.025)	.1025	22.2 (72)	9.86 (1.43)	7.79 (1.13)
	1	Cycle 2	Flat	14.45 (2.24)	2602.2 (585.0)	1800.63 (261.16)	4	.620 (.244)	.127 (.050)	.2049	22.2 (72)	10.41 (1.51)	9.86 (1.43)
	1	Cycle 3	Flat	14.45 (2.24)	4399.3 (989.0)	3044.17 (441.52)	4	.620 (.244)	.1796 (.050)	.2898	22.2 (72)	16.00 (2.32)	11.79 (1.71)
	1	Cycle 4	Flat	14.45 (2.24)	2402.2 (540.0)	1662.12 (241.07)	4	.620 (.244)	.1321 (.050)	.2131	22.2 (72)	10.96 (1.59)	9.79 (1.42)
	2	Stack 2 Cycle 1	Flat	14.45 (2.24)	1290.0 (290.0)	892.60 (129.46)	4	.620 (.244)	.0940 (.0370)	.1516	190 (374)	5.31 (0.77)	5.72 (0.83)
	2	Stack 2 Cycle 2	Flat	14.45 (2.24)	1158.8 (260.5)	801.79 (116.29)	4	.620 (.244)	.0940 (.0370)	.1516	190 (374)	6.83 (0.99)	7.10 (1.03)
	2	Stack 2 Cycle 3	Flat	14.45 (2.24)	1568.8 (352.5)	1085.03 (157.37)	4	.620 (.244)	.1250 (.0492)	.2016	190 (374)	7.86 (1.14)	8.00 (1.16)
	2	Stack 2 Cycle 4	Flat	14.45 (2.24)	1514.6 (340.5)	1048.07 (152.01)	4	.620 (.244)	.1252 (.0493)	.2020	190 (374)	7.03 (1.02)	9.17 (1.33)
	2	Stack 2 Cycle 5	Flat	14.45 (2.24)	1512.4 (340.0)	1046.56 (151.79)	4	.620 (.244)	.1252 (.0493)	.2020	190 (374)	7.03 (1.02)	9.17 (1.33)
	2	Stack 2 Cycle 6	Flat	14.45 (2.24)	4403.7 (990.0)	3047.21 (441.96)	4	.620 (.244)	.1242 (.0489)	.2004	22.2 (72)	13.10 (1.90)	14.89 (2.16)
Viton	2	Cycle 1[2]	Flat	24.80 (3.844)	3647.5 (820.0)	1474.1 (213.8)	6	.940 (.370)	.183 (.072)	.195	22.2 (72)	8.27 (1.20)	7.52 (1.09)
	3	Cycle 4[2,3]	Flat	19.35 (3.01)	2668.9 (600.0)	1379.0 (200.0)	6	.940 (.370)	.188 (.074)	.20	201.7 (395)	4.83 (0.70)	6.89 (1.00)

---

(1) Measured with a 5 lb. (2.23 psi) preload applied.

(2) This data was obtained from previously conducted tests and documented in Reference 3.

(3) Viton stack 3 had been previously cycled according to the following sequence:
Cycle 1 - compression cycle at ambient temperature
Cycle 2 - (thermal cycle) - 5-hr. soak at 201.7°C (395°F)
Cycle 3 - compression cycle at ambient temperature.

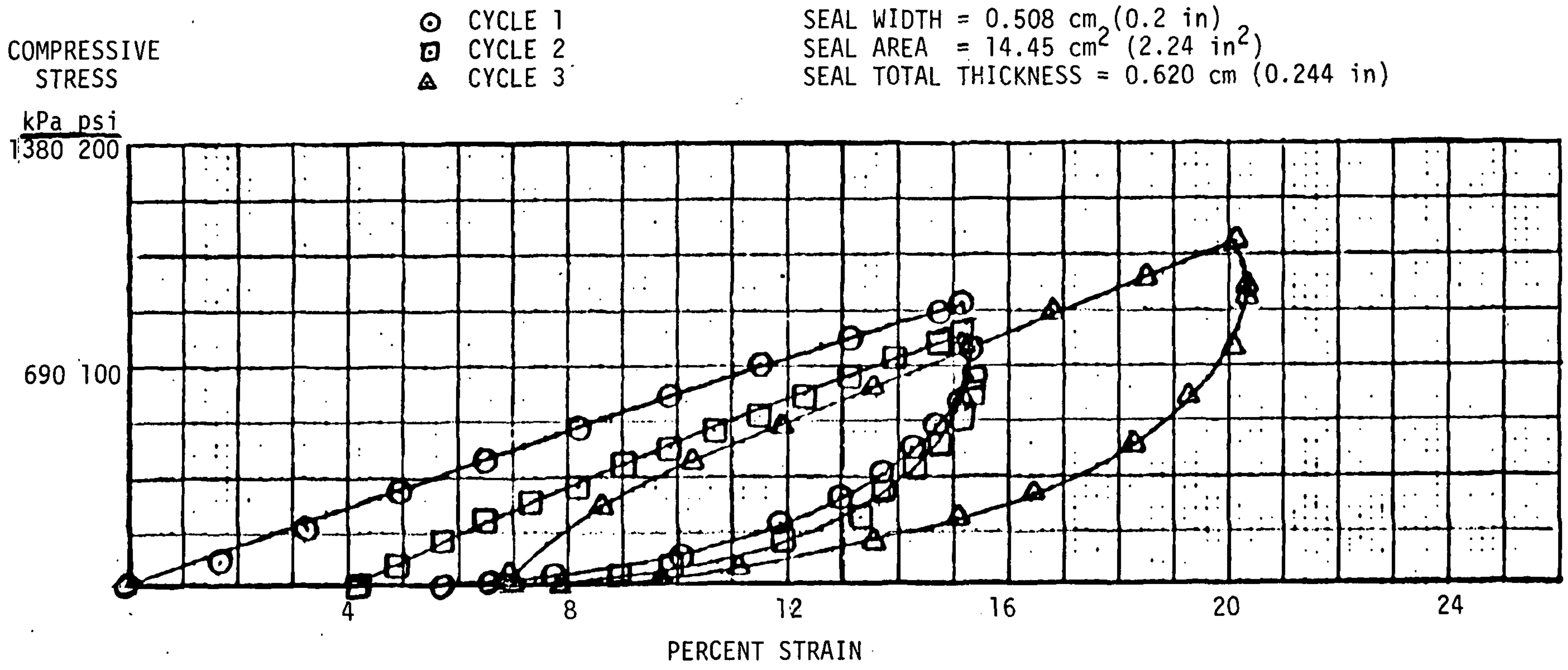

Figure 3-37. Compressive Seal Stress Vs. Seal Strain for Kalrez Seal Configuration at Operating Temperature (190°C)

Another key aspect of the mechanical testing is that of permanent set at both ambient and operating temperatures. The results of this study indicated after one cycle at ambient temperature Kalrez exhibited a 2.75 percent permanent compression set, and after four cycles permanent compression set of 4.8 percent occurred. Kalrez demonstrated larger compression sets of 5.8 percent and 7.8 percent after one and four cycles at operating temperature. These values are consistent with other elastomers which have been tested.

As part of this study, a comparison of material characteristics was made between Kalrez and Viton. A comparison of modulus of elasticity values at ambient temperature, operating temperature, and finally at ambient temperature after being at 193°C (380°F) for a period of time is shown on Figure 3-38. It was found that the Kalrez seals were slightly stiffer than Viton seals at both ambient and operating temperatures where the elastic moduli of Viton are 8270 kPa (1200 psi) and 4830 kPa (700 psi), respectively. Kalrez seals incurred a smaller permanent compression set after four cycles at ambient temperature than did Viton seals. Kalrez demonstrated a permanent compression set of only 16.5 percent of the maximum compressive strain developed during testing; Viton exhibited a permanent set of 51.3 percent of the maximum compressive strain developed during its testing. Both materials demonstrated good sealing capabilities under compressive loads normally encountered and with internal pressurization of 135.5 kPa (5.0 psig).

A short compression/seal leakage test stack made of Armalon seal material was assembled and tested. The Teflon coated fiber material, which indicated acceptable acid resistance, was tested at ambient temperature conditions. The dry stack was compressed and leak tested at three compression levels of 10, 15, and 20 percent strain. At all three loading conditions, the seals showed leakage at 135.5 kPa (5 psig) internal nitrogen pressurization. This leakage decreased at the higher compression strains. The exact source of this leakage could not be located due to a limitation of the size of the test unit and the test assembly. The material exhibited large permanent strains and very nonlinear behavior at ambient temperature conditions. Even though the tangent modulus values are on the order of 13.79 MPa (2000 psi), the large permanent

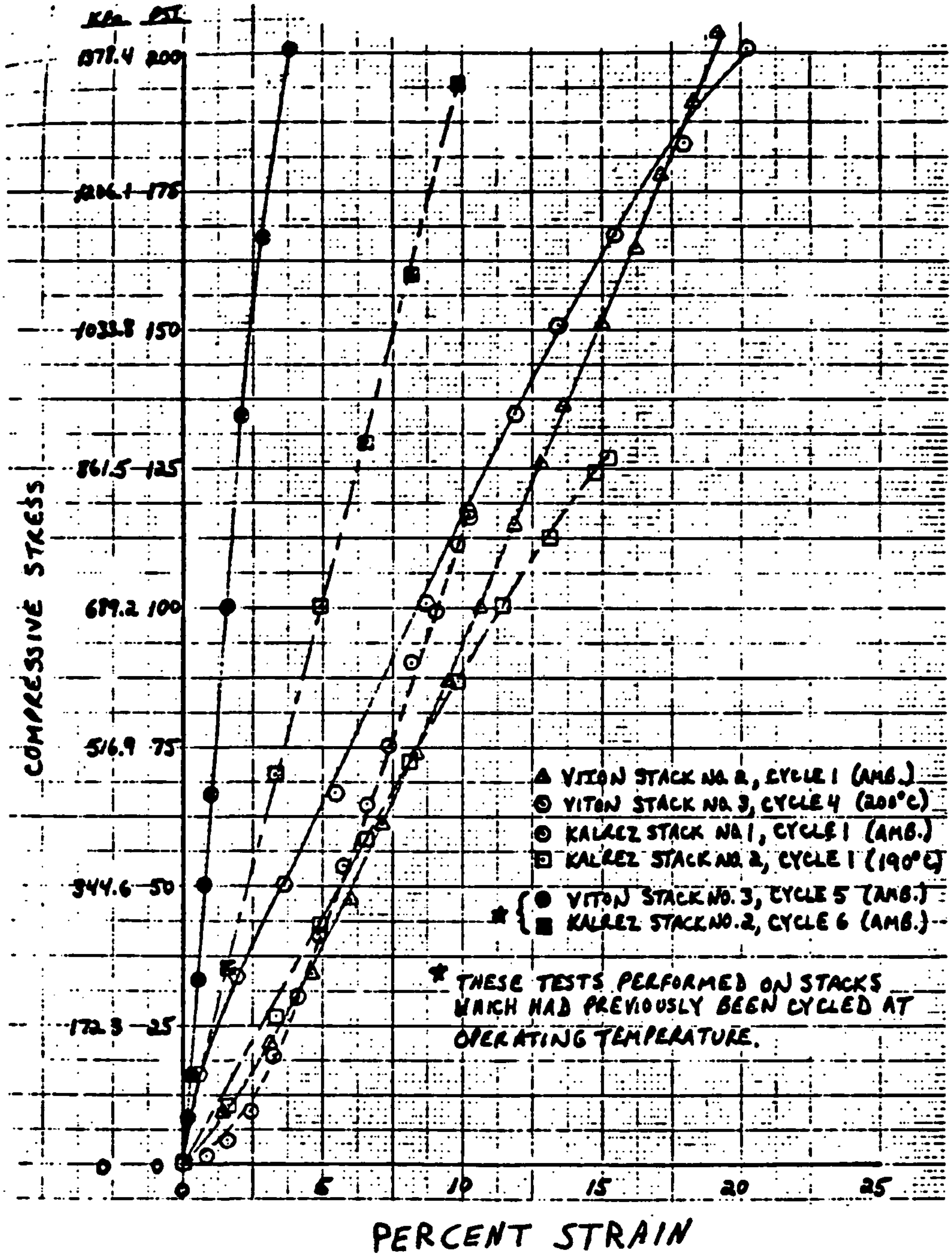

Figure 3-38. Compressive Stress Vs. Seal Strain for Viton/Viton Cement and Kalrez/Viton Cement Seal Comparative Tests

strains (95 percent of maximum strain obtained) indicate a lack of compliance. This lack of compliance of the material has precluded consideration of Armalon as a viable candidate seal material.

Mechanical testing of candidate seal material Kel-F was completed for both ambient temperature and operating temperature of 198°C (390°F). This seal material has similar elastomer characteristics to the Viton compound. Ambient temperature tests were conducted using four compression cycles for seal strain values ranging from 15 to 30 percent. The Kel-F exhibited tangent modulus of elasticity values on the order of 8.67 MPa to 10.45 MPa (1258 psi to 1515 psi). The original hardness of this seal was measured as 61 Shore durometer. The seal material exhibited a relatively small amount of permanent strain (3 percent) after two cycles to a maximum of 20 percent strain. The test unit indicated good sealing characteristics over the range of 108.6 kPa to 135.5 kPa (1.1 psig to 5 psig). A 10 percent strain working range is available for sealing once the seal has been loaded to 30 percent strain. At ambient temperature, no evidence of seal leakage could be detected for compressive stresses greater than 853 kPa (109 psi) under an internal pressure of 135.5 kPa (5 psig). The Kel-F seal material also demonstrated the ability to withstand internal pressures of up to 445 kPa (50 psig) under a normal compressive stress of 2.5 MPa (352 psi). Since the Kel-F material exhibited excellent seal characteristics at ambient temperatures, no leak tests were performed at operating temperatures.

A second Kel-F mechanical test performed at 198°C (390°F) was completed and the material exhibited relatively linear characteristics over the range of 4 percent to 20 percent strain. The Kel-F material did not soften during the 198°C (390°F) test phase. The increase in modulus of elasticity values for first cycle loading was on the order of 33 percent. The modulus of elasticity value changed from 8.674 MPa (1258 psi) to 11.69 MPa (1696 psi) for the ambient to operating temperature conditions. It should be noted for both ambient and operating temperature conditions, the amount of permanent strain developed was on the order of 4 percent after the seals had been compressed to 15 percent and 20 percent strain values. This is considerably less permanent strain than any Viton compound previously tested.

The seal stiffening effect after exposure to high temperature was also evaluated during this test phase. The evaluation indicated the Kel-F material increased in stiffness from 11.610 MPa (1684 psi) at 198°C (390°F) to 19.305 MPa (2800 psi) at ambient temperature after exposure at 198°C (390°F) for ~40 hours. This stiffness increase is consistent with Viton type elastomers.

Compression creep tests of the Viton edge seal material were initiated. Four units are currently being tested at the following conditions:

Test Condition	Test Unit No. 1	Test Unit No. 2	Test Unit No. 3	Test Unit No. 4
Temperature	149°C/300°F	198°C/390°F	198°C/390°F	54°C/130°F
Compressive Pressure (using Constant Load)	1.72 MPa/ 250 psi	0.689 MPa/ 100 psi	1.72 MPa/ 250 psi	2.76 MPa/ 400 psi
Test Time as of 6/1/84	400 hours	1000 hours	1600 hours	400 hours

Each test unit consists of five layers of Viton seal material separated by graphite disks, Figure 3-36. The specimens were loaded, and deflection versus time data are presently being recorded. Each specimen will be tested until a sustained creep limit has been reached. Documentation of the test results will be presented upon completion of the entire test.

Assessment of acid exposure of various fluoroelastomer material being considered for cell to cell and manifold to stack seals was initiated. Samples, as received, were leached in 94 w/o acid for 150 hours at 185°C (365°F), and ion chromatography (Dionex Model 14 Ion Chromatograph) was performed on the resultant acid after filtering through 8000 Å opening Millipore filter and dilution to 47 w/o H_3PO_4. An H_3PO_4 sample was run in the Teflon beaker used for leaching to establish the blank. In addition, weight gain/loss tests were performed on the various samples. Test results, Table 3-40, indicate rather substantial removal of F^- and SO_4^{2-} from the samples as a result of leaching. Selected samples were re-leached and relatively minor

TABLE 3-40

LEACHING EFFECT ON SEVERAL AS-RECEIVED FLUOROELASTOMER MATERIALS

(Leached in 94% H_3PO_4 at 185°C after 150 hours. Ion chromatography used for analysis. Samples washed to neutral and dried in vacuo before weighing.)

Sample	Description	Wt. Change (%)	ANALYSIS, PPM BY WEIGHT F^-	Cl^-	NO_3^-	SO_4^{2-}	Comments
VMOAC-1	Viton 10125 Cured 164°C, 3 hrs	+ 6.1	890	5	8	212	Electrolyte black
VMOAC-2	Viton 10149 Cured 164°C, 3 hrs	+ 11.4	900	5	5	112	Electrolyte black
KALAR-1	Kalrez K00506	+ 0.08	712	6	4	100	Electrolyte straw colored
KLFAR-1	KEL-F 06-3655 As received	+ 0.4	512	3	8	112	Electrolyte amber
VPAAR-1	Pelmor	+ 7.3	460	3	5	252	Light straw
VPRAR-1	Precision Rubber No. 42679	- 0.5	172	60	5	112	Acid dark brown
VMDAR-1	MOSITE	+ 33.1	752	10	6	106	Electrolyte black
GRAY VITON	Pelmor, PLV-10059	+ 4.2	316	6	5	100	Electrolyte black
BLACK VITON	Precision Rubber No. 19356	+ 3.5	418	11	8	144	Electrolyte black
BLANK	H_3PO_4 in Teflon		3	3	5	4	No color change

changes in the anionic species levels were noted, Table 3-41. A third group of samples heated at 190°C (374°F) in air for 100 hours prior to leaching show a large increase for several samples in the F^- due to prior heat treatment, Table 3-42. These data indicate that all of the fluoroelastomer materials examined as possible seal materials have the potential of being a source of F^- and SO_4^{2-} contamination or poison to the cell.

3.7.4 Electrode Materials

Characterization of finished electrodes by half cell measurements was initiated and other evaluations were continued.

3.7.4.1 Design and Optimization of Half Cell Fixture

The design and optimization of a half cell assembly for electrochemical evaluation of individual electrodes (both cathodes and anodes) was accomplished. Several generations of cell designs were evaluated in the optimization process. As shown in Figure 3-39, the final half cell fixture machined from Teflon utilizes standard existing subscale test hardware (compression plate, carbon end plate, current collector, heating element and insulation). A reference DHE was fabricated and calibrated in the half cell over the temperature range of 18 - 193°C (64 - 380°F). At 0.1 mA/cm^2 (0.09 A/ft^2), the potential of this reference electrode was measured with respect to a RHE in the same electrolyte. Preliminary tests were run in this cell to identify optimum testing conditions, establish electrode pre-treatment conditions, and to select the electrochemical method for polarization measurements.

3.7.4.2 Effect of Sintering Temperature on Cathode Performances: Half Cell Studies

The baseline manufacturing practice requires the fuel cell electrodes be sintered to enhance the Teflon binding strength. The sintering temperature is thought to be one of the key parameters affecting the wetting characteristics

TABLE 3-41
SECOND LEACHING EFFECT ON SELECTED FLUOROELASTOMER MATERIALS

(Selected gasket materials releached with 94% H_3PO_4 at 185°C for 150 hours.)

Sample	Description	Wt. Change (%)	ANALYSIS, PPM BY WEIGHT				Comments
			F	Cl	NO_3	SO_4	
KALAR-1	Kalrez K00 506 As received	+ 2.0	320	<5	<3	220	Electrolyte dark amber
KLFAR-1	KEL-F 06-3655 As received	+ 6.5	320	<5	<3	400	Electrolyte very light amber
VPAAR-1	Pelmor	+ 36.1	72	<5	<3	88	Electrolyte very light amber
VPAAR-1	Precision Rubber No. 42679	+ 1.7	180	<5	<3	224	Electrolyte dark brown

TABLE 3-42

LEACHING EFFECT ON HEAT TREATED FLUOROELASTOMER MATERIALS*

(Leached in 94% H_3PO_4 on several polymer materials at 190°C for 150 hours. Samples were washed to neutral in hot deionized water and dried in vacuo before weighing.)

Sample	Description	Wt. Change (%)	ANALYSIS, PPM BY WEIGHT				Comments
			F^-	Cl^-	NO_3^-	SO_4^{2-}	
VPR HT-1	Precision Rubber No. 42679	- 1.9	130	<5	<5	52	Electrolyte amber
VPA HT-1	Pelmor	- 21.1	610	<5	<5	156	Electrolyte light amber
VMDAC HT-2	Cured Viton No. 10149	- 7.0	29,500	<5	<5	320	Sample broken
VMDAC HT-1	Cured Viton No. 10125	-	5,284	<5	<5	256	Sample fractured into small fragments
VMO HT-1	MOSITE	+ 17.0	7,300	<5	<5	80	
KLF HT-1	KEL-F 06-3655 Compound	-	1,300	<5	<5	184	Sample fractured into small fragments
KAL-HT-1	Kalrez Keo Sol Compound	+ 1.2	80	<5	<5	112	Electrolyte clear

*HEAT TREATED FOR 100 HOURS AT 190°C IN AIR PRIOR TO LEACHING

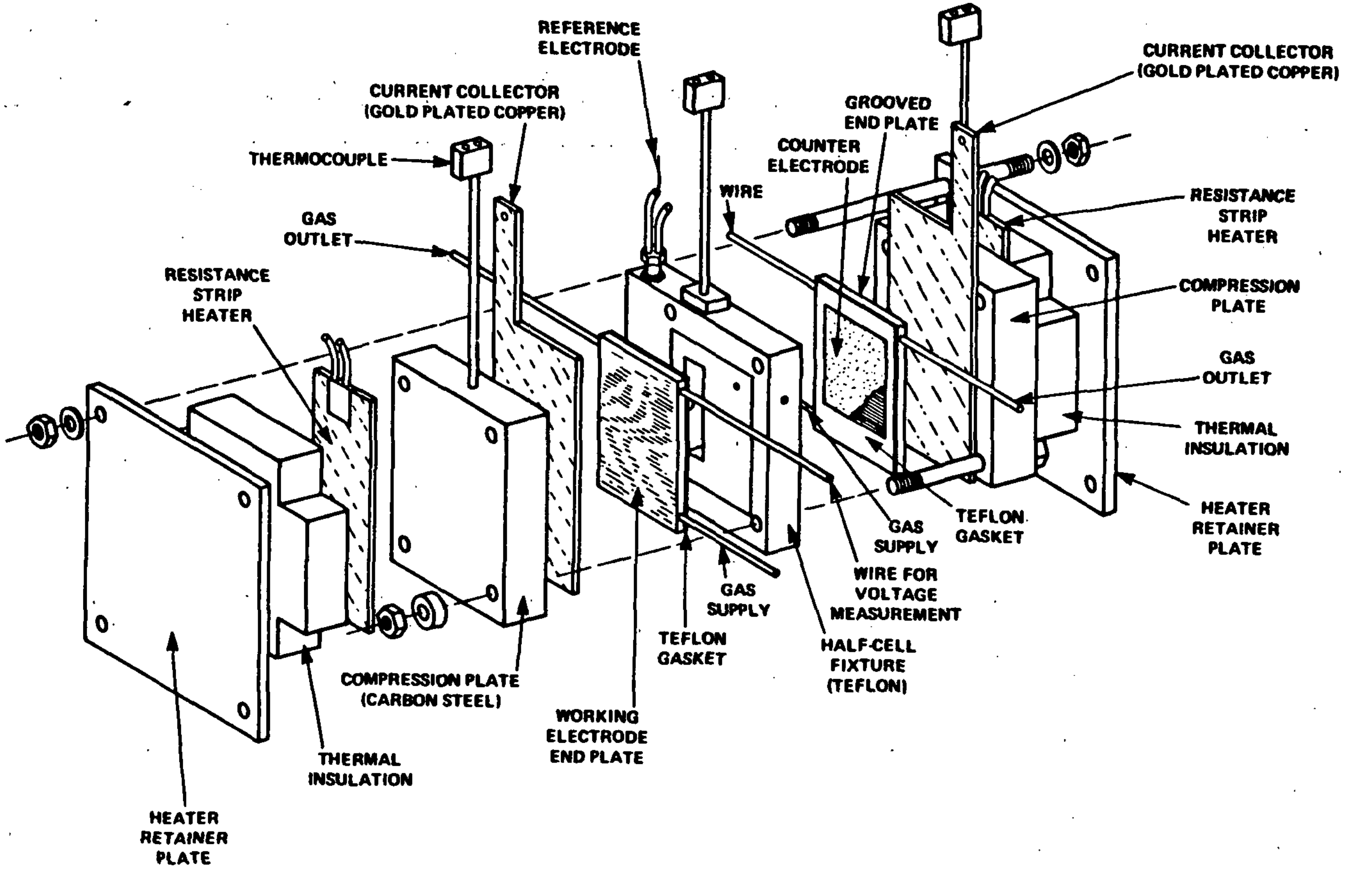

Figure 3-39. Exploded View of a Half Cell Assembly

of the Teflon-bonded catalyst layer. Electrochemical behaviors of three "oversintered" and two baseline cathode samples were studied in the half cell at 190°C (374°F) and 101 kPa (1 atm). The "oversintered" cathodes were heated an additional 6°C and 12°C (11°F and 22°F).

Throughout the current density region of this study, the polarization data were highly reproducible on the two baseline cathodes. The increased sintering temperature produced a substantial reduction in the achievable electrode potential. At 200 mA/cm^2 (186 A/ft^2), for example, the high temperature sintered cathode exhibited a potential of only 650 mV versus RHE, about 60 mV less than the baseline samples. Furthermore, the measured Tafel slopes also increased slightly with increased sintering temperature.

After polarization at 200 mA/cm^2 (186 A/ft^2) for 40 hours or longer, only slight improvements (less than 5 mV) were observed on the two baseline cathodes. The performance of "oversintered" cathodes was significantly improved, but was still 20-30 mV below the baseline level. This result suggests that increasing the sintering temperature improves the hydrophobicity of the catalyst layer and thus retards the penetration of electrolyte into the porous structure. It also raises a question as to whether reducing the sintering temperature below the 360°C (680°F) baseline level would result in improved cathode performance.

3.7.4.3 Half Cell Evaluation on Alternate Electrocatalysts

The electrochemical behaviors of several alternate catalysts were investigated in the half cell apparatus at 190°C (374°F) and atmospheric pressure. Shown in Figure 3-40 is the Tafel plot for oxygen reduction on DC-06 catalyst as compared to two present baseline cathode samples, C234-4 and C249-8. To optimize the catalyst utilization, each electrode was pretested at 200 mA/cm^2 (186 A/ft^2) for approximately 90 hours. The polarization curve of DC-06 catalyst was nearly parallel to those on the baseline cathodes. However, the observed electrode potentials on DC-06 were $\sim$30 mV higher than the baseline cathodes in the current density range of 5-600 mA/cm^2 (4.7-560 A/ft^2). At

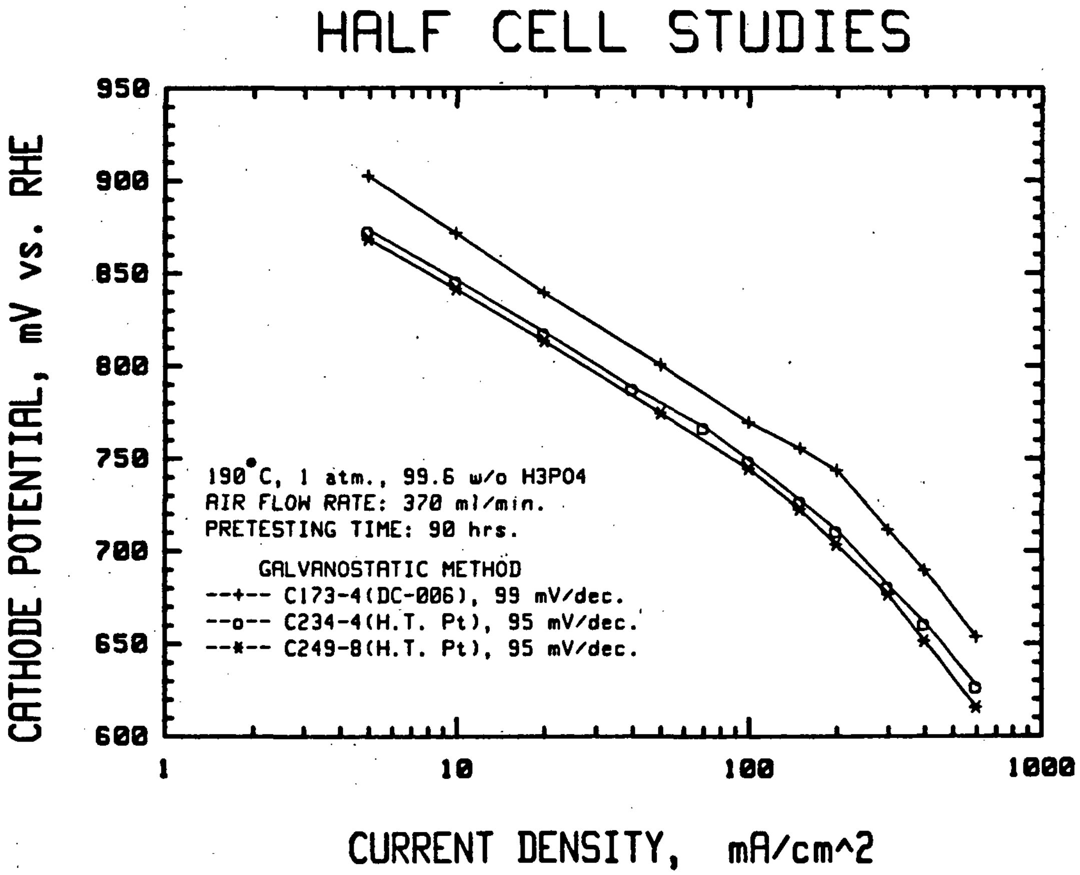

Figure 3-40. Tafel Plots for Oxygen Reduction on an Alternate Catalyst and Two Baseline Cathodes

200 mA/cm^2 (186 A/ft^2), for instance, the measured cathode potential on DC-06 was ∿740 mV versus RHE, as compared to the baseline performance of ∿710 mV.

Tafel plots for oxygen reduction on alternate catalyst DC-10 and DC-05 are illustrated in Figure 3-41. Electrochemical behavior of DC-10 was quite similar to the two baseline cathodes, showing a Tafel slope of ∿96 mV/decade. However, DC-05 exhibited slightly better performance than the baseline cathodes. The measured electrode potential was 726 mV versus RHE at 200 mA/cm^2 (186 A/ft^2).

Figure 3-42 shows the polarization curves for hydrogen oxidation on a baseline anode, A212-2, and an alternate anode catalyst, DC-03. The anodic overpotentials increased significantly with increasing current density; consequently, no linear Tafel region was obtainable on either electrode. The alternate anode, DC-03, exhibited lower overpotentials than the baseline anode. At 200 mA/cm^2 (186 A/ft^2), the observed hydrogen overpotential was ∿15 mV at the anode A212-2, ∿50 percent higher than the literature reference value. This suggests that the platinum catalyst at this baseline anode may have been contaminated by impurities from the Vulcan XC-72 carbon support and/or the wetproofed backing paper.

3.7.4.4 Effect of Electrolyte Contamination by Viton Gasket Corrosion Products on the Anode Performance

Half cell tests were performed to investigate the impact of electrolyte contamination from Viton gasket-acid reactions on the anode performance for hydrogen oxidation. The contaminated electrolyte, prepared by immersing and soaking Viton gaskets in 97 w/o H_3PO_4 at 190°C (374°F) and 485 kPa (4.8 atm) for N170 hours, contained 320 ppm F^- and 68 ppm SO_4^{2-} as determined by ion chromatography. This contaminated solution was then mixed with various proportions of fresh electrolyte to provide a series of test electrolytes containing a range of contaminant concentrations.

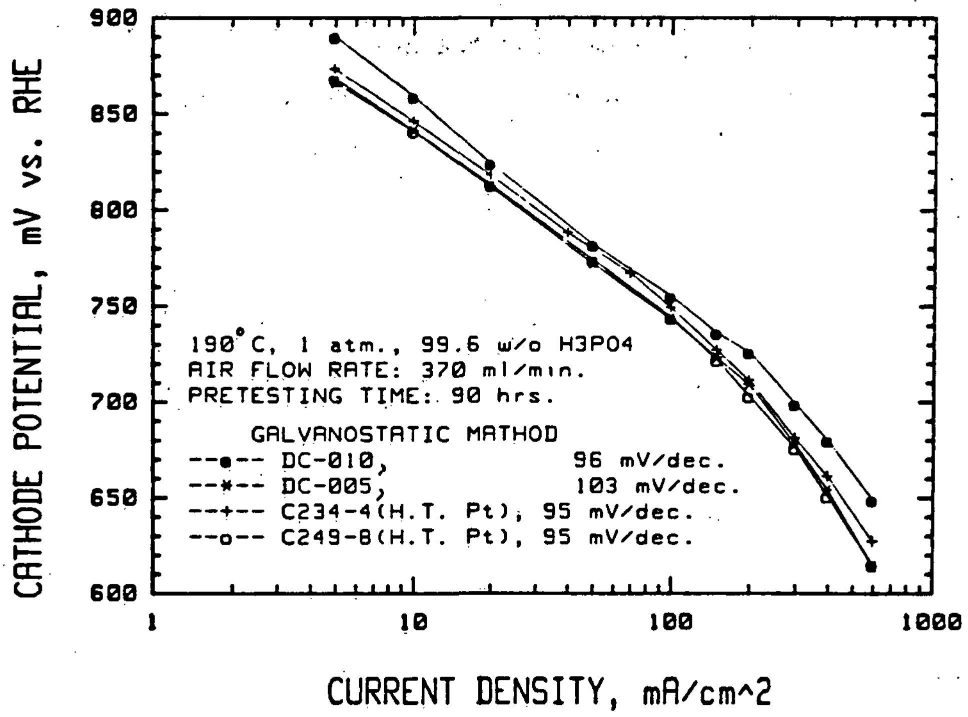

Figure 3-41. Tafel Plots for Oxygen Reduction on Two Alternate Catalysts and Two Baseline Cathodes

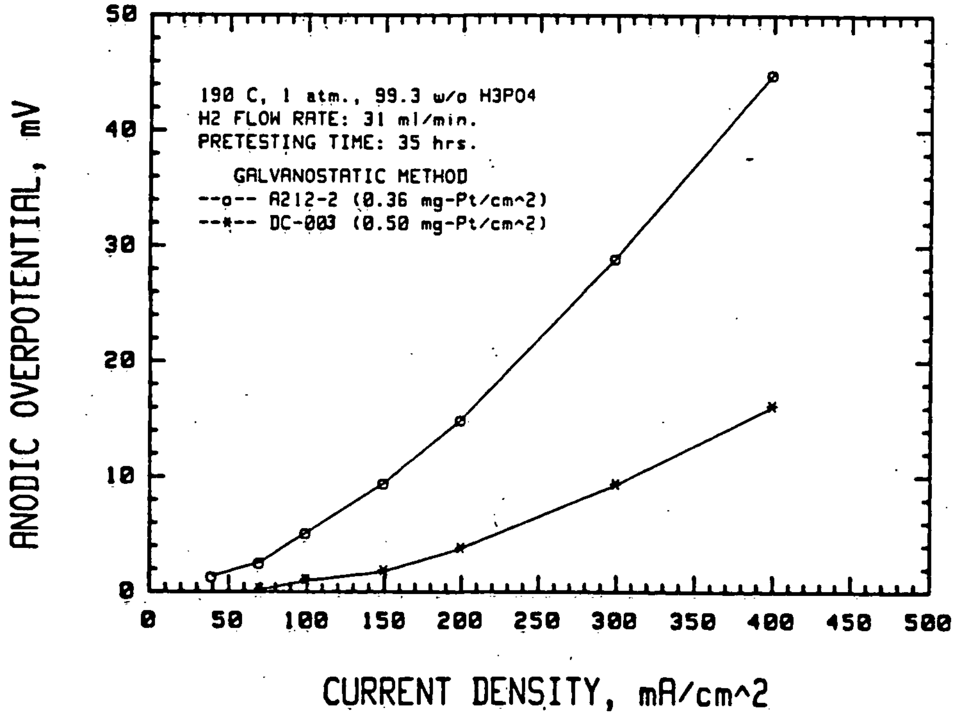

Figure 3-42. Polarization Curves for Hydrogen Oxidation on an Alternate Catalyst and a Baseline Anode

Using pure hydrogen, the equilibrium potential of a typical WAESD-produced anode, A212-2, decreased with increasing concentration of impurities in the electrolyte. At the highest impurity level used (i.e., 320 ppm F^- and 68 ppm SO_4^{2-}), the equilibrium potential decreased by ∿20 mV. In the practical current density region of 200-400 mA/cm^2 (186-372 A/ft^2), however, the contaminated electrolyte resulted in about 5 mV higher polarization potential than that measured for the uncontaminated electrolyte.

3.7.4.5 Baseline Catalyst Characterization

Characterization of Lot No. 3 catalyst was performed in both the as-received condition and after heat treatment at 900°C (1650°F). The data is in relatively good agreement with both the vendor data and the PDS requirements. In the case of Lot No. 3, the as-received metal surface area is somewhat larger, 16.3 m^2/g (79.6×10^4 ft^2/lb), than that of Lot No. 2, 13.6 m^2/g (66.4×10^4 ft^2/lb), or the PDS value (11 ± 2 m^2/g). Heat treatment of the catalyst to 900°C (1650°F) results primarily in changes in the platinum. The metal surface area decreases from about 190 to 40 - 45 m^2/g (9.28×10^5 to 1.95×10^5 - 2.20×10^5 ft^2/lb) while the surface area of the carbon support remains unchanged. The particle size as determined by both transmission electron microscopy and X-ray line broadening increases from 15 to 20 Å to 39 to 44 Å as a result of heat treatment. Increases in Fe, Ni and Cr have been noted in the heat treated catalyst; this may be related to either non-uniform distribution of foreign particles in the as-received catalyst or to possible contaminant pickup from the metal trays used to contain the catalyst during heat treatment.

3.7.4.6 Compression Behavior of Electrode Materials

Compressibility tests were performed on Stack W-009-09 anode-cathode components and Stack W-009-11 anode-matrix-cathode components. Both sets of components were fabricated using the following procedure: Cathode (900°C (1650°F) heat treated catalyst, dry laminated, argon sintered) and anode (as-received catalyst, dry laminated, argon sintered). However, the Stack 09 components incorporated a thicker SiC layer and higher platinum loadings than the Stack 11 components.

Three assemblies were tested. The first assembly consisted of five layers of Stack 09 anode-cathode components wetted with 1.1 cm^3 (0.07 in^3) of 98 percent w/o phosphoric acid (H_3PO_4) per cell layer. This specimen was subjected to five cycles at 56°C (133°F). The second unit consisted of five layers of dry Stack 09 anode-cathode components and was subjected to four cycles at 56°C (133°F) and two additional cycles at 198°C (390°F). The third specimen consisted of five layers of dry Stack 11 components and was subjected to three cycles at 55°C (130°F), two cycles at 191°C (375°F) and then one cycle at 55°C (130°F). A typical compression cycle was as follows:

- load to 1000 N (225 pounds)
- 30 minute load relaxation
- unload to 8.89 N (2 pounds)

Although each compression cycle followed this general pattern, there was some variation in maximum load and relaxation time. A LVDT and a load cell were used to record displacement and load as a function of time. The data were reduced and evaluated to determine stress-strain relationships, permanent set characteristics and load relaxation effects for use in the stack analyses.

At the operating temperature of 56°C (133°F), the wet test unit with Stack 09 anode-cathode components exhibited a very nonlinear stress-strain curve. In the 0 to 15 percent strain range, the material was extremely soft as indicated by a low modulus of elasticity. The 15 to 19 percent strain range is a transition region which was strongly nonlinear. From 19 percent to the maximum strain range, it is characterized by relatively stiff, linear behavior. After the third compression cycle, the stress-strain curves demonstrated good repeatability. In the range from 19 to 22 percent strain, the average modulus of elasticity (based on nominal area) for cycles 3, 4 and 5 was 5.49 MPa (796 psi). After five cycles, the wet specimen incurred a 10 percent permanent set. This permanent set represents 43 percent of the maximum strain developed during the compression loading. During the 30 minute relaxation periods, this specimen showed a load relaxation of 10 to 20 percent of the initial load. Although this relaxation did not reach a steady state value, the amount of additional relaxation for longer time periods would be relatively small.

The structural properties of the dry W-009-09 anode-cathode components at 56°C (133°F) exhibited a strong correlation to the wet structural properties. Although the permanent set values were slightly lower, the modulus of elasticity and load relaxation effects were nearly the same for both test assemblies. Overall, the phosphoric acid had a negligible effect on the structural properties of the W-009-09 anode-cathode components.

At 190°C (374°F) the Stack 09 components appeared significantly softer than at 56°C (133°F). Additional tests are being considered to fully determine the structural properties of the Stack 09 components at this elevated temperature.

At the operating temperature of 55°C (130°F), the Stack W-009-11 anode-matrix-cathode components also exhibited a very nonlinear stress-strain curve. For example, the cycle 2 test data indicate a modulus of elasticity (based on nominal area) of 117 kPa (17.0 psi) in the 0 to 10.6 percent strain range and a modulus of elasticity of 4.09 MPa (593 psi) in the 15.0 to 18.0 percent strain range. At 191°C (376°F) the Stack 11 components exhibited a fairly linear and repeatable stress-strain curve. The average tangent modulus of elasticity at this temperature was 6.45 MPa (936 psi). After three cycles, Stack 11 specimen accumulated a constant permanent set of 11.5 percent strain. No additional permanent set is expected for a higher number of cycles.

Figure 3-43 compares the stress-strain behavior of the Stack 09 components, the Stack 11 components and the standard anode-matrix-cathode components. (Standard components refer to the electrodes used in Stacks W-009-01 through W-009-08). Note the Stack 09 components and Stack 11 components were significantly softer than the standard components. This difference was primarily due to the soft behavior of the Stack 09 and Stack 11 components in

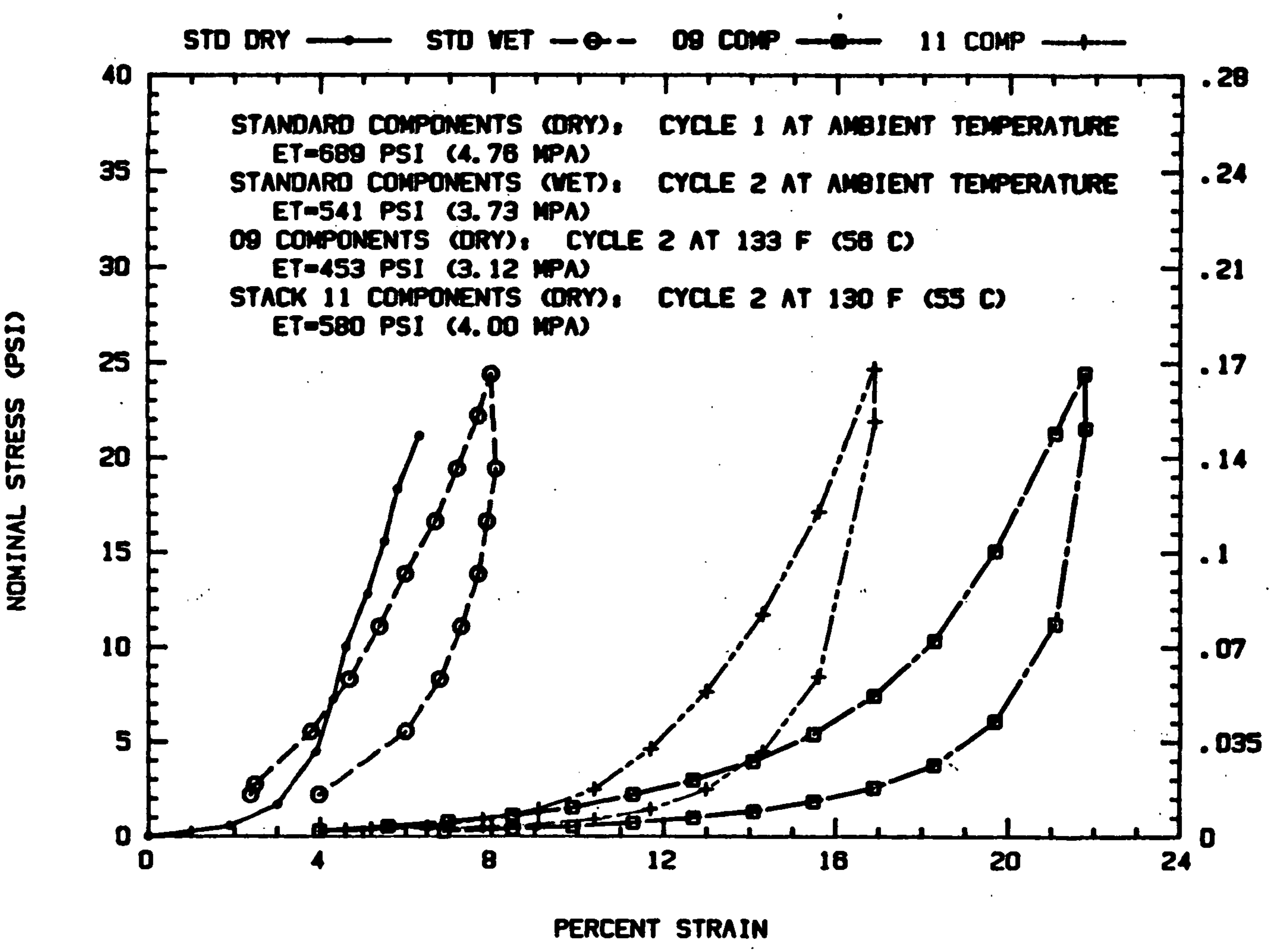

Figure 3-43. Strain Comparison Between Standard and Stacks W009-09 and -11 Cell Components

the low strain range. The increased stiffness of the Stack 11 components as compared to the Stack 09 electrodes is the result of the thinner SiC layer and reduced loadings on the Stack 11 cell components.

The primary design impact of the softer Stack 09 and Stack 11 electrodes occurs with the stress distribution in the cell. Due to the soft electrode material, the stresses will tend to redistribute around the outside seal regions. This redistribution is being investigated in the nine cell stack finite element models.

3.7.4.7 Silicon Carbide Layers and Powder

Helium bubble pressures were determined for various thickness layers of silicon carbide (all acid-filled for 15 minutes with 98.4 w/o H_3PO_4) from Cathode C204-4. The ambient temperature data obtained are tabulated in Table 3-43. There is no apparent relationship of bubble pressure with coating thickness. The bubble pressure varies from 89.7 kPa (13 psi) to 165.6 kPa (24 psi). These data are in agreement with previously reported bubble pressures for acid filled silicon carbide layers.

An all-Teflon Gelman in-line filter holder was modified to perform elevated temperature bubble pressures up to 230°C (446°F). Data were obtained over the range from 190°C to 228°C (374°F to 442°F) and are given in Table 3-44. The bubble pressure is somewhat lower than the ambient temperature average data, but not below 65 kPa (9.5 psi).

A second lot of SiC used for cathode insulation layer was evaluated. Comparison of the particle size distribution of this lot of material with that of the previous lot indicates the two lots of powder have relatively similar particle distribution.

Bubble pressure was determined at ambient temperature for cathode C214-2 fabricated with this new lot of SiC. The values ranged from 82.8 to 117.2 kPa (12 to 17 psi), which are similar to values obtained with the previous lot of SiC.

TABLE 3-43
HELIUM BUBBLE PRESSURE OF VARIOUS THICKNESS SiC LAYERS (CATHODE C204-4)

Sample Ident.	SiC Thickness		Bubble Pressure	
	mm	in	kPa	psi
1	0.10	0.004	165.6	24
2	0.10-0.14	0.004-0.0055	144.9	21
3	0.14	0.0055	103.5	15
4	0.11-0.14	0.0045-0.0055	103.5	15
5	0.11	0.0045	124.2	18
6	0.22	0.0085	96.6	14
7	0.22-0.27	0.0085-0.0105	124.2	18
8	0.27	0.0105	96.6	14
9	0.18-0.27	0.007-0.0105	110.4	16
10	0.18	0.007	89.7	13

TABLE 3-44
ELEVATED TEMPERATURE BUBBLE PRESSURE OF TYPICAL CATHODE (C204-4)

Sample No.	Test Temperature (°C)	BUBBLE PRESSURE kPa	BUBBLE PRESSURE psi
1	190	65.46	9.5
2	193	78.55	11.4
3	208	77.17	11.2
4	228	65.46	9.5

Initial evaluation of zirconium pyrophosphate applied as an alternate to SiC was performed on cathode C221-5. Bubble pressure for a 0.13 mm (0.005 in.) layer at ambient temperature ranged from 131 to 172 kPa (19 to 25 psi), and was slightly higher and more uniform than data on SiC layers.

3.7.4.8 Backing Paper

A limited evaluation of Kureha E715 carbon paper was performed. This paper was evaluated as a possible alternative to the Stackpole PC-206 paper currently in use. Comparison data are given in Table 3-45. The thickness variation of the E715 sample measured was larger than that of the PC-206 and the average in-plane electrical resistivity of the E715 was about double that of the PC-206. Based on these data and subscale cell resistances, the decision was made that E715 was not an acceptable alternative to the PC-206.

X-ray diffraction of as-received samples of PC-206 and E715 are shown in Figure 3-44. These data indicate that the PC-206 is somewhat more "graphitic" than the E715, having both a lower d_{002} and higher L_{002}.

Evaluation of the structural properties of the Kureha paper E715 was initiated. The Kureha paper is an alternative replacement candidate for the electrode layer support as well as a possible acid transport member. Compression tests of E715 at both ambient and operating temperatures were completed. Two test units, each 20 pieces thick, were compressed in a dry (no acid) flat loading configuration. A typical compression cycle consists of loading to a specified strain and then unloading to a 22 N (5 lb) reference load. Figure 3-45 indicates the compressive stress versus strain curve for three cycles at ambient temperature. According to Figure 3-45, a compressive stress of 480 kPa (70 psi) would produce a 12 percent strain in the Kureha paper. A similar test of MAT-1 (carbon layer) indicates the same 480 kPa (70 psi) would induce only a 4.1 percent strain in the MAT-1. This verifies the Kureha paper (E715) is much more compliant than the MAT-1 (carbon layer) at ambient temperature.

TABLE 3-45
BACKING PAPER COMPARISON SUMMARY

	Stackpole PC-206[1]	Kureha E715
Dimensional (3 sheets of each)		
Min. Thickness, mm (mils)	0.368 (14.5)	0.406 (16.0)
Max. Thickness, mm (mils)	0.457 (18.0)	0.560 (26.1)
Average Thickness, mm (mils)	0.406 (16.0)	0.477 (18.8)
Calculated Density, g/cc	0.307	0.318
Measured Density, g/cc	0.375	-
Porosity, percent[2]	62	-
Wetproofed, Paste Process	-	-
Wetproofed, Dip Process	-	-
Resistivity, ohm-cm	0.009-0.018[3]	0.021-0.022
Sulfur Analysis, w/o	0.034[4]	-
Corrosion[5] 0.9 V vs. RHE, mA/cm^2	0.004	-
1.0 V vs. RHE, mA/cm^2	0.037	-
1.1 V vs. RHE, mA/cm^2	0.9	-

---

[1] Baseline P. O. 74351 unless noted
[2] Hg porosimetry technique
[3] P.O. 74351 (3 samples) and P. O. 60816 (4 samples)
[4] P.O. not identified
[5] 190°C, 100 percent H_3PO_4, 1 atm

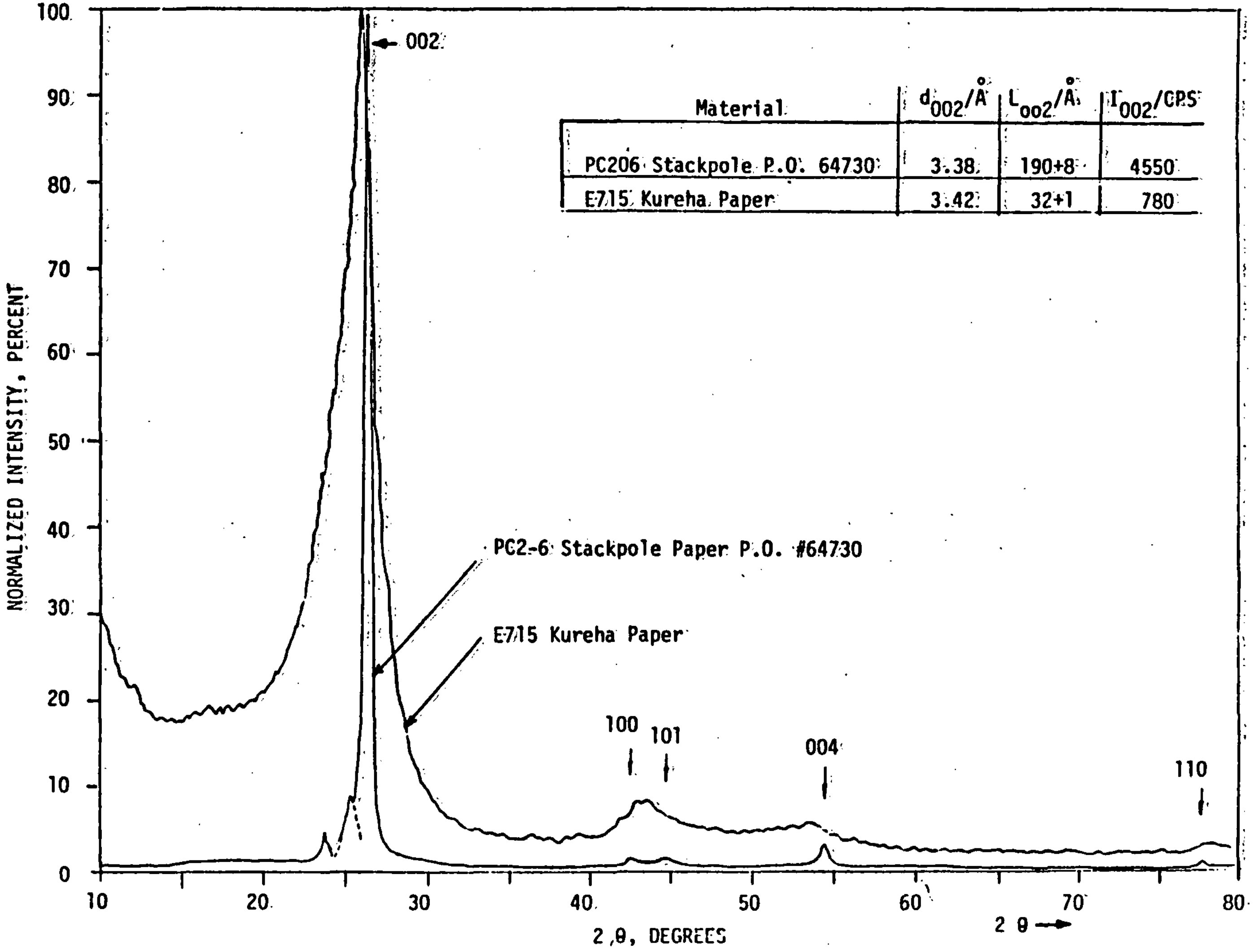

Material	$d_{002}/\mathring{A}$	$L_{002}/\mathring{A}$	I_{002}/CPS
PC206 Stackpole P.O. 64730	3.38	190+8	4550
E715 Kureha Paper	3.42	32+1	780

Figure 3-44. X-ray Diffraction Profiles of Stackpole vs. Kureha Papers

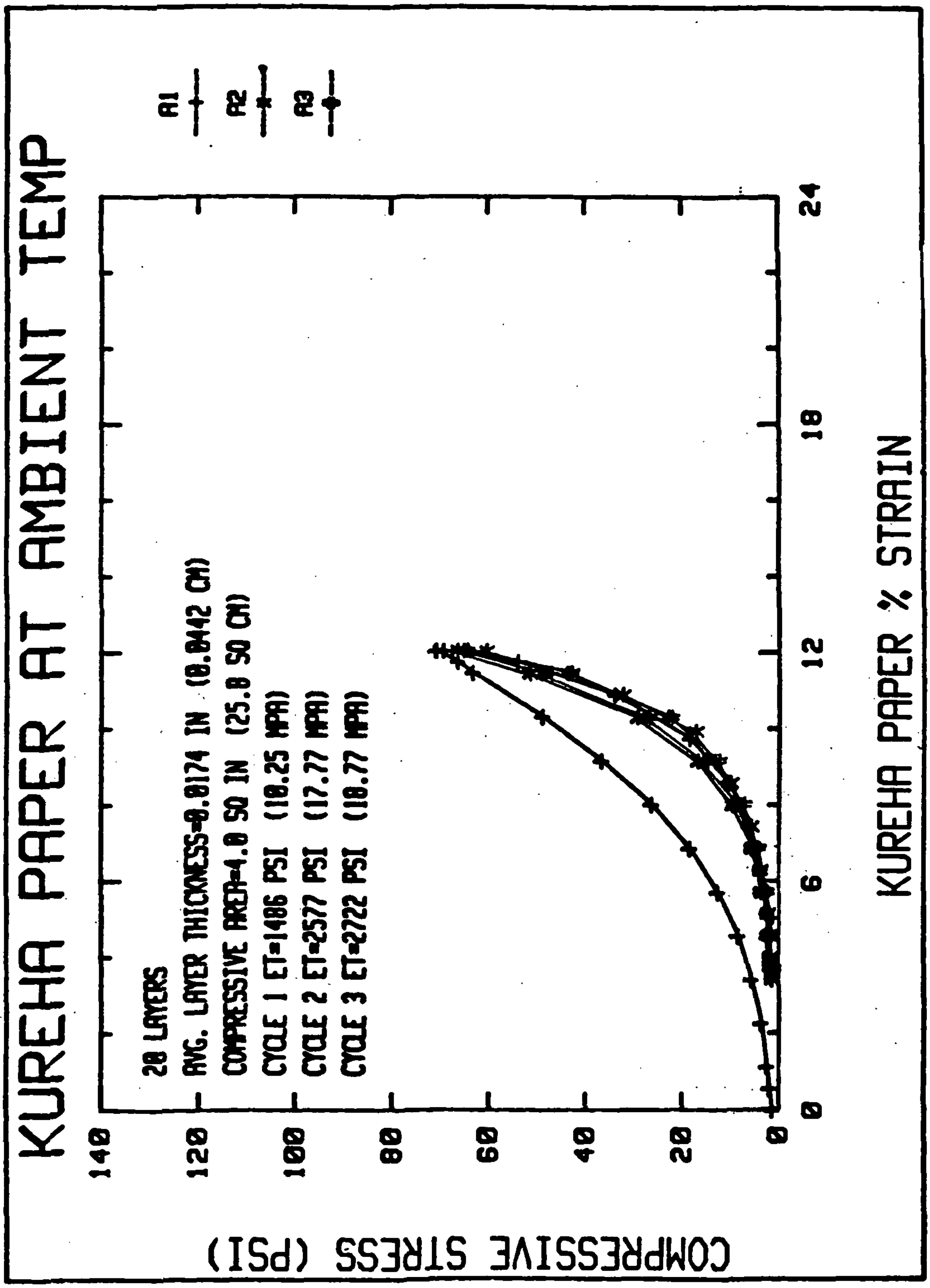

Figure 3-45. Compressive Stress-Strain Data for Kureha E715 Paper at Ambient Temperature

The second Kureha paper stack was tested at operating temperatures. Figures 3-46 and 3-47 present the stress-strain curves at temperature. Note that cycle 1, cycle 2 (loading only) and cycle 5 are at 55°C (130°F), whereas, cycle 2 (unloading), cycle 3 and cycle 4 are at 198°C (390°F). In addition, the cycle 4 data (Figure 3-47) indicate a yield stress at approximately 500 kPa (80 psi). The plastic strain associated with this yielding accounts for the offset of cycle 5.

3.7.4.9 Differential Scanning Calorimetry

Characterization of Teflon 6C powder as-received, in a non-sintered electrode layer (C209-1) and in a sintered electrode layer (C233-8) was performed using differential scanning calorimetry (DSC). The thermogram of the Teflon 6C is shown in Figure 3-48, data from a computer-controlled DuPont 1090 analyzer. The glass transitions around 20 and 30°C (68 and 86°F) are in agreement with the values reported for polytetrafluoroethylene (PTFE).(1) The virgin material has a melting point peaking at 339°C (642°F). Upon cooling, only a portion of the virgin crystalline phase resolidifies at about 310°C (590°F). The recrystallized portion of Teflon melts at a lower temperature than the virgin material, at about 326°C (619°F), as reported.(2) No further changes, both in the temperature and heat of melting, are observed upon continued cycling between 200 and 400°C (392 and 752°F). The thermal data are summarized in Table 3-46.

Figure 3-49 is a thermogram of a catalyst layer (C209-1) that had only been heated to 93°C (200°F) to drive off the NH_4HCO_3. On first heating, a broad exothermic transition peaking occurs at about 180°C (356°F). This transition was not observed in as-received TFE 6C. It was also absent on a second heating scan. This is attributed to the exothermic effect with the stress relaxation of the cold-worked, fibrillated Teflon. The enthalpy of the solid-state reaction was found to be different in different samples, 25.2, 27.7, and 8.6 J/g (10.8, 11.9, and 3.7 Btu/lb).(*) These data may be an

---

(*) Based on the portion of Teflon in the catalyst layer (40 w/o).

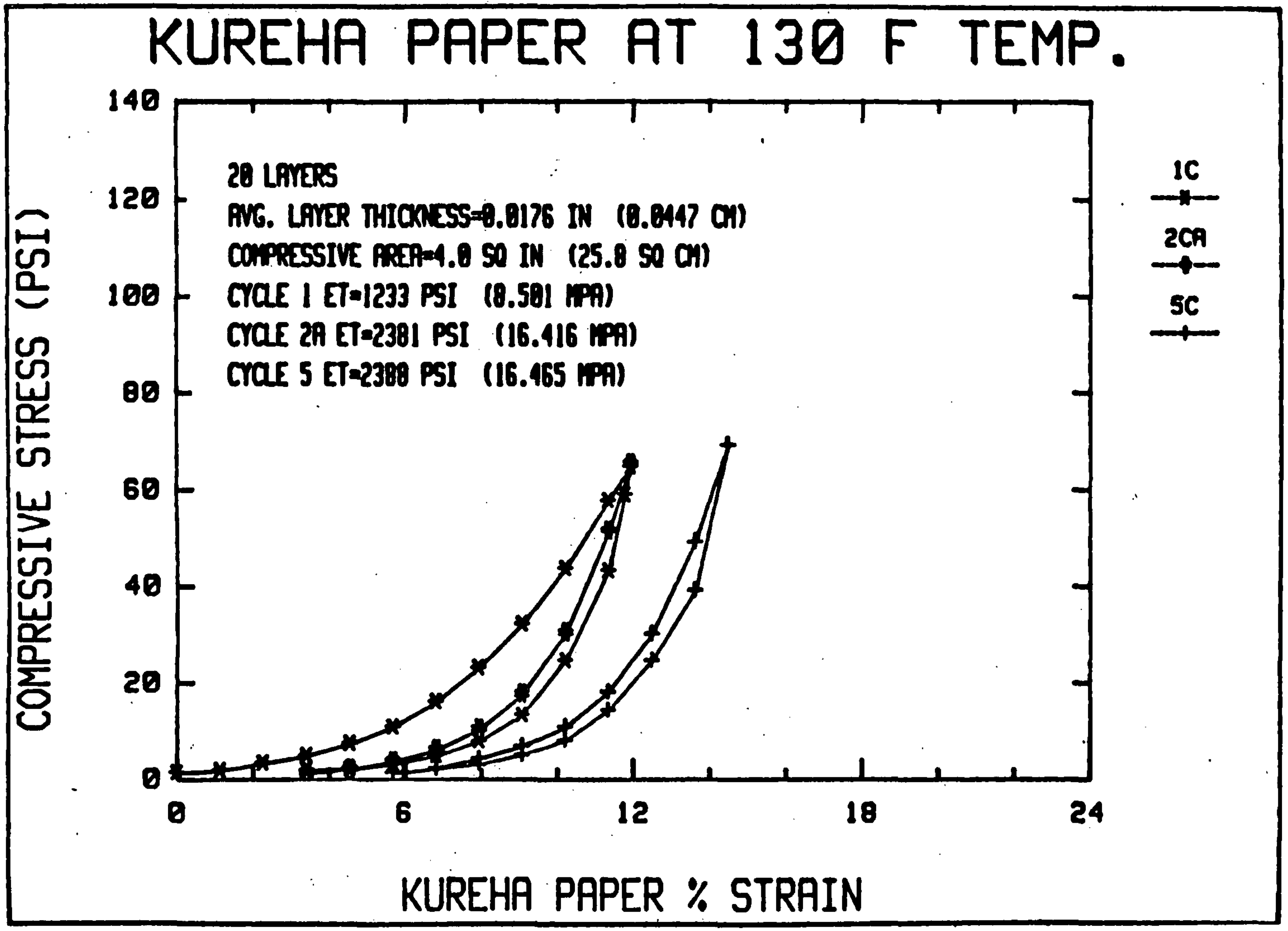

Figure 3-46. Kureha Paper Stress-Strain Data at 55°C (130°F)

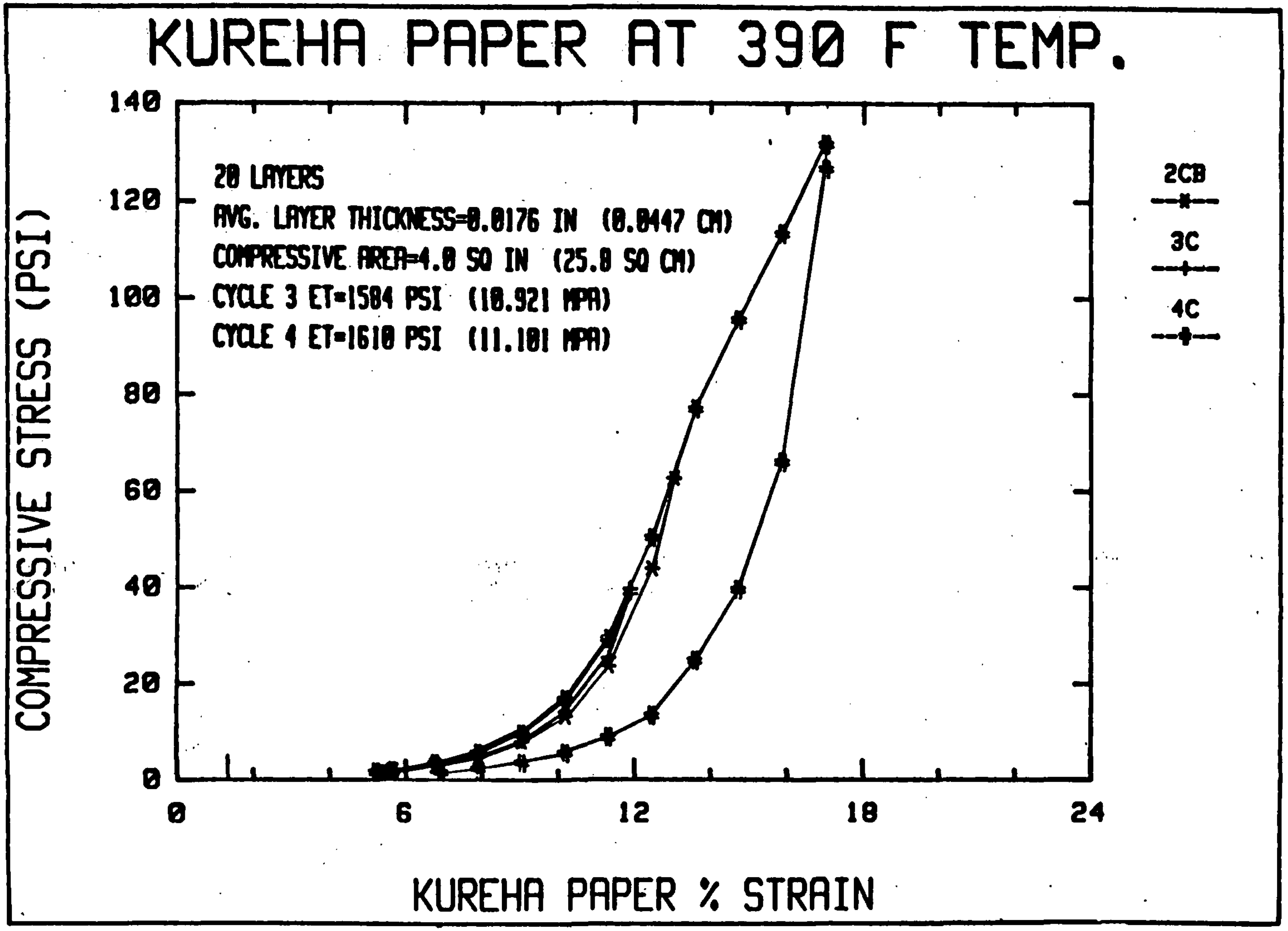

Figure 3-47. Kureha Paper Stress-Strain Data at 199°C (390°F)

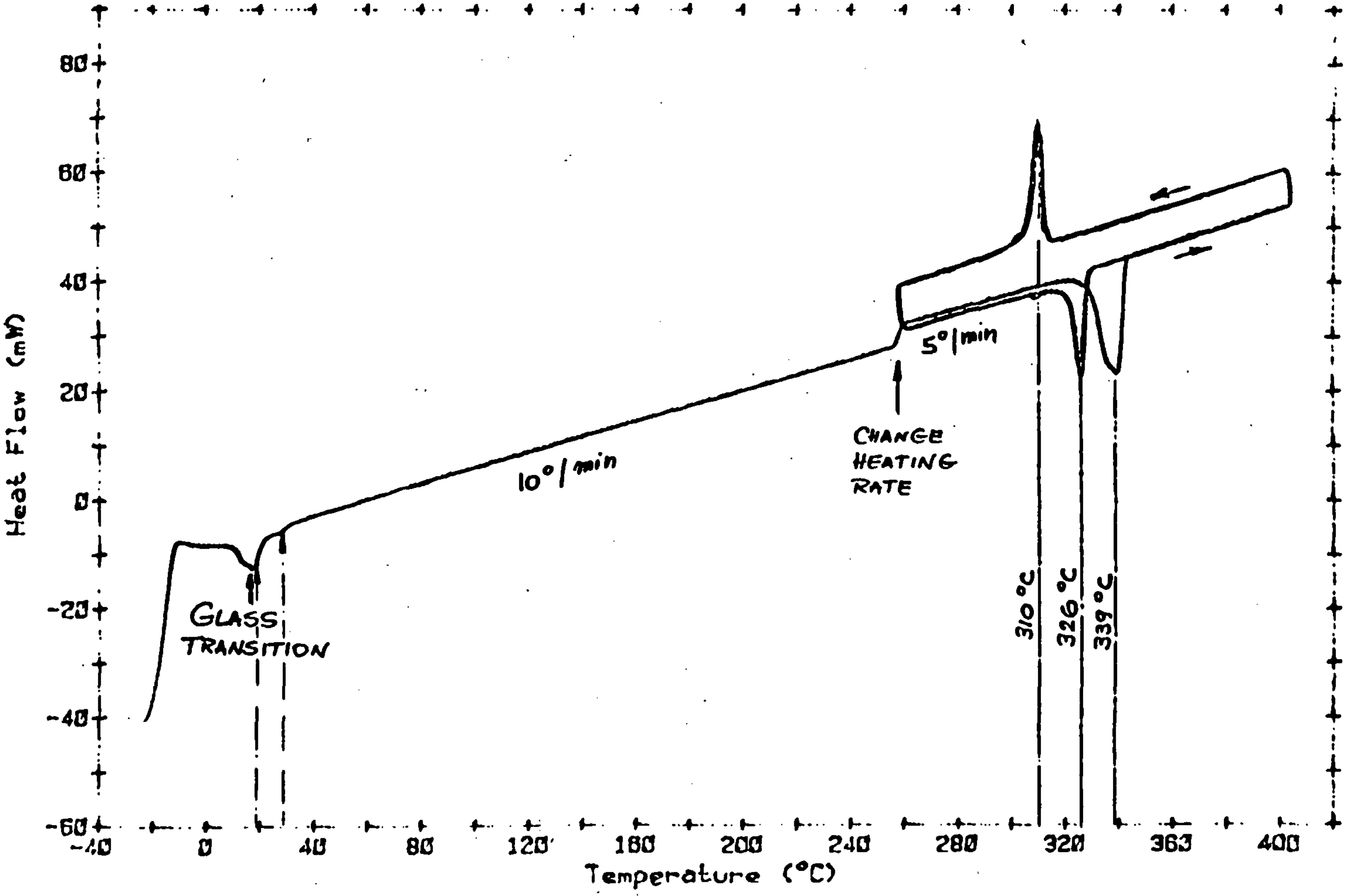

Figure 3-48. DSC Thermogram of TFE 6C

TABLE 3-46
MELTING POINT DATA FOR TFE 6C

Transition	Onset Temperature (°C)	Peak Temperature (°C)	Enthalpy Change J/g
1 Melting	329	340	+ 40.5
Freezing	314	311	- 23.2
2 Melting	320	325	+ 23.1

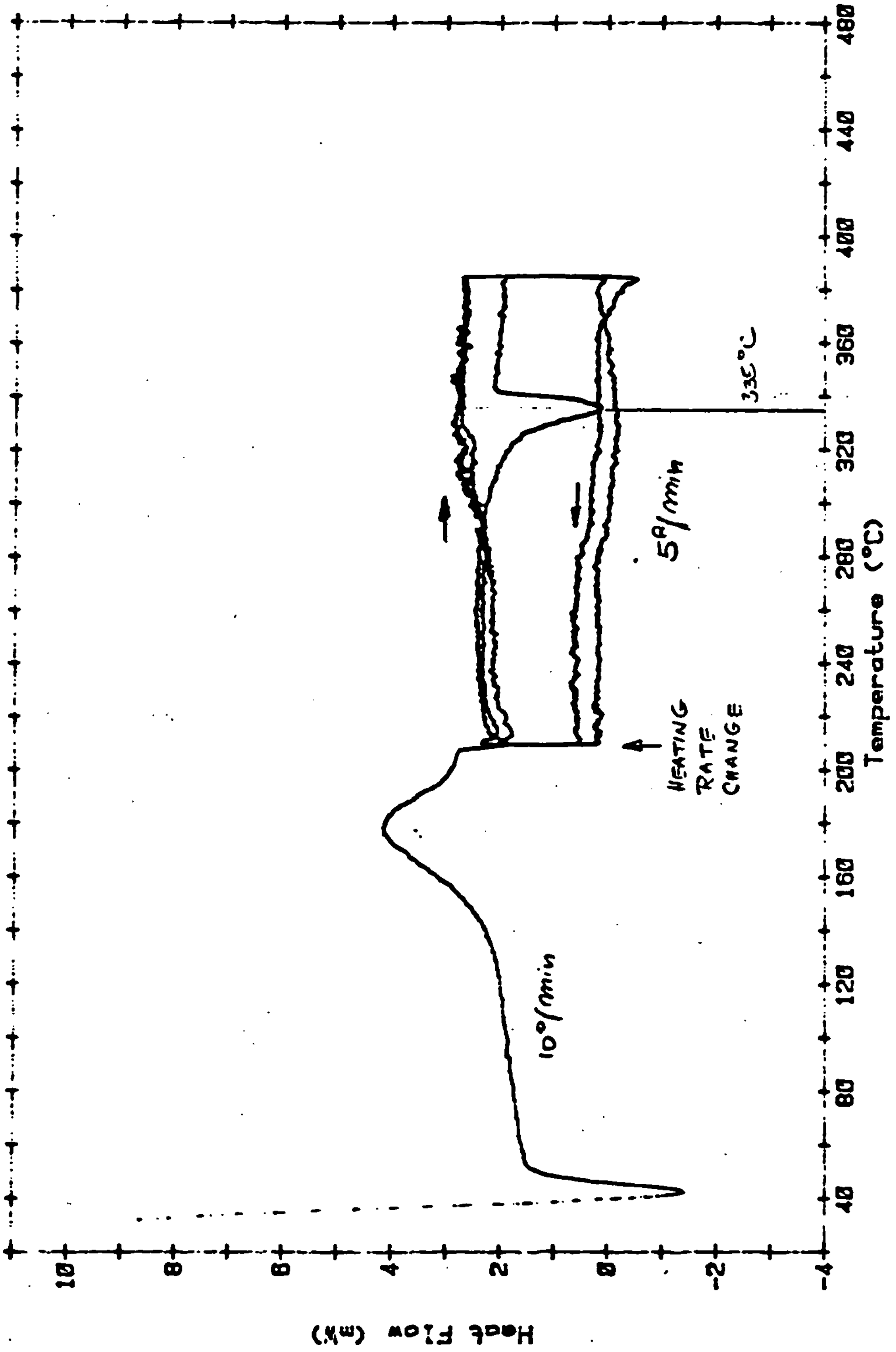

Figure 3-49. DSC Thermogram of an Unsintered Catalyst Layer (C209-1)

important indicator of the state of fibrillation. Further work in this area is suggested, including thermomechanical and dilatometric studies on catalyst layers.

Unsintered catalyst layers (including the one shown in Figure 3-49) have a melting transition peaking at around 335°C (635°F) which is reasonably close to the peak melting point of virgin TFE 6C; however, the heat of melting is only about half that of as-received Teflon (∿20 J/g).

After melting, no further transition is observed, either on cooling or reheating. This suggests that the Teflon, once melted in the Pt/C matrix, is totally amorphous. It is thought that Teflon penetrates into the carbon pores and forms thin films around carbon/platinum aggregates, thereby disallowing any opportunity for crystallinity. For the same reason, no success has been experienced in obtaining electron diffraction patterns of Teflon in electrodes.

Catalyst layers that have been sintered at 360°C (680°F) on Stackpole supports show no transition at all.

3.7.4.10 Ammonium Bicarbonate

Emphasis was placed on determining a satisfactory technique to determine the particle size distribution of ground ammonium bicarbonate. Utilization of the Microtrac particle size analyzer with either isopropyl alcohol, toluene or Shell Sol as the fluid proved satisfactory. A number of wet grinding results were analyzed to assess the effect of the ball jar size on particle distribution. This work was in support of manufacturing and had as its goal the preparation of layer grinding batches of bicarbonate. Initial dry grinding experiments were analyzed for particle size distribution as well.

3.7.5 Other Stack Materials

3.7.5.1 Manifold Material

Evaluation of polyethersulfone (PES) was initiated for possible stack manifold application. Coefficient of thermal expansion tests for this material confirmed that it is anisotropic. The material expands differently in all three directions and some shrinkage occurs between cycles. The critical coefficient of thermal expansion in the "X" direction of measurement was found to be 2.02×10^{-5}/°C (1.12×10^{-5}/°F). The coefficients of thermal expansion in the "Y" and "Z" directions were 2.55×10^{-5}/°C (1.41×10^{-5}/°F) and 2.17×10^{-5}/°C (1.20×10^{-5}/°F), respectively. These values are based on an average of two tests per direction. Compressive creep tests were initiated for the Victrex (PES) manifold material. Two specimens are being tested for 1000 hours at 199°C (390°F) and 20.75 MPa (3010 psi). The results of the test will help predict orthotropic creep rates for the Victrex material.

3.7.5.2 Stack End Insulation Material

The thermal expansion of the insulating block material (H-18408) was evaluated in three directions up to a maximum temperature of 232.2°C (450°F). Preliminary results indicate that the material has nonlinear expansion characteristics and is anisotropic. The largest variation occurs in the "Z" direction. The "X" and "Y" directions are relatively consistent with values of 1.99×10^{-5}/°C (1.11×10^{-5}/°F) and 1.95×10^{-5}/°C (1.08×10^{-5}/°F), respectively. The "Z" direction expansion is greater by a factor of 3.74, for a value of 13.2×10^{-5}/°C (7.37×10^{-5}/°F). This value affects the amount of compressive force developed in the stack during thermal excursions. The second cycles indicate that some shrinkage occurs during the first cycle. Therefore, it may be necessary to thermally cycle the finished parts made from this material at least twice to minimize the shrinkage effect.

3.7.5.3 Phosphoric Acid

Ion chromatography was performed on three samples of H_3PO_4, Table 3-47. The data indicate that all three are essentially the same with regard to F^-, Cl^-, NO_3^- and SO_4^{2-}.

3.8 Advanced Fuel Cell Development

To achieve the plant performance goals, the fuel cell technology needs to be developed to obtain an average start of life performance of 680 mV/cell at 325 mA/cm^2 (300 A/ft^2), 190°C (374°F), 480 kPa (70 psia), 83 percent fuel utilization and 50 percent oxidant utilization. A performance degradation rate of 2 mV/1000 hours was considered desirable. Although significant progress has been achieved in the development effort to obtain the above goals, further improvements are required. Problem areas and potential solutions were identified and a Performance Improvement Work Plan was developed to achieve these goals.

Performance improvements are being sought by:

- improving catalysts.
- reducing the cell resistance.
- better understanding of operational parameters.

Efforts are also underway to reduce cell performance variance by:

- reducing the matrix thickness variations.
- improving quality control techniques.
- improving fabrication and assembly procedures.

Performance degradation rates are expected to be lowered by the use of a more corrosion resistant catalyst support, improved corrosion resistance of the plates, and acid management improvements. The advanced development effort is described in the following areas:

TABLE 3-47
ION CHROMATOGRAPHY OF VARIOUS SAMPLES OF PHOSPHORIC ACID

	Analysis, ppm by weight			
Acid	F^-	Cl^-	NO_3^-	SO_4^{2-}
Baker Analyzed (0260-3)	2	4	1	6
Fisher Certified ACS (A242)	3	4	2.5	13
MCB, Reagent Grade	3	5	4	11

- alternate catalyst evaluation.
- alternate catalyst support.
- electrode manufacturing.
- cell resistance.
- acid management.
- plate corrosion.
- plate coatings.
- impurity effects.

3.8.1 Alternative Catalysts

Heat treated platinum is being used as the cathode catalyst in the present electrodes. Improved catalyst activity with alloy catalysts has been reported in the literature by several investigators. Evaluation of developmental catalysts DC-05 and DC-06 was, therefore, initiated according to test specification TSE 2x2-008A. A heat treated platinum cathode was also evaluated to provide a baseline for comparison.

Initial performance of the developmental catalysts was 25 to 30 mV better than the heat treated platinum/Vulcan. Catalyst DC-06 showed the best performance. A total of 1,760 hours of pressurized, 480 kPa (4.76 atm), testing showed that the IR-free performance degradation rate of the developmental catalyst is 15 to 25 mV/1000 hours. This is much higher than observed for the baseline heat treated platinum/Vulcan catalyst. Cell performance data are shown in Table 3-48 and Figure 3-50.

The performance level of the alloy catalysts decreased to that of the heat treated platinum/Vulcan in 1,760 hours of testing. Similar results were previously obtained with alloy catalysts tested at ERC. An increase in cell resistance during testing was noted in all cells. This is presently thought to be due largely to the corrosion of the 900°C (1650°F) heat treated plates used in these cells. Cells containing 2700°C (4900°F) heat treated plates will be tested to verify this hypothesis. Testing of all cells will continue in order to obtain long term degradation rates.

TABLE 3-48

ENDURANCE TESTING OF DEVELOPMENTAL CATALYST CELLS ECPS-05 THRU -08

(TEST SPEC. TSE 2X2-008A)

Operating Conditions: 70 psia, 190°C, 325 mA/cm^2, 83% fuel (H_2) and 50% oxidant (air) utilizations.

Cell No.	Cathode Catalyst	Anode Catalyst	Cell Matrix	Hours Tested (As of 5/25/84)	Terminal Cell Voltage, mV		
					Initial	Peak	Most Recent
ECPS-05	DC-05	DC-03	MAT-1	1759	693 (740)*	693 (750)	652 (710)
ECPS-06	DC-06	DC-03	MAT-1	1759	697 (761)	697 (761)	650 (731)
ECPS-07	DC-06	DC-03	MAT-1	1759	696 (765)	696 (765)	657 (738)
ECPS-08	HT Pt	Pt	MAT-1	1759	667 (729)	669 (731)	650 (734)

*Numbers in parentheses are IR-free voltages

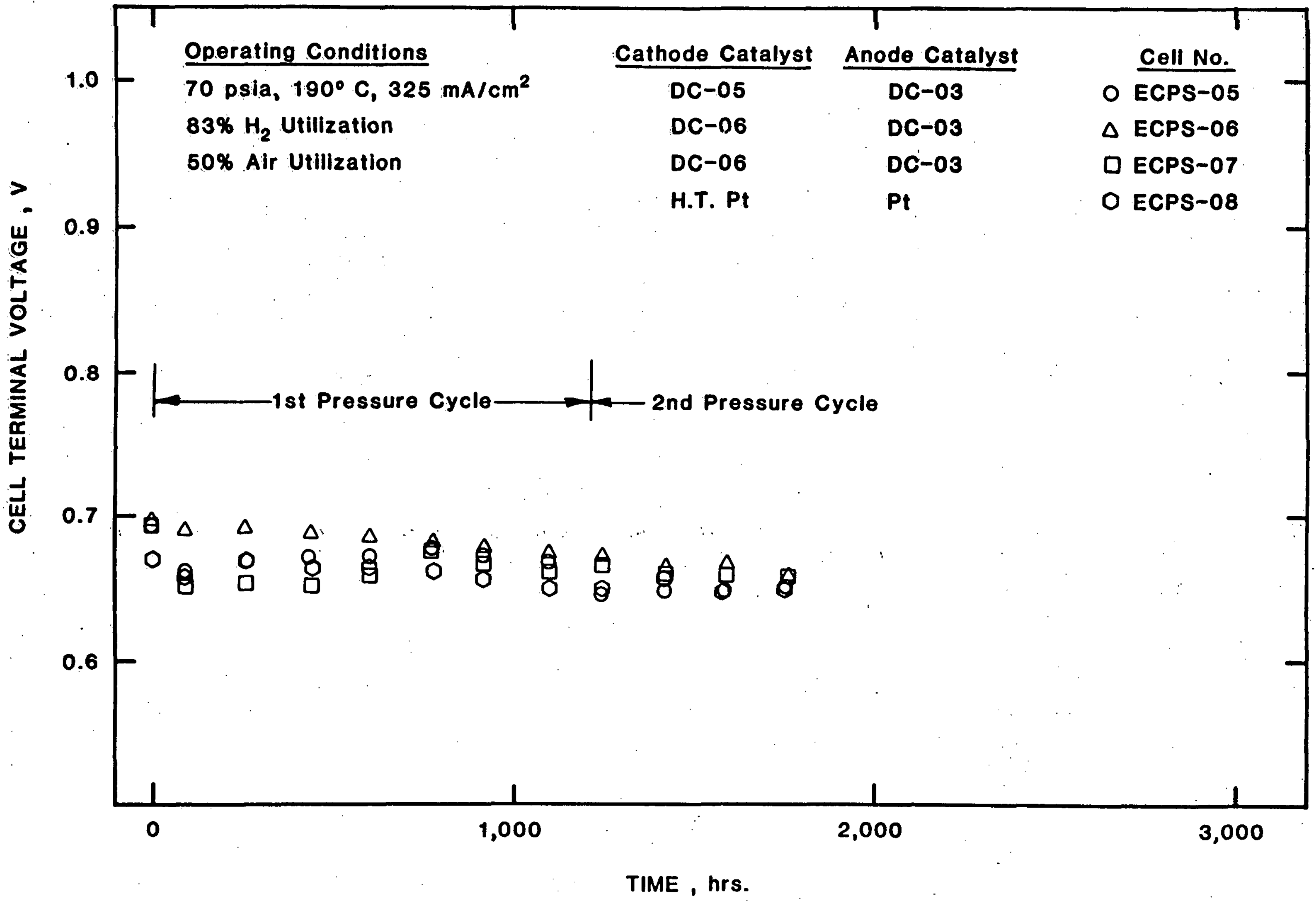

Figure 3-50. Lifegraphs of Developmental Catalyst Cells ECPS-05 Thru -08

Six additional cells (ST-01 thru ST-06) were tested to compare the performance stability of developmental catalyst cathodes with the 900°C (1650°F) heat treated platinum/Vulcan cathodes under atmospheric stress test conditions (870 mV terminal voltage) and nominal atmospheric operating conditions, per Test Specification TSE 2x2-008. The cell performance at 200 mA/cm^2 (186 A/ft^2) is presented in Table 3-49. The IR-free performance of developmental catalyst cells degraded faster than that of the cells with heat treated platinum catalyst, both under stress conditions and at nominal atmospheric operating conditions. Of the developmental catalysts, performance of cathodes with DC-06 catalyst degraded much slower (36 mV/1000 hours) than cathodes with DC-05 catalyst (77 mV/1000 hours). Performance of the cells with the heat treated platinum cathode increased during the test period. This may be due to continued wetting of the catalyst layer.

Based on the data available, it appears that the performance of cathodes containing developmental catalysts DC-05 and DC-06 is less stable under stress test conditions than under nominal atmospheric operating conditions, and degrades faster than the heat treated platinum catalyst.

Cell 3009 containing a 900°C (1650°F) heat treated platinum/Vulcan cathode has been tested at 101 kPa (1 atm) and 200 mA/cm^2 (186 A/ft^2) for 11,000 hours. A lifegraph of Cell 3009 is shown in Figure 3-51. During this period its terminal voltage dropped from 643 mV (peak) to 619 mV. This represents an overall degradation rate of $\sim$ 2 mV/1000 hours. The performance degradation appears mainly to be related to a decrease in catalyst activity. The cell resistance appears to be quite stable.

3.8.2 Alternate Catalyst Support

Analysis of stack and subscale cell data obtained under pressurized test conditions during the First Logical Unit of Work indicated that the performance degradation rates of cells containing heat treated platinum/Vulcan electrodes could be as high as 25 mV per 1,000 hours. Currently, performance

TABLE 3-49

STRESS TESTING OF DEVELOPMENTAL CATALYST CELLS ST-01 THRU -06

(TEST SPEC. TSE 2X2-008)

Operating Conditions: 15 psia, 190°C, 100 mA/cm^2, 83% fuel (H_2) and 25% oxidant (air) util.

Cathode Catalyst	Test Objective	Cell No.	Anode Catalyst	Cell Matrix	CELL TERMINAL (IR-FREE) VOLTAGE, mV			Change In IR-Free Voltage, mV
					Before stress testing	After 336 hrs of stress testing	After 1008 hrs of stress testing	
DC-05	Stress	ST-01	Pt	SiC	681 (708)	644 (674)	600 (631)	-77
DC-05	Control	ST-02	Pt	SiC	671 (701)	663 (698)	654 (691)	-10
DC-06	Stress	ST-03	Pt	SiC	679 (715)	659 (707)	620 (679)	-36
DC-06	Control	ST-04	Pt	SiC	697 (726)	697 (729)	697 (726)	- 0
HT Pt	Stress	ST-05	Pt	SiC	628 (669)	634 (688)	608 (671)	+ 2
HT Pt	Control	ST-06	Pt	SiC	623 (663)	636 (679)	635 (681)	+18

Control: 15 psia, 190°C, 100 mA/cm^2, 83% fuel (H_2) and 25% oxidant (air) utilizations.

Stress Testing Conditions: 15 psia, 190°C, 83% fuel (H_2) and 5.2% oxidant (O_2) utilizations and 870 mV/cell terminal voltage. Oxidant (O_2) utilizations of 5.2% is selected to ensure the same electrolyte concentration as in the control cells.

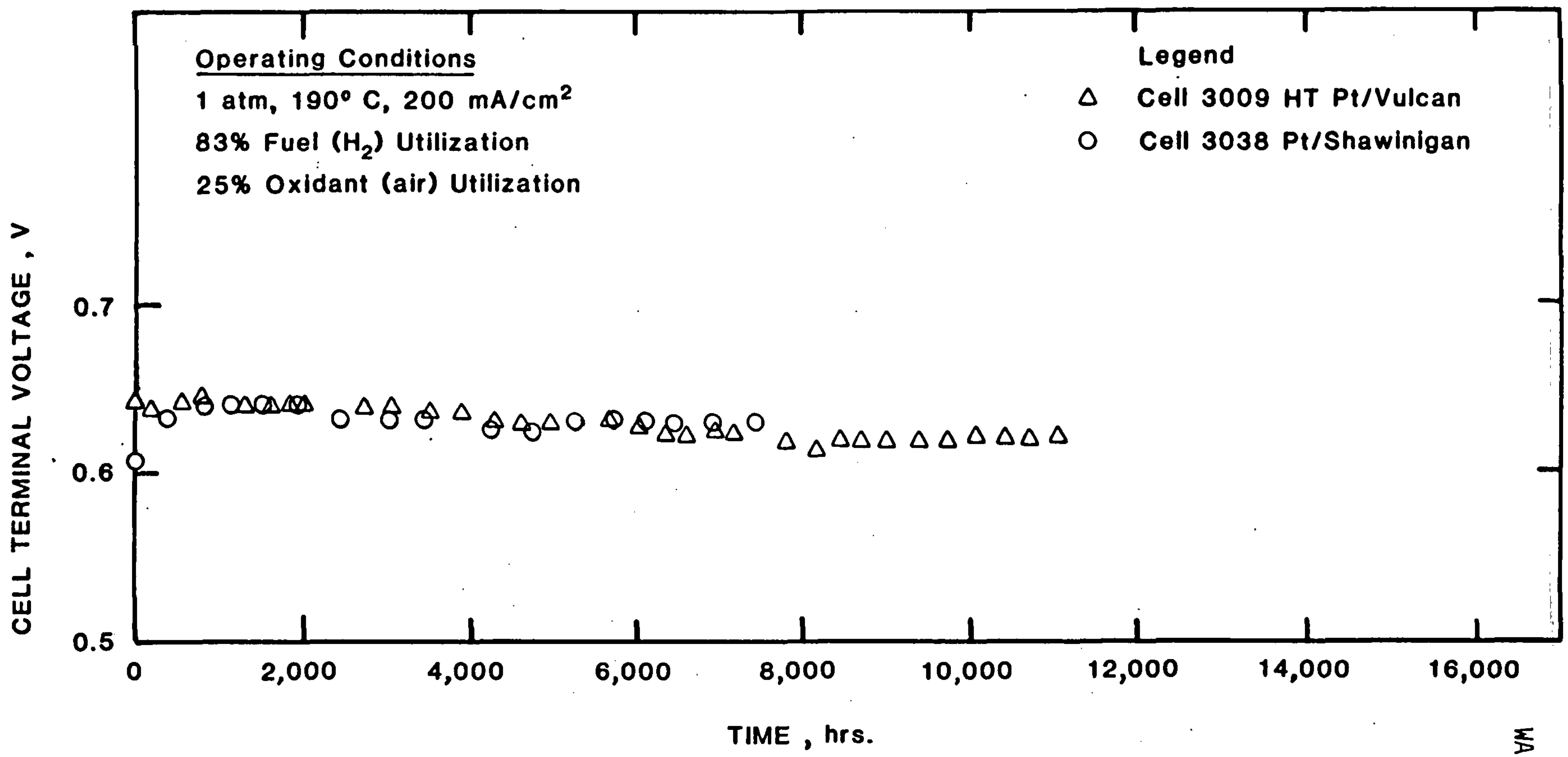

Figure 3-51. Lifegraph of Cells 3009 and 3038

degradation rates of similar cells, based on short-term test results, is 8 to 12 mV per 1,000 hours. It is important to note that the 2 mV/1,000 hours degradation rate was demonstrated in Stack 431 operated at atmospheric pressure for more than 16,000 hours (Table 3-50) and Stack 560 (Figure 3-52). Recently, this rate was confirmed in subscale Cell 3009 which has been running for over 11,000 hours (Figure 3-51).

During the Second Logical Unit of Work, Gulf Corporation's Shawinigan Acetylene Black and 2700°C (4900°F) heat treated Vulcan XC-72 were selected as alternative catalyst support materials. A suitable catalyst support material should have a low corrosion rate, high surface area, and be electrochemically clean. Shawinigan Black carbon has a low sulfur content (0.01 percent). As-received Shawinigan Black has a surface area, 90 m^2/g (4.40×10^5 ft^2/lb), similar to that of 2700°C (4900°F) heat treated Vulcan, 80 m^2/g (3.90×10^5 ft/lb). The corrosion rate of Shawinigan carbon at 0.8 volt is at least an order of magnitude lower than that of Vulcan XC-72. These desirable properties formed the basis for its selection.

Platinum/Shawinigan electrodes with 25 percent and 30 percent polytetrafluoroethylene were fabricated. Fabrication of Shawinigan electrodes was more difficult than Vulcan electrodes. Platinum/Shawinigan electrodes were tested for over 7,500 hours at 101 kPa (1 atm). Performance data for the cells tested are summarized in Table 3-51. The electrode performance is ∿ 20 mV lower than that of heat treated Platinum/Vulcan at 101 kPa (1 atm). The performance decay rate (2 mV/1,000 hours), however, is similar to that of heat treated platinum/Vulcan electrodes.

Performance of 2500°C (4550°F) heat treated platinum/heat treated Vulcan electrodes was very low. Platinum/heat treated Vulcan electrodes tested in other ERC programs showed better results than those obtained here. The performance in this program was still 20 to 30 mV lower than that of heat treated platinum/Vulcan electrodes. The poor performance of heat treated platinum/heat treated Vulcan electrodes may be due to a large platinum crystallite size. This hypothesis, however, needs to be investigated further.

TABLE 3-50

TERMINAL PERFORMANCE STABILITY OF STACK 431, mV

CELL NO.	INITIAL PERFORMANCE	PERFORMANCE AT 16,382 HRS.	PERFORMANCE DEGRADATION RATE, mV/1,000 HOURS
1	670	630	2.4
2	660	630	1.8
3	670	620	3.1
4	670	630	2.4
5	650	630	1.2
AVG. CELL	660	630	1.8

OPERATING CONDITIONS:

PRESSURE:	1 atm
TEMPERATURE:	180-185°C
REACTANTS:	H_2/AIR
CURRENT DENSITY:	100 mA/cm^2
CATALYST:	Pt/Vulcan
PLATES:	900°C HEAT TREATED MK-I
MATRIX:	MAT-1
CONTRACT:	DEN3-205

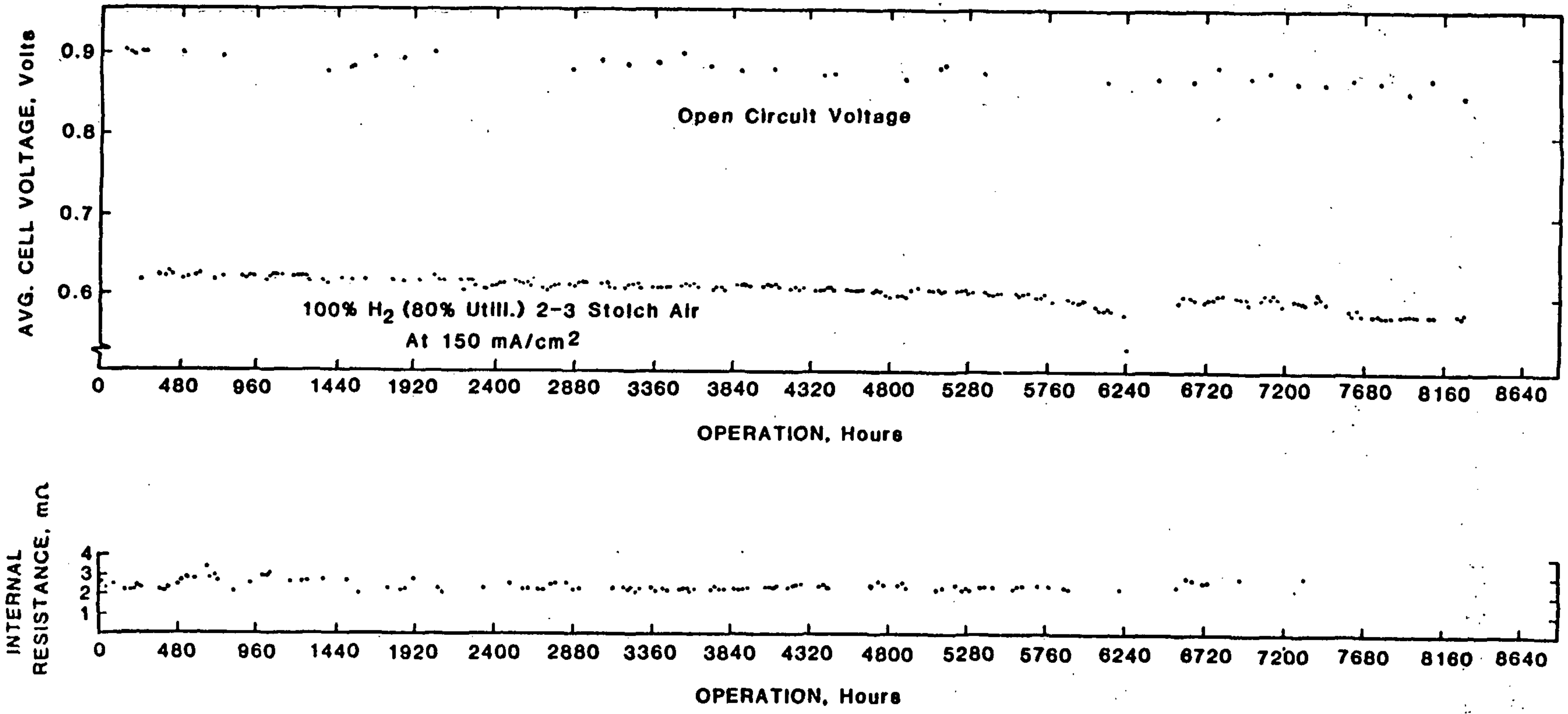

Figure 3-52. Lifegraph of Stack 560

TABLE 3-51

PERFORMANCE OF ALTERNATE CATALYST SUPPORT CELLS, mV

(*TEST SPEC. TSE 2X2-002*)

	CATHODE							TERMINAL (IR-FREE) VOLTAGE		
SUPPORT	TEFLON CONTENT %	LAMINATION PRESSURE	AMOUNT OF FILLER USED	CATALYST	CATALYST LOADING, mg/cm^2	CELL NO.	HOURS TESTED AS OF 5/25/84	INITIAL	PEAK	MOST RECENT
Shawinigan, 1200°C HT	25	0.13 x Std	Std	HT Pt	0.6	AS-02	2,088	636 (677)	654 (690)	647 (683)
Shawinigan, 1200°C HT	30	0.13 x Std	None	HT Pt	0.6	AS-05	528	595 (635)	623 (659)	614 (651)
Shawinigan, as-received	30	0.13 x Std	Std	HT Pt	0.6	AS-06	2,088	622 (668)	637 (680)	634 (678)
Shawinigan, 1200°C HT	30	Std	Std	HT Pt	0.5	AS-08	1,152	644 (680)	648 (680)	579 (618)
Vulcan, 2500°C HT	25	0.13 x Std	Std	HT Pt	0.6	AS-09	360	303 (380)	--- ---	280 (359)
Vulcan, 2500°C HT	30	Std	Std	HT Pt	0.6	AS-12	360	435 (497)	--- ---	423 (489)
Shawinigan, as-received	30	Std	Std	Pt	0.5	3037	2,040	622 (656)	641 (672)	576 (607)
Shawinigan, as-received	30	Std	Std	Pt	0.5	3038	7,584	608 (640)	643 (668)	630 (654)

Operating Conditions

Pressure: 1 atm
Temperature: 190°C
Reactants: H_2/Air
Current Density: 200 mA/cm^2

3.8.3. Electrode Manufacturing

Some of the performance variations observed in subscale cells and stacks may be attributed to the variations in electrode manufacturing processes. Occasionally, partial burning of the electrodes has been observed during the air sintering process. Subscale cell and out-of-cell tests were, therefore, conducted to study the effect on cell performance of the following variables:

- sintering gas environment.
- electrode lamination pressure.
- amount of filler ammonium bicarbonate used in the electrode fabrication process.

Cathodes sintered in various gas environments were tested in subscale Cells MF-01 thru -04 at atmospheric conditions. Although no significant difference in cell performance was observed in the limited number of tests conducted, it was decided to use an argon gas environment to prevent the possibility of electrode burning.

Thermogravimetric analysis (TGA) of the unsintered electrode layers in air had shown that burning occurred around 160°C (320°F). It is known, however, that heat treatment of the catalyst powder is carried out at 900°C (1650°F) in a nitrogen environment without any noticeable burning. Experiments indicated that burning can be limited by reducing the amount of air available at the catalyst surface.

Effects of electrode lamination pressure and the amount of filler used in electrode fabrication on cell performance was studied in Cells MF-05 thru MF-08 at atmospheric pressure. No difference in the cell performance associated with these manufacturing variables was observed. However, very low lamination pressure sometimes resulted in poor lamination of the electrode. A more detailed study is necessary to optimize the required lamination pressure. Elimination of the filler from the manufacturing process can result in a simplified process with significant cost savings. Further testing in stacks is required to confirm the above results.

3.8.4 Cell Resistance

Subscale cell tests indicated that a 31 mV performance improvement could be achieved by reducing the present matrix thickness, 0.043 cm (0.017 in.), by 50 percent, 0.023 cm (0.009 in.). These results were further verified in nine cell stacks. It was recognized that manufacturing processes would need to be refined to fabricate thin and defect-free matrices. A brief account of the cell resistance model and experimental results are presented in this section.

Previous effort under DOE/NASA contract DEN3-67 identified the potential resistance contribution of various individual cell components. Significant reduction in cell resistance was achieved in that program by heat treating the graphite-resin plates. Initial estimates indicated that the electrolyte matrix accounted for a large part of the measured cell resistance.

The present MAT-1 matrix consists of a carbon layer, 0.025 cm (0.010 in.), and a SiC layer, .018 cm (0.007 in.) thick. It has become apparent that the resistance of the carbon layer is not directly measured by the AC milliohmeter normally used to measure resistance. Two subscale cells were tested to obtain a preliminary estimate of the resistance of the carbon layer. Although the thickness of the matrix in Cell 3028 was 60 percent greater than that in Cell 3029, the measured resistances of both cells were the same. The peak IR-free performance of Cell 3029 was ∿ 20 mV higher than that of Cell 3028. This suggested that the resistance of the carbon layer is not being measured by the present resistance measurement technique. A similar gain in performance for cells without carbon layers in matrices had also been observed in Stack E-009-02.

Understanding of the effective cell resistance network was, therefore, desired. The previous resistance model did not include the interaction of electronic and ionic resistance of the electrode catalyst layers and the carbon layer in the cell matrix. The model was modified to include this interaction. Figure 3-53 presents the revised model. When the cell resistance is measured using a milliohmmeter, current from the meter passes through all the resistances. The path of the current generated in the cell is different than in the milliohmmeter case. Thus, the actual cell resistance is different that the measured value. Resistance equations for the new model were derived and individual component resistances estimated using these equations. The estimates also confirmed that the matrix accounts for most of the cell resistance.

Resistance of the cell matrix can be reduced by reducing the thickness of the SiC and carbon layers in it. However, these thicknesses may only be reduced to the minimum required for these layers to perform their functions. The main function of the SiC layer is to serve as an electrical insulator between anode and cathode, while that of the carbon layer is to provide a bubble pressure barrier to prevent gas crossover between the electrodes. Very thin layers of SiC and carbon are sufficient to perform these functions.

As a first attempt, the thickness of the SiC layer was reduced from 0.018 to 0.008 cm (0.007 to 0.003 in.) and that of the carbon layer from 0.025 to 0.015 cm (0.010 to 0.006 in.). These thin matrix layers were evaluated in subscale cells (TH-01 thru TH-06) at atmospheric pressure. Performance and resistance data are presented in Table 3-52. Individual resistances of the SiC layer, carbon layer, and hardware (electrodes, plates, and contact) in standard cells (2 x 2 in. and 12 x 17 in.) were estimated using the test data. It is again apparent from these estimates that the matrix layers offer most of the resistance. A resistance reduction of ∿ 2 mΩ resulted from 0.01 cm (0.004 in.) reduction in the SiC layer thickness, which represents a performance gain of ∿ 10 mV at 200 mA/cm^2 (186 A/ft^2). A carbon layer thickness reduction of 0.01 cm (0.004 in.) resulted in a performance gain of ∿ 9 mV at 200 mA/cm^2 (186 A/ft^2). The total observed gain at 200 mA/cm^2 (186 A/ft^2) was 19 mV. At power plant operating conditions, 325 mA/cm^2 (300 A/ft^2), a performance gain of ∿ 31 mV can be expected. This was verified in nine cell Stack E-009-01 and is a significant improvement in cell performance.

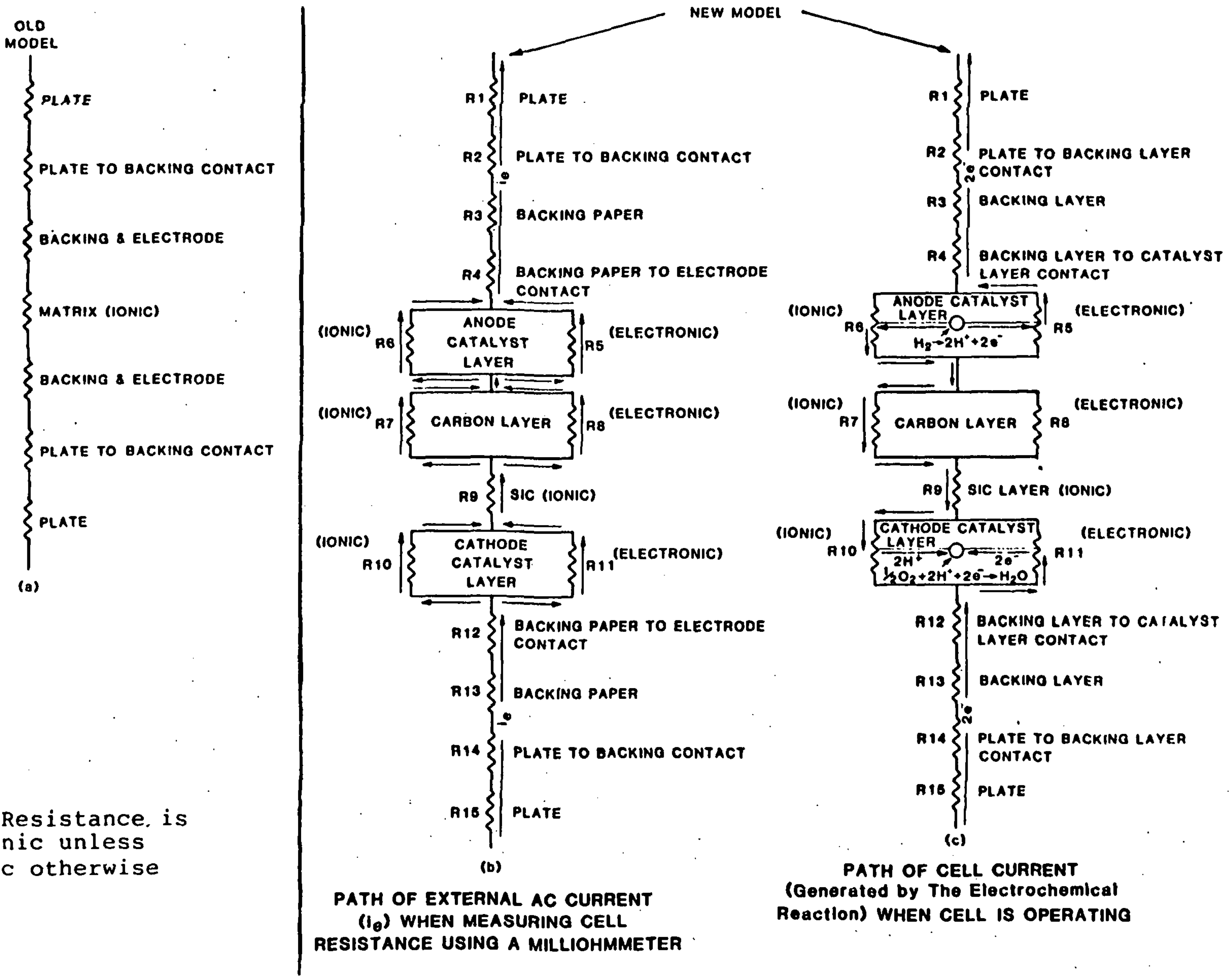

PATH OF EXTERNAL AC CURRENT (I_e) WHEN MEASURING CELL RESISTANCE USING A MILLIOHMMETER

PATH OF CELL CURRENT (Generated by The Electrochemical Reaction) WHEN CELL IS OPERATING

NOTE: Resistance is electronic unless specific otherwise

Figure 3-53. Modified Resistance Model Compared with Old Model

TABLE 3-52

EFFECT OF MATRIX THICKNESS ON CELL PERFORMANCE AND RESISTANCE

OPERATING CONDITIONS: 1 atm, 190°C, 200 mA/cm^2, 83% fuel (H_2) and 25% oxidant (air) util.

Cell Matrix Thickness, mil				Cell Terminal (IR-Free*) Voltage, mV			Cell Resistance, mΩ		
SiC Layer	Carbon Layer	Cell No.	Hours Tests	Initial	Peak	Last	Initial	At Peak Voltage	Last
3	0	TH-05	740	679 (697)	687 (704)	673 (694)	3.5	3.3	4.1
3	6	TH-01	740	668 (686)	677 (695)	677 (695)	3.4	3.5	3.5
3	10	TH-02	740	675 (694)	686 (706)	684 (705)	3.8	4.0	4.0
7	0	TH-06	740	670 (701)	681 (712)	681 (712)	6.0	6.1	6.1
7	6	TH-03	740	668 (692)	674 (698)	670 (695)	4.7	4.7	4.8
7	10	TH-04	740	642 (673)	659 (690)	658 (689)	6.1	6.0	6.1

*IR correction for the carbon layer not included.

The 0.008 cm (0.003 in.) thick SiC layer did, however, cause an electrical short resulting in low OCV and cell performance. The manufacturing of thin SiC layer should be improved to yield a stronger, uniformly thin layer.

The 0.008 cm (0.003 in.) thick SiC layer was also evaluated in a nine cell stack (E-009-04) at pressure. Performance and average cell resistance data are presented in Table 3-53. A performance gain of 14 mV was expected based on the measured resistance reduction. The observed gain at 325 mA/cm^2 (300 A/ft^2) was 18 mV.

3.8.5 Bipolar Plate Corrosion

Corrosion of the cathode side of bipolar plates has been observed in subscale cells and stacks after pressurized operation. The following factors are suspected to play a significant role in plate corrosion:

- acid volume expansion.
- high water partial pressure in oxidant exhaust stream.
- defective wetproofing of backing paper.
- fuel starvation in a cell driven by other cells.
- oxidant starvation in a cell driven by other cells.

The objectives of this task were to identify the cause(s) and to gain an understanding of the mechanism of bipolar plate corrosion. Conditions suspected of causing bipolar plate corrosion were investigated by introducing these conditions into subscale cells and evaluating their effects on plate corrosion. The ultimate goal is to find a means to prevent or protect against bipolar plate corrosion.

Subscale Cells PC-01 thru PC-08 were tested for ∿ 600 hours at atmospheric pressure to evaluate the suspected contributors to corrosion. Acid expansion and higher water partial pressure in the cathode exhaust stream were obtained by running these cells with pure oxygen at greater than 60 percent utilization

TABLE 3-53

EFFECT OF MATRIX THICKNESS ON PERFORMANCE AND RESISTANCE OF STACK E-009-04 AT PRESSURE

(1) DECREASE IN MEASURED RESISTANCE

	Matrix Thickness, mil		Average Cell (12 x 17 in.) Resistance, mΩ At 325 mA/cm^2, 70 psia, 190°C
	SiC Layer	Carbon Layer	
	7	10	0.12
	3	10	0.08
Difference	4	0	0.04 mΩ

Average Resistance of SiC layer = 0.01 mΩ/mil

(2) MEASURED VOLTAGE GAIN

Cell No.	Matrix Thickness, mil		Cell Terminal Voltage, mV At 70 psia, 325 mA/cm^2, 190°C	
	SiC Layer	Carbon Layer		
1	7	10	662	
2	7	10	654	
3	7	10	676	Avg. 669.8
4	7	10	673	
5	7	10	684	
6	3	10	641*	
7	3	10	678	Avg. 676.5
8	3	10	708	
9	3	10	680	

*Cells 6, 7, 8, 9 were diagnosed to have electronic shorts

(3) CONCLUSIONS

Based on resistance reduction:

predicted gain = 14 mV
observed gain, Cells 6-9 = 7 mV
observed gain, Cells 7, 8 and 9 = 18 mV

and then running them on air. This operation is referred to as an oxygen cycle. Fuel and oxidant starvation due to gas maldistribution were simulated by restricting the gas flow and fixing the current density via an external power supply.

Maximum acid expansion was expected in Cell PC-01. No change in performance, however, was observed after two oxygen cycles. Cell PC-02 could not be operated at 84 percent oxygen utilization, (partial pressure of water corresponding to plant conditions) hence it was operated at 78 percent oxygen utilization. Performance of the cell decayed by 25 mV after two oxygen cycles. Upon disassembly of Cell PC-02, a platinum deposit was found on the SiC matrix and on the anode graphite plate in the acid reservoir area. There was no apparent reason for this rather strange occurence. No significant decay was observed in the other two cell (PC-03 and PC-04). During oxygen cycles, acid was seen to have expanded in the acid fill tubes for all four cells. Upon disassembly, no visible softness was found on any of the cathode plates.

Cell PC-05 was operated in an oxidant starved mode and driven by an external power supply. A decay of 31 mV was observed after two oxygen cycles. No softness of the cathode plate was evident upon disassembly.

Cell PC-06 was run in a fuel starved mode during the oxygen cycle. This cell required nearly 2V from the external power supply. After one hour of operation in this mode, a significant increase in cell resistance was noted (from ∿ 4 mΩ to 60 mΩ). Testing was terminated when acid in the fill tube turned black. Significant corrosion was observed in the acid channel area on the anode plate.

The results of these experiments may be summarized as follows:

- Up to 12 percent acid expansion and corresponding high water partial pressure did not cause any apparent softness of the cathode plate or the backing paper. This may be due to the lateral transport of electrolyte in the 2 x 2 cells allowing the acid to escape from the edges. The above experiments also suggest that similar acid expansion experiments in 12 x 17 stacks would be helpful in isolating the effects of acid expansion from any other effects of high pressure operation.

- Oxidant and fuel starvation caused significant performance loss in fuel cells in a driven mode. Fuel starvation is more detrimental than oxidant starvation although fuel starvation causes anode plate corrosion; no apparent cathode plate corrosion was found in either of these cells.

Cell PC-07 was tested to evaluate defective wetproofing of the backing paper on plate corrosion. The cathode backing paper in this cell had a non-wetproofed area (∿ 1.3 cm (0.5 in.) diameter) in the center. This cell was first conditioned and tested at 200 mA/cm^2 (186 A/ft^2), 101 kPa (1 atm) pressure, 25 percent oxidant (air) and 80 percent fuel (hydrogen) utilizations. It was then tested at 325 mA/cm^2 (300 A/ft^2), 101 kPa (1 atm) pressure, 84 percent oxidant (oxygen) utilization and 80 percent fuel (hydrogen) utilization to simulate acid expansion and high water partial pressure in the oxidant stream. After two cycles of acid expansion, no significant decay in cell performance was observed. After ∿ 600 hours of testing, the cell was disassembled, and no corrosion was visually apparent underneath the non-wetproofed area of the backing paper. A small area of the cathode plate near the acid reservoir was found to be corroded.

Cell PC-08 was assembled with a specially fabricated cathode. The backing paper of this cathode had a 1.3 cm (1/2 in.) wide SiC strip in the middle in place of standard backing paper. This provided an acid path from the catalyst layer to the cathode plate. Cell PC-08 was first conditioned and tested at 200 mA/cm^2 (186 A/ft^2), 190°C (374°F), 101 kPa (1 atm), 25 percent oxidant (air) utilization, and 80 percent fuel (hydrogen) utilization. It was then tested at 325 mA/cm^2 (300 A/ft^2), 190°C (374°F), 101 kPa (1 atm), 84 percent oxidant (oxygen) utilization and 80 percent fuel (hydrogen) utilization to provide a 8 percent acid expansion and high water partial pressure in the oxidant stream. After two cycles of acid expansion, a steady decline in cell performance was observed. Testing of this cell was terminated after 580 hours.

Careful examination of the cell components during post-test disassembly revealed no apparent corrosion of the plates. The anode backing paper and the lower half of the anode plate were found to be wet and may have been the cause of the poor cell performance.

Potentiostatic corrosion testing of as-received and wetproofed Stackpole backing paper was also conducted. Test results are presented in Figure 3-54. Corrosion behavior of this material was very similar to that of pyrolitic graphite. The corrosion current at 1.05 V for the as-received backing paper was $\sim 7 \times 10^{-3}$ mA/cm^2 (6.5×10^{-3} A/ft^2) (in comparison to ~ 4 mA/cm^2 (3.7 A/ft^2) for the 900°C (1650°F) heat treated A-99 graphite/resin plate material). The corrosion current for a wetproofed backing paper at 1.05V was $\sim 2.5 \times 10^{-2}$ mA/cm^2 (2.3×10^{-2} A/ft^2). This is higher than the value obtained for the plain backing paper. This may be due to some residual dispersing agent from the flourinated ethylene-propylene (FEP) emulsion. These results suggest that the backing paper is graphitic and any further heat treatment of the backing paper may not be helpful.

Corrosion testing of Asbury A-99, Asbury 4221 and Superior 9026 molded plates was completed. The Asbury 4421 plates showed the best corrosion resistance in these tests. At 0.85V, wet-mixed Asbury 4421 plates showed a three-fold reduction in corrosion current as compared with standard Asbury A-99 dry-mixed plates. The dry-mixed Superior 9026 plate showed no improvement over the standard Asbury A-99 dry-mixed plates. The improved corrosion resistance of the Asbury 4421 plate may be attributed to the higher purity of the graphite and to the wet mixing process.

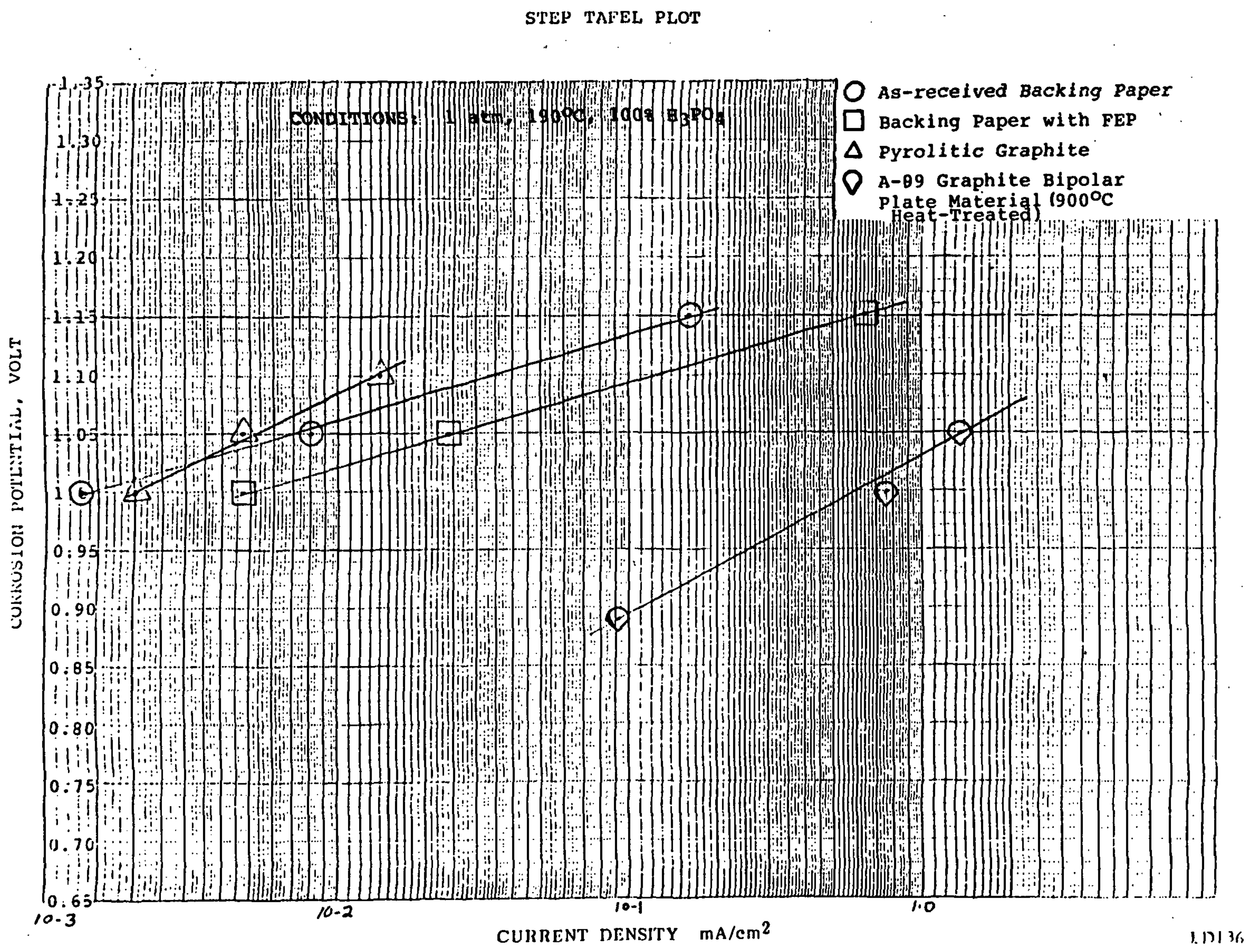

Figure 3-54. Corrosion Behavior of Stackpole Backing Paper

3.8.6 Bipolar Plate Coatings

A possible solution to prevent or minimize plate corrosion is to apply a Teflon (e.g. FEP) coating on the cathode side of plate (except the rib area) and thereby reduce the plate surface area in contact with phosphoric acid. Another solution may be to heat treat the plates to a high temperature (e.g. 2700°C (4900°F)) to form a structure which is more corrosion resistant. Because Teflon (FEP, PFA) is a poor conductor of electrons, the bulk of the coating should be sanded off the rib area to minimize the electrical resistance added by the coating. Another option which minimizes the electrical resistance of Teflon coating is to use carbon or graphite filling.

A test plan was written to evaluate plate coatings which includes the following items:

- Evaluate the corrosion resistance of FEP, FEP/Graphite A-99, PFA/Vulcan XC-72 coated plates, and 2700°C (4900°F) heat treated plates.
- Determine the stability of each coating.
- Determine the effect of coating thickness on measured cell resistance, coating stability, and corrosion resistance.
- Demonstrate subscale cell performance.

The objective of plate coating is to form a protective layer against acid penetration into the graphite/resin plates and thus prevent plate corrosion. The development of a protective coating with a minimum increase in fuel cell electrical resistance is being pursued through vendors and at ERC. The current status of the development is presented below.

Two subscale cathode plates were coated by a vendor with FEP to yield 0.0013 cm and 0.0025 cm (0.0005 in. and 0.001 in.) thick coatings. Preliminary tests indicated that these coatings were electrical insulators. By shaving most of the coating off the ribs, the increase in electrical resistance due to coating was reduced; however, the cell resistance was still high.

To lower the electrical resistance of Teflon coatings, development of a conductive graphite/Teflon composite coating was initiated. Materials and plans for a composite coating were submitted to a vendor for formulation and supplying coated subscale plates for future testing.

DuPont's "Topcoat Finish Black" (dispersion of Teflon and graphite) was received and evaluated. The electrical resistance of a coating less than 0.0013 cm (0.0005 in.) thick was not acceptable. Discussion with DuPont also revealed that an unacceptable anionic wetting agent was used in "Topcoat Finish Black". Further work with DuPont is planned to establish materials suitable for fuel cell use.

Presently, bipolar plates are heat treated to 900°C (1650°F). Higher heat treatment temperatures are expected to increase the corrosion resistance of the bipolar plates. Ten sets of Westinghouse subscale cell graphite/resin plates were successfully heat treated to 1150°C (2100°F). Five sets of these plates were heat treated to 1500°C (2732°F) by a vendor. Heat treatment cycles for these trials have been developed by ERC under in-house programs. The other five sets of subscale plates were successfully heat treated to 2700°C (4900°F) by a vendor using ERC procedures. Visual inspection of these plates indicated no delamination or blistering but the plates were bowed. Careful sanding of the plate reduced bowing satisfactorily. Dimensional changes due to heat treatment above 900°C (1650°F) were less than 1 percent and current MK-II stack hardware should accommodate these changes. As expected, the porosity measured by mercury porosimetry (pore diameters between 50 microns (2 mils) to .006 microns (2.4×10^{-4} mils)) increased for materials heat treated at 2700°C (4900°F).

3.8.7 Acid Management

A comprehensive acid management system study was submitted during the First Logical Unit of Work. Some experimental effort on different acid management-related issues was also initiated during that period. The effort during the Second Logical Unit of Work focused on four different areas as identified in the Performance Improvement Work Plan document:

- Improve lateral transfer of electrolyte during non-steady state operation and acid addition by improving matrix and transport and an alternate seal design.
- Test acid volume control methods.
- Estimate acid requirements based on individual component characteristics.
- Establish criteria and procedures for acid replenishment during stack operation.

Three nine cell stacks were tested in support of this activity. Stack E-009-02 was assembled with a seal design which extended the silicon carbide coated cathode and the carbon layer over the acid replenishment channel. A diagram depicting this design is shown in Figure 3-55. The design improves the wicking of acid into cells. The effectiveness of this design was demonstrated by acid addition to Stack E-009-02 after its first pressure cycle. The cell OCV increased significantly as shown in Table 3-54. This stack had five standard cells and four cells which contained no carbon layer in the matrix. Cells without a carbon layer had very low OCV before the acid addition, but increased to the level of the standard cells after acid addition. Apparently, acid was effectively transported to the cells. This data supports the recommendation that this seal design be used in future cells.

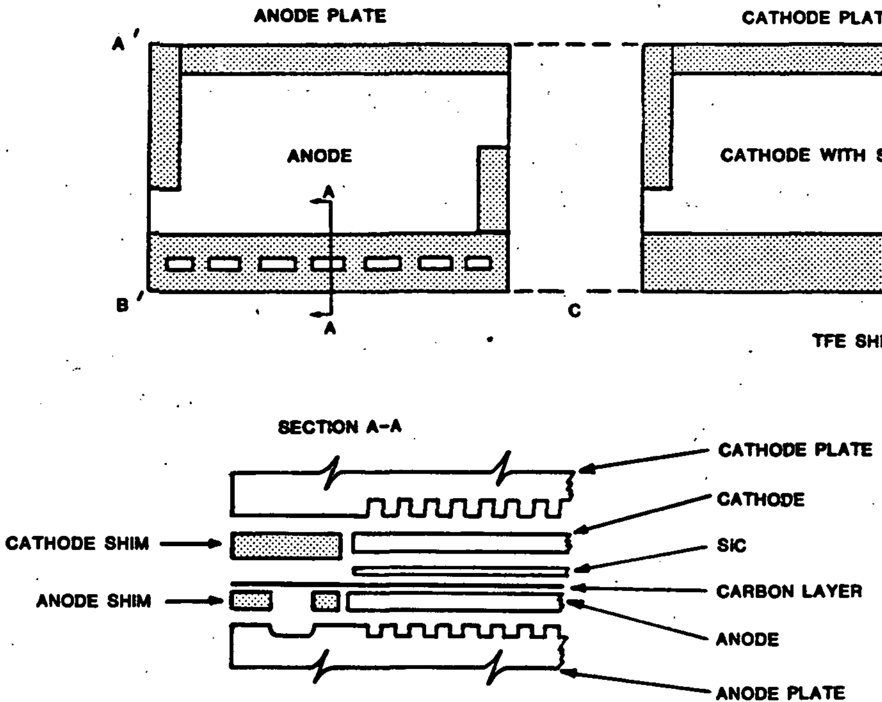

a) STANDARD SEAL DESIGN

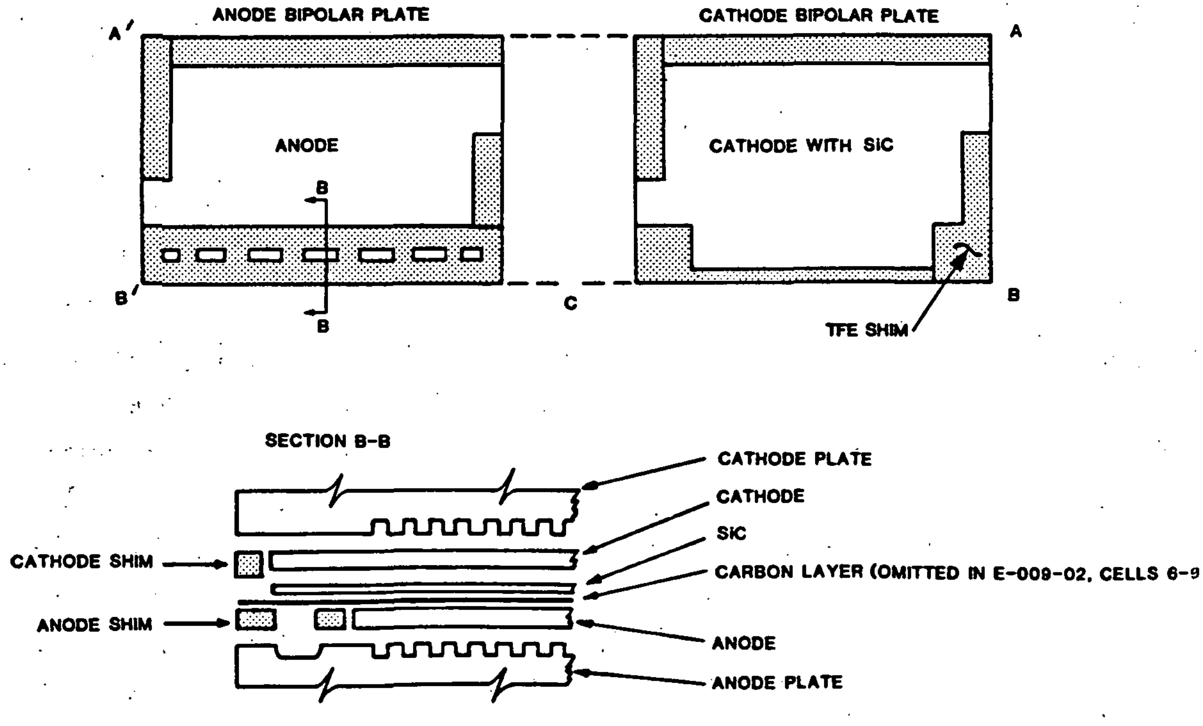

b) ALTERNATE SEAL DESIGN FOR IMPROVED ACID TRANSPORT

Figure 3-55. Cell Seal Design

TABLE 3-54

STACK E-009-02 OPEN CIRCUIT VOLTAGES, mV

Operating Conditions: 1 atm, 125°C, H_2/Air

CELL NO.	MAT-1	BEFORE ACID ADDITION	AFTER ACID ADDITION
1	Yes	888	896
2	Yes	878	895
3	Yes	923	937
4	Yes	913	943
5	Yes	886	988
6	No	71	772
7	No	9	1003
8	No	46	895
9	No	137	903
Avg. MAT-1 Matrix Cells		898	932
Avg. SiC Matrix Cells		66	893

Total Acid Addition ∿ 65 cc 97% H_3PO_4

Stack E-009-03 was assembled with Cells 1 - 5 containing Kureha 604 paper instead of Vulcan carbon layer. This material was tested to see if it improved the lateral transport of acid during operational changes that result in acid volume expansion. The stack was tested for a total of ∿ 160 hours, including ∿ 90 hours at 480 kPa (70 psia). An average performance of 653 mV/cell in Cells 1-5 containing Kureha paper in cell matrices and 661 mV/cell in Cells 6-9 containing MAT-1 matrices was observed at 480 kPa (70 psia), 190°C (374°F), 325 mA/cm^2 (300 A/ft^2), 83 percent fuel (hydrogen) and 40 percent oxidant (air) utilizations. A reversal of polarity in Cell 3 caused stack testing to be terminated. Kureha paper in the cell matrices resulted in a slightly lower average cell performance (∿ 10 mV/cell) as compared to cells containing MAT-1 matrices. Several other differences were observed between Cells 1-5 containing the Kureha paper matrices and Cells 6-9 containing MAT-1 matrices:

- Open circuit voltages of Cells 1-5 were lower (∿ 50 mV/cell) than those in Cells 6-9. This may have been due to internal short circuits or slight gas cross leaks.

- Due to the more porous structure (and thus higher electronic resistance) of Kureha paper compared to the standard carbon layer, the measured resistances of Cells 1-5 were ∿ 50 percent higher than those of Cells 6-9. This higher electronic resistance was not expected to adversely affect cell performance since ionic resistance of the matrix has a much more significant effect on performance than does electronic.

- SRG loss in Cells 1-5 was 82 mV/cell at the design point compared to a loss of 34 mV/cell for the cells containing MAT-1. Overheating also occurred in several cells containing Kureha paper in the matrices which was attributed to reactant crossover.

Post-test disassembly showed degradation of the Cell 1 cathode plate near the oxidant inlet and both the Cell 3 anode plate and anode backing paper near the fuel inlet.

Based on the limited experience thus far with Kureha paper in cell matrices, Kureha paper is not satisfactory as a barrier to crossleaks. Post-test disassembly also showed that it does not prevent plate wetting by transporting the electrolyte laterally.

During upset conditions it is possible to get relatively large changes in acid volume. There are two methods for dealing with this potential problem:

- allow the acid to expand laterally and collect in the replenishment channel (modified matrix tested in Stack E-009-03)
- allow acid expansion perpendicular to the electrode (tested in Stack E-009-01).

An acid inventory control member (AICM) was initially developed and tested on Contract DEN3-205. The best component design from that effort was incorporated into the anode of Cells 6-9 in Stack E-009-01. The basic design of this member is shown in Figure 3-56.

The stack was operated for ∿ 530 hours, of which 100 hours were at 480 kPa (70 psia). As shown in Figure 3-57, Cell 6-9 containing AICM anodes had performance equivalent to the other cells. Disassembly inspection showed that one cell with the AICM and one cell without an AICM had cathode plate corrosion. Apparently, the AICM did not prevent this type of corrosion.

The amount of acid required to fill standard or modified components is obtained from analysis of ERC electrolyte take-up (ETU) data and from Westinghouse calculations. Since components can vary in thickness and density, the amount of acid to completely fill them during the assembly procedure cannot be ascertained with any significant accuracy. This variability, however, can be accommodated by applying a constant amount during the initial assembly and then adding acid through the acid replenishment channel in each cell after assembly. The optimum conditions for post-assembly acid addition remain to be determined.

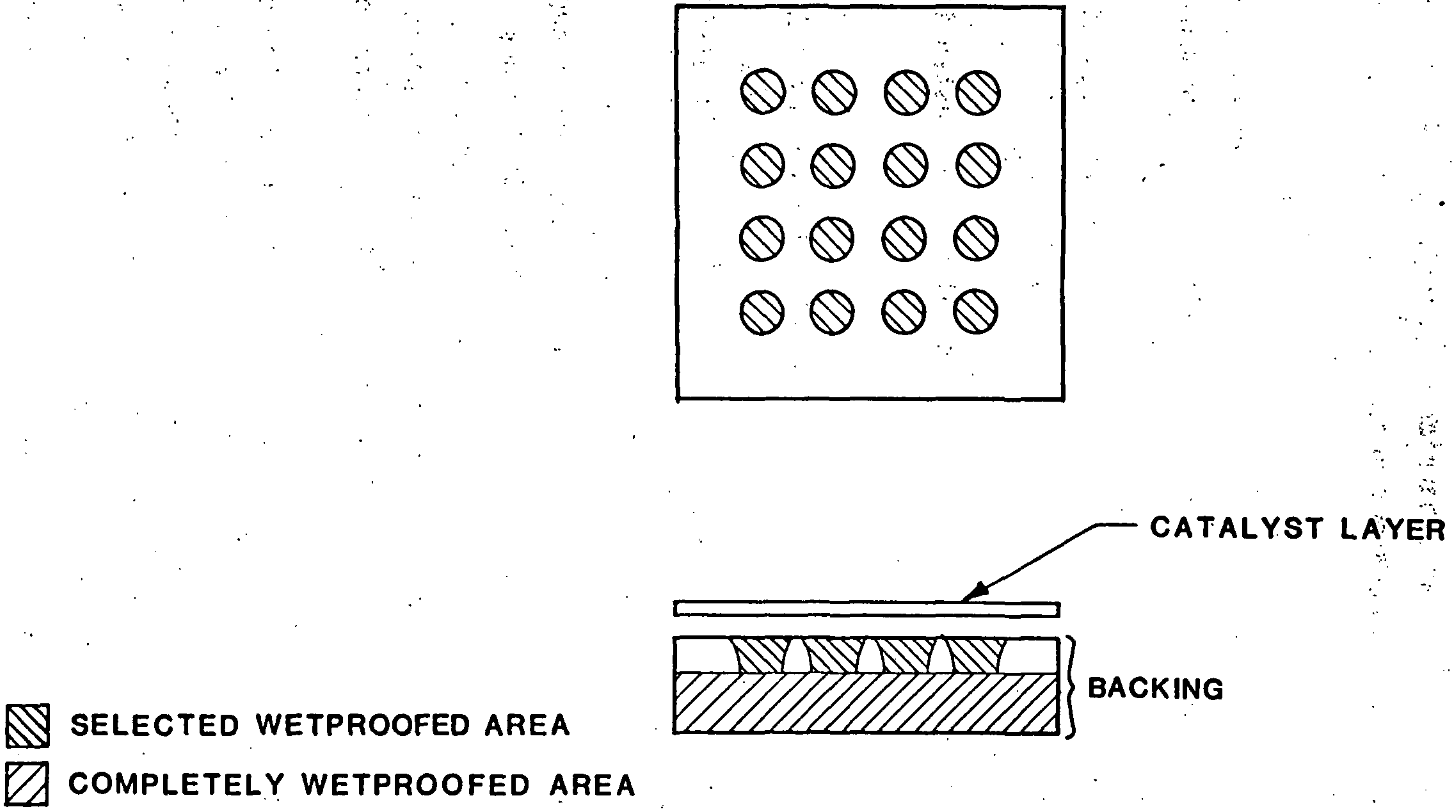

Figure 3-56. AICM-Anode Backing for Nine Cell Stack E-009-01

ORIGINAL PAGE IS
OF POOR QUALITY

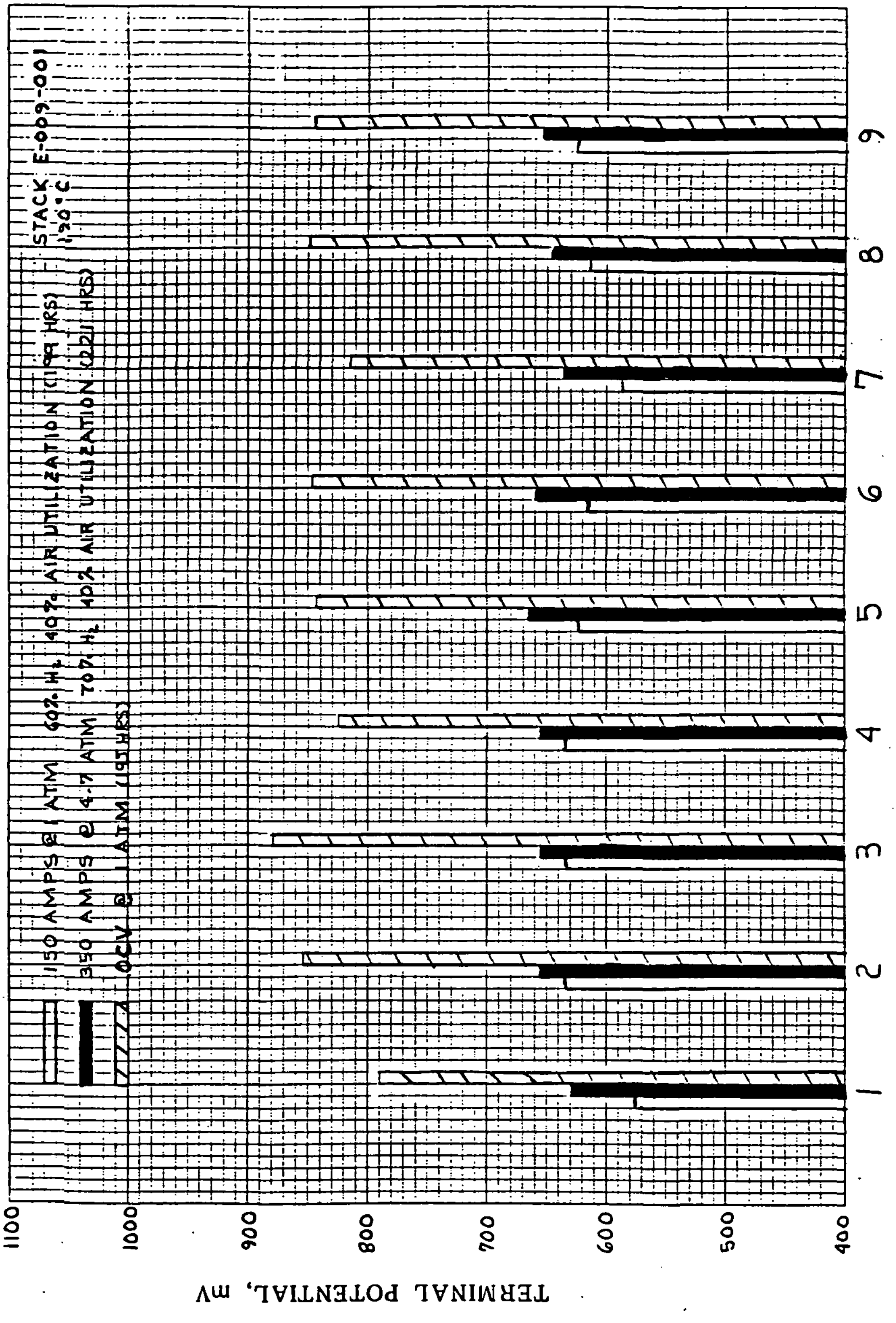

Figure 3-57. Initial Performance Data for Stack E-009-01

Analysis of acid replenishment requirements during stack operation has been limited by the relatively short periods of operation for each stack and the variations of the cell components built into the stacks. Each stack was found to accept acid when it was added. A summary of the acid additions is presented in Table 3-55. Apparently the cells had not received enough acid before operation. Improved procedures for acid addition prior to operation are required for the future.

3.8.8 Impurity Effects

An effort to catalog and understand the level of impurities in various starting materials was initiated during the First Logical Unit of Work. Spectrographic analyses showed that as-received Vulcan XC-72 (standard catalyst support) contained ∿ 1 percent sulfur. Because high levels of sulfur may cause catalyst poisoning and create problems during plant startup, an effort to remove these impurities was undertaken. Various pretreatments including leaching in phosphoric acid and heat treatments at 900°C, 1800°C, and 2500°C (1650°F, 3300°F, and 4550°F) were examined as shown in Table 3-56. Both free sulfur and total sulfur were measured. Acid leaching removed only a small amount of sulfur. Similarly, heat treatment to 900°C (1650°F) ("standard" heat treatment temperature after catalyzation) did not change the sulfur content. Thus, as expected, sulfur appears to be strongly bound within the carbon structure. Further heat treatment to 1800°C (3300°F) and 2500°C (4550°F) did remove ∿ 95 percent of the sulfur. It is possible that an intermediate temperature between 900°C (1650°F) and 1800°C (3300°F) may also provide a similar reduction in sulfur levels. However, such heat treatments do change the chemical and physical properties of carbon and may also be expensive.

The sulfur content of Shawinigan Black, a purer carbon support, was also analyzed. As shown in Table 3-56, the sulfur level is ∿ 160 ppm in the as-received material. Heat treatment to 1200°C (2200°F) and 1800°C (3300°F) reduced this level slightly.

TABLE 3-55

SUMMARY OF ACID ADDITIONS TO NINE CELL STACKS, cm^3

	Stack Number			
Addition No.	E-009-01	E-009-02	E-009-04	E-009-06
1	25	12	10	28
2	-	40	43	-
3	-	20	54	-
Total	25	72	107	28

TABLE 3-56

TOTAL AND FREE SULFUR CONTENTS OF CARBON SUPPORTS

Material	Sulfur Content % Total	Sulfur Content % Free
As-received Vulcan XC-72	0.93	0.53
Hot Phosphoric Acid (190°C) Leached Vulcan XC-72	0.88	0.27
900°C heat treated Vulcan XC-72 (in N_2 atmosphere)	0.89	0.51
1800°C heat treated Vulcan XC-72 (in N_2 atmosphere)	0.025	Not detectable*
2500°C heat treated Vulcan XC-72 (in N_2 atmosphere)	0.024	Not detectable*
As-received Shawinigan	0.016	Not detectable*
1200°C heat treated (in N_2 atmosphere) Shawinigan Acetylene Black	0.013	Not detectable*
1800°C heat treated (in N_2 atmosphere) Shawinigan Acetylene Black	0.012	Not detectable*

---

*Less than 40 ppm.

4.0 ERC NINE CELL STACK TEST FACILITIES DEVELOPMENT

A pressurized test facility to accommodate a 12 x 17 in. nine cell stack was completed. This facility improved upon the past ERC facilities in the following areas:

- capable of testing up to a nine cell stack.
- measurement of fuel, oxidant, and cooling flow pressure drops (bringing the total number of ΔP measurements to six).
- cooling inlet temperature control.
- redundant flow monitoring.
- fine control of electrical load.
- automatic failure mode control system.
- load transients with greater than 3 milliseconds switching time able to be studied.

A schematic flow diagram for the improved facility is presented in Figure 4-1. This facility was designed for the following range of operating conditions:

Pressure Range:	0 to 1037 kPa (0 to 135 psig), pressurization rate of approximately 13.8 kPa (2 psi) per minute
Standard Gases:	Hydrogen fuel, air oxidant, auxiliary inputs for special gases
Current Density Range:	50 to 460 mA/cm^2 (47 to 430 A/ft^2)

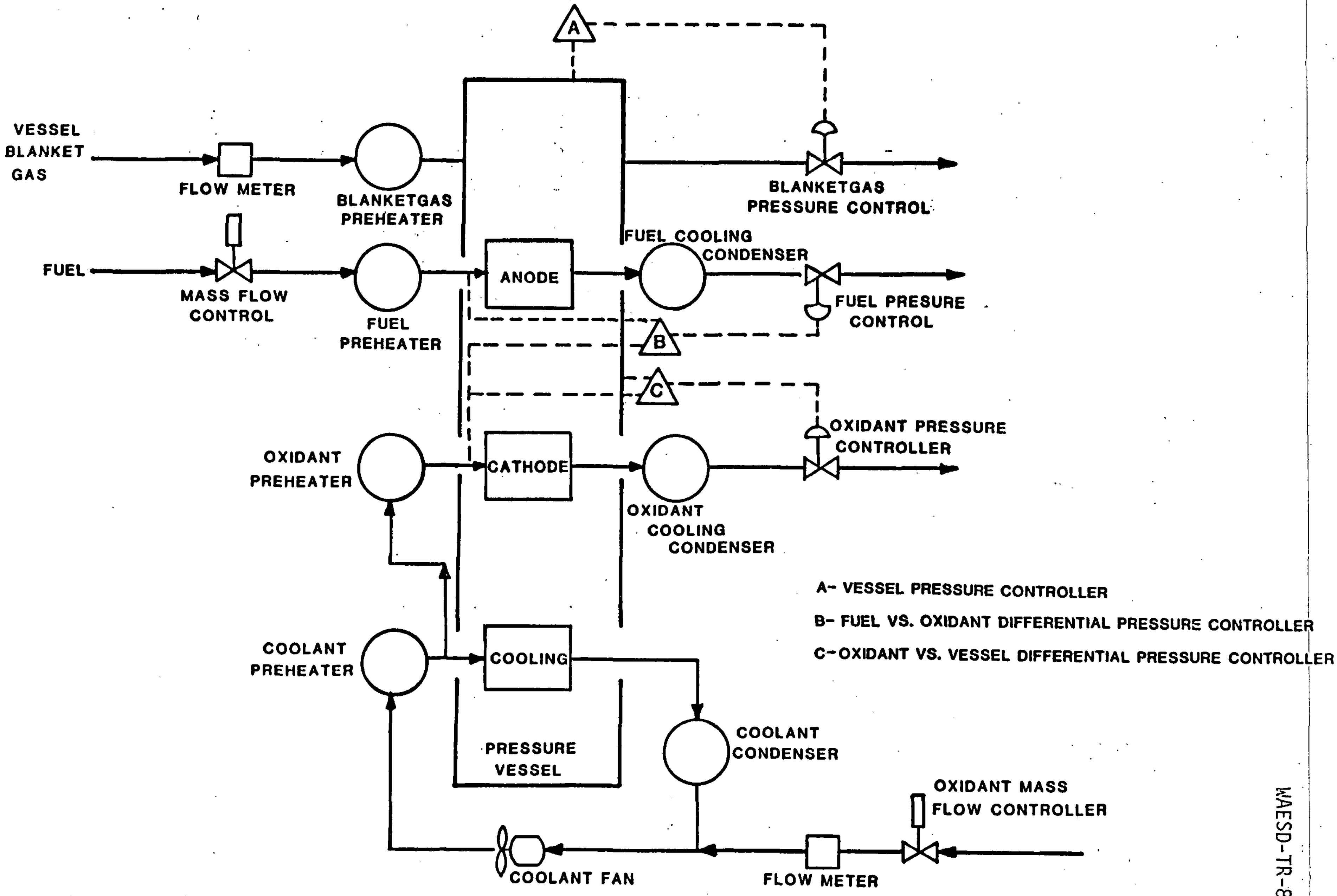

Figure 4-1. Schematic Flow Diagram for Nine Cell Stack Pressurized Facility (SE-1)

Fuel FLow Range: Up to 80 percent utilization at 50 mA/cm^2 (47 A/ft^2) 50 to ∿ 100 percent utilization at 460 mA/cm^2 (430 A/ft^2)

Oxidant Flow Range: Up to 50 percent utilization at 50 mA/cm^2 (47 A/ft^2) 20 to ∿ 100 percent utilization at 460 mA/cm^2 (430 A/ft^2)

Temperature Range: 30 to 250°C (86 to 480°F), independently controlled end plate temperatures

Cooling: 100 scfm air, Ambient to 130°C (265°F)*

Unattended operation of the facility is made possible by the use of a Failure Mode Control System (FMCS). This system continuously monitors the facility for conditions that could have a harmful effect on either the facility or the stack. The FMCS monitors several stack voltages, several temperatures, line power, and hydrogen concentration in the vessel cover gas. The specifications for the FMCS are presented in Table 4-1.

Construction and checkout of the first nine cell stack pressurized test facility, SE-1, was completed. The checkout of facility SE-1 was conducted by testing Stack E-009-06 and when completed, the facility was put into service. Stacks have been tested in this facility up to 825 kPa (120 psia) and 400 mA/cm^2 (372 A/ft^2) using pure hydrogen as fuel with a 55°C (100°F) coolant ΔT. The verified operating condition ranges are presented in Table 4-2. The facility has accumulated ∿ 3,500 hours of testing.

Several recommended modifications to the original design were identified during the testing of facility SE-1. These changes are outlined below:

---

*At blower element

TABLE 4-1
SPECIFICATIONS OF THE FMCS FOR 12 X 17 STACK PRESSURIZED TEST FACILITY

Problem	Trip Point (Adjustable)	Action
Stack Undervoltage (group of 2 or 3 cells)	0.5 - 3.0 V	Remove Load
Stack Over Temperature	150 - 250°C	Remove Load
Vessel Over Temperature	100 - 175°C	Remove Load Stop Process Flows Depressurize System
H_2 in Vessel Gas	1% or 4%	Remove Load Stop Process Flows Depressurize System
Power Failure	Longer than 1 min.	Remove Load
	Longer than 30* min.	Remove Load Stop Process Flows Depressurize System

---

*Due to loss of backup power and supply air.

TABLE 4-2
VERIFIED OPERATING CONDITIONS (USING NINE CELL STACK IN PRESSURIZED TEST FACILITY SE-1)

	OPERATING CONDITIONS	COMMENTS
Pressure Range:	14.7 to 120 psia (Pressurization Rate of ∿ 0.5 psi per min.)	Pressure above 120 psia not tested. Pressurized at 83 mA/cm^2 load, 50% H_2 utilization 40% oxidant utilization.
Standard Gases:	H_2 fuel, air oxidant auxiliary inputs for other gases	Modification for long term SRG planned
Current Range:	At 14.7 psia-up to 150 mA/cm^2 At 70 psia-86 to 400 mA/cm^2	
Fuel Flow Range:	Up to 83% utilization at 86 mA/cm^2, 50 to 85% utilization at 325 mA/cm^2	
Oxidant Flow Range:	Up to 50% utilization at 86 mA/cm^2, 40 to 65% utilization at 325 mA/cm^2	
Stack Temp Range:	Ambient to 250°C (independently controlled for each end plate)	
Cooling ΔT:	∿ 55°C (100°F) at 325 mA/cm^2 with 120°C (250°F) inlet manifold temperature	Coolant ΔT higher than the design value of 100°F above 400 mA/cm^2. Modification for increased coolant flow capacity submitted to Westinghouse to reduce coolant ΔT from 100 to 68°F.

- Addition of a flow control/gas blending system for extended operation on SRG. This system should allow incremental addition of the various component gases to investigate their effect on stack performance. Minor adjustments in gas compositions should also be possible.

- Addition of a temperature controller in the fuel inlet line to achieve a more uniform thermal profile and to simulate the temperature of the fuel gas entering the stack from a reformer.

- Increase in cooling loop capacity. The program specification of 55°C (100°F) temperature rise in the cooling air system from inlet manifold to outlet manifold was revised after the design of test facility SE-1. The new specification of 38°C (68°F) rise and increased pressure drop in the cooling plate, along with other factors, will require modification of the design to single pass cooling and installation of a dedicated compressed air system.

- Single pass cooling design to eliminate the blowers presently in use. The blowers are unreliable for long term continuous operation. By replacing them with a dedicated compressor system, overall system reliability will increase.

- Oil-free compressors are recommended because oil decomposition products generated at elevated temperatures in the compression process may poison fuel cell catalysts. Although filters can be used to remove oil particles, they do not remove vapors and gases. Periodic compressor shutdowns required to replenish the oil also reduce the compressor availability and may require unwarranted stack shutdowns. The air in these compressors is thoroughly mixed with the oil and a filter malfunction can introduce oil in the compressed air lines, requiring a long shutdown to decontaminate.

A comparison of the design for recirculation and single pass cooling is presented in Figure 4-2.

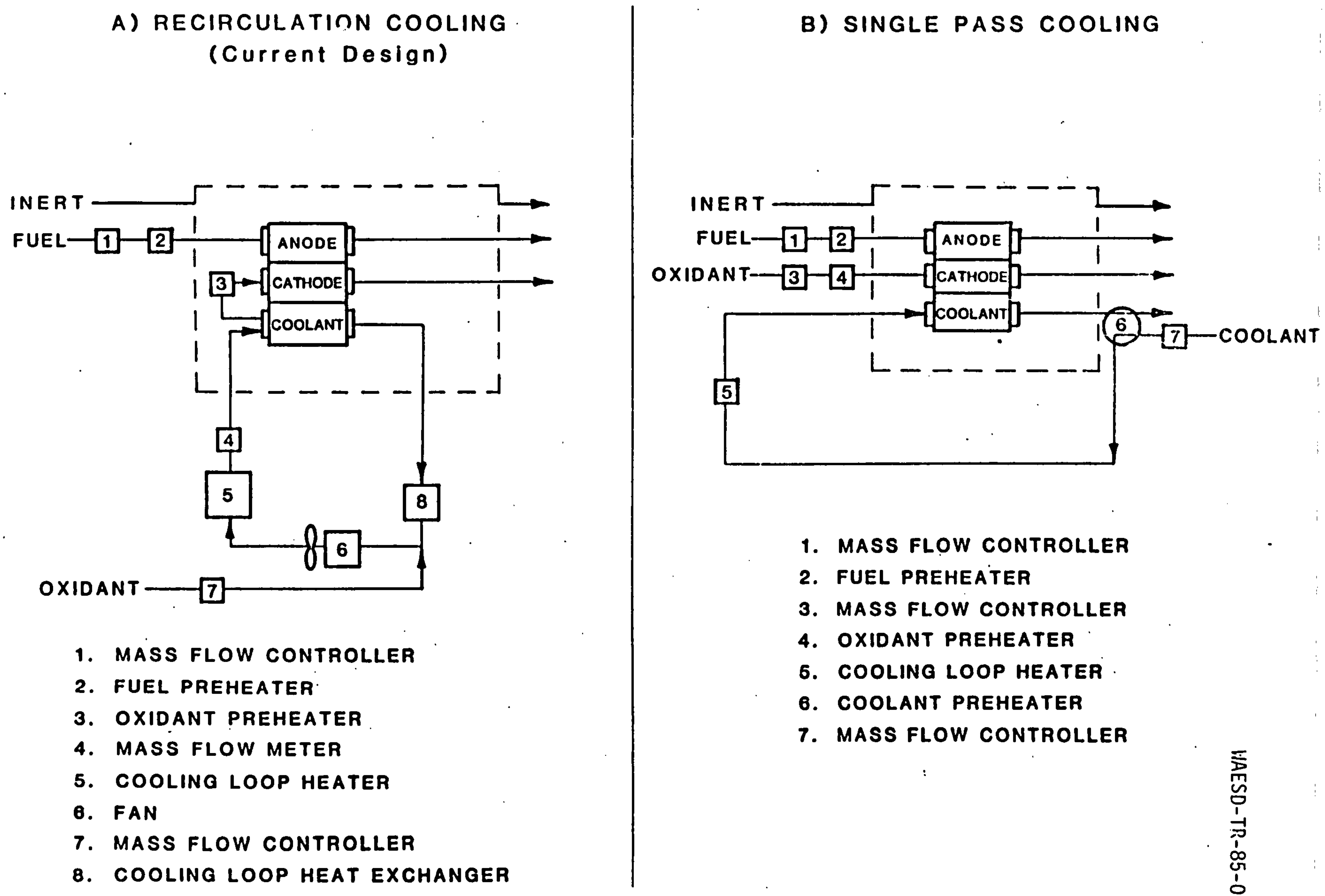

Figure 4-2. Current Nine Cell Pressurized Recirculation Design and Proposed Single Pass Cooling Design

Work on modification of the second nine cell stack pressurized test facility SE-2 was initiated.

Test facility SE-3 is planned for construction in the next logical unit of work. After it is completed, facility SE-1 will be modified to the single pass cooling scheme.

5.0 REFERENCES

1. B. Ke, J. Polymer Sci., BI, 1967-70 (1963).

2. B. Wunderlich and E. Hellmuth, Dupont Thermogram, _1_, 5 (1964).

Report No.
NASA CR-175047

2. Government Accession No.
---

3. Recipient's Catalog No.
---

4. Title and Subtitle
Gas Cooled Fuel Cell Systems Technology Development
Final Report for the Second Logical Unit of Work

5. Report Date
August 1986

6. Performing Organization Code
XAL-78010-AL

7. Author(s)
J. M. Feret

8. Performing Organization Report No.
WAESD-TR-85-0030

10. Work Unit No.

9. Performing Organization Name and Address
Westinghouse Electric Corporation
Advanced Energy Systems Division
P. O. Box 10864
Pittsburgh, PA 15236-0864

11. Contract or Grant No.
DEN3-290

13. Type of Report and Period Covered
Contractor Report
May 1983 - May 1984

12. Sponsoring Agency Name and Address
U. S. Department of Energy
Morgantown Energy Technology Center
Morgantown, WV 26505

14. Sponsoring Agency Code
DOE/NASA/0290-01

15. Supplementary Notes
Prepared under Interagency Agreement DE-AI01-80ET17088. Project Manager, Robert B. King, Energy Technology Division, NASA Lewis Research Center, Cleveland, Ohio 44135

16. Abstract

This report summarizes the work performed by Westinghouse Electric Corp. and Energy Research Corp. during the second phase of a planned multiphase program to develop a Phosphoric Acid Fuel Cell (PAFC) for Electric Utility Prototype Power Plant Application. The results of this effort include: 1) establishment of the final system level requirements for the Fuel Cell, Fuel Processing, Power Conditioning, Rotating Equipment, and Instrumentation and Control Systems, 2) advancement of fuel cell technology through innovative improvements in the areas of acid management, catalyst selection, electrode materials, and quality assurance programs, and 3) demonstration of improved fuel cell stack performance.

17. Key Words (Suggested by Author(s))
Fuel Cells. Phosphoric Acid. Energy Conversion. Energy Systems. Advanced Power. Carbon Corrosion. Carbon Compounds. Alloy Catalysts.

18. Distribution Statement
Unclassified - Unlimited
Star Category - 44
DOE Category - UC-97d

19. Security Classif. (of this report)	20. Security Classif. (of this page)	21. No. of Pages	22. Price*
Unclassified	Unclassified	279	

*For sale by the National Technical Information Service, Springfield, Virginia 22161

NASA-C-168 (Rev. 10-75)

REPORT SUMMARY FORM

1. **SECURITY CLASSIFICATION:** N/A

2. **REPORT NO.:** WAESD-TR-85-0030

3. **PROPRIETARY CLASS:** N/A

4. **AVAILABILITY:** AESD-WM-LIB

5. **ORIGINATING SOURCE:** AESD-L

6. **CONTRACT NO.:** DEN3-290

7. **FUNDING SOURCE:** U. S. Dept. of Energy/NASA Lewis Research Center

8. **NOTES:** N/A

9. **AUTHOR(S):** Feret, J. M.

10. **TITLE:** GAS COOLED FUEL CELL SYSTEMS TECHNOLOGY DEVELOPMENT FINAL REPORT FOR THE SECOND LOGICAL UNIT OF WORK

11. **DATE--YYMMDD:** 860800

12. **PAGES, REF., ILLUS.:** 279 P. 2 Ref. 69 Illus.

13. **DOCUMENT TYPE:** Report

14. **KEYWORDS:** FUEL CELLS. PHOSPHORIC ACID. ENERGY CONVERSION. ENERGY SYSTEMS. ADVANCED POWER. CARBON CORROSION. CARBON COMPOUNDS. ALLOY CATALYSTS

15. **ABSTRACT--PURPOSE, SCOPE, APPROACH, RESULTS, CONCLUSIONS, SIGNIFICANCE: (MAXIMUM: 200 WORDS)**

This report summarizes the work performed by Westinghouse Electric Corp. and Energy Research Corp. during the second phase of a planned multiphase program to develop a Phosphoric Acid Fuel Cell (PAFC) for Electric Utility Prototype Power Plant Application. The results of this effort include: 1) establishment of the final system level requirements for the Fuel Cell, Fuel Processing, Power Conditioning, Rotating Equipment, and Instrumentation and Control Systems, 2) advancement of fuel cell technology through innovative improvements in the areas of acid management, catalyst selection, electrode materials, and quality assurance programs, and 3) demonstration of improved fuel cell stack performance.

16. **THIS WAESD-TN SHOULD BE DESTROYED AFTER ______ MONTH ______ YEAR.**

FORM AESD-00130A

DOCUMENT DISTRIBUTION LIST

INTERNAL AESD				EXTERNAL AESD		
NAME, DEPT, LOCATION	FULL TEXT*	RSF ONLY+	COPY NO.●	NAME AND ADDRESS	NO. OF COPIES	COPY NO.●
See Fuel Cell Distribution List				R. B. KING PROJECT MANAGER MAIL STOP 301-5 NASA LEWIS RESEARCH CENTER 21000 BROOKPARK RD. CLEVELAND, OHIO 44135		

* INDICATE NUMBER OF COPIES OF FULL TEXT
\+ REPORT SUMMARY FORM ONLY
● CONTROLLED DISTRIBUTION, IF APPLICABLE

FORM NO. AESD-00130B